Flows, intersections, and stability on hyperbolic arrangements

by

Samuel Carwyn Lewis

A thesis submitted in fulfilment of the requirements
for the degree of

Doctor of Philosophy

at the

School of Mathematics & Statistics
College of Science & Engineering
University of Glasgow

September 2024

To Sophie

Abstract

This thesis studies various aspects of stability theory, hyperplane arrangements, and Coxeter combinatorics, often in the hyperbolic setting. We provide a large family of examples of real variation of stability conditions, and fully classify hyperbolic intersection arrangements in dimension two. Our work establishes new connections between generalised Coxeter arrangements and stability conditions for K3 categories. It is motivated by the belief that the hyperbolic (minimally wild) setting is a rich one; combinatorially, representation theoretically, and geometrically, and worthy of further study.

Contents

Acknowledgements

First and foremost, I would like to express my sincere gratitude to my supervisors, Gwyn Bellamy and Michael Wemyss, for their unwavering support and patience over the past four years. Without their consistent encouragement and faith, this thesis would not have been possible.

I would also like to thank the members of the research groups I have been lucky enough to be a part of and learn from. In particular, I am grateful to Simone Castellan, Rhys Davies, Marina Godinho, Isambard Goodbody, Charlotte Llewellyn, Caroline Namanya, and Parth Shimpi for many illuminating chats. A big thanks is also owed to Matthew Pressland and Franco Rota for often providing their time and guidance to answer lots of naive questions, mathematical or otherwise.

I am extremely thankful to Martin Vrabec for help with `Mathematica`, and to Robin Ammon for advice on `Magma` (and for introducing me to bubble tea). Being completely unfamiliar with hyperbolic geometry before starting this project, I am indebted to Philipp Bader and Jim Belk for all the helpful discussions on the subject. I wish to thank Xiuping Su for introducing me to quiver representation theory during a Master's project at the University of Bath, as well as inspiring my study of the hyperbolic setting through her research into wild quivers.

I would also like to thank my fellow PhD students and my office mates in 230 for always making work a fun and unpredictable place to be, particularly Julian for his excellent playlist of classical music which got this thesis over the line. I am grateful to everyone in the department (many of whom are named above) who joined me for my parkruns around Scotland.

This research was made possible by funding from both the EPSRC and ERC. The template used for this thesis was designed and implemented by Okke van Garderen and Ross Paterson. Many thanks to my examiners, Jim Belk and Joseph Chuang, for their thorough reading of this thesis and for giving many helpful corrections.

Finally, I wish to thank my family for helping me get this far, as well as my partner Sophie for always believing in me, and for providing most of the commas in this thesis.

Author's declaration

I declare that, except where explicit reference is made to the contribution of others, this dissertation is the result of my own work and has not been submitted for any other degree at the University of Glasgow or any other institution.

Chapter 1

Introduction

The research in this thesis lies within algebra and geometry, and solves geometry-inspired questions in an algebraic context, with applications to homological algebra, Coxeter theory, and stability conditions.

The prolific trichotomy of finite, tame, and wild permeate across mathematics, from Cartan and Killing's classification of simple Lie algebras [Kil88], to Gabriel's theorem for quivers [Gab72] and the McKay correspondence [McK80]. This thesis investigates what happens when we take algebro-geometric questions, answers, and objects in the first two cases and push them to the 'hyperbolic' tame–wild boundary.

In the context of undirected graphs, the hyperbolic case comprises the *overextended* ADE families

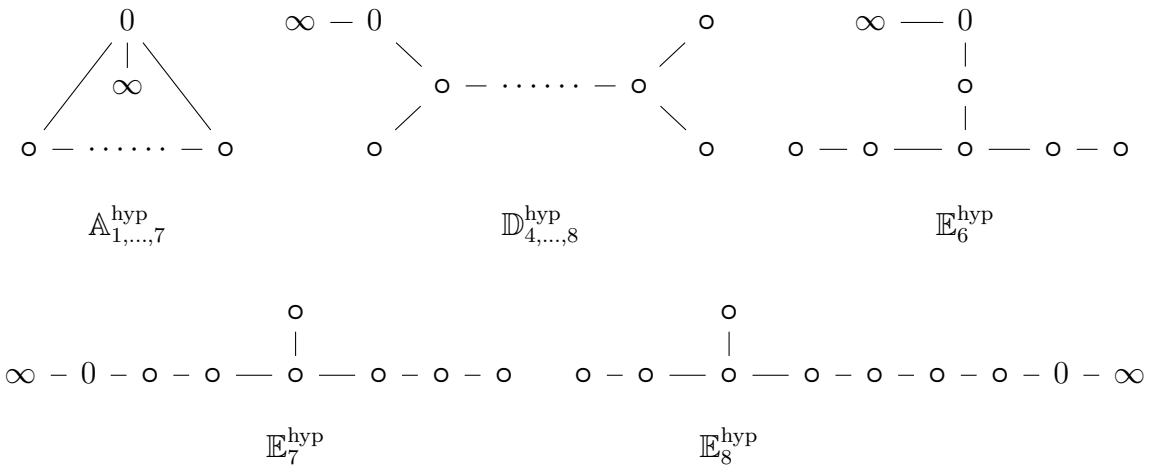

as well as some exceptional graphs. Our key insight is that there are particularly fruitful and exciting new results and structures to be found within this hyperbolic setting.

In line with the the title of this thesis, we investigate the role of the above diagrams in three key areas.

(1) Flows — categorifying hyperplane arrangements by connecting wall-crossing and monodromy with derived autoequivalences and mutation functors.

(2) Intersections — generalising Coxeter theory via intersection arrangements, classifying a new family of rich combinatorial structures.

(3) Stability — notions related to Bridgeland stability conditions on triangulated categories and their real variations, applied to K3 categories associated with preprojective algebras.

A general theme is to use combinatorial structures such as hyperplane arrangements and their wall-crossings, to understand bounded hearts in triangulated categories. To this end, we create novel combinatorial models which allow us to explore a wealth of new t-structures on K3 categories associated with preprojective algebras for hyperbolic graphs. Our results demonstrate the potential that comes from considering this family of diagrams, extracting combinatorial insights and visualisations from wild type behaviour, with algebraic corollaries.

§ 1.1 | Overview

In the theory of quiver representations, much attention has been given to the finite and affine cases due to finite-dimensionality and noetherianity of their preprojective algebras, respectively. This has important geometric consequences in dimension two, but loses meaning in the wild.

Coxeter theory is the study of reflections and symmetry, arising as kaleidoscopic tessellations of space known as hyperplane arrangements. The research in this thesis generalises classical Coxeter theory and connects the representation theory of preprojective algebras to the resulting arrangements. From the perspective of Coxeter combinatorics, it is known that in the finite/tame/wild trichotomy, a meaningful distinction can be made between the strictly wild (indefinite) and minimally wild (hyperbolic), via the existence of a 'real level'.

§ 1.1.1 | Real stability on noncommutative K3 categories

As in the work [Ike14] of Ikeda, to a graph $\Delta = (\Delta_0, \Delta_1)$ of *rank* $\mathsf{rk} := |\Delta_0|$ we can associate the triangulated category $\mathcal{D}_\Delta$, the derived category of nilpotent representations of the preprojective algebra Π_Δ. We are motivated by the realisation of the space $\operatorname{Stab} \mathcal{D}_\Delta$ of Bridgeland stability conditions on $\mathcal{D}_\Delta$ as a covering space of the complexification of a hyperplane arrangement $\mathcal{H}_\Delta$, coming from the root data of Δ. To avoid the technical issue of whether or not a functor that fixes all simples is the identity functor, we take an alternative approach to Bridgeland stability conditions via real variations, leveraging Coxeter theory to investigate homological properties of Π_Δ.

Generally, let $\mathcal{D}$ be a triangulated category and let $\mathcal{H}$ be a locally finite arrangement of real hyperplanes equipped with a direction $\prec$ on its alcoves (connected components of the complement). Introduced in [ABM15], a real variation of stability conditions on $\mathcal{D}$, parametrised by $\mathcal{H}$ in the direction of $\prec$, consists of the following data:

(1) a real central charge Z,

(2) an assignment of hearts (of bounded t-structures on $\mathcal{D}$) to alcoves.

This data needs to satisfy positive pairing and t-structure compatibility conditions for neighbouring alcoves, such that if an alcove is 'above' another with respect to $\prec$, then the associated hearts differ by an appropriate homological shift. Full details are given in Definition 4.1. If the assigned hearts are *faithful*, this compatibility constraint can be thought of as a perverse equivalence of triangulated categories, in the sense of [CR17].

Returning to the setting of the K3 category $\mathcal{D}_\Delta$ arising from Δ, it is well-known that $\mathcal{D}_\Delta$ and the Coxeter arrangement $\mathcal{H}_\Delta$ are closely related via tilting theory, with mutation functors categorifying simple reflections. However, it is clear that the definition of 'direction' given in [ABM15] does not generalise to this setting. We give a general definition of real variations of stability that is applicable in many more situations. First we introduce the new notion of a *real flow* on a Coxeter arrangement, which we sketch here, with full details given in Section 4.2.

Definition 1.1. Let $\mathcal{H}$ be a locally finite arrangement of real hyperplanes. A *real flow* on $\mathcal{H}$ is a choice of $\succ$ or $\prec$ at every codimension one wall between neighbouring alcoves, such that around every codimension two wall there is a unique 'source' alcove A_s, opposite which is a unique 'target' alcove A_t, as illustrated below.

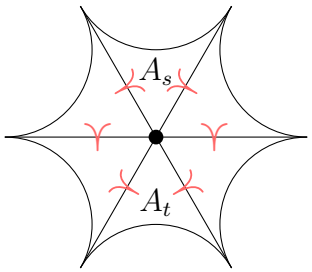

This is given a categorical interpretation in Section 4.2, where the choice of above or below corresponds to a choice of positive or negative power of the mutation functors between the hearts assigned to the alcoves. We show that a real flow on an affine or hyperbolic Coxeter arrangement gives rise to a real variation of stability conditions, in the more general sense defined in this thesis. In fact, we demonstrate in Theorem 4.20 that choosing such a real variation is equivalent to choosing a real flow on $\mathcal{H}_\Delta$.

§ 1.1.2 | Generalising Coxeter combinatorics

A real arrangement of hyperplanes is a collection of codimension one 'subspaces' in a finite-dimensional real space. In the classical theory arrangements consisted of finitely many affine-linear hyperplanes, but have seen generalisations to infinite arrangements of possibly nonzero curvature. Starting from the data of a connected graph Δ and a subset of shaded vertices $\mathcal{J}$, Iyama and Wemyss in [IW] introduced the notion of intersection arrangements, generalising arrangements coming from classical Coxeter theory.

Definition 1.2. The *intersection arrangement* associated with the data $(\Delta, \mathcal{J})$ is the

collection of hyperplanes $\mathcal{H}_\mathcal{J}$ obtained by taking the Coxeter arrangement of Δ and setting all variables indexed by $j \in \mathcal{J}$ to be zero.

Classical Lie theory in the affine setting asserts that it is possible to take a *real level* in the Coxeter arrangement, which gives a reduction in dimension by one. Thus, tilings of the affine plane arise from Δ an affine ADE graph and $\mathcal{J}$ with *corank* $\mathsf{crk} := |\mathcal{J}^c| = 3$. Iyama and Wemyss fully classify the affine intersection arrangements in dimension two.

Theorem 1.3 ([IW, 0.5])**.** *Let Δ a graph of affine type and let $\mathcal{J} \subseteq \Delta$ be of corank three. Then $H_\mathcal{J}$ is one the following sixteen hyperplane arrangements in $\mathbb{R}^2$.*

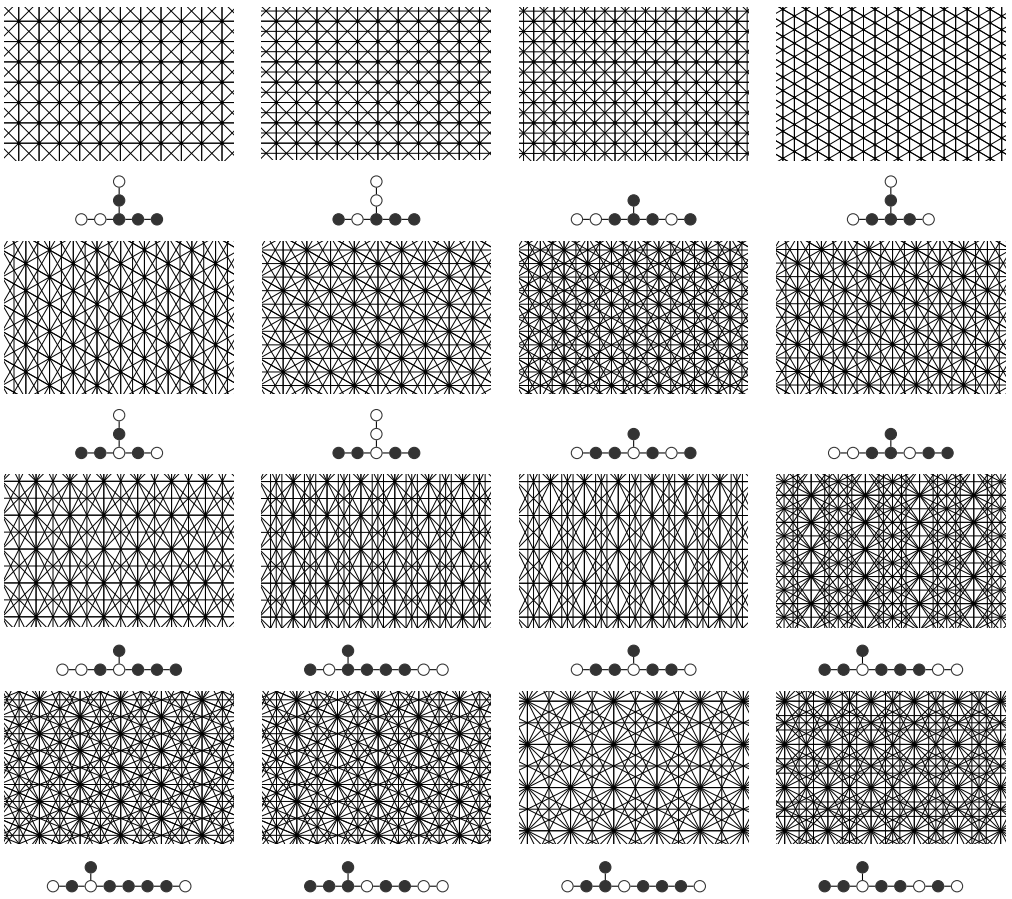

Intersection arrangements provide an opportunity to produce new ways to construct stability conditions. In this thesis, we fully classify tilings of the hyperbolic plane $\mathbb{H}^2$ that arise as hyperbolic intersection arrangements. Importantly, this gives a large class of non-global real hyperplane arrangements.

§ 1.2 | Summary of results

§ 1.2.1 | Real variations of stability conditions (Chapter 4)

After providing a hyperbolic analogue of the classical affine level using Moody's characterisation for the Tits cone, we introduce a real central charge map from hyperbolic $(\mathsf{rk}-1)$-space to the space of stability functions on our category $\mathcal{D}_\Delta$. Our definition generalises the affine real variations of stability in [ABM15] in two ways. Firstly, we

allow for a central charge compatible with hyperbolic space, where we cannot easily translate hyperplanes to the 'origin', and secondly, we categorify their notion of direction on alcoves away from an affine setting, giving rise to the idea of real flows. Our first main result is that real flows (as in Definition 1.1) on the Coxeter arrangement are very common.

Proposition 1.4 (4.10)**.** *Real flows are precisely those assignments of mutation functors to wall-crossings that descend to the arrangement groupoid of $\mathcal{H}_\Delta$. Equivalently, $\mathbb{F}$ is a real flow if and only if braid relations hold around every codimension two wall in $\mathcal{H}_\Delta$.*

A functor from the arrangement groupoid to the groupoid of autoequivalences of $\mathcal{D}_\Delta$ induces a homomorphism from the fundamental group of the complexified arrangement complement to the autoequivalence group. We show that this induced 'monodromy homomorphism' is the trivial morphism for real flows. This makes precise the notion that real variations of stability conditions are those that have trivial monodromy, and motivates the term 'real' in real flow.

We next prove a result that may be of independent interest regarding *faithfulness* of the standard heart in $\mathcal{D}_\Delta$, explored in the hereditary case in [EL21, Lemma 3.2]. Indeed, Bridgeland in [Bri09] raises the 'slightly subtle' problem of whether $\mathcal{D}_\Delta$ is equivalent to $\mathrm{D^b}(\operatorname{nilp}\Pi_\Delta)$. We answer this in the affirmative.

Theorem 1.5 (4.14)**.** *The standard heart* $\operatorname{nilp}\Pi_\Delta$ *in* $\mathcal{D}_\Delta$ *is faithful. In other words,*

$$\mathrm{D^b}(\operatorname{nilp}\Pi_\Delta) \cong \mathrm{D^b_{nilp}}(\Pi_\Delta) = \mathcal{D}_\Delta,$$

where the equivalence is induced by the inclusion $\operatorname{nilp}\Pi_\Delta \hookrightarrow \operatorname{Mod}\Pi_\Delta$.

This allows us to rephrase the main compatibility condition of real variations in terms of perverse equivalences with respect to the filtration of $\mathcal{D}_\Delta$ by thick triangulated subcategories generated by vertex simple modules. Our main result is the following.

Theorem 1.6 (4.20)**.** *Let Δ be a connected graph of affine or hyperbolic type and choose a real flow $\mathbb{F}$ on its Coxeter arrangement $\mathcal{H}_\Delta$. Then there exists a real variation of stability conditions on $\mathcal{D}_\Delta$, where the bounded t-structure at each alcove A is determined by the image of the corresponding Weyl group element under $\mathbb{F}$.*

Through doing this we provide first steps to understanding the Bridgeland stability manifold in this more general setting and prepare for more local approaches via contracted preprojective algebras.

§ 1.2.2 | Hyperbolic intersection arrangements (Chapter 5)

It turns out that the intersection arrangements described in Section 1.1.2 are very interesting in their own right. They are beautiful tessellations of the hyperbolic plane $\mathbb{H}^2$,

containing rich, non-global combinatorial information. Specifically, we show that taking intersections with Coxeter arrangements in type $\mathbb{A}^{\text{hyp}}, \mathbb{D}^{\text{hyp}}, \mathbb{E}^{\text{hyp}}$ give novel tilings of $\mathbb{H}^2$, viewed in the Poincaré disk, and we completely classify all possibilities that can arise in this way.

We first give a full classification of symmetric mutation classes in the hyperbolic setting, a useful combinatorial invariant for intersection arrangements linked to derived equivalences of *contracted preprojective algebras*. This reduces the upper bound on possible arrangements as follows.

Theorem 1.7 (5.24)**.** *There are* 827 *corank three subsets of hyperbolic graphs, which partition into* 200 *symmetric mutation classes.*

Then we directly compute the intersection arrangements in two ways. On the one hand, we compute a large region of the infinite restricted root system in `Magma` [BCP97], using this data to draw the arrangements directly in `Mathematica` [Inc]. On the other hand, we use the mutation computations for the symmetric mutation classes to understand the minimal 'angle' data that determines the arrangement, in terms of a list of hyperbolic triangles. Using both approaches to distinguish the intersection arrangements that can arise cuts the possibility of 200 new arrangements roughly in half, giving a hyperbolic version of the classification in [IW]. This is our second main result.

Theorem 1.8 (5.45)**.** *There are* 102 *hyperbolic intersection arrangements* $\mathcal{H}_\mathcal{J}$ *in dimension two,* 15 *of which are Coxeter arrangements.*

All 102 arrangements are drawn in Chapter 5, but for this introduction we illustrate eight of these arrangements below, all of which are governed by intricate local combinatorics. In particular, they are not determined by an underlying Coxeter group.

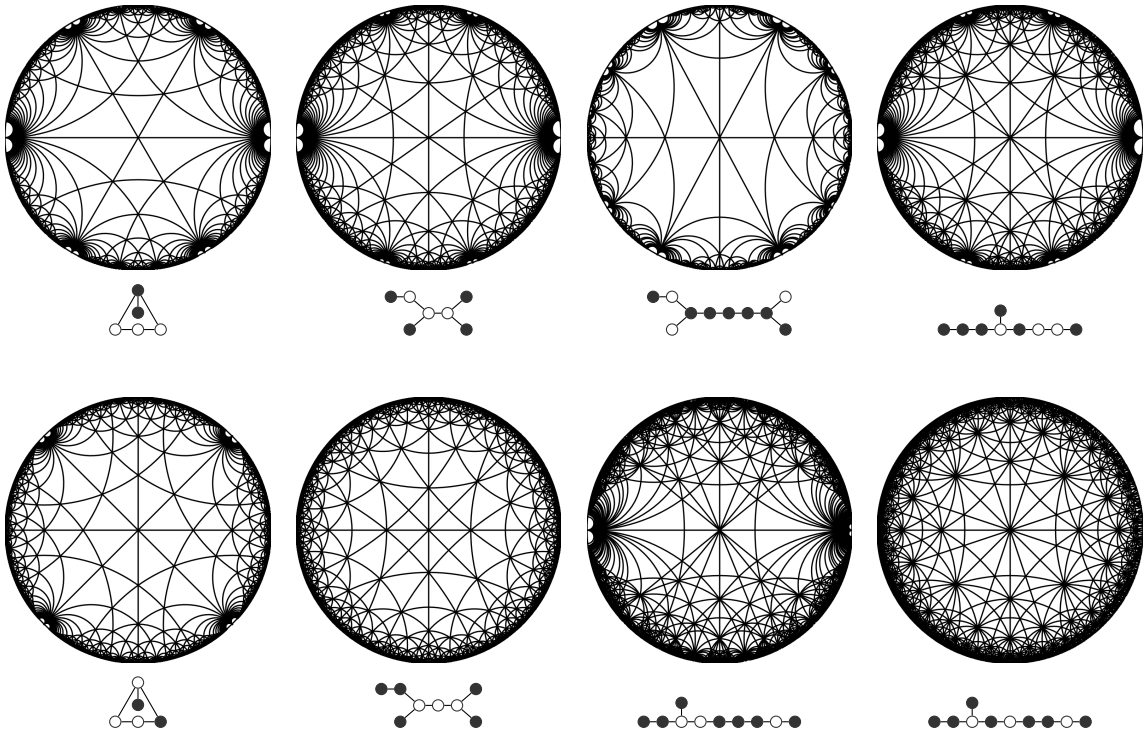

The 87 non-Coxeter intersection arrangements give a generalisation of hyperbolic triangle groups, providing a surplus of potential new examples for tilting theory on contracted preprojective algebras and the study of $K(\pi, 1)$.

As a more general result, we also obtain the number of symmetric mutation classes of any (nontrivial) corank. This includes the above corank three example as a special case and motivates studying intersection arrangements in higher dimensional hyperbolic space.

Theorem 1.9 (5.42)**.** *There are* 800 *proper hyperbolic symmetric mutation classes,* 485 *of which are in corank three or above.*

§ 1.3 | Structure of the thesis

We give an outline of how the work in this thesis is organised.

§ 1.3.1 | Prerequisite material

Chapter 2 and Chapter 3 are dedicated to giving preliminary material on Coxeter combinatorics and homological algebra. In Chapter 2 we introduce the combinatorial regions and hyperplane arrangement $\mathcal{H}_\Delta$ associated with a graph Δ, whilst in Chapter 3 we introduce the main triangulated category $\mathcal{D}_\Delta$ of interest and describe its basic properties. In particular, we cover background material on Coxeter combinatorics, with an emphasis on hyperbolic type, and the tilting theory of preprojective algebras, with an emphasis on complexes with nilpotent cohomology. These are the input for our real variations of stability.

§ 1.3.2 | Research outcomes

In Chapter 4 we introduce the notion of a *real flow* on a hyperplane arrangement, a categorified version of partial order on alcoves. We discuss real variations of stability parametrised by affine and hyperbolic arrangements, and show that they come from a choice of real flow. In Chapter 5 we describe intersection arrangements in the hyperbolic setting, giving a complete classification of dimension two phenomena. We also highlight the computational differences between the affine and hyperbolic case.

§ 1.3.3 | Further directions

To conclude, we discuss in Chapter 6 possible future research stemming from the work in this thesis. Research directions include the full stability manifold, higher dimensional intersection arrangements, and local systems of categories. Appendix A contains the supplementary computer algebra code used to create the hyperplane arrangements and provides computer verification of the classification results.

§ 1.4 | Notation and conventions

We summarise below common notation used in the thesis.

- We work over the field $\mathbb{C}$ of complex numbers.
- Rings Λ will be generally noncommutative.
- All modules will be right modules.
- All subcategories and subgraphs are assumed to be strict and full.
- Throughout we use the term *graph* to refer to a connected undirected graph with finitely many vertices, and diagram to refer to a graph that may have additional data, such as a Dynkin or Coxeter diagram.
- When objects depend on the graph Δ, in particular the edge data and not just the rank, we use a subscript. In Chapter 5 this is superseded by the choice of shaded vertices $\mathcal{J}$. Since we are viewing $\mathcal{J}$ as a full subgraph of Δ, this implicitly contains its data.
- We use the term *bounded heart* for the heart of a bounded t-structure.
- For a subcategory $\mathcal{E}$ of a triangulated category $\mathcal{D}$, the smallest thick subcategory of $\mathcal{D}$ containing $\mathcal{E}$ is denoted $\langle \mathcal{E} \rangle$.

Chapter 2

Coxeter preliminaries

Our first preliminary chapter focuses on the combinatorial aspects of the work, that being reflection arrangements and root systems. These come from the input data of a graph, or more generally a generalised Cartan matrix. From this data, we define the Coxeter arrangement $\mathcal{H}_\Delta$ in Section 2.3, and then construct a category known as the arrangement groupoid in Section 2.4. The latter is the first step towards categorifying real flows on hyperplane arrangements.

§ 2.1 | Generalised Cartan matrices

To conveniently package and compute this combinatorial data, we use a fundamental object from Lie theory known as the generalised Cartan matrix. Let $\Delta = (\Delta_0, \Delta_1)$ be a connected graph, where Δ_0 is the set of vertices and Δ_1 is the set of edges, both of which we assume throughout to be finite. The *rank* of Δ is the number of vertices, written $\mathsf{rk} := |\Delta_0|$. As running examples, consider the *Kronecker*, *affine*-$\mathbb{A}$, and *hyperbolic*-$\mathbb{A}$ graphs

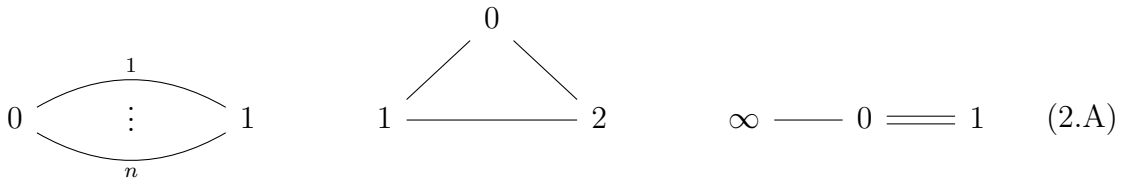

$\mathbb{K}_{n\geq 1}$ $\qquad$ $\mathbb{A}_2^{\text{aff}}$ $\qquad$ $\mathbb{A}_1^{\text{hyp}}$ $\qquad$ (2.A)

which all have $\mathsf{rk} \leq 3$ and whose nomenclature is soon made apparent.

§ 2.1.1 | The Cartan matrix

Definition 2.1. A *generalised Cartan matrix* (GCM) is a integer-valued square matrix $C = (C_{ij})$ with

(1) $C_{ii} = 2$ for all i,

(2) $C_{ij} \leq 0$ for all $i \neq j$,

(3) $C_{ij} = 0$ if and only if $C_{ji} = 0$.

If there exists a diagonal matrix D such that DC is symmetric, then C is called *symmetrisable*.

If Δ contains no loops, then we may uniquely associate with Δ a $\mathsf{rk} \times \mathsf{rk}$ GCM

$$C_\Delta \coloneqq 2I_{\mathsf{rk}} - \operatorname{adj}\Delta = (C_{ij})_{i,j\in\Delta_0},$$

with I_{rk} the identity matrix and $\operatorname{adj}\Delta$ the adjacency matrix of Δ. In other words, if i and j are distinct vertices in Δ then $-C_{ij}$ is the number of edges they share. By definition this is a symmetric matrix, and so there is a one-to-one correspondence between graphs without loops and symmetric generalised Cartan matrices. More generally, GCMs correspond to Dynkin diagrams, which in turn determine generalised Kac–Moody Lie algebras. In this context, asymmetric off-diagonal elements represent 'longest' roots in the systems of Section 2.3. Through the identification above, the diagram Δ is connected precisely when C_Δ is *indecomposable*, that is, there does not exist a nonempty proper subset $J \subset \Delta_0$ with $C_{ij} = 0$ for all $i \notin J$ and $j \in J$.

Example 2.2. The GCMs associated with the graphs (2.A) are

$$C_{\mathbb{K}_n} = \left(\begin{smallmatrix} 2 & -n \\ -n & 2 \end{smallmatrix}\right), \qquad C_{\mathbb{A}_2^{\text{aff}}} = \left(\begin{smallmatrix} 2 & -1 & -1 \\ -1 & 2 & -1 \\ -1 & -1 & 2 \end{smallmatrix}\right), \qquad C_{\mathbb{A}_1^{\text{hyp}}} = \left(\begin{smallmatrix} 2 & -1 & 0 \\ -1 & 2 & -2 \\ 0 & -2 & 2 \end{smallmatrix}\right).$$

Remark 2.3. We may encode the possibility of Δ having $\ell_i \geq 1$ loops at vertex $i \in \Delta_0$ by defining the corresponding diagonal to be $C_{ii} = 2 - 2\ell_i$. For example, the *loop graph*

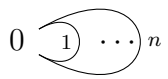

$\mathbb{L}_n$

has 1×1 GCM $C_{\mathbb{L}_n} = (2 - 2n)$. This weakens Definition 2.1(1) to requiring that C_{ii} is at most two, and is even, for all i. This more general definition of GCM was introduced by Kac in [Kac80].

In this thesis, all GCMs of interest are symmetric (trivially symmetrisable via the identity matrix), indecomposable, and have all diagonal elements being two. However, we shall see that much of the theory has generalisations to the asymmetric but symmetrisable case, discussed in Section 6.2.

§ 2.1.2 | A trichotomy of types

We now recall a ubiquitous trichotomy in mathematics, appearing in various contexts such as Lie algebras and quiver representation theory. At the level of GCMs, this starts with the following important theorem. Recall that a principal minor of C is the determinant of a principal submatrix, that is, a submatrix obtained by removing the same set of rows and columns from C.

Theorem 2.4 (Cf. [Kac90, Theorem 4.3])**.** *Each indecomposable generalised Cartan matrix C satisfies precisely one of the following:*

(1) *C is of* finite type *— all principal minors are positive.*

(2) *C is of* affine type *— all principal minors are non-negative and* $\det C = 0$.

(3) *C is of* indefinite type *— at least one principal minor is negative.*

In other words, C is of finite/affine/indefinite type if and only if it is positive definite/positive semidefinite/indefinite, respectively. The generalised Cartan matrices of finite type classify finite-dimensional complex simple Lie algebras which, through the work of Cartan and Killing, have types $\mathbb{A}$, $\mathbb{B}$, $\mathbb{C}$, $\mathbb{D}$, $\mathbb{E}$, $\mathbb{F}$, and $\mathbb{G}$.

For graphs (equivalently, symmetric GCMs), we adopt the commonly used terms from representation theory, pertinent for Chapter 3.

Definition 2.5. A connected graph Δ is *finite* (or *spherical*) if C_Δ is of finite type, *tame* (or *affine*) if C_Δ is of affine type, and *wild* if C_Δ is of indefinite type.

By Theorem 2.4, every graph Δ is either finite, tame, or wild. The connected graphs of the first type are the ubiquitous ADE diagrams

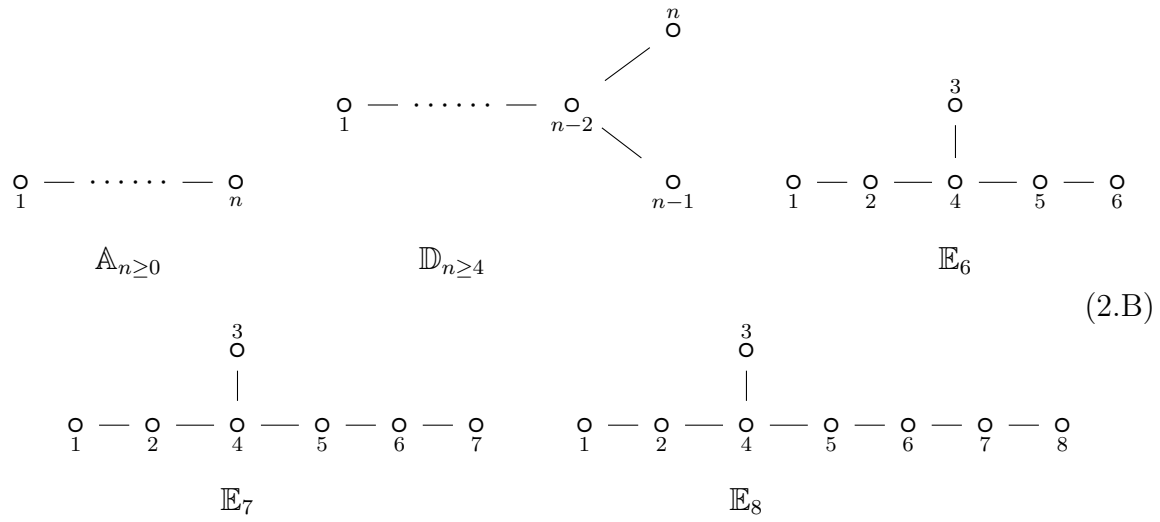

(2.B)

consisting of two infinite families and three exceptional cases. By convention, the graph $\mathbb{A}_0$ is the *empty graph* with no vertices, and $\mathbb{A}_1$ is the *trivial graph* with a single vertex and no edges. All graphs considered in this thesis derive from (2.B) in some way. The vertex indices above are those used in our computations and the code of Appendix A, but this choice is not important and we often keep it suppressed.

If we consider a 'tree' graph consisting of a central vertex and three 'arms' of length (including the central vertex) a, b, and c, then the trees satisfying $\frac{1}{a} + \frac{1}{b} + \frac{1}{c} > 1$ are precisely the graphs in (2.B). Indeed, $\mathbb{A}_n$ has arms of length $\{2, 1, n-1\}$, $\mathbb{D}_n$ has arms of length $\{2, 2, n-2\}$, and $\mathbb{E}_n$ has arms of length $\{2, 3, n-3\}$. In this way one sees that the family $\mathbb{E}_n$ cannot be continued in finite type past $\mathbb{E}_8$.

The tame graphs are also known as affine/extended ADE diagrams. They are obtained by adding an *extended vertex* 0 to the finite type graphs, namely

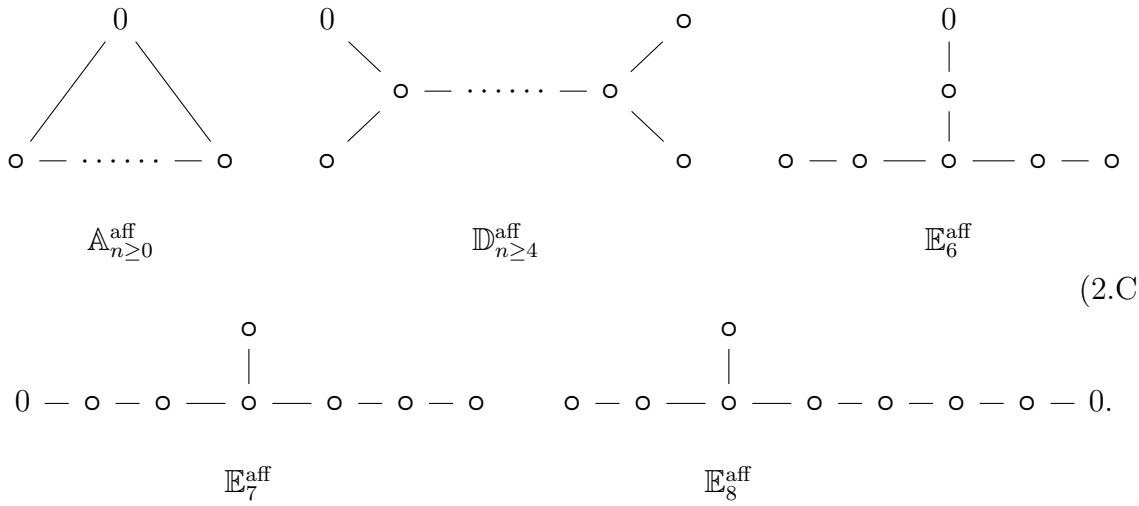

(2.C)

The graph $\mathbb{A}^{\mathrm{aff}}_0$ can be thought of as the one-loop graph $\mathbb{L}_1$, and $\mathbb{A}^{\mathrm{aff}}_1$ coincides with $\mathbb{K}_2$. Such an extension also exists for the Dynkin diagrams $\mathbb{B}_n$, $\mathbb{C}_n$, $\mathbb{F}_4$, and $\mathbb{G}_2$. The diagrams (2.C) are special in that they admit a labelling by positive integers such that twice any label is the sum of the adjacent labels. This labelling gives rise to the *minimal imaginary root* in the associated affine root system, see Section 2.3.

Example 2.6. Consider our running examples (2.A). For the Kronecker graph, we have $\det C_{\mathbb{K}_n} = 4 - n^2$, so $\mathbb{K}_1 = \mathbb{A}_2$ is finite, $\mathbb{K}_2 = \mathbb{A}^{\mathrm{aff}}_1$ is tame, and $\mathbb{K}_n$ is wild for all $n \geq 3$. The graph $\mathbb{A}^{\mathrm{aff}}_2$ appears above as one of the tame graphs, as every principal minor is either 0, 2, or 3. The graph $\mathbb{A}^{\mathrm{hyp}}_1$ is wild, which we can see by computing the full principal minor $\det C_{\mathbb{A}^{\mathrm{hyp}}_1} = -2$. However, notice that both of the wild examples are 'minimally wild', in the sense that any full proper subgraph is either finite or tame.

The above discussion motivates an *overextension* of the ADE graphs (2.B), such as $\mathbb{A}^{\mathrm{hyp}}_1$ in (2.A), as a way to study wild behaviour in the simplest case.

§ 2.2 | Hyperbolic graphs

This section is dedicated to the first step into the wild — hyperbolic type. We recall the definition of hyperbolic generalised Cartan matrices and then give a recap of the classification of hyperbolic graphs, of which there are twenty-three in ranks three to ten and four infinite families in rank one and two. We see in Section 2.3 that it is possible to explicitly describe the Tits cone (and thus the Coxeter arrangement) in the hyperbolic case, giving a distinct upshot to considering this setting. Hyperbolic graphs have appeared in the representation theory literature in the context of framed quiver varieties, for example the recent work [BCS23], from which we take the index ∞ to denote the overextended vertex.

§ 2.2.1 | Hyperbolic GCMs

Definition 2.7. A generalised Cartan matrix C is of *hyperbolic type* if it is of indefinite type, but every proper principal submatrix decomposes into GCMs of finite or affine type. If Δ is a graph and its GCM C_Δ is of hyperbolic type, then Δ is said to be *hyperbolic*.

Equivalently, a wild graph Δ is hyperbolic if all full proper subgraphs Δ' are a possibly disjoint union of tame or finite graphs, as in Definition 2.5.

Example 2.8. For $\mathsf{rk} = 2$, any generalised Cartan matrix of the form

$$C = \begin{pmatrix} 2 & -a \\ -b & 2 \end{pmatrix}$$

is hyperbolic, provided that $ab > 4$. This includes the Kronecker GCM $C_{\mathbb{K}_n}$ as the special case $a = b = n > 2$.

Example 2.9. The wild graphs $\mathbb{K}_{n\geq 3}$ and $\mathbb{A}_1^{\text{hyp}}$ of (2.A) are hyperbolic. Indeed, the only (nontrivial) full proper subgraph of the former is $\mathbb{A}_1$, and for the latter we have subgraphs $\mathbb{A}_1^{\text{aff}}$, $\mathbb{A}_2$, $\mathbb{A}_1$, and $\mathbb{A}_1 \sqcup \mathbb{A}_1 =: \mathbb{A}_1^2$.

The first rationale for the term 'hyperbolic' comes from the signature of the GCM, which later manifests itself in the associated hyperboloid quadratic form.

Lemma 2.10 ([Moo79, 1.2])**.** *If C is a $\mathsf{rk} \times \mathsf{rk}$ hyperbolic GCM, then it is nonsingular with signature $(\mathsf{rk} - 1, 1)$. In other words, C has $\mathsf{rk} - 1$ positive eigenvalues and 1 negative eigenvalue. In particular, the determinant of C is negative.*

Whilst these conditions are necessary for a generalised Cartan matrix to be of hyperbolic type, they are not sufficient, as the following example demonstrates.

Example 2.11. Consider the wild graph

$$\Delta = \quad , \qquad C_\Delta = \begin{pmatrix} 2 & -2 & 0 & -3 \\ -2 & 2 & -3 & 0 \\ 0 & -3 & 2 & -2 \\ -3 & 0 & -2 & 2 \end{pmatrix}$$

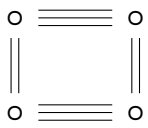

whose GCM can be readily seen to have eigenvalues -3, 1, 3, and 7. Hence C_Δ has signature $(3, 1)$ but is not hyperbolic, for example it contains $\mathbb{K}_3$ as a subgraph. If we replace each pair of vertical edges with a single edge, then $\det C_\Delta = 0$, and so there are also wild graphs with singular generalised Cartan matrices.

In the previous subsection we discussed the (finite) ADE diagrams and the (tame) extended ADE diagrams. Since the idea behind hyperbolic graphs is to be minimally wild, it is natural to expect such graphs to arise from a further extension of extended

ADE. Indeed, the *overextended* ADE diagrams

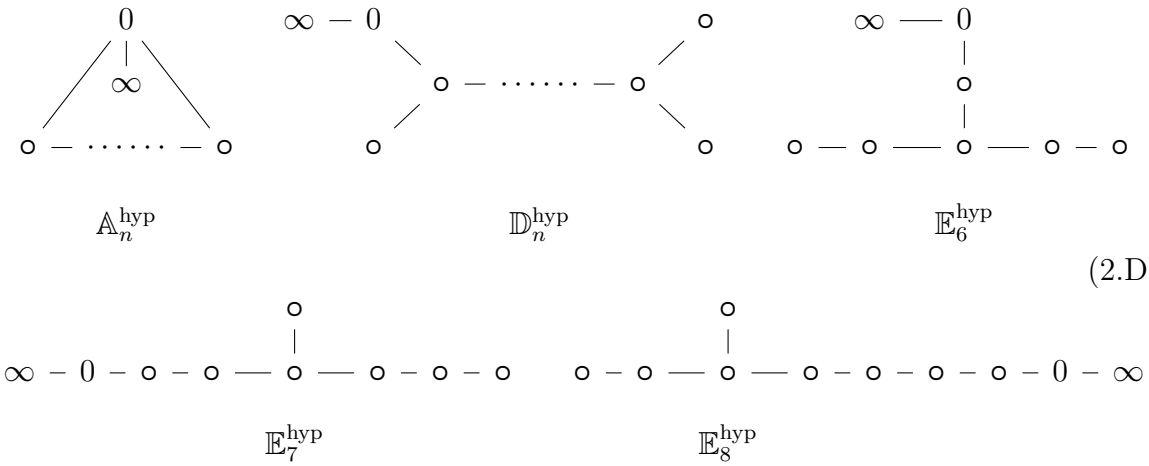

(2.D)

comprise most of the hyperbolic graphs. Perhaps surprisingly, it turns out that only finitely many of the hyperbolic graphs take the form of (2.D) above; further there are hyperbolic graphs and infinite families not of this form that arise as exceptional cases. For the overextended hyperbolic graphs, there is a relationship with the determinant of the underlying ADE graph.

Lemma 2.12. *Let C be a generalised Cartan matrix of finite type and let C^{hyp} be its hyperbolic overextension. Then $\det C^{\text{hyp}} = -\det C$. In particular, if Δ^{hyp} is an overextended ADE diagram of rank rk, then its GCM has determinant*

$$\det C_{\Delta^{\text{hyp}}} = \begin{cases} 1-\mathsf{rk} & \text{if } \Delta = \mathbb{A}_{\mathsf{rk}-2}, \\ -4 & \text{if } \Delta = \mathbb{D}_{\mathsf{rk}-2}, \\ \mathsf{rk}-11 & \text{if } \Delta = \mathbb{E}_{\mathsf{rk}-2}. \end{cases}$$

Proof. It follows from the definition of hyperbolic extension that C^{hyp} is the matrix

$$\begin{pmatrix} 2 & -1 \\ -1 & C^{\text{aff}} \end{pmatrix},$$

with all other entries zero, where C^{aff} is the affine extension of C. Computing the determinant recursively along the first row, we then have

$$\det C^{\text{hyp}} = \det \begin{pmatrix} 2 & -1 & 0 \\ -1 & 2 & -1 \\ 0 & -1 & C \end{pmatrix} = 2\det C^{\text{aff}} + \det \begin{pmatrix} -1 & -1 \\ 0 & C \end{pmatrix} = -\det C,$$

as $\det C^{\text{aff}} = 0$. A simple computation shows $\det C_{\mathbb{A}_n} = n+1$, $\det C_{\mathbb{D}_n} = 4$, and $\det C_{\mathbb{E}_n} = 9-n$, and so the second claim follows. □

§ 2.2.2 | Classification of hyperbolic graphs

The classical references [Li88, §2] and [Saç89, §3] give a classification of hyperbolic Dynkin diagrams, which include hyperbolic graphs as a special case. A more recent classification is given in [CCC+10], which fixes some errata in the original lists. For

reference, we now classify all hyperbolic graphs, a special case of the classification of hyperbolic Dynkin diagrams.

A hyperbolic GCM is said to be *compact* if every proper principal submatrix is actually of finite type. The following lemma shows that for hyperbolic graphs we never have compactness, outside of low rank.

Lemma 2.13. *Any connected hyperbolic graph of rank* $\mathsf{rk} \geq 3$ *contains a full connected affine subgraph of rank* $\mathsf{rk} - 1$.

Proof. It suffices to argue that Δ contains some full affine subgraph, as this subgraph would be contained in a full connected subgraph Δ' of rank $\mathsf{rk} - 1$, and one affine graph cannot be properly contained in another or in a finite type graph. This is easily observed from (2.C). Hence the affine subgraph must equal Δ'. Assume that every proper subgraph of Δ is finite type. Then Δ cannot contain any loops, multiple edges, or cycles, so Δ must be a tree. Since $\mathbb{D}^{\mathrm{aff}}_{n\geq 4}$ is not a subgraph, Δ can have no vertices of valency at least four and has at most one vertex of valency three. If Δ has no vertex of valency three, then $\Delta = \mathbb{A}_{\mathsf{rk}}$, a contradiction. If Δ has a single vertex of valency three, then as $\mathbb{E}^{\mathrm{aff}}_6$ is not a subgraph, there is at least one arm of length at most two (recall from Section 2.1 that this includes the branch vertex). Similarly, having no subgraph of type $\mathbb{E}^{\mathrm{aff}}_7$ (respectively $\mathbb{E}^{\mathrm{aff}}_8$) implies that Δ must contain at least one arm of length at most three (respectively five). Therefore Δ is either $\mathbb{E}_6$, $\mathbb{E}_7$, or $\mathbb{E}_8$, a contradiction. □

Next we show that there is an upper bound on the rank in hyperbolic type.

Lemma 2.14. *Let* Δ *be a connected graph of rank* rk. *If* Δ *is hyperbolic then* $\mathsf{rk} \leq 10$.

Proof. Suppose that Δ has rank $\mathsf{rk} > 10$. We specialise the proof of [Li88, Proposition 2] to the case of symmetric matrices, which considerably simplifies the types of subgraphs that can occur.

First observe that only for $\mathsf{rk} \leq 3$ is more than one edge permitted between a pair of vertices, otherwise Δ would be strictly wild, as the only tame graph with doubled edges is $\mathbb{K}_2 = \mathbb{A}^{\mathrm{aff}}_1$. If Δ contains a cycle as a subgraph, then this cycle must contain $\mathsf{rk} - 1$ vertices. Otherwise there would exist a proper subgraph which in turn contains a cycle as a proper subgraph, but no finite or tame graph has a proper affine subgraph. Then $\Delta = \mathbb{A}^{\mathrm{hyp}}_n$ for some $n \geq 9$, which contains the wild subgraph $\mathbb{E}^{\mathrm{hyp}}_8$, contradicting the fact that Δ is hyperbolic. If Δ contains a branch vertex, then it must be of the form $\mathbb{D}_4$, because otherwise Lemma 2.13 would imply that Δ itself must be $\mathbb{D}^{\mathrm{aff}}_4$.

If Δ has two branch vertices, then it must have $\mathbb{D}^{\mathrm{aff}}_{\mathsf{rk}-2}$ as an affine subgraph and hence $\Delta = \mathbb{D}^{\mathrm{hyp}}_n$ for some $n \geq 9$. As before, this has the wild subgraph $\mathbb{E}^{\mathrm{hyp}}_8$, and so Δ must have at most one branch point. In this case, Δ has the finite subgraph $\mathbb{D}_{\mathsf{rk}-1}$, but there is no way to get a hyperbolic graph from this just by adding one vertex. The only case that remains is when Δ is just a chain of vertices, but as $\mathsf{rk} > 3$, all pairs of vertices share at most one edge and this forces $\Delta = \mathbb{A}_{\mathsf{rk}}$. Thus no such hyperbolic graph can exist. □

The proof of Lemma 2.14 shows that $\mathbb{E}_8^{\text{hyp}}$ is, in a sense made precise through [Vis08], the 'largest' hyperbolic graph. Notice that $C_{\mathbb{E}_8^{\text{hyp}}}$ has signature $(9, 1)$ and determinant -1, which is the smallest magnitude possible for a hyperbolic determinant. Outwith a combinatorial argument, there is also a heuristic for this rank restriction coming from reflection groups. Indeed, the largest hyperbolic space in which a 'Coxeter simplex' can live is $\mathbb{H}^9$, see [VS93, Chapter 5, §2.3]. With this upper bound on rank and Lemma 2.13, it is relatively easy to list the hyperbolic graphs by starting with the affine graphs in ranks up to 9, and considering possible extensions.

Proposition 2.15. *If Δ is a graph of hyperbolic type, then it is either one of the overextended ADE diagrams $\mathbb{A}_{1,\dots,7}^{\text{hyp}}$, $\mathbb{D}_{4,\dots,8}^{\text{hyp}}$, $\mathbb{E}_{6,7,8}^{\text{hyp}}$ from* (2.D)*, or a member of one of the following infinite families*

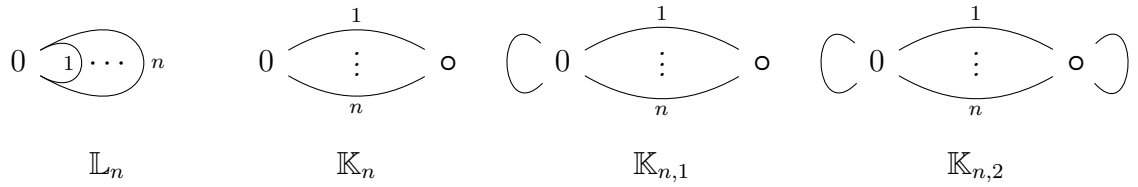

or one of the following exceptional graphs

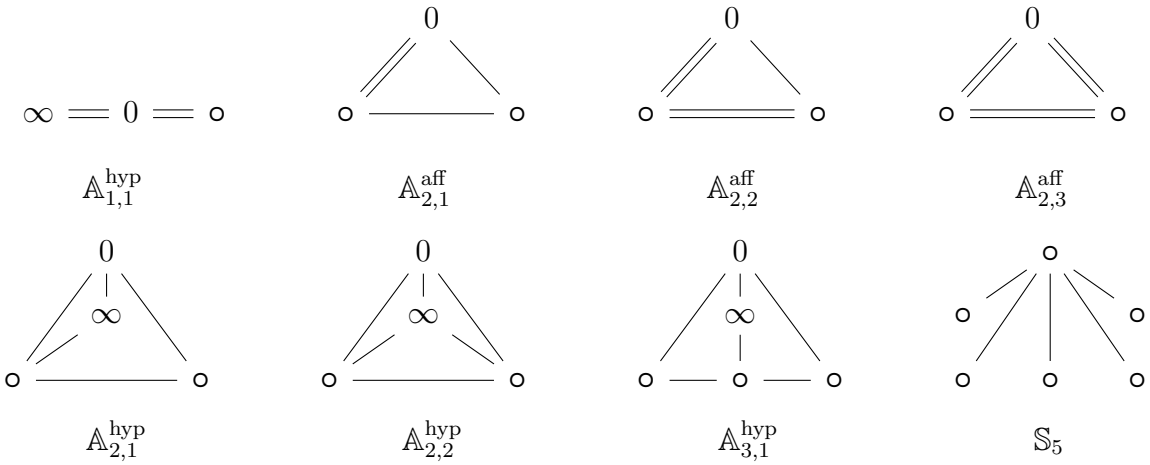

where the vertex ∞ is overextended, in the sense that the full subgraph without this node is affine ADE. Of the 23 *graphs and* 4 *infinite families in hyperbolic type,* 18 *are simply laced,* 15 *are overextended ADE,* 7 *are extended or overextended ADE with extra edges, and* 3 *contain loops.*

Proof. We proceed by rank, starting with an affine graph in rank rk or $\mathsf{rk} - 1$ and adding edges or vertices to create a hyperbolic graph. By Lemma 2.13 we only need to consider *maximal* full proper subgraphs of Δ.

(1) In rank one, consider the tame graph $\mathbb{A}_0^{\text{aff}}$, which is also the 1-loop graph $\mathbb{L}_1$. The only way to make this wild is to add more loops, obtaining $\mathbb{L}_n$ for some $n \geq 2$. This is vacuously hyperbolic because any full proper subgraph is the empty graph.

(2) In rank two, we have already seen that the n-Kronecker graph is hyperbolic for $n \geq 3$, so the only other way of getting new graphs of rank two is by adding loops. Notice that we can add at most one loop to each vertex, as otherwise there would be a subgraph of the form $\mathbb{L}_n$ for $n \geq 2$, which is wild. Since $\mathbb{L}_1$ is tame this is permitted as a subgraph, and so the options are no loops ($\mathbb{K}_n$), with one looped vertex ($\mathbb{K}_{n,1}$), and with two looped vertices ($\mathbb{K}_{n,2}$). Note that n can be any positive integer for the Kronecker graphs with loops.

(3) From rank three and above it is easy to see that Δ cannot have any loops, since no finite or affine graphs of rank two have loops. Similarly, creating any triple edges would leave a $\mathbb{K}_3$ subgraph, giving an upper bound on edge multiplicity. Hence the hyperbolic graphs in rank three are the connected graphs that have no loops, have edge multiplicity at most two, and have not already appeared as finite or affine graphs. These are $\mathbb{A}_1^{\text{hyp}}$, $\mathbb{A}_{1,1}^{\text{hyp}}$, $\mathbb{A}_{2,1}^{\text{aff}}$, $\mathbb{A}_{2,2}^{\text{aff}}$, and $\mathbb{A}_{2,3}^{\text{aff}}$.

(4) As discussed in Lemma 2.14, in rank four and above all pairs of vertices in Δ share at most one edge. Consider again the rank three extended ADE diagram $\mathbb{A}_2^{\text{aff}}$, which we overextended to obtain $\mathbb{A}_2^{\text{hyp}}$. From here it is possible to increase the incidence of the new vertex ∞, as subgraphs will all just be $\mathbb{A}_2^{\text{aff}}$ or simpler. Therefore we also have the graphs $\mathbb{A}_{2,1}^{\text{hyp}}$ and $\mathbb{A}_{2,2}^{\text{hyp}}$, where the former has two vertices connected to ∞ and the latter is the full graph on four vertices.

(5) The rank five case is very similar to rank four above, where now we overextend the tame graph $\mathbb{A}_3^{\text{aff}}$ to $\mathbb{A}_3^{\text{hyp}}$. Unlike in rank four however, we can no longer connect the overextended vertex to every other vertex, as this runs the risk of inducing a subgraph of type $\mathbb{A}_2^{\text{hyp}}$. Indeed, the only vertex that ∞ can also be connected to is the vertex not connected to original extended vertex in the tame graph, resulting in $\mathbb{A}_{3,1}^{\text{hyp}}$.

(6) In rank six, type $\mathbb{D}$ makes an appearance, so we must consider extensions of both $\mathbb{A}_4^{\text{aff}}$ and $\mathbb{D}_4^{\text{aff}}$. In type $\mathbb{A}$ the only option is the standard overextension $\mathbb{A}_4^{\text{hyp}}$, as any extra incidence on the vertex ∞ will create an $\mathbb{A}_2^{\text{hyp}}$ or $\mathbb{A}_3^{\text{hyp}}$ subgraph, and this trick is no longer possible for any graph. For $\mathbb{D}_4^{\text{aff}}$ there are two options, the first is the overextension $\mathbb{D}_4^{\text{hyp}}$ and the second is connecting an extra vertex directly to the branch point. The second case is the five-star graph $\mathbb{S}_5$, which has only two meaningfully different subgraphs in $\mathbb{A}_1$ and $\mathbb{D}_4^{\text{aff}}$.

(7) From rank seven onwards, the only viable options are the overextended graphs of the required rank. No other vertices admit extensions and the overextended vertex may only have incidence one, giving $\mathbb{A}_5^{\text{hyp}}$ and $\mathbb{D}_5^{\text{hyp}}$ for this rank.

(8) Starting at rank eight, we now also have to consider type $\mathbb{E}$, but using the above the only options are $\mathbb{A}_6^{\text{hyp}}$, $\mathbb{D}_6^{\text{hyp}}$, and $\mathbb{E}_6^{\text{hyp}}$.

(9) The argument for rank nine proceeds completely analogously to the previous case $\mathsf{rk} = 8$, which gives $\mathbb{A}_7^{\mathrm{hyp}}$, $\mathbb{D}_7^{\mathrm{hyp}}$, and $\mathbb{E}_7^{\mathrm{hyp}}$.

(10) Finally for rank ten, it remains to be shown that $\mathbb{A}_8^{\mathrm{hyp}}$ is actually strictly wild, so that the only hyperbolic graphs of maximal rank are $\mathbb{D}_8^{\mathrm{hyp}}$ and $\mathbb{E}_8^{\mathrm{hyp}}$. By deleting a vertex at the middle of the underlying $\mathbb{A}_8$, a tree subgraph occurs with branch lengths 2, 4, and 5, which is wild (indeed, it is the graph $\mathbb{E}_7^{\mathrm{hyp}}$).

By Lemma 2.14, since $\mathsf{rk} \leq 10$, we are done. □

To conclude this section, we summarise the hyperbolic graphs in the following table, in light of Proposition 2.15. The simply laced hyperbolic graphs are those with $\mathsf{rk} \geq 4$. For completion, we include the determinants of the associated GCMs, which one can compare with Lemma 2.12.

rk	Δ	#	$\det C_\Delta$
1	$\mathbb{L}_n$	$\mathbb{N}$	$2-2n$
2	$\mathbb{K}_n \quad \mathbb{K}_{n,1} \quad \mathbb{K}_{n,2}$	$3\mathbb{N}$	$4-n^2 \quad -n^2 \quad -n^2$
3	$\mathbb{A}_1^{\mathrm{hyp}} \quad \mathbb{A}_{1,1}^{\mathrm{hyp}} \quad \mathbb{A}_{2,1}^{\mathrm{aff}} \quad \mathbb{A}_{2,2}^{\mathrm{aff}} \quad \mathbb{A}_{2,3}^{\mathrm{aff}}$	5	$-2 \quad -8 \quad -8 \quad -18 \quad -32$
4	$\mathbb{A}_2^{\mathrm{hyp}} \quad \mathbb{A}_{2,1}^{\mathrm{hyp}} \quad \mathbb{A}_{2,2}^{\mathrm{hyp}}$	3	$-3 \quad -12 \quad -27$
5	$\mathbb{A}_3^{\mathrm{hyp}} \quad \mathbb{A}_{3,1}^{\mathrm{hyp}}$	2	$-4 \quad -16$
6	$\mathbb{A}_4^{\mathrm{hyp}} \quad \mathbb{D}_4^{\mathrm{hyp}} \quad \mathbb{S}_5$	3	$-5 \quad -4 \quad -16$
7	$\mathbb{A}_5^{\mathrm{hyp}} \quad \mathbb{D}_5^{\mathrm{hyp}}$	2	$-6 \quad -4$
8	$\mathbb{A}_6^{\mathrm{hyp}} \quad \mathbb{D}_6^{\mathrm{hyp}} \quad \mathbb{E}_6^{\mathrm{hyp}}$	3	$-7 \quad -4 \quad -3$
9	$\mathbb{A}_7^{\mathrm{hyp}} \quad \mathbb{D}_7^{\mathrm{hyp}} \quad \mathbb{E}_7^{\mathrm{hyp}}$	3	$-8 \quad -4 \quad -2$
10	$\mathbb{D}_8^{\mathrm{hyp}} \quad \mathbb{E}_8^{\mathrm{hyp}}$	2	$-4 \quad -1$

(2.E)

§ 2.3 | Coxeter arrangements

In this section we consider hyperplane arrangements arising associated with a GCM C, namely reflection arrangements. These arrangements are topologically determined, in the sense of the fundamental group of the complexified complement, by a Coxeter group known as the Weyl group.

§ 2.3.1 | The Weyl group

Definition 2.16. Let $C = (C_{ij})$ be a generalised Cartan matrix, and for $i \neq j$, define $m_{ij} = m_{ji}$ according to the following table

$C_{ij}C_{ji}$	0	1	2	3	≥ 4
m_{ij}	2	3	4	6	∞

.

The *Weyl* group W is generated by $\{s_i \mid C_{ii} = 2\}$ with relations

(1) $\langle s_i, s_j \rangle^{m_{ij}} = \langle s_j, s_i \rangle^{m_{ji}}$ for all $i \neq j$,

(2) $s_i^2 = 1$ for all i,

where $\langle s_i, s_j \rangle^{m_{ij}}$ is the alternating word $s_i s_j \cdots$ of length m_{ij}. The case $m_{ij} = \infty$ is interpreted to mean that there is no relation between s_i and s_j.

Note that Definition 2.16(2) implies $(s_i s_j)^{m_{ij}} = 1$ for all i, j, taking as convention $m_{ii} = 1$. A group of this form is known as a *Coxeter group*, where more generally $m_{ij} \in \{1, 2, \ldots, \infty\}$. Removing the relation Definition 2.16(2), one obtains the (Artin) braid group Br associated with C, so only the braid relations hold and there is a natural quotient map $\mathrm{Br} \twoheadrightarrow W$. The kernel of this map is the *pure braid group* PBr, giving a short exact sequence of groups

$$1 \longrightarrow \mathrm{PBr} \longrightarrow \mathrm{Br} \longrightarrow W \longrightarrow 1. \tag{2.F}$$

If we specialise Definition 2.16 to the symmetric GCM C_Δ of a graph Δ, then for all distinct $i, j \in \Delta_0$ we have $C_{ij} C_{ji} = C_{ij}^2 \in \{0, 4, 9, \ldots\}$; hence $m_{ij} \in \{2, 3, \infty\}$. This simplifies the braid relations of W_Δ to three cases, which we can visualise using the *Cayley graph* and summarise in the following table.

$\mathbb{A}_1^2$	$\mathbb{A}_2$	$\mathbb{K}_{n\geq 2}$
i — / — j	i —— j	i ≡≡ … j
$\lvert C_{ij}\rvert = 0$	$\lvert C_{ij}\rvert = 1$	$\lvert C_{ij}\rvert \geq 2$
$s_i s_j = s_j s_i$	$s_i s_j s_i = s_j s_i s_j$	$s_i s_j s_i \cdots = s_j s_i s_j \cdots$
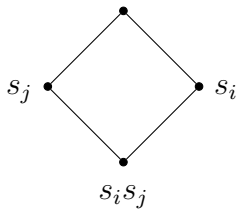	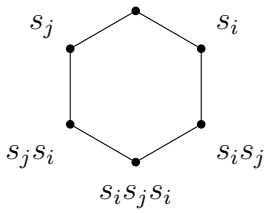	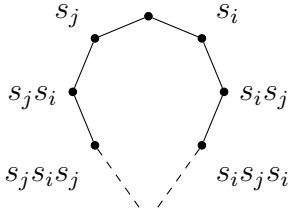

(2.G)

These three polygons occur throughout the thesis, with 8-gons, 10-gons, 12-gons, and 16-gons also appearing when we pass to intersection arrangements in Chapter 5.

Example 2.17. The running examples (2.A) have Weyl groups:

(1) $W_{\mathbb{K}_1} = \mathrm{Sym}_3$ and $W_{\mathbb{K}_{n\geq 2}} = \mathrm{Dih}_\infty$,

(2) $W_{\mathbb{A}_2^{\mathrm{aff}}} = \mathrm{Sym}_3^{\mathrm{aff}}$,

(3) $W_{\mathbb{A}_1^{\mathrm{hyp}}} = \langle s_\infty, s_0, s_1 \mid s_i^2 = 1, s_\infty s_0 s_\infty = s_0 s_\infty s_0, s_\infty s_1 = s_1 s_\infty \rangle$.

Here $\mathrm{Sym}_n^{(\mathrm{aff})}$ is the (affine) symmetric group on n symbols, and $\mathrm{Dih}_\infty = \mathrm{Sym}_2^{\mathrm{aff}}$ is the infinite dihedral group. In $W_{\mathbb{A}_1^{\mathrm{hyp}}}$, we have s_0 and s_1 generating a free subgroup due to the two edges they share in the graph.

In light of Remark 2.3, we see that the requirement $C_{ii} = 2$ in specifying the set of generators means that vertices with loops do not correspond to generators. This

means that $W_{\mathbb{L}_n}$ is trivial as it has no vertices without loops and hence has an empty generating set. Similarly the Weyl group of $\mathbb{K}_{n,1}$ is the cyclic group of order 2, with the generator corresponding to the single vertex without a loop.

In Example 2.17 the Weyl group of the graph $\mathbb{A}_1^{\text{hyp}}$ may also be described as the hyperbolic triangle group $(2, 3, \infty)$, which concisely describes the angles occurring in its Coxeter arrangement: $\frac{\pi}{2}$, $\frac{\pi}{3}$, and $\frac{\pi}{\infty} = 0$. More generally, hyperbolic triangle groups have the form (p, q, r), where $\frac{1}{p} + \frac{1}{q} + \frac{1}{r} < 1$, and there are infinitely many. See [Mag74] for more details.

Coxeter classified in [Cox34, Theorem 9] the finite Coxeter groups. These are the Weyl groups in finite type, as well as types $\mathbb{H}$ and $\mathbb{I}$ which do not arise as Weyl groups. The term *simply laced* is typically used for the case where $m_{ij} \in \{2, 3\}$ only, and it is well-known that the simply laced finite Coxeter groups are precisely the Weyl groups of the diagrams (2.B).

Theorem 2.18 (Cf. [Kac90, Proposition 4.9])**.** *The finite Weyl groups are precisely those associated with generalised Cartan matrices of finite type.*

§ 2.3.2 | Root systems

An important combinatorial and Lie theoretic structure is that of the root system, which gives rise to both the hyperplanes in the Coxeter arrangements and the Tits cone in which they live. In finite type there is a finite root system consisting of only 'real' roots, but in all other cases the set of real roots is infinite and there are also 'imaginary' roots.

Definition 2.19. If $C = (C_{ij})$ is a $\mathsf{rk} \times \mathsf{rk}$ generalised Cartan matrix, then its rk-dimensional *root lattice* is defined to be

$$V \coloneqq \bigoplus_{i \in \mathrm{row} C} \mathbb{Z}\alpha_i \cong \mathbb{Z}^{\mathsf{rk}},$$

where the basis vectors α_i are called *simple roots*.

A nonzero $v \in V$ is called *positive* if $v_i \geq 0$ for all i. If C is symmetrisable (replacing C with DC from Definition 2.1 if necessary), then V can be equipped with the symmetric bilinear *Euler form*, which is defined on the simple roots as

$$(\alpha_i, \alpha_j) \coloneqq (DC)_{ij}.$$

This form is nondegenerate if and only if $\det C \neq 0$, so extra care must be taken when trying to dualise in affine type.

Definition 2.20. Let $C = (C_{ij})$ be a symmetrisable GCM and let i be such that $C_{ii} = 2$. The *simple reflection* of $v \in V$ by $s_i \in W$ is

$$s_i v \coloneqq v - (v, \alpha_i)\alpha_i.$$

This defines a linear action of W on V, with s_i a reflection in the hyperplane orthogonal to the simple root α_i. Hence it should be no surprise that $s_i\alpha_i = -\alpha_i$ for all i and $(s_i v)_j = v_j$ for all $i \neq j$.

Example 2.21. We revisit our running examples (2.A) and see how their Weyl groups W_Δ from Example 2.17 act on $v \in V$.

(1) If $\Delta = \mathbb{K}_n$, then $V = \mathbb{Z}\alpha_0 \oplus \mathbb{Z}\alpha_1$ and

$$s_0 v = \left(\begin{smallmatrix} -v_0+nv_1 \\ v_1 \end{smallmatrix}\right), \qquad s_1 v = \left(\begin{smallmatrix} v_0 \\ nv_0-v_1 \end{smallmatrix}\right).$$

(2) If $\Delta = \mathbb{A}_2^{\text{aff}}$, then $V = \mathbb{Z}\alpha_0 \oplus \mathbb{Z}\alpha_1 \oplus \mathbb{Z}\alpha_2$ and

$$s_0 v = \begin{pmatrix} -v_0+v_1+v_2 \\ v_1 \\ v_2 \end{pmatrix}, \qquad s_1 v = \begin{pmatrix} v_0 \\ v_0-v_1+v_2 \\ v_2 \end{pmatrix}, \qquad s_2 v = \begin{pmatrix} v_0 \\ v_1 \\ v_0+v_1-v_2 \end{pmatrix}.$$

(3) If $\Delta = \mathbb{A}_1^{\text{hyp}}$, then $V = \mathbb{Z}\alpha_\infty \oplus \mathbb{Z}\alpha_0 \oplus \mathbb{Z}\alpha_1$ and

$$s_\infty v = \begin{pmatrix} -v_\infty+v_0 \\ v_0 \\ v_1 \end{pmatrix}, \qquad s_0 v = \begin{pmatrix} v_\infty \\ v_\infty-v_0+2v_1 \\ v_1 \end{pmatrix}, \qquad s_1 v = \begin{pmatrix} v_\infty \\ v_0 \\ 2v_0-v_1 \end{pmatrix}.$$

Next we wish to define root systems in V based on this W-action. A root system is an abstract collection of vectors in a finite-dimensional vector space with important geometric properties. The roots considered in the thesis are defined as the image of W applied to a 'fundamental set' in V. For real roots, the fundamental set is just the set of simple roots, but for imaginary roots we consider the set K of nonzero $v \in V$ with connected support, all entries non-negative, and $(v, \alpha_i) \leq 0$ for all i. The *support* of $v \in V$ is the graph with vertices i corresponding to $v_i \neq 0$ and an edge between $i \neq j$ if $C_{ij} \neq 0$.

Definition 2.22. Let $C = (C_{ij})$ be a symmetrisable GCM with Weyl group W. Then $\alpha \in V$ is

(1) a *real root* if there exists a simple root α_i such that $\alpha = w\alpha_i$ for some $w \in W$,

(2) an *imaginary root* if there exists $v \in \pm K$ such that $\alpha = wv$ for some $w \in W$.

Write $\mathsf{R}^{\mathsf{re}}_{(+)}$ and $\mathsf{R}^{\mathsf{im}}_{(+)}$ for the set of (positive) real and imaginary roots, respectively.

By Theorem 2.18, there are finitely many real roots if and only if C is a finite type GCM, since positive real roots are in bijection with reflections (conjugations of simple reflections) in W. Furthermore (see [Kac90, §5.2]) it is easy to see that both types of roots are integral and either positive or negative vectors, so each set of roots is a disjoint union of positive and negative roots. By [Kac90, Theorem 5.6], the root systems for indecomposable GCMs can be summarised as follows:

(Fin) There are finitely many real roots and no imaginary roots.

(Aff) There are infinitely many real roots and a ray of imaginary roots spanned by the (positive) *minimal imaginary root* δ.

(Ind) There are infinitely many real roots and a region of imaginary roots known as the *imaginary cone*.

For affine root systems, it turns out that the minimal imaginary root coincides with the vertex labelling discussed below (2.C). For example $\Delta = \mathbb{A}_2^{\text{aff}}$ has $\delta = \left(\begin{smallmatrix}1\\1\\1\end{smallmatrix}\right)$ which satisfies the property that twice any entry is the sum of its neighbours in Δ. The following Kronecker example demonstrates the above trichotomy.

Example 2.23. We continue from Example 2.21 to compute the positive roots for the graph $\mathbb{K}_n$. Since $\operatorname{supp} v$ is connected for any $v \in V \cong \mathbb{Z}^2$, the fundamental set of imaginary roots is

$$K = \{v \in V \setminus \{0\} \mid 0 \leq \tfrac{2}{n} v_0 \leq v_1 \leq \tfrac{n}{2} v_0\},$$

as $(v, \alpha_0) = 2v_0 - nv_1$ and $(v, \alpha_1) = 2v_1 - nv_0$. In the cases $n = 1$, $n = 2$, and $n = 3$, drawn in Figure 2.1 below, a direct computation shows that:

(Fin) $\mathsf{R}_+^{\text{re}} = \{\alpha_0, \alpha_1, \alpha_0 + \alpha_1\}$ and $\mathsf{R}_+^{\text{im}} = \varnothing$.

(Aff) $\mathsf{R}_+^{\text{re}} = \left\{ \binom{k}{k+1}, \binom{k+1}{k} \,\middle|\, k \in \mathbb{Z}_{\geq 0} \right\}$ and $\mathsf{R}_+^{\text{im}} = \{\binom{k}{k} \mid k \in \mathbb{Z}_{\geq 1}\}$.

(Ind) $\mathsf{R}_+^{\text{re}} = \{\binom{1}{0}, \binom{0}{1}, \binom{1}{3}, \binom{3}{1}, \binom{3}{8}, \binom{8}{3}, \ldots\}$ and R^{im} is the image of the region $\frac{2}{3} v_0 \leq v_1 \leq \frac{3}{2} v_0$ under W, which comprises a dense family of rays.

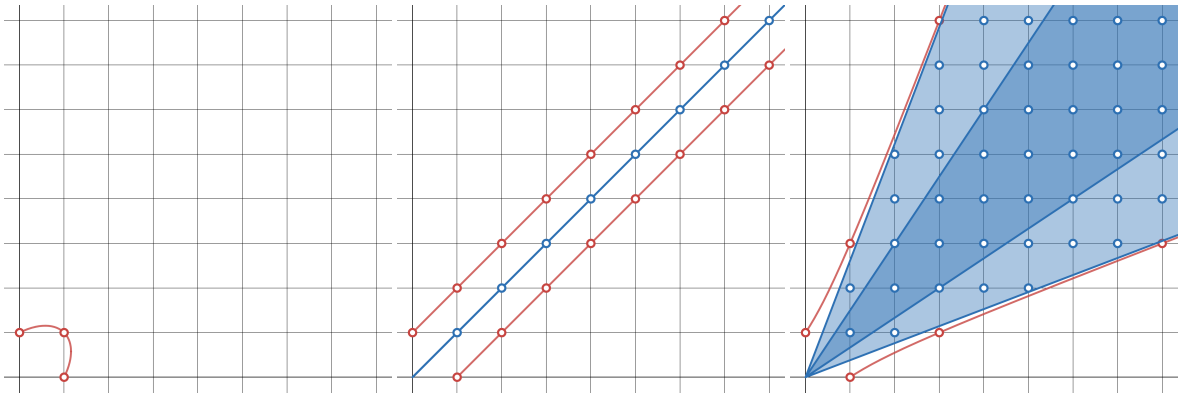

Figure 2.1: Positive roots associated with $\mathbb{K}_n$ for $n \in \{1, 2, 3\}$, with real roots in red and imaginary roots in blue. The darker region is the fundamental set of imaginary roots and the lighter region is the imaginary cone.

As Example 2.23 demonstrates, understanding root systems in the indefinite (wild) case can be difficult. We will see that hyperbolic root systems are better behaved than arbitrary wild root systems.

Definition 2.24. If $C = (C_{ij})$ is a symmetrisable GCM, then its associated Tits form is the real quadratic form

$$q \colon V \to \mathbb{R}, \qquad v \mapsto \tfrac{1}{2} v^\top (DC) v = \sum_i v_i^2 + \sum_{i>j} (DC)_{ij} v_i v_j.$$

Example 2.25. We compute the Tits form for the running examples. Notice that the type (spherical, affine, hyperbolic) of the graph agrees with the signature of the quadratic form.

(1) $q_{\mathbb{K}_n}(v) = v_0^2 - nv_0v_1 + v_1^2$. In $V \cong \mathbb{R}^2$ this is an ellipse for $n = 1$, a pair of straight lines for $n = 2$, and a hyperbola for $n \geq 3$. Compare with Example 2.23.

(2) $q_{\mathbb{A}_2^{\mathrm{aff}}}(v) = v_0^2 + v_1^2 + v_2^2 - v_0v_1 - v_0v_2 - v_1v_2$. In $V \cong \mathbb{R}^3$ this is a pair of planes.

(3) $q_{\mathbb{A}_1^{\mathrm{hyp}}}(v) = v_\infty^2 + v_0^2 + v_1^2 - v_\infty v_0 - 2v_0v_1$. In $V \cong \mathbb{R}^3$ this is a hyperboloid.

The following root criterion is the key combinatorial motivation for studying hyperbolic type.

Theorem 2.26 ([Moo79, Theorem 1])**.** *Let C be a symmetrisable GCM of either finite, affine, or hyperbolic type, and let q be its Tits form. Then*

$$\mathsf{R}^{\mathsf{re}} = \{\alpha \in V \mid q(\alpha) = 1\}, \qquad \mathsf{R}^{\mathsf{im}} = \{\alpha \in V \mid q(\alpha) \leq 0\}.$$

In other words, the Tits form can detect real and imaginary roots when we are no wilder than hyperbolic type. This allows the classical notion of *affine level* to be extended to the hyperbolic setting. Unfortunately, the inclusion $q_\Delta^{-1}(\mathbb{Z}_{\leq 0}) \supset \mathsf{R}_+^{\mathsf{im}}$ is proper in general.

Example 2.27. To see how the criterion in Theorem 2.26 does not apply for graphs 'wilder' than hyperbolic, consider the slight modification of $\mathbb{A}_1^{\mathrm{hyp}}$ given by

$$\Delta = \quad \infty \text{ —— } 0 \text{ ═══ } 1, \qquad C_\Delta = \begin{pmatrix} 2 & -1 & 0 \\ -1 & 2 & -3 \\ 0 & -3 & 2 \end{pmatrix}.$$

This contains the hyperbolic graph $\mathbb{K}_3$ as a full proper subgraph, so Δ is strictly wild, with

$$q_\Delta(v) = v_\infty^2 + v_0^2 + v_1^2 - v_\infty v_0 - 3v_0v_1.$$

This satisfies $q_\Delta(\alpha) = -1 \leq 0$ for $\alpha \coloneqq \left(\begin{smallmatrix} 4 \\ 3 \\ 2 \end{smallmatrix}\right)$. However, α is not a positive imaginary root; if it were then so would be $w\alpha$ for all $w \in W$, but we have $s_\infty \alpha = \left(\begin{smallmatrix} -1 \\ 3 \\ 2 \end{smallmatrix}\right)$ which is not positive.

§ 2.3.3 | The Tits cone

We are now ready to define Coxeter arrangements, which consist of hyperplanes dual to positive real roots. To this end, consider the real space

$$\Theta \coloneqq \mathrm{Hom}_{\mathbb{Z}}(V, \mathbb{Z}) \otimes_{\mathbb{Z}} \mathbb{R} = \bigoplus \mathbb{R}\alpha_i^*,$$

where the α_i^* comprise the dual basis. This is often called the space of *stability parameters*. There is a canonical pairing $\langle -, - \rangle \colon \Theta \times V \to \mathbb{R}$, and the action of W on V induces the contragredient action on Θ, defined for $w \in W$ and $\vartheta \in \Theta$ by

$$w\vartheta \coloneqq \langle \vartheta, w^{-1} - \rangle \colon V \to \mathbb{R}.$$

Definition 2.28. Let C be a symmetrisable GCM and let α be a positive real root within its root system. Then the *root hyperplane* corresponding to α is

$$H_\alpha \coloneqq \{\vartheta \in \Theta \mid \langle \vartheta, \alpha \rangle = 0\} \subset \Theta.$$

If $\alpha = \alpha_i$ is a simple root, we write $H_i \coloneqq H_{\alpha_i} = \{\vartheta \in \Theta \mid \vartheta_i = 0\}$. The *Coxeter arrangement* associated with C is the collection

$$\mathcal{H} \coloneqq \bigcup_{\alpha \in \mathsf{R}^{\mathsf{re}}_+} H_\alpha \subseteq \Theta.$$

Due to the existence of imaginary roots, the Coxeter arrangement does not always fill the space Θ.

Definition 2.29. The *Tits cone* associated with a symmetrisable GCM C is

$$\mathsf{TC} \coloneqq \bigcup_{w \in W} w\overline{\Theta_+},$$

where $\Theta_+ \coloneqq \{\vartheta \in \Theta \mid \langle \vartheta, \alpha_i \rangle > 0 \text{ for all } i\} \subset \Theta$ is the positive orthant known as the *standard (Weyl) chamber* and $\overline{\Theta_+}$ is its real closure.

The fact that the Coxeter arrangement $\mathcal{H}$ is contained in TC is immediate from the contragredient action of W on Θ. The *real complement* $\mathsf{TC} \backslash \mathcal{H}$ is thus a collection of connected components known as *chambers*, and it is well-known (see, for example [Hal13, Propositions 8.23 and 8.27]) that W acts simply transitively on the set of chambers.

Proposition 2.30 ([Kac83, §3])**.** *The Tits cone is a convex cone in* Θ*, and the standard chamber is a fundamental domain for the action of* W *on* TC*. Furthermore,* $\mathsf{TC} = \Theta$ *if and only if* C *is finite type, and if* C *is of affine type then* $(\mathsf{TC} \cup -\mathsf{TC}) \backslash \{0\} = \Theta \backslash H_\delta$*.*

§ 2.3.4 | The real level

The characterisation of roots given in Theorem 2.26 can be dualised to obtain an explicit description of the Tits cone in the hyperbolic case. First, consider the dual Tits form

$$q^* \colon \Theta \to \mathbb{R}, \qquad \vartheta \mapsto \tfrac{1}{2}\vartheta^\top (\operatorname{Adj} C)\vartheta,$$

where $\operatorname{Adj} C$ is the adjugate matrix. We use $\operatorname{Adj} C$ instead of C^{-1} so that q^* is well-defined even in affine type where C is singular. Then the result [Kac90, 5.10.2] says that

$$\mathsf{TC} \cup -\mathsf{TC} = \{\vartheta \in \Theta \mid q^*(\vartheta) \geq 0\}$$

in finite, affine, or hyperbolic type. If we take a level set of this expression (say, $\{q^*(\vartheta) = 1\}$), then it is possible to slice the Tits cone and hence the Coxeter arrangement. This retains all of the same combinatorial information, due to W acting simply transitively, but in one dimension less. This allows for easier visualisation of $\mathcal{H}$.

Definition 2.31. Let $C = (C_{ij})$ be a $\mathsf{rk} \times \mathsf{rk}$ symmetrisable GCM of finite, affine, or hyperbolic type. Then the (upper) *real level* is the set

$$\mathsf{Level} := \left\{ \vartheta \in \mathsf{TC} \;\middle|\; \sum\nolimits_{i \in \Delta_0} \vartheta_i \geq 0,\ q^*(\vartheta) = 1 \right\}.$$

Example 2.32. We draw the Coxeter arrangement for $\mathbb{K}_n$ in the cases $n = 1$, $n = 2$, and $n = 3$, giving a picture dual to Example 2.23. In the latter two cases, this is asymptotically parallel to the Tits cone, which has slopes

$$m_n^{\pm 1} := \frac{n \pm \sqrt{n^2 - 4}}{2},$$

a value that we call the *Kronecker constant* and satisfies $m_n + m_n^{-1} = n$.

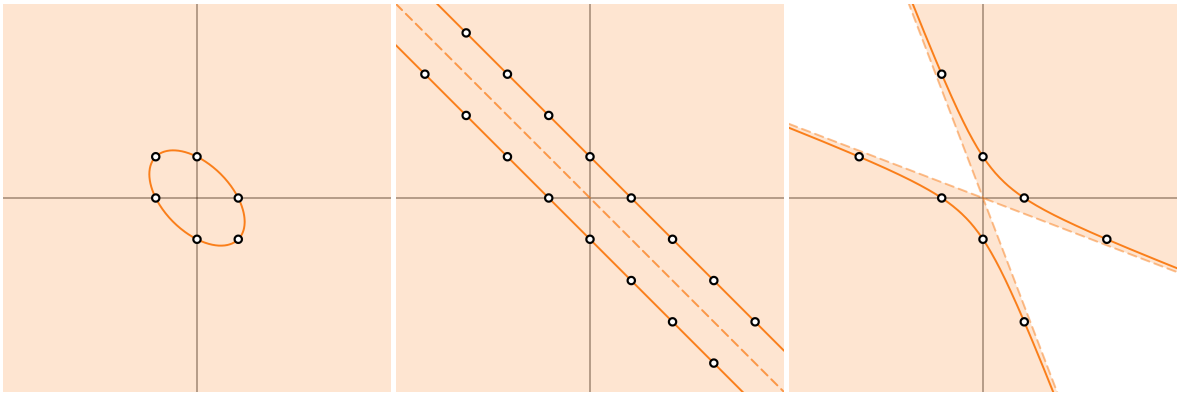

Figure 2.2: Tits cone for $\mathbb{K}_n$ in the cases $n = 1$, $n = 2$, and $n = 3$. Shaded region is $\mathsf{TC} \cup -\mathsf{TC}$, dotted line is its boundary, and solid line is Level satisfying $q(\vartheta) = \vartheta_0^2 + n\vartheta_0\vartheta_1 + \vartheta_1^2 = 1$. Link to `Desmos` interactive version.

If C is a hyperbolic GCM, then $\det C \neq 0$ by Lemma 2.10 and we may equivalently use C^{-1} to define q^*. In this case $\mathsf{Level} \cup -\mathsf{Level}$ is the preimage of -1, which is a hyperboloid in Θ and is the same as Definition 2.31 after rescaling. It turns out that Level generalises the classical notion of the *affine level* $H_\delta + \mathbb{Z}$, which under translation sweeps out TC, to the hyperbolic setting despite lacking a minimal imaginary root.

Proposition 2.33. *Let C be a symmetrisable GCM of affine type and let q^* be its dual Tits form. Then for all $\vartheta \in \Theta$ we have*

$$q^*(\vartheta) = \det(C^{\mathrm{fin}}) \langle \vartheta, \delta \rangle^2,$$

where C^{fin} is the underlying finite type GCM.

Proof. Without loss of generality (using symmetrisability), we may assume that C is symmetric. By definition $C \operatorname{Adj} C = (\det C) I = 0$, so $(\operatorname{Adj} C)\vartheta$ is in the nullspace of C for all $\vartheta \in \Theta$. By [Hum90, §2.6], the nullspace of an affine type GCM is

$$\{\alpha \in V \otimes_{\mathbb{Z}} \mathbb{R} \mid \alpha^\top C \alpha = 0\} = \mathbb{R}\{\delta\},$$

so it follows that $(\operatorname{Adj} C)\vartheta = a_\vartheta \delta$ for some $a_\vartheta \in \mathbb{R}$. Then, for all $\eta \in \Theta$,

$$\eta^\top (\operatorname{Adj} C)\vartheta = a_\vartheta \langle \eta, \delta \rangle = a_\eta \langle \vartheta, \delta \rangle = \vartheta^\top (\operatorname{Adj} C)\eta,$$

follows from the fact that C is symmetric. Taking $\eta = (1, 0, \dots, 0)$ gives the result, since by definition of the adjugate matrix we have

$$q^*(1, 0, \dots, 0) = (\operatorname{Adj} C)_{00} = \det(C^{\mathrm{fin}}). \qquad \square$$

Whilst $\mathcal{H}$ is a (generally infinite) collection of linear hyperplanes, the intersection $\mathcal{H} \cap \mathsf{Level}$ is a locally finite non-linear arrangement. In affine or hyperbolic type we thus abuse notation and redefine the Coxeter arrangement as

$$\mathcal{H} \coloneqq \bigcup_{\alpha \in \mathsf{R}^{\mathsf{re}}_+} H_\alpha \cap \mathsf{Level}.$$

However, this is not too dangerous as the Cayley graph of W is still the dual graph to $\mathcal{H}$. We call the connected components of $\mathsf{Level} \backslash \mathcal{H}$ *alcoves*, denoting their set by Alc.

Definition 2.34. The connected component $A_+ \coloneqq \Theta_+ \cap \mathsf{Level} \subseteq \mathsf{Level} \backslash \mathcal{H}$ is called the *standard alcove* in the Coxeter arrangement.

We finish this section by considering the rank three hyperbolic Coxeter arrangements, since they demonstrate how one can use the the real level to view hyperbolic Coxeter arrangements in $\mathbb{H}^2$.

Example 2.35. Suppose that Δ is a hyperbolic graph of rank three, which by Proposition 2.15 is either $\mathbb{A}_1^{\mathrm{hyp}}$, $\mathbb{A}_{1,1}^{\mathrm{hyp}}$, $\mathbb{A}_{2,1}^{\mathrm{aff}}$, $\mathbb{A}_{2,2}^{\mathrm{aff}}$, or $\mathbb{A}_{2,3}^{\mathrm{aff}}$. Then, via a change of coordinates, Level_Δ takes the form of the standard two-sheeted hyperboloid in $\mathbb{R}^3$. Our running example $\Delta = \mathbb{A}_1^{\mathrm{hyp}}$ has dual Tits form

$$q^*_\Delta(\vartheta) = 2\vartheta_0^2 + \tfrac{3}{2}\vartheta_1^2 + 2\vartheta_\infty\vartheta_0 + 2\vartheta_\infty\vartheta_1 + 4\vartheta_0\vartheta_1,$$

computed using $\operatorname{Adj} C_\Delta$. Using the eigenvalues 2, $2 + \sqrt{5}$, and $2 - \sqrt{5}$ of C_Δ we may diagonalise this to obtain

$$-\eta_\infty^2 + \eta_0^2 + \eta_1^2 = -1. \tag{2.H}$$

Applying this change of coordinates to the real root hyperplanes H_α and intersecting the hyperplanes with the above hyperboloid yields a collection of curves, which may be stereographically projected onto the unit disc via the point $(0, 0, -1)$ on the bottom sheet. In this way we can view the Coxeter arrangement in the Poincaré disc model of the hyperbolic plane. In other words, $\mathsf{Level}_\Delta \cong \mathbb{H}^2$, and each $A \in \mathsf{Alc}$ is a hyperbolic triangle with angles $(\frac{\pi}{2}, \frac{\pi}{3}, 0)$. See Section 5.2 for computational details. Each intersection $H_\alpha \cap \mathsf{Level}_\Delta$ corresponds to a geodesic in the Poincaré disc, and all five cases are

drawn below with their descriptions as hyperbolic triangle groups.

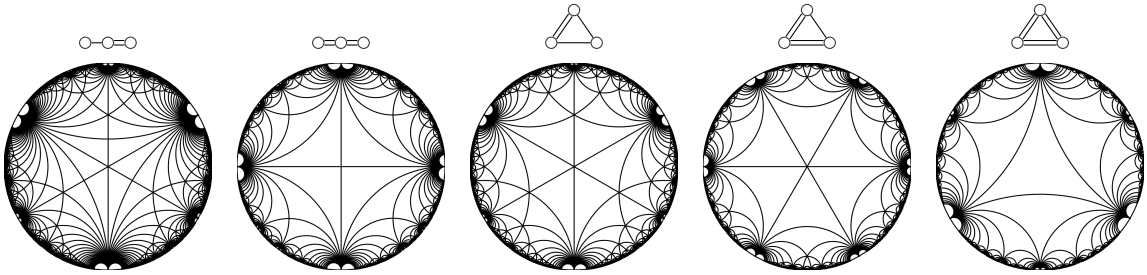

$(2,3,\infty)$ $(2,\infty,\infty)$ $(3,3,\infty)$ $(3,\infty,\infty)$ (∞,∞,∞)

Furthermore, the Cayley graph of W_Δ can be seen as the dual graph of $\mathcal{H}_\Delta$, as the 'faces' corresponding to ∞-gons lie on the boundary of the disc, which is not in $\mathbb{H}^2$.

This identification of hyperbolic Coxeter arrangements with an arrangement in the Poincaré disc also holds for higher-rank cases, and provides justification for the term 'hyperbolic arrangement'. Indeed, the Tits cone acts as the 'light cone' to the hyperbolic level and every geodesic in the Poincaré ball model corresponds to the intersection of a linear hyperplane with the unit hyperboloid one dimension higher. We refer the reader to [CFKP97] for more details on the hyperbolic geometry.

§ 2.4 | Arrangement groupoids

We finish the chapter by associating a combinatorial groupoid to $\mathcal{H}_\Delta$, the *arrangement groupoid*, which captures codimension two information. We borrow terminology and notation from [AW22] and [Del10]. Henceforth, let Δ be a finite connected graph of affine or hyperbolic type and let W_Δ and $\mathcal{H}_\Delta$ be its Weyl group and Coxeter arrangement, respectively.

Definition 2.36. A small category $\mathcal{C}$ is a *groupoid* if every morphism is invertible.

§ 2.4.1 | Coxeter consequences

The data (W_Δ, Δ_0) from Definition 2.16 is an example of a *Coxeter system* (W, S), that is a Coxeter group together with a chosen set of generators. As a result, we may apply fundamental results from Coxeter theory, following the standard reference [BB05].

Definition 2.37. Let (W, S) be a Coxeter system. Then each 'word' $w \in W$ can be expressed as $w = s_\ell \cdots s_1$ with $s_i \in S$. If ℓ is minimal amongst all such expressions for w then $s_\ell \cdots s_1$ is *reduced*. In this case, $\ell = \ell(w)$ is called the *length* of w.

This idea is important to us as we are interested in 'minimal positive paths' between regions in a hyperplane arrangement, which correspond to reduced expressions for words in the Weyl group.

Example 2.38. Recall Example 2.17. In $W_{\mathbb{A}_2^{\text{aff}}} = \text{Sym}_3^{\text{aff}}$ the word $w = s_1 s_2 s_1 s_0 s_2 s_0$ has reduced expression $s_2 s_1 s_0 s_2$, and so $\ell(w) = 4$. In the 'free' setting $W_{\mathbb{K}_{n\geq 2}} = \text{Dih}_\infty$, the lack of braid relations means that every reduced expression is unique.

In general $w \in W$ may admit more than one reduced expression. The *word property* for Coxeter groups, due to Matsumoto, explains the relationship between different reduced expressions.

Theorem 2.39 ([Mat64])**.** *Let (W, S) be a Coxeter system. Then any two reduced expressions for $w \in W$ are connected by a finite sequence of braid moves in W, that is, replacements of the form $\langle s_i, s_j \rangle^{m_{ij}} \longleftrightarrow \langle s_j, s_i \rangle^{m_{ji}}$.*

Another useful notion from Coxeter theory is the weak (left/right) Bruhat order, a partial order on Coxeter systems which says that two words are comparable if one word is a suffix/prefix of the other.

Definition 2.40. Let (W, S) be a Coxeter system and let $w, x \in W$. Then $x \leq_L w$ in the *(weak left) Bruhat order* if and only if there exist $s_1, \ldots, s_k \in S$ such that

$$w = s_k s_{k-1} \cdots s_1 x$$

with $\ell(w) = \ell(x) + k$. In other words, some reduced expression for w has a reduced expression for x as a final substring. The right Bruhat order $\leq_R$ is defined similarly.

The Bruhat order on W gives rise to the simplest example of a direction on alcoves, which we prove in Section 4.2.

Example 2.41. Continuing Example 2.38, in $W_{\mathbb{A}_2^{\text{aff}}} = \text{Sym}_3^{\text{aff}}$, we have

$$s_1 s_2 \leq_L s_0 s_1 s_2 s_1 = s_0 s_2 s_1 s_2$$

in the Bruhat order.

If $\mathbf{\Delta}$ is finite type, then W_Δ is a finite group by Theorem 2.18, and hence must have a unique *longest element* w_Δ in the sense of Definition 2.37. Such a graph $\mathbf{\Delta}$ also admits a *Dynkin involution*, the unique graph automorphism ι_Δ such that for all $i \in \mathbf{\Delta}_0$

$$w_\Delta s_i w_\Delta = s_{\iota_\Delta(i)}. \tag{2.I}$$

We summarise this below, giving only the length of w_Δ, but explicit expression can be found in [BKOP14, Table 1]. As in [IW, (1.2.B)], ! denotes the unique nontrivial involution of $\mathbf{\Delta}$.

$\mathbf{\Delta}$	$\mathbb{A}_n$	$\mathbb{D}_{2n}$	$\mathbb{D}_{2n+1}$	$\mathbb{E}_6$	$\mathbb{E}_7$	$\mathbb{E}_8$
$\ell(w_\Delta)$	$\frac{n(n+1)}{2}$	$n(n-1)$	$n(n-1)$	36	63	120
ι_Δ	!	id	!	!	id	id

. (2.J)

The data in (2.J) is important for the local wall-crossing rules of Section 5.1.

§ 2.4.2 | Arrangement groupoids

Definition 2.42. The *free category* (or *Deligne quiver*) $\text{Free}\,\mathcal{H}_\Delta$ is the freely generated category with objects Alc_Δ and morphisms generated by the wall-crossing pairs $(A \to B, B \to A)$, whenever $A, B \in \mathsf{Alc}_\Delta$ are adjacent.

Note that in $\operatorname{Free}\mathcal{H}_\Delta$ the morphisms $A \to B$ and $B \to A$ are *not* inverse to each other. A concatenation of morphisms β is called a *(positive) path*, and we say that such a path is *minimal* if it doesn't cross the same hyperplane twice. Since $\mathcal{H}_\Delta$ is locally finite, this is the same ([Sal87, Lemma 2]) as $\beta\colon A_1 \to A_2$ having minimal length among all paths between the alcoves A_1 and A_2.

An *atom* is a minimal path of length one, which for a fixed source we may identify with the generators s_i of W_Δ. This is possible because if $A = wA_+$ is an alcove, then its walls are the hyperplanes $H_{w\alpha_i}$ for $i \in \Delta_0$, and a neighbouring alcove is of the form $B = ws_iA$. This formalises the idea that the Cayley graph lives on the Coxeter arrangement.

Definition 2.43. The *(positive) path category* is $\operatorname{Path}\mathcal{H}_\Delta \coloneqq \operatorname{Free}\mathcal{H}_\Delta/\!\sim$, where $\sim$ is the smallest equivalence relation (compatible with morphism composition) that identifies minimal positive paths.

Since W_Δ acts simply transitively on Alc_Δ, for all $A \in \mathsf{Alc}_\Delta$ there exists a unique $w \in W_\Delta$ such that $A = wA_+$. In general, there are multiple reduced expressions for w, but Theorem 2.39 shows that they differ by a finite sequence of braid relations, which is codimension two information. The relations above are generated by polygon face relations, namely the two shortest path around the polygon are identified.

Definition 2.44 ([Del72, (1.25)])**.** The *arrangement groupoid* of $\mathcal{H}_\Delta$ is the groupoid completion $\mathcal{G}_\Delta$ of $\operatorname{Path}\mathcal{H}_\Delta$. This simply means that every morphism in $\operatorname{Path}\mathcal{H}_\Delta$ is formally inverted.

Definition 2.45. The *complexification* of a hyperplane $H \subseteq \Theta$ is the hyperplane $H^{\mathbb{C}} \subseteq \Theta^{\mathbb{C}} \coloneqq \Theta \otimes_{\mathbb{R}} \mathbb{C}$ having the same equation as H. In other words, $\Theta^{\mathbb{C}} = \Theta \oplus \Theta$ equipped with complex scalar multiplication $(a + bi)(\vartheta, \eta) \coloneqq (a\vartheta - b\eta, b\vartheta + a\eta)$.

The topological space $\Theta^{\mathbb{C}} \setminus \mathcal{H}_\Delta^{\mathbb{C}}$ now contains holes as the complexified hyperplanes are in codimension two. This creates monodromy, which in the real picture we can encode as a choice of going under or over a particular wall by moving a dimension higher. A well-known fact (see, for example, [Par00, §2.1]) is that for all $A \in \mathsf{Alc}_\Delta$ and $\vartheta \in A$ there is an isomorphism

$$\operatorname{End}_{\mathcal{G}_\Delta} A \cong \pi_1(\mathsf{Level}_\Delta^{\mathbb{C}} \setminus \mathcal{H}_\Delta^{\mathbb{C}}, \vartheta) =: \operatorname{PBr}_\Delta, \tag{2.K}$$

where the left hand side is called the *vertex group* and the right hand side is the *pure braid group*.

Definition 2.46 ([Sal87, Part One])**.** The *Salvetti complex* $\operatorname{Sal}\mathcal{H}_\Delta$ is a CW complex which is a W_Δ-equivariant homotopy model for $\mathsf{Level}_\Delta \setminus \mathcal{H}_\Delta$. The 1-skeleton of this complex is $\operatorname{Free}\mathcal{H}_\Delta$, and there is a 2-cell for each pair (F, A), where F is a flat and $A \in \mathsf{Alc}_\Delta$ is adjacent to F. The attaching map identifies the two minimal positive paths from A to B, the alcove opposite across the flat F.

The Salvetti complex allows us to formally reduce the data of the Coxeter arrangement to its codimension two information, useful in Section 4.2.

Chapter 3

Homological preliminaries

With the combinatorial aspects of the work established, this chapter gives the required background on stability conditions, preprojective algebras, nilpotent modules, and mutation functors. In particular, we discuss the main category of interest $\mathcal{D}_\Delta$, connecting it with $\mathcal{H}_\Delta$ using tilting theory.

§ 3.1 | Stability conditions

We recall the work of Bridgeland [Bri07] defining stability conditions on triangulated categories, and then give Anno, Bezrukavnikov, and Mirković's notion of real variation of stability conditions. Recall that a triangulated category is an additive category $\mathcal{D}$ equipped with an autoequivalence [1], known as the *shift functor*, along with a class of *distinguished triangles*

$$X \xrightarrow{f} Y \xrightarrow{g} Z \xrightarrow{h} X[1]$$

satisfying certain axioms, which we do not recall here. See [KS06] for these and further details. For $X \in \mathcal{D}$ and $k \in \mathbb{Z}$ it is common to write $X[k] \coloneqq [1]^k X$.

The triangulated categories studied in this thesis will all be full subcategories of $\mathrm{D}^{\mathrm{b}}(\mathcal{A})$, the bounded derived category of an abelian category $\mathcal{A}$. This is the localisation of the homotopy category $\mathrm{K}^{\mathrm{b}}(\mathcal{A})$ of (bounded) cochain complexes, with respect to quasi-isomorphisms. The objects in this category are (bounded) cochain complexes of objects in $\mathcal{A}$ and morphisms $X \to Y$ are equivalence classes $[E^\bullet, q, f]_{\mathcal{A}}$ of 'roof diagrams'

$$\begin{array}{ccc} & E^\bullet & \\ {\scriptstyle q}\swarrow & & \searrow{\scriptstyle f} \\ X & & Y, \end{array} \tag{3.A}$$

where q is a quasi-isomorphism and two such morphisms are equivalent if there exists a common 'overroof'. The exact triangles in $\mathrm{D}^{\mathrm{b}}(\mathcal{A})$ are precisely the triangles that are isomorphic to

$$X \xrightarrow{f} Y \longrightarrow \operatorname{Cone} f \longrightarrow X[1]$$

for some chain map f.

§ 3.1.1 | t-structures

A key concept in the theory of triangulated categories is that of a t-structure, a way to abstract the properties of $\mathrm{D}^{\mathrm{b}}(\mathcal{A})$, introduced in [BBD82]. This is a core part of stability conditions, and relating different t-structures using combinatorial approaches provides an effective way to understand categories like the derived category of a nonnoetherian preprojective algebra in Section 3.2.

Definition 3.1. A *t-structure* on a triangulated category $\mathcal{D}$ is a pair of full subcategories $(\mathcal{D}^{\leq 0}, \mathcal{D}^{\geq 0})$, the *aisle* and *coaisle*, satisfying

(1) $\mathrm{Hom}_{\mathcal{D}}(\mathcal{D}^{\leq 0}, \mathcal{D}^{\geq 0}[-1]) = 0$,

(2) $\mathcal{D}^{\leq 0}[1] \subseteq \mathcal{D}^{\leq 0}$ and $\mathcal{D}^{\geq 0}[-1] \subseteq \mathcal{D}^{\geq 0}$,

(3) for all $D \in \mathcal{D}$ there exists a triangle $X \to D \to Y \to X[1]$ with $X \in \mathcal{D}^{\leq 0}$ and $Y \in \mathcal{D}^{\geq 0}[-1]$.

The *heart* of a t-structure is $\mathcal{D}^{\heartsuit} \coloneqq \mathcal{D}^{\leq 0} \cap \mathcal{D}^{\geq 0}$, and a t-structure is said to be *bounded* if $\mathcal{D} = \bigcup_{\ell,m\in\mathbb{Z}} \mathcal{D}^{\leq 0}[\ell] \cap \mathcal{D}^{\geq 0}[m]$.

If we write $\mathcal{T} \coloneqq \mathcal{D}^{\leq 0}$ then it follows that

$$\mathcal{D}^{\geq 0}[-1] = \{X \in \mathcal{D} \mid \mathrm{Hom}_{\mathcal{D}}(\mathcal{T}, X) = 0\} =: \mathcal{T}^{\perp},$$

so any t-structure is determined solely by its aisle. The heart $\mathcal{A} = \mathcal{T} \cap \mathcal{T}^{\perp}[1]$ is an abelian category by [BBD82, Théorème 1.3.6], and if $\mathcal{T}$ is the aisle of a *bounded* t-structure then it is recovered by its heart via the extension closed subcategory $\langle \mathcal{A}[\geq 0] \rangle = \mathcal{T}$.

Example 3.2. If $\mathcal{A}$ is an abelian category then the *standard t-structure* on the triangulated category $\mathrm{D}^{\mathrm{b}}(\mathcal{A})$ has aisle and coaisle

$$\mathcal{D}^{\leq 0} \coloneqq \{X \in \mathrm{D}^{\mathrm{b}}(\mathcal{A}) \mid H^{>0}(X) = 0\}, \qquad \mathcal{D}^{\geq 0} \coloneqq \{X \in \mathrm{D}^{\mathrm{b}}(\mathcal{A}) \mid H^{<0}(X) = 0\},$$

respectively. It is easy to see that this t-structure is bounded and has heart $\mathcal{A}$.

However, not all t-structures satisfy $\mathrm{D}^{\mathrm{b}}(\mathcal{D}^{\heartsuit}) = \mathcal{D}$, a useful property which we capture in the following.

Definition 3.3 (Cf. [Woo10, §2.1])**.** Let $\mathcal{A}$ be the heart of a bounded t-structure in a triangulated category $\mathcal{D}$. Then $\mathcal{A}$ is called *faithful* if the inclusion $\mathcal{A} \subset \mathcal{D}$ induces an equivalence of triangulated categories $F\colon \mathrm{D}^{\mathrm{b}}(\mathcal{A}) \to \mathcal{D}$, called the *realisation functor*.

In full generality, such a realisation functor may not even exist, requiring additional structure on $\mathcal{D}$ known as an *f-category*, introduced in [Bei87, §A]. However $\mathcal{D} = \mathrm{D}^{\mathrm{b}}(\mathcal{A})$ admits a canonical f-category structure and hence for each t-structure there exists a canonical realisation functor.

Abstracting Example 3.2, any t-structure $(\mathcal{D}^{\leq 0}, \mathcal{D}^{\geq 0})$ on $\mathcal{D}$ with heart $\mathcal{A}$ induces *truncation functors*

$$\tau_{\mathcal{A}}^{\leq 0} \colon \mathcal{D} \to \mathcal{D}^{\leq 0}, \qquad \tau_{\mathcal{A}}^{\geq 0} \colon \mathcal{D} \to \mathcal{D}^{\geq 0},$$

the right and left adjoints to the inclusions $\iota^{\leq 0} \colon \mathcal{D}^{\leq 0} \hookrightarrow \mathcal{D}$ and $\iota^{\geq 0} \colon \mathcal{D}^{\geq 0} \hookrightarrow \mathcal{D}$, respectively. In particular, every triangle in $\mathcal{D}$ is isomorphic to one of the form

$$\tau_{\mathcal{A}}^{\leq 0} X \longrightarrow X \longrightarrow \tau_{\mathcal{A}}^{\geq 0} X[-1] =: \tau_{\mathcal{A}}^{\geq 1} X \longrightarrow \tau_{\mathcal{A}}^{\leq 0} X[1]. \tag{3.B}$$

See [Mil, §4.1.2] for further details.

Definition 3.4. Let $\mathcal{A}$ be the heart of a bounded t-structure on a triangulated category $\mathcal{D}$. Then the k-th *cohomology functor* is defined

$$H_{\mathcal{A}}^k(-) \colon \mathcal{D} \to \mathcal{A}, \qquad X \mapsto \tau_{\mathcal{A}}^{\leq 0} \tau_{\mathcal{A}}^{\geq 0} X[k].$$

In the case of the standard t-structure on $\mathcal{D} = \mathrm{D}^{\mathrm{b}}(\mathcal{A})$, the above functors and their shifts reduce to the well-known 'good' truncation functors and the usual notion of cohomology for complexes $E^\bullet$, defined as below:

$$\begin{array}{ccccccccc}
\cdots & \longrightarrow & E^{m-1} & \longrightarrow & \ker d^m & \longrightarrow & 0 & \longrightarrow & \cdots \\
 & & \downarrow & & \downarrow & & \downarrow & & \\
\cdots & \longrightarrow & E^{m-1} & \xrightarrow{d^{m-1}} & E^m & \xrightarrow{d^m} & E^{m+1} & \longrightarrow & \cdots \\
 & & \downarrow & & \downarrow & & \downarrow & & \\
\cdots & \longrightarrow & 0 & \longrightarrow & \operatorname{coker} d^{m-1} & \longrightarrow & E^{m+1} & \longrightarrow & \cdots
\end{array} \qquad \begin{array}{c} \tau^{\leq m} E^\bullet \\ \downarrow \\ E^\bullet \\ \downarrow \\ \tau^{\geq m} E^\bullet. \end{array}$$

The cohomology of the above complexes is useful when inducting on length of bounded complexes, as

$$H^k(\tau^{\leq m} E^\bullet) = \begin{cases} H^k(E^\bullet) & \text{if } k \leq m, \\ 0 & \text{otherwise,} \end{cases} \qquad H^k(\tau^{\geq m} E^\bullet) = \begin{cases} H^k(E^\bullet) & \text{if } k \geq m, \\ 0 & \text{otherwise.} \end{cases} \tag{3.C}$$

It will be useful for later to determine the relationship between the cohomology functors of Definition 3.4 and exact (triangle preserving) autoequivalences of $\mathcal{D}$.

Lemma 3.5. *Let $\mathcal{A}$ and $\mathcal{B}$ be hearts of bounded t-structures on a triangulated category $\mathcal{D}$, and suppose that $F \colon \mathcal{D} \to \mathcal{D}$ is an exact autoequivalence satisfying $F\mathcal{A} = \mathcal{B}$. Then for all $X \in \mathcal{D}$ with image $FX =: Y$ we have*

$$H_{\mathcal{B}}^\bullet(Y) = F H_{\mathcal{A}}^\bullet(X).$$

Proof. We first show F commutes with the corresponding truncation functors, namely

$$\tau_{\mathcal{B}}^{\geq 0} F \cong F \tau_{\mathcal{A}}^{\geq 0}, \qquad \tau_{\mathcal{B}}^{\leq 0} F \cong F \tau_{\mathcal{A}}^{\leq 0}. \tag{3.D}$$

To this end, let $\mathcal{T}$ and $\mathcal{F}$ be the aisles of the t-structures corresponding to $\mathcal{A}$ and $\mathcal{B}$, so

$$\mathcal{A} = \mathcal{T} \cap \mathcal{T}^{\perp}[1], \qquad \mathcal{B} = \mathcal{F} \cap \mathcal{F}^{\perp}[1].$$

Since $\mathcal{T}$ is the extension-closed subcategory generated by $\mathcal{A}[k]$ for $k \in \mathbb{Z}_{\geq 0}$, it follows that $F(\mathcal{T})$ is the extension-closed subcategory generated by all $\mathcal{B}[k]$, and analogously for $\mathcal{F}$. Thus F restricts to an equivalence between $\mathcal{T}$ and $\mathcal{F}$, and an equivalence between $\mathcal{T}^{\perp}[1]$ and $\mathcal{F}^{\perp}[1]$. Then for all $f \in \mathcal{F}$ we have

$$\begin{aligned}
\operatorname{Hom}_{\mathcal{F}}(f, \tau_{\mathcal{B}}^{\leq 0} Y) &\cong \operatorname{Hom}_{\mathcal{D}}(f, Y) & \operatorname{Hom}_{\mathcal{F}^{\perp}[1]}(\tau_{\mathcal{B}}^{\geq 0} FX, f) &\cong \operatorname{Hom}_{\mathcal{D}}(Y, f) \\
&\cong \operatorname{Hom}_{\mathcal{D}}(F^{-1}f, X) & &\cong \operatorname{Hom}_{\mathcal{D}}(X, F^{-1}f) \\
&\cong \operatorname{Hom}_{\mathcal{T}}(F^{-1}f, \tau_{\mathcal{A}}^{\leq 0} X) & &\cong \operatorname{Hom}_{\mathcal{T}^{\perp}[1]}(\tau_{\mathcal{A}}^{\geq 0} X, F^{-1}f) \\
&\cong \operatorname{Hom}_{\mathcal{F}}(f, F\tau_{\mathcal{A}}^{\leq 0} X), & &\cong \operatorname{Hom}_{\mathcal{F}^{\perp}[1]}(F\tau_{\mathcal{A}}^{\geq 0} X, f).
\end{aligned}$$

The first isomorphisms are adjunctions, the second isomorphisms are applications of F^{-1}, the third isomorphisms are adjunctions, and the last isomorphisms are applications of F. Since all of the above isomorphisms are functorial, by both the covariant and contravariant Yoneda embeddings, (3.D) holds. Thus

$$H_{\mathcal{B}}^{k}(Y) \coloneqq \tau_{\mathcal{B}}^{\leq 0}\tau_{\mathcal{B}}^{\geq 0} Y[k] = \tau_{\mathcal{B}}^{\leq 0}\tau_{\mathcal{B}}^{\geq 0} F(X[k]) \cong F\tau_{\mathcal{A}}^{\leq 0}\tau_{\mathcal{A}}^{\geq 0} X[k] =: FH_{\mathcal{A}}^{k}(X)$$

for all $k \in \mathbb{Z}$, using the fact that F is exact. □

The following well-known lemma is invaluable for results regarding bounded hearts.

Lemma 3.6 (Cf. [MS17, Exercise 5.6])**.** *Let $\mathcal{D}$ be a triangulated category. If $\mathcal{A}$ and $\mathcal{B}$ are hearts of bounded t-structures on $\mathcal{D}$, then $\mathcal{A} \subseteq \mathcal{B}$ implies $\mathcal{A} = \mathcal{B}$.*

§ 3.1.2 | Bridgeland stability

We can now define the original notion of stability for triangulated categories, a generalisation of [Mum65]'s slope stability on vector bundles introduced in algebraic geometry.

Definition 3.7. The *Grothendieck group* of an abelian category $\mathcal{A}$ is the abelian group $K(\mathcal{A})$ generated by isomorphism classes $[M]$ of objects in $\mathcal{A}$, subject to the relation $[M] = [L_1] + [L_2]$ whenever

$$0 \longrightarrow L_1 \longrightarrow M \longrightarrow L_2 \longrightarrow 0$$

is a short exact sequence in $\mathcal{A}$. Informally, $[M]$ is called the *K-theory class* of M.

One can similarly define the Grothendieck group for a triangulated category $\mathcal{D}$, where instead relations are induced by exact triangles. However, if $\mathcal{A}$ is a bounded heart in $\mathcal{D}$ then it can be shown (see, for example, [Ach21, Proposition A.9.5]) that

$$K(\mathcal{D}) = K(\mathcal{A}). \tag{3.E}$$

Definition 3.8. A *stability function* on an abelian category $\mathcal{A}$ is a group homomorphism $Z\colon K(\mathcal{A}) \to \mathbb{C}$, such that if $M \in \mathcal{A}$ is nonzero then

$$Z[M] \in \mathbb{R}_{>0} e^{i\pi\varphi}$$

for some $\varphi = \varphi(M) \in (0, 1]$, known as the *phase* of M.

Two important potential properties of stability functions are the following. If Z is a stability function on $\mathcal{A}$ then $M \in \mathcal{A}$ is said to be *Z-semistable* if $\varphi(L) \leq \varphi(M)$ for all $L \subseteq M$. The *Harder-Narasimhan (HN)* property for Z is that every nonzero object in $\mathcal{A}$ has a unique filtration

$$0 = E^{(0)} \subset \cdots \subset E^{(\ell)} = E$$

with Z-semistable factors $E^{(k)}/E^{(k-1)}$ of phase φ_k, satisfying $\varphi_1 > \cdots > \varphi_\ell$. A stability function has the *support property* if, for any norm $\|-\|\colon K(\mathcal{D}) \to \mathbb{R}_{\geq 0}$,

$$\inf \left\{ \frac{|Z[M]|}{\|[M]\|} \;\middle|\; 0 \neq M \in \mathcal{A} \right\} > 0. \tag{3.F}$$

Definition 3.9 ([Bri07])**.** Let $\mathcal{D}$ be a triangulated category. A *stability condition* on $\mathcal{D}$ is a pair $\sigma = (Z, \mathcal{A})$, where $\mathcal{A}$ is the heart of a bounded t-structure on $\mathcal{D}$ and Z is a stability function on $\mathcal{A}$ with the HN property.

Bridgeland's original definition of a stability condition uses the notion of a slicing of $\mathcal{D}$, but by [Bri07, Proposition 5.3], this is equivalent to Definition 3.9.

Theorem 3.10 ([Bri07])**.** *Let $\mathcal{D}$ be a triangulated category. Then the set* $\operatorname{Stab}\mathcal{D}$ *of stability conditions on $\mathcal{D}$ (with the support property) has the structure of a complex manifold, with a local homeomorphism*

$$\operatorname{Stab}\mathcal{D} \to K(\mathcal{D})^* \coloneqq \operatorname{Hom}_{\mathbb{C}}(K(\mathcal{D}), \mathbb{C}), \qquad (Z, \mathcal{A}) \mapsto Z.$$

The topological behaviour of this complex manifold is unknown in most cases, with connectedness and contractibility (possibly of some connected component) being of great interest.

§ 3.2 | The preprojective algebra

In this section we dive into the world of quiver representation theory and preprojective algebras. Recall that a *quiver* is simply an oriented graph $Q = (Q_0, Q_1, s, t)$ with sets of vertices and edges as in Section 2.1, but now with source and target maps $s, t\colon Q_1 \to Q_0$ that encode the orientation of each edge. A *path* in Q is a string of arrows such that the target of each arrow coincides with the source of the following arrow. A quiver Q is called *acyclic* if no path in Q has the same start and end point.

§ 3.2.1 | Quivers, representations, and paths

Definition 3.11. A *representation* of a quiver Q is a choice of a finite-dimensional complex vector space V_i for each $i \in Q_0$ and a $\mathbb{C}$-linear map $V_{s(a)} \to V_{t(a)}$ for each $a \in Q_1$. The *dimension vector* of a quiver representation is $(\dim V_i)_{i \in Q_0} \in \mathbb{Z}_{\geq 0}^{|Q_0|}$.

Remarkably, this notion is closely related to ideas in Section 2.3.

Theorem 3.12 ([Gab72])**.** *The quivers that admit only finitely many isoclasses of indecomposable representations are precisely those with underlying graphs Δ of types $\mathbb{A}_n$, $\mathbb{D}_n$, $\mathbb{E}_6$, $\mathbb{E}_7$, and $\mathbb{E}_8$. Moreover the dimension vector gives a one-to-one correspondence between indecomposable representations and positive real roots in the root system of Δ.*

A theorem by Kac extends this correspondence to arbitrary quivers, and shows that if α is a positive imaginary root then there exists infinitely many isoclasses of indecomposable representations of Q with dimension vector α. This motivates the terms 'tame' and 'wild' used for graphs in Section 2.1.

Definition 3.13. The *path algebra* of Q is the unital associative $\mathbb{C}$-algebra $\mathbb{C}Q$ with basis the set of paths in Q, with multiplication given by (by convention, left-to-right) concatenation of paths when compatible and zero otherwise.

It is easy to see that $\dim_{\mathbb{C}} \mathbb{C}Q < \infty$ if and only if Q is acyclic, and in general $\mathbb{C}Q$ is noncommutative. For each $i \in Q_0$, there exists a *trivial path* (or *empty path*, in the sense of the string of arrows mentioned prior) e_i which give a family of pairwise orthogonal idempotents in $\mathbb{C}Q$, the sum of which give rise to the unit in $\mathbb{C}Q$.

We will frequently make use of the well-known equivalence between representations of Q and (finite-dimensional) modules over the path algebra of Q. See [ARS95, Theorem III.1.5] for full details of the correspondence.

§ 3.2.2 | Quiver algebras and Π_Δ

Definition 3.14. A *quiver algebra* is an algebra of the form $\Lambda = \mathbb{C}Q/R$, where Q is a quiver and R is an admissible ideal, that is, a two-sided ideal of $\mathbb{C}Q$ satisfying $\langle Q_1 \rangle^m \subseteq R \subseteq \langle Q_1 \rangle^2$ for some $m \in \mathbb{Z}_{\geq 2}$.

To construct the preprojective algebra from Δ first consider the *doubled quiver* $\overline{\Delta}$, which has vertex set Δ_0 and two oppositely oriented arrows a, a^* replacing each edge in Δ. We view arrow reversal as an involution $(-)^* \colon \overline{\Delta}_1 \to \overline{\Delta}_1$.

Definition 3.15 ([GP79])**.** Let Δ be a graph and choose any map $\varepsilon \colon \overline{\Delta}_1 \to \{-1, 1\}$ such that $\varepsilon(a) \neq \varepsilon(a^*)$ for all $a \in \overline{\Delta}_1$. The *preprojective algebra* of (Δ, ε) is the quiver algebra

$$\Pi_\Delta \coloneqq \frac{\mathbb{C}\overline{\Delta}}{\left(\rho \coloneqq \sum_{a \in \overline{\Delta}_1} \varepsilon(a) a a^*\right)}.$$

Importantly, the orientation of Δ will not matter, as [CH98, Lemma 2.2] shows that two different choices of the map ε induce isomorphic preprojective algebras. Going forward we make an implicit choice of ε.

Remark 3.16. We may equivalently describe Π_Δ by taking a relation at each vertex. Indeed, premultiplying ρ by e_i gives rk relations such that

$$\Pi_\Delta = \frac{\mathbb{C}\overline{\Delta}}{\left(\rho_i \coloneqq \sum_{s(a)=i} \varepsilon(a) a a^* \;\middle|\; i \in \Delta_0\right)}.$$

Example 3.17. Now return to the running examples (2.A), which have the following doubled quivers

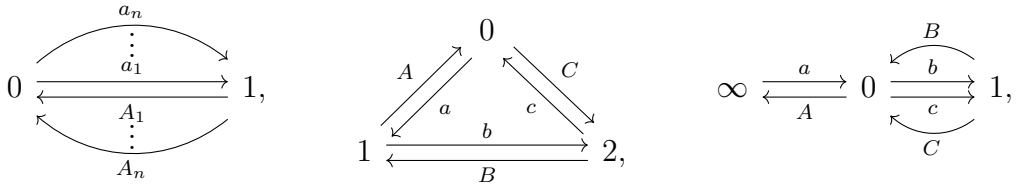

$\mathbb{K}_n$ $\quad$ $\mathbb{A}_2^{\mathrm{aff}}$ $\quad$ $\mathbb{A}_1^{\mathrm{hyp}}$

where we have used lowercase for the arrows with $\varepsilon(a) = 1$ and capitalised the reversed arrows. By Remark 3.16, their preprojective algebras are the path algebra of the above quivers, modulo the following:

(1) $\Pi_{\mathbb{K}_n}$ has relations $\sum_{k=1}^n a_k A_k = 0$ (ρ_0) and $\sum_{k=1}^n A_k a_k = 0$ (ρ_1).

(2) $\Pi_{\mathbb{A}_2^{\mathrm{aff}}}$ has relations $aA = Cc$ (ρ_0), $bB = Aa$ (ρ_1), and $cC = Bb$ (ρ_2).

(3) $\Pi_{\mathbb{A}_1^{\mathrm{hyp}}}$ has relations $aA = 0$ (ρ_∞), $Aa = bB + cC$ (ρ_0), and $Bb + Cc = 0$ (ρ_1).

Notice that for $\Delta = \mathbb{L}_1$ the preprojective algebra is simply the polynomial algebra in two variables.

The algebraic behaviour of Π_Δ across the trichotomy of Section 2.1 is captured in the following result.

Theorem 3.18 ([BGL87, §6])**.** *If Δ is a graph without loops, then the following statements hold.*

(1) Π_Δ *is finite-dimensional (thus noetherian) if and only if Δ is finite type.*

(2) Π_Δ *is infinite-dimensional and noetherian if and only if Δ is tame.*

(3) Π_Δ *is not noetherian if and only if Δ is wild.*

Hence $\Pi_{\mathbb{K}_1}$ is finite-dimensional, $\Pi_{\mathbb{K}_2}$ is infinite-dimensional noetherian, and $\Pi_{\mathbb{K}_{n\geq 3}}$ is nonnoetherian. The fact that the preprojective algebra of a wild graph, such as $\Pi_{\mathbb{A}_1^{\mathrm{hyp}}}$ in Example 3.17(3), is always nonnoetherian will create technical difficulties. For example the category $\operatorname{mod}\Pi_\Delta$ of finitely generated modules is not abelian, and so we must work

with the full module category $\operatorname{Mod}\Pi_\Delta$ in order to construct the derived category $\mathrm{D}(\Pi_\Delta)$. It is still unknown whether the weaker condition of *coherence*, discussed in Section 6.4, holds for Π_Δ in general.

In any case, Π_Δ admits an $\mathbb{N}$-grading

$$\Pi_\Delta = (\Pi_\Delta)_{\geq 0} = \bigoplus_{\ell \in \mathbb{N}} (\Pi_\Delta)_\ell. \tag{3.G}$$

by path length, in which the ℓ-th graded piece is spanned by paths of length ℓ For a graded Π_Δ-module M we write $(M)_\ell$ for its ℓ-th piece, and $(M)_{\geq \ell}$ for the direct sum of pieces in grades at least ℓ.

§ 3.2.3 | Vertex modules

We discuss the main modules of interest for the preprojective algebra, and quiver algebras more generally, which correspond to vertices in the underlying graph Δ.

Definition 3.19. Let $i \in \Delta_0$. The *vertex simple* is defined $S_i \coloneqq \mathbb{C}e_i$, the one dimensional Π_Δ-module on which e_i acts as the identity, and all other arrows act as zero. As a quiver representation of $\overline{\Delta}$, S_i has $V_j = \delta_{ij}\mathbb{C}$ for each vertex and $0 \colon V_{s(a)} \to V_{t(a)}$ for each arrow.

We see that the dimension vector of S_i is the simple root α_i of Definition 2.19, so it is tempting to think of quiver algebra modules as being built up out of vertex simples. However, in general a quiver may admit infinitely many non-vertex simples when its path algebra has infinite dimension. For example giving an orientation to $\mathbb{L}_1$ we see that the simple module induced by the representation

$$\mathbb{C} \circlearrowleft 1 \tag{3.H}$$

is not a vertex simple as in Definition 3.19.

By the 2-Calabi–Yau property (outside of finite type) discussed in Definition 3.35, for Δ without loops there is a connection between the edges in Δ and extensions of vertex simples. Namely, for all $i, j \in \Delta_0$ and $k \in \mathbb{Z}_{\geq 0}$ we have

$$\dim \operatorname{Ext}^k_{\Pi_\Delta}(S_i, S_j) = \begin{cases} \delta_{ij} & \text{if } k \in \{0, 2\}, \\ \Delta_{ij} & \text{if } k = 1, \\ 0 & \text{otherwise.} \end{cases} \tag{3.I}$$

Definition 3.20. Let $i \in \Delta_0$. The *vertex projective* is defined $P_i \coloneqq e_i\Pi_\Delta$, the Π_Δ-module spanned by all paths in $\overline{\Delta}$ that start at i.

This is clearly a projective module as it is a direct summand of $\Pi_\Delta = \bigoplus_{i \in \Delta_0} P_i$. By definition of the vertex modules above, it follows that

$$\dim \operatorname{Hom}_{\Pi_\Delta}(P_i, S_j) = \delta_{ij}. \tag{3.J}$$

Proposition 3.21 ([BBK02, 4.2])**.** *Let Δ be a connected graph without loops that is not of finite type. Then for every $i \in \Delta_0$ the vertex simple S_i admits a projective resolution*

$$0 \longrightarrow P_i \xrightarrow{\boldsymbol{a}^*} Q_i \coloneqq \bigoplus_{s(b)=i} P_{t(b)} \xrightarrow{\boldsymbol{a}^\top} P_i \xrightarrow{f_i} S_i \longrightarrow 0,$$

in Π_Δ. Here $\boldsymbol{a}$ is a vector consisting of all arrows in $\overline{\Delta}$ that start at i, $\boldsymbol{a}^*$ is its componentwise reverse, and f_i is the unique map in (3.J)*.*

§ 3.3 | Category $\mathcal{D}_\Delta$

Having introduced the Coxeter arrangement $\mathcal{H}_\Delta$ in Section 2.3, we now introduce the triangulated category with which the hyperplane structure will interact. We start by defining nilpotent modules which, in light of Theorem 3.18, attempt to keep the representation theory as close to the noetherian situation as possible. We specialise to the preprojective algebra of a given graph Δ, but most of what follows applies to a general quiver algebra $\Lambda = \mathbb{C}Q/R$. We follow [SY13, §2].

§ 3.3.1 | Nilpotent modules

Definition 3.22. The *arrow ideal* I of Π_Δ is the two-sided ideal which is generated by all arrows (length one paths) in $\mathbb{C}\overline{\Delta}$.

From the definition above we have $\Pi_\Delta/I = \mathbb{C}\Delta_0$ and for all $i \in \Delta_0$, $S_i = e_i(\Pi_\Delta/I)$. As $\overline{\Delta}$ contains cycles, there may not exist a power of I that vanishes, but there may still be modules annihilated by some power of I.

Definition 3.23. Let N be a finite-dimensional right Π_Δ-module. Then N is *nilpotent* if $NI^\ell = 0$ for some $\ell \in \mathbb{Z}_{\geq 0}$.

We write $\operatorname{nilp}\Pi_\Delta$ for the category of nilpotent Π-modules.

Example 3.24. The $\mathbb{C}\mathbb{L}_1$-module corresponding to the representation (3.H) extends to a $\Pi_{\mathbb{L}_1}$-module M which is not nilpotent, since $MI^\ell = M$ for all $\ell \in \mathbb{Z}_{\geq 1}$.

Now we prove some useful results about nilpotent modules and their relationship with vertex simples.

Lemma 3.25. *Suppose there is a short exact sequence of Π_Δ-modules*

$$0 \longrightarrow L_1 \xrightarrow{f} M \xrightarrow{g} L_2 \longrightarrow 0.$$

Then M is nilpotent if and only if both L_1 and L_2 are nilpotent.

Proof. If $MI^\ell = 0$ for some $\ell \in \mathbb{Z}_{\geq 0}$ then

$$L_1 I^\ell \subseteq MI^\ell = 0, \qquad L_2 I^\ell = (MI^\ell + L_1)/L_1 = L_1/L_1 = 0,$$

so both L_1 and L_2 are nilpotent. Conversely, if $L_1 I^{\ell_1} = 0$ and $L_2 I^{\ell_2} = 0$ for some $\ell_1, \ell_2 \in \mathbb{Z}_{\geq 0}$ then $MI^{\ell_2} \subseteq L_1$, so M is nilpotent, since

$$MI^{\ell_1+\ell_2} = MI^{\ell_2} I^{\ell_1} \subseteq L_1 I^{\ell_1} = 0. \qquad \square$$

We now give an equivalent characterisation of nilpotent modules which motivates their study. As $N \in \operatorname{nilp} \Pi_\Delta$ is necessarily finite-dimensional as a vector space, N has finite length (in particular it is artinian and noetherian as a module) and so there exists a finite composition series

$$0 = N^{(0)} \subset N^{(1)} \subset \cdots \subset N^{(m)} = N, \tag{3.K}$$

with simple factors $N^{(k)}/N^{(k-1)}$.

Proposition 3.26 (Cf. [Rin12, §2.4])**.** *A Π_Δ-module M is nilpotent if and only if M has finite length, and every factor in its composition series is isomorphic to a vertex simple.*

Proof. Suppose that $M \in \operatorname{nilp} \Pi_\Delta$ and let $\ell \in \mathbb{Z}_{\geq 1}$ be minimal such that $MI^\ell = 0$. Then $L \coloneqq MI^{\ell-1} \neq 0$ is a submodule of M, and the short exact sequence

$$0 \longrightarrow L \longrightarrow M \longrightarrow M/L \longrightarrow 0$$

implies that L and M/L are nilpotent by Lemma 3.25. By induction on ℓ it thus suffices to prove that L has vertex simple factors, but $LI = 0$ and so L must be a direct sum of vertex simples.

Conversely, we use induction on dimension of M to show that $MI^{\dim_{\mathbb{C}} M} = 0$ for all $M \in \operatorname{fd} \Pi_\Delta$ with vertex simple composition factors. If $\dim_{\mathbb{C}} M = 1$ then $M = S_i$ for some $i \in \Delta_0$, and so $Ma = 0$ for all $a \in \overline{\Delta}_1$, in other words $MI = 0$. If M has a composition series with vertex simple factors then there is an exact sequence

$$0 \longrightarrow L \longrightarrow M \longrightarrow S_i \longrightarrow 0,$$

for some $L \in \operatorname{fd} \Pi_\Delta$ also having vertex simple factors and some $i \in \Delta_0$. Since $S_i I = 0$, we have $(M/L)I = 0$ and so $MI \subseteq L$. By induction $LI^{\ell-1} = 0$ where $\ell = \dim_{\mathbb{C}} L + 1$, so $MI^\ell = 0$. $\square$

One must be careful not to conflate the length of a nilpotent module N with the power of the arrow ideal that annihilates it, which is sometimes called the *nilpotency index* of N. For example if $i \neq j$ the nilpotent module $N = S_i \oplus S_j$ has length two but $NI = 0$.

The following consequence of the characterisation in Proposition 3.26 allows us to regain control over the representation theory of Π_Δ even in the wild setting.

Corollary 3.27. *If $S \in \operatorname{nilp} \Pi_\Delta$ is simple, then S is isomorphic to a vertex simple.*

Proof. As S is simple its composition series (3.K) is just $0 = S^{(0)} \subset S^{(1)} = S$, hence by Proposition 3.26 the nilpotent assumption gives $S = S^{(1)}/S^{(0)} \cong S_i$ for some $i \in \Delta_0$. □

§ 3.3.2 | Serre subcategories

Definition 3.28 ([Ser53])**.** Let $\mathcal{A}$ be an abelian category. Then a strictly full subcategory $\mathcal{S}$ is said to be *Serre* (or *dense*) if for all short exact sequences

$$0 \longrightarrow L_1 \longrightarrow M \longrightarrow L_2 \longrightarrow 0$$

in $\mathcal{A}$ we have $M \in \mathcal{S}$ if and only if $L_1, L_2 \in \mathcal{S}$. In other words, $\mathcal{S}$ is Serre if it is closed under inclusions, quotients, and extensions.

Example 3.29. The category of nilpotent modules $\operatorname{nilp} \Pi_\Delta$ is a Serre subcategory of the abelian category $\operatorname{Mod} \Pi_\Delta$. Indeed, this is precisely the statement of Lemma 3.25.

From Definition 3.28 we see that in particular a Serre subcategory $\mathcal{S} \subset \mathcal{A}$ is itself an abelian category, so we may consider the triangulated category $\mathrm{D}^{\mathrm{b}}(\mathcal{S})$. An important subcategory of $\mathrm{D}^{\mathrm{b}}(\mathcal{A})$ is the full subcategory consisting of complexes with cohomology in $\mathcal{S}$, that is

$$\mathrm{D}^{\mathrm{b}}_{\mathcal{S}}(\mathcal{A}) \coloneqq \{X \in \mathrm{D}^{\mathrm{b}}(\mathcal{A}) \mid H^\bullet(X) \in \mathcal{S}\}.$$

Lemma 3.30. *If $\mathcal{S}$ is a Serre subcategory of an abelian category $\mathcal{A}$, then $\mathrm{D}^{\mathrm{b}}_{\mathcal{S}}(\mathcal{A})$ is a thick triangulated subcategory of $\mathrm{D}^{\mathrm{b}}(\mathcal{A})$. In other words, $\mathrm{D}^{\mathrm{b}}_{\mathcal{S}}(\mathcal{A})$ it is closed under triangles and direct summands.*

Proof. As $\mathrm{D}^{\mathrm{b}}_{\mathcal{S}}(\mathcal{A})$ is preserved under translation and is an additive subcategory, we need to show that for any triangle

$$X \longrightarrow Y \longrightarrow Z \longrightarrow Y[1]$$

with $X, Y \in \mathrm{D}^{\mathrm{b}}_{\mathcal{S}}(\mathcal{A})$, Z is also in $\mathrm{D}^{\mathrm{b}}_{\mathcal{S}}(\mathcal{A})$. Considering the cohomology long exact sequence

$$\cdots \longrightarrow H^k(X) \longrightarrow H^k(Y) \longrightarrow H^k(Z) \longrightarrow H^{k+1}(X) \longrightarrow \cdots$$

then $H^k(Z) \in \mathcal{S}$ for all $k \in \mathbb{Z}$, as $\mathcal{S}$ is Serre. To show thickness, now assume that $X \oplus Y \in \mathrm{D}^{\mathrm{b}}_{\mathcal{S}}(\mathcal{A})$, so that $H^\bullet(X \oplus Y) = H^\bullet(X) \oplus H^\bullet(Y) \in \mathcal{S}$. Since $H^\bullet(X)$ is a subobject and $H^\bullet(Y)$ is a quotient, they must both be in $\mathcal{S}$. Hence $X, Y \in \mathrm{D}^{\mathrm{b}}_{\mathcal{S}}(\mathcal{A})$. □

Recall that if $\mathcal{A}$ is an abelian category and $\mathcal{S}$ be a Serre subcategory, then the *Gabriel quotient* (or *Serre quotient*) $\mathcal{A}/\mathcal{S}$ is the localisation of $\mathcal{A}$ with respect to the multiplicative system

$$\{f \in \operatorname{Mor} \mathcal{A} \mid \ker f, \operatorname{coker} f \in \mathcal{S}\}.$$

The canonical functor $\mathcal{A} \to \mathcal{A}/\mathcal{S}$ is exact and surjective on objects, with kernel $\mathcal{S}$. There is a similar notion, the *Verdier quotient* $\mathcal{D}/\mathcal{E}$ for thick triangulated subcategories $\mathcal{E} \subseteq \mathcal{D}$, where now we localise with respect to the class of morphisms f with $\operatorname{Cone} f \in \mathcal{E}$.

Lemma 3.31. *If $\mathcal{S}$ is a Serre subcategory of an abelian category $\mathcal{A}$, then there exists a fully faithful functor*

$$\mathcal{A}/\mathcal{S} \to \mathrm{D}^{\mathrm{b}}(\mathcal{A})/\mathrm{D}^{\mathrm{b}}_{\mathcal{S}}(\mathcal{A}).$$

Proof. First consider the exact sequence of abelian categories

$$0 \longrightarrow \mathcal{S} \longrightarrow \mathcal{A} \xrightarrow{\pi} \mathcal{A}/\mathcal{S} \longrightarrow 0,$$

which, by [Miy91, Theorem 3.2], induces an exact sequence of triangulated categories

$$0 \longrightarrow \mathrm{D}^{\mathrm{b}}_{\mathcal{S}}(\mathcal{A}) \longrightarrow \mathrm{D}^{\mathrm{b}}(\mathcal{A}) \longrightarrow \mathrm{D}^{\mathrm{b}}(\mathcal{A}/\mathcal{S}) \longrightarrow 0. \tag{3.L}$$

Now, the fully faithful functor $\mathcal{A}/\mathcal{S} \to \mathrm{D}^{\mathrm{b}}(\mathcal{A}/\mathcal{S})$ factors as

$$\mathcal{A}/\mathcal{S} \longrightarrow \mathrm{D}^{\mathrm{b}}(\mathcal{A})/\mathrm{D}^{\mathrm{b}}_{\mathcal{S}}(\mathcal{A}) \xrightarrow{\sim} \mathrm{D}^{\mathrm{b}}(\mathcal{A}/\mathcal{S}),$$

where the second functor is an equivalence using (3.L). Hence the first functor must be fully faithful. □

With Example 3.29 in mind, we make the following definition, writing $\mathrm{D}^{\mathrm{b}}(\Pi_\Delta)$ for $\mathrm{D}^{\mathrm{b}}(\operatorname{Mod}\Pi_\Delta)$, as is standard. This is our main category of interest.

Definition 3.32. Let Π_Δ be the preprojective algebra of a connected graph Δ without loops. Define the *K3 category* associated with Δ to be the full subcategory

$$\mathcal{D}_\Delta \coloneqq \mathrm{D}^{\mathrm{b}}_{\mathrm{nilp}}(\Pi_\Delta) \subseteq \mathrm{D}^{\mathrm{b}}(\Pi_\Delta).$$

Specifically, $\mathcal{D}_\Delta$ is the thick (by Lemma 3.30) triangulated subcategory of the bounded derived category of Π_Δ consisting of complexes with nilpotent cohomology.

§ 3.3.3 | Properties of $\mathcal{D}_\Delta$

Lemma 3.33. *Let $\mathcal{S}$ be a Serre subcategory of an abelian category $\mathcal{A}$. The the standard t-structure of Example* 3.2 *on $\mathrm{D}^{\mathrm{b}}(\mathcal{A})$ restricts to a t-structure on $\mathrm{D}^{\mathrm{b}}_{\mathcal{S}}(\mathcal{A})$ with heart $\mathcal{S}$.*

Proof. Define the triangulated subcategories of $\mathrm{D}^{\mathrm{b}}_{\mathcal{S}}(\mathcal{A})$:

$$\mathcal{D}^{\leq 0} \coloneqq \{X \in \mathrm{D}^{\mathrm{b}}_{\mathcal{S}}(\mathcal{A}) \mid H^k(X) = 0 \text{ for all } k > 0\},$$
$$\mathcal{D}^{\geq 0} \coloneqq \{X \in \mathrm{D}^{\mathrm{b}}_{\mathcal{S}}(\mathcal{A}) \mid H^k(X) = 0 \text{ for all } k < 0\}.$$

By (3.B) we need to show that $\tau^{\leq 0}X \in \mathcal{D}^{\leq 0}$ and $\tau^{\geq 1}X \in \mathcal{D}^{\geq 0}[-1]$ for all $X \in \mathcal{D}$, but

$$H^{>0}(\tau^{\leq 0}X) = 0, \qquad H^{\leq 0}(\tau^{\leq 0}X) = H^{\leq 0}(X) \in \mathcal{S},$$
$$H^{<1}(\tau^{\geq 1}X) = 0, \qquad H^{\geq 1}(\tau^{\geq 1}X) = H^{\geq 1}(X) \in \mathcal{S},$$

using the definition of $\mathrm{D}^{\mathrm{b}}_{\mathcal{S}}(\mathcal{A})$ and the truncations. The remaining properties are inherited via Lemma 3.30. □

By Lemma 3.33, the standard t-structure on $\mathrm{D}^{\mathrm{b}}(\Pi_\Delta)$ given in Example 3.2 restricts to a t-structure on $\mathcal{D}_\Delta$ with heart $\mathcal{A}_+ \coloneqq \operatorname{nilp}\Pi_\Delta$, which we call the *standard heart* in $\mathcal{D}_\Delta$. This suggests a link with the standard alcove A_+ (Definition 2.34) in the Coxeter arrangement $\mathcal{H}_\Delta$, which is now made precise.

Remark 3.34. The standard heart $\mathcal{A}_+ \subseteq \mathcal{D}_\Delta$ is *algebraic*, meaning it is a length category with finitely many isoclasses of simple objects $\{S_i \mid i \in \Delta_0\}$. Since every nilpotent module is built out of vertex simples, we have

$$K(\mathcal{D}_\Delta) \overset{(3.\mathrm{E})}{=} K(\mathcal{A}_+) = \bigoplus_{i\in\Delta_0} [S_i] \cong \mathbb{Z}^{\mathsf{rk}}.$$

Definition 3.35. Let $\mathcal{D}$ be a triangulated category with shift functor [1] and finite-dimensional Hom spaces. Let $d \in \mathbb{Z}$. Then $\mathcal{D}$ is said to be *d-Calabi–Yau* if

$$\operatorname{Hom}_{\mathcal{D}}(X, Y) \cong \operatorname{Hom}_{\mathcal{D}}(Y, X[d])^*$$

is a functorial isomorphism for all $X, Y \in \mathcal{D}$.

In other words, a triangulated category is d-Calabi–Yau if $[1]^d$ is a Serre functor, in the sense of [BK89, §3]. Using a Koszul argument, Keller shows the following.

Proposition 3.36 ([Kel08, §4])**.** *The triangulated category $\mathcal{D}_\Delta$ is 2-Calabi–Yau whenever Δ is not of finite type.*

Since the bounded derived category of coherent sheaves on a K3 surface is also 2-Calabi–Yau, $\mathcal{D}_\Delta$ is often referred to as an example of a *K3 category*. We may then think of $\mathcal{D}_\Delta$ as a *noncommutative K3 surface*, from the fact that Π_Δ has global dimension two.

Definition 3.37. An *Ext-finite* (or *finite-type*) category is a $\mathbb{C}$-linear triangulated category $\mathcal{D}$ such that

$$\dim_{\mathbb{C}} \left(\bigoplus_{k\in\mathbb{Z}} \operatorname{Hom}_{\mathcal{D}}(X, Y[k]) \right) < \infty$$

for all $X, Y \in \mathcal{D}$. In this case we may define in K-theory the bilinear *Euler form*

$$\chi\colon K(\mathcal{D}) \times K(\mathcal{D}) \to \mathbb{Z}, \qquad ([X], [Y]) \mapsto \sum_{k\in\mathbb{Z}} (-1)^k \dim_{\mathbb{C}} \operatorname{Hom}_{\mathcal{D}}(X, Y[k]).$$

Proposition 3.36 implies that $\mathcal{D}_\Delta$ is Ext-finite and in particular χ is symmetric, with $-\chi([S_i], [S_j]) = C_{ij}$ for all $i, j \in \Delta_0$. Therefore we have an identification

$$(K(\mathcal{D}_\Delta), \chi) \cong (V, (-,-)), \qquad [S_i] \mapsto \alpha_i \tag{3.M}$$

with the root lattice of Δ given in Definition 2.19. Dually, we may identify Θ with $K(\mathcal{D}_\Delta)^* \otimes_{\mathbb{Z}} \mathbb{R}$, so that stability functions in the sense of Definition 3.8 can be thought of as elements of Θ.

In the nonnoetherian setting of Δ wild, we may consider the algebraic question as to whether $\mathrm{D}^{\mathrm{b}}_{\mathrm{nilp}}(\Pi_\Delta)$ is equivalent to $\mathrm{D}^{\mathrm{b}}(\operatorname{nilp}\Pi_\Delta)$. In other words, is the standard heart in $\mathcal{D}_\Delta$ faithful, in the sense of Definition 3.3, via the canonical realisation functor $F\colon \mathrm{D}^{\mathrm{b}}(\mathcal{S}) \to \mathcal{D}_\Delta$. This is answered in the affirmative in Section 4.1, allowing us to simplify the compatibility conditions of real variations of stability. This is in general a subtle problem, but for $\mathcal{D}_\Delta$ reduces to an Ext^2 problem by the 2-Calabi–Yau property in Proposition 3.36. Sufficient conditions include [GM94, Theorem 3.7.3] and [Ver96, III.2.4.1]. It is known ([IR08, Lemma 2.5]) that if Λ is a module finite algebra, that is, finitely generated as a module over Λ, then faithfulness holds for finite length modules.

§ 3.4 | Tilting t-structures

We finish this chapter, and our preliminaries, with a discussion of ways to obtain new hearts from old, so that the standard heart can be 'mutated' into neighbouring alcoves in the Coxeter arrangement.

§ 3.4.1 | Torsion theories

Recall that for an abelian category $\mathcal{A}$ containing a strictly full subcategory $\mathcal{B}$, the *left orthogonal* and *right orthogonal* to $\mathcal{B}$ are the full subcategories

$$
\begin{aligned}
{}^{\perp}\mathcal{B} &\coloneqq \{M \in \mathcal{A} \mid \operatorname{Hom}_{\mathcal{A}}(M, L) = 0 \text{ for all } L \in \mathcal{B}\},\\
\mathcal{B}^{\perp} &\coloneqq \{M \in \mathcal{A} \mid \operatorname{Hom}_{\mathcal{A}}(L, M) = 0 \text{ for all } L \in \mathcal{B}\}.
\end{aligned}
$$

Definition 3.38. A *torsion theory* on an abelian category $\mathcal{A}$ is a full subcategory $\mathcal{T}$ such that every $M \in \mathcal{A}$ fits into a short exact sequence

$$0 \longrightarrow L_1 \longrightarrow M \longrightarrow L_2 \longrightarrow 0,$$

with $L_1 \in \mathcal{T}$ and $L_2 \in \mathcal{F} \coloneqq \mathcal{T}^{\perp}$.

The pair $(\mathcal{T}, \mathcal{F})$ is called a *torsion pair* in $\mathcal{A}$, where $\mathcal{T}$ is the *torsion class* and $\mathcal{F}$ is the *torsion-free class*. This is motivated by the subcategories of torsion and torsion-free groups in the category of abelian groups. Similarly to t-structures in Section 3.1 (indeed, the two notions are closely related), a torsion pair is determined by $\mathcal{T}$.

Example 3.39. If S is a simple object in a finite length heart $\mathcal{A}$, then $\langle S\rangle$ and ${}^{\perp}\langle S\rangle$ are torsion theories, where $\langle S\rangle \subseteq \mathcal{A}$ is the full subcategory of objects whose simple factors are isomorphic to S. Recall that $\operatorname{add} S_i \subseteq \mathcal{A}$ is the full subcategory closed under direct sums and summands. If Δ has no loops, we have $\mathrm{Ext}^1_{\Pi_\Delta}(S_i, S_i) = 0$ by (3.I), and hence $\operatorname{add} S_i$ coincides with $\langle S_i\rangle$. In this case $\operatorname{add} S_i$ and ${}^{\perp}(\operatorname{add} S_i)$ are two torsion theories on $\operatorname{nilp}\Pi_\Delta$.

If $\mathcal{A}$ is the heart of of a t-structure admitting a torsion theory $(\mathcal{T}, \mathcal{F})$, then there is a notion of 'tilting' with respect to it. This gives a new t-structure with tilted heart.

Definition 3.40 ([HRS96])**.** If $\mathcal{A}$ is a bounded heart in a triangulated category $\mathcal{D}$ and $(\mathcal{T}, \mathcal{F})$ is a torsion pair in $\mathcal{A}$, then the left and right tilt of $\mathcal{A}$ are the hearts

$$\mathcal{L}_{\mathcal{T}}(\mathcal{A}) \coloneqq \{X \in \mathcal{D} \mid H^0_{\mathcal{A}}(X) \in \mathcal{F}, H^1_{\mathcal{A}}(X) \in \mathcal{T}, H^{\bullet}_{\mathcal{A}}(X) = 0 \text{ otherwise}\},$$
$$\mathcal{R}_{\mathcal{T}}(\mathcal{A}) \coloneqq \{X \in \mathcal{D} \mid H^0_{\mathcal{A}}(X) \in \mathcal{T}, H^{-1}_{\mathcal{A}}(X) \in \mathcal{F}, H^{\bullet}_{\mathcal{A}}(X) = 0 \text{ otherwise}\}.$$

The idea is that $\mathcal{L}_{\mathcal{T}}(\mathcal{A})$ is obtained from $\mathcal{A}$ by replacing $\mathcal{T}$ with $\mathcal{T}[-1]$, and $\mathcal{R}_{\mathcal{T}}(\mathcal{A})$ is obtained by replacing $\mathcal{F}$ with $\mathcal{F}[1]$. Furthermore, $\mathcal{F}$ is a torsion class in the new heart $\mathcal{L}_{\mathcal{T}}(\mathcal{A})$ and $\mathcal{R}_{\mathcal{F}}(\mathcal{L}_{\mathcal{T}}(\mathcal{A})) = \mathcal{A}$. Following Example 3.39, we are particularly interested in tilting with respect to the simple objects $\{S_i \mid i \in \Delta_0\}$ in $\operatorname{nilp}\Pi_\Delta$, giving a 'minimal' way to modify t-structures within $\mathcal{D}_\Delta$.

Example 3.41. For Δ without loops, consider the left and right *simple tilts* of the standard heart, that is

$$\mathcal{L}_i(\operatorname{nilp}\Pi_\Delta) \coloneqq \mathcal{L}_{\operatorname{add} S_i}(\operatorname{nilp}\Pi_\Delta), \qquad \mathcal{R}_i(\operatorname{nilp}\Pi_\Delta) \coloneqq \mathcal{R}_{\perp_{(\operatorname{add} S_i)}}(\operatorname{nilp}\Pi_\Delta).$$

The cohomology $H^k(X)$ of objects in these simple tilts is summarised below.

$$H^k(X) \in \begin{array}{c|cc} k & \mathcal{L}_i(\operatorname{nilp}\Pi_\Delta) & \mathcal{R}_i(\operatorname{nilp}\Pi_\Delta) \\ \hline \leq -2 & 0 & 0 \\ -1 & 0 & \operatorname{add} S_i \\ 0 & (\operatorname{add} S_i)^{\perp} & {}^{\perp}(\operatorname{add} S_i) \\ 1 & \operatorname{add} S_i & 0 \\ \geq 2 & 0 & 0 \end{array} \tag{3.N}$$

§ 3.4.2 | Tilting and mutation

Definition 3.42. A *tilting module* (of projective dimension at most $d \in \mathbb{Z}_{\geq 0}$) over a ring Λ is $T \in \operatorname{mod}\Lambda$ such that:

(1) There exists a resolution of T by finitely generated projectives

$$0 \longrightarrow P_d \longrightarrow \cdots \longrightarrow P_0 \longrightarrow T \longrightarrow 0.$$

(2) The self extensions of T are $\operatorname{Ext}^k_\Lambda(T, T) = 0$ for all $k \in \{1, \ldots, d\}$.

(3) There is an exact sequence in $\operatorname{mod}\Lambda$

$$0 \longrightarrow \Lambda \longrightarrow T^{(0)} \longrightarrow \cdots\cdots \longrightarrow T^{(d)} \longrightarrow 0,$$

with each $T^{(k)} \in \operatorname{add} T$.

If $d = 1$ then T is called *classical tilting*.

Example 3.43 ([BIRS09, §III.1])**.** Assume Δ is not of finite type and without loops and let $i \in \Delta_0$. Then the ideal $T_i \coloneqq \Pi_\Delta(1 - e_i)\Pi_\Delta$ is classical tilting for all $i \in \Delta_0$ and

satisfies $\Pi_\Delta/T_i \cong S_i$. Furthermore if $T = T_{i_\ell} \cdots T_{i_1}$ for some $i_1, \ldots, i_\ell \in \Delta_0$, then T is also classical tilting and satisfies $\operatorname{End}_{\Pi_\Delta} T \cong \Pi_\Delta$.

We can view the classical tilting Π_Δ-module T_i as being spanned by all paths in Π_Δ that pass through at least one vertex other than i, so that

$$e_j T_i = \begin{cases} e_i I & \text{if } j = i, \\ P_j & \text{otherwise.} \end{cases} \tag{3.O}$$

Moreover, there is a short exact sequence of Π_Δ-bimodules

$$0 \longrightarrow T_i \longrightarrow \Pi_\Delta \longrightarrow S_i \longrightarrow 0. \tag{3.P}$$

The following classical result is fundamental to this section.

Theorem 3.44 ([Ric89, §6])**.** *Let Λ be a $\mathbb{C}$-algebra, let $T \in \operatorname{mod}\Lambda$ be tilting, and let $\Gamma \coloneqq \operatorname{End}_\Lambda T$. Then there is an equivalence of triangulated categories*

$$\mathrm{D^b}(\Lambda) \underset{-\overset{\mathbb{L}}{\otimes}_\Gamma T}{\overset{\mathbb{R}\mathrm{Hom}_\Lambda(T,-)}{\rightleftarrows}} \mathrm{D^b}(\Gamma).$$

In light of Example 3.43, we see that the *mutation functors*

$$\Phi_i \coloneqq \mathbb{R}\mathrm{Hom}_{\Pi_\Delta}(T_i, -), \qquad \Phi_i^{-1} = - \overset{\mathbb{L}}{\otimes}_{\Pi_\Delta} T_i,$$

are derived autoequivalences of $\mathrm{D^b}(\operatorname{End}_{\Pi_\Delta} T_i) \cong \mathrm{D^b}(\Pi_\Delta)$ for each $i \in \Delta_0$, provided that Δ is tame or wild and has no loops. By definition of derived functors, we have

$$H^\bullet(\Phi_i X) = \operatorname{Ext}^\bullet_{\Pi_\Delta}(T_i, X), \qquad H^\bullet(\Phi_i^{-1} Y) = \operatorname{Tor}_\bullet^{\Pi_\Delta}(Y, T_i),$$

for all $X, Y \in \mathrm{D^b}(\Pi_\Delta)$. To compute $\Phi_i X$ as a complex of abelian groups we can either apply $\operatorname{Hom}_{\Pi_\Delta}(-, X)$ to a projective resolution of T_i or apply $\operatorname{Hom}_{\Pi_\Delta}(T_i, -)$ to an injective resolution of X. Since T_i is classical tilting, there will be at most two terms in the image of Φ_i.

Now consider the *dimension vector*

$$[-] \colon \mathrm{D^b_{fd}}(\Pi_\Delta) \to V, \qquad M^\bullet \mapsto \sum_{k \in \mathbb{Z}} (-1)^k \underline{\dim} H^k(M^\bullet),$$

named as such because $[M]$ coincides with the dimension vector of M from Definition 3.11. Since $\operatorname{nilp}\Pi_\Delta \subset \operatorname{fd}\Pi_\Delta$, the dimension vector $[-]$ restricts to $\mathcal{D}_\Delta$. Then [SY13, Lemma 2.22 and Theorem 2.28] imply a commutative diagram

$$\begin{array}{ccc} \mathcal{D}_\Delta & \underset{\Phi_i^{-1}}{\overset{\Phi_i}{\longleftrightarrow}} & \mathcal{D}_\Delta \\ {\scriptstyle [-]}\downarrow & & \downarrow{\scriptstyle [-]} \\ V & \underset{s_i}{\longleftrightarrow} & V \end{array} \tag{3.Q}$$

for all $i \in \Delta_0$.

Lemma 3.45. *If $i, j \in \Delta_0$ are distinct, then the image of vertex simples, viewed as a complex in degree zero, under the mutation functor Φ_i satisfy*

$$\Phi_i^{\pm} S_i \cong S_i[\mp 1], \qquad \Phi_i S_j \cong \operatorname{Hom}_{\Pi_\Delta}(T_i, S_j), \qquad \Phi_i^{-1} S_j = S_j \otimes_{\Pi_\Delta} T_i.$$

Moreover, these have dimension vector $[\Phi_i(S_j)] = s_i \alpha_j$.

Proof. This follows from the proof of [SY13, Theorem 2.28], or equivalently [Wem18, Lemma 5.7], combined with (3.Q). □

Lemma 3.46 ([SY13, Lemma 2.22])**.** *If $T_w = T_{i_\ell} \cdots T_{i_1}$ then $\Phi_w \coloneqq \mathbb{R}\operatorname{Hom}_{\Pi_\Delta}(T_w, -)$ is a triangle autoequivalence of $\mathcal{D}_\Delta$. In other words, Theorem 3.44 restricts to $\mathcal{D}_\Delta$*

We write $\operatorname{Auteq} \mathcal{D}_\Delta$ for the *automorphism group* associated with $\mathcal{D}_\Delta$, where by convention all autoequivalences are exact. Strictly speaking we only need to work with the subgroup $\operatorname{Br} \mathcal{D}_\Delta \coloneqq \langle \Phi_i \mid i \in \Delta_0 \rangle$. Importantly, the mutation functors and simple tilts are related as follows.

Lemma 3.47 (Cf. [DW22, §4.2])**.** *For all $i \in \Delta_0$ we have equalities*

$$\mathcal{L}_i(\operatorname{nilp} \Pi_\Delta) = \Phi_i(\operatorname{nilp} \Pi_\Delta), \qquad \mathcal{R}_i(\operatorname{nilp} \Pi_\Delta) = \Phi_i^{-1}(\operatorname{nilp} \Pi_\Delta)$$

of bounded hearts in $\mathcal{D}_\Delta$.

Proof. Since every abelian category in the statement is a bounded heart, it suffices by Lemma 3.6 to show that $\Phi_i^{-1}(\operatorname{nilp} \Pi_\Delta) \subseteq \mathcal{R}_i(\operatorname{nilp} \Pi_\Delta)$ and similarly for the left tilt. As every $N \in \operatorname{nilp} \Pi_\Delta$ is built out of vertex simples, we just check $\Phi_i^{-1}(S_i), \Phi_i^{-1}(S_j) \in \mathcal{R}_i(\operatorname{nilp} \Pi_\Delta)$. By Lemma 3.45, $\Phi_i^{-1}(S_i)$ and $\Phi_i^{-1}(S_j)$ are in cohomological degree -1 and 0 respectively. Firstly

$$H^{-1}(\Phi_i^{-1}(S_i)) = H^{-1}(S_i[1]) = S_i \in \operatorname{add} S_i,$$

as required. Then adjunction, along with Lemma 3.45 again, implies

$$\begin{aligned} \operatorname{Hom}_{\text{nilp}}(H^0(\Phi_i^{-1} S_j), S_i) &\cong \operatorname{Hom}_{\mathcal{D}}(\Phi_i^{-1} S_j, S_i) \\ &\cong \operatorname{Hom}_{\mathcal{D}}(S_j, \Phi_i S_i) \\ &= \operatorname{Hom}_{\mathcal{D}}(S_j, S_i[-1]), \end{aligned}$$

which is zero and so $H^0(\Phi_i^{-1} S_j)$ is torsion. This implies that $\Phi_i^{-1}(S_j) \in \mathcal{R}_i(\operatorname{nilp} \Pi_\Delta)$. □

Chapter 4

Real variations of stability

In this chapter we introduce the notion of real variations of stability conditions on a triangulated category, and construct a wide class of examples for the category $\mathcal{D}_\Delta$ from Chapter 3. With the Coxeter arrangement and triangulated category now established, we seek to unify their structures in order to construct real variations. In this chapter we give results demonstrating the existence of real variations of stability conditions on $\mathcal{D}_\Delta$ for all graphs without loops of affine and hyperbolic type. Much of this chapter comprises [Lew24, §3,4].

§ 4.1 | Setup

We start by discussing the main definition of this chapter, a type of stability on triangulated categories first introduced by Anno, Bezrukavnikov, and Mirković.

§ 4.1.1 | What is a real variation of stability?

Definition 4.1 (Cf. [ABM15, Definition 1])**.** Let $\mathcal{D}$ be an (Ext-finite) triangulated category and let $\mathcal{L}$ be a finite-dimensional Euclidean or hyperbolic space containing a discrete collection of hyperplanes $\mathcal{H}$. Let Alc be the set of *alcoves*, the connected components of $\mathcal{L}\setminus\mathcal{H}$. Suppose also that Alc carries the notion of 'above/below' for neighbouring alcoves A, B, denoted $\prec$. A *real variation of stability conditions* on $\mathcal{D}$, parametrised by $\mathcal{L}\setminus\mathcal{H}$ in the direction of $\prec$, consists of the following:

(a) A real (analytic) map $Z\colon \mathcal{L} \to K(\mathcal{D})^*_{\mathbb{R}},\ \vartheta \mapsto Z_\vartheta$, the *central charge*,

(b) a map $\heartsuit\colon \mathsf{Alc} \to \{\mathcal{A} \subseteq \mathcal{D} \text{ bounded heart}\}$,

satisfying the following properties for all $A \in \mathsf{Alc}$.

(1) If $M \in \mathcal{A} \coloneqq \heartsuit(A)$ is nonzero, then $\langle Z_\vartheta, [M]\rangle > 0$ for all $\vartheta \in A$.

(2) If $B \succ A$ is an alcove neighbouring A across a hyperplane $H \in \mathcal{H}$, consider for $k \in \mathbb{Z}_{\geq 0}$ the full subcategories

$$\mathcal{A}^{(k)}_H \coloneqq \{M \in \mathcal{A} \mid \langle Z_-, [M]\rangle\colon \mathcal{L} \to \mathbb{R} \text{ has a zero of order at least } k \text{ along } H\},$$
$$\mathcal{D}^{(k)}_{A,H} \coloneqq \{X \in \mathcal{D} \mid H^\bullet_{\mathcal{A}}(X) \in \mathcal{A}^{(k)}_H\}.$$

Then $\mathcal{B} \coloneqq \heartsuit(B)$ is compatible with the filtration $\mathcal{D}^{(\bullet)}_{A,H}$ of $\mathcal{D}$ in the sense that

$$\mathcal{B}^{(k)}_H = \mathcal{B} \cap \mathcal{D}^{(k)}_{A,H} \tag{4.A}$$

$$\frac{\mathcal{B}^{(k)}_H}{\mathcal{B}^{(k+1)}_H} = \frac{\mathcal{A}^{(k)}_H}{\mathcal{A}^{(k+1)}_H}[k] \subset \mathcal{D}/\mathcal{D}^{(k)}_{A,H} \tag{4.B}$$

for all $k \in \mathbb{Z}_{\geq 0}$, where $\mathcal{B}^{(k)}_H$ is defined analogously to $\mathcal{A}^{(k)}_H$.

Notice that in Definition 4.1 the first axiom gives a map from the space $\mathcal{L}$ into the space of Bridgeland stability conditions $\operatorname{Stab}\mathcal{D}$, by taking a 'real slice' of the usual central charge. The second axiom connects neighbouring alcoves as $\mathcal{L} \setminus \mathcal{H}$ is disconnected. Ours is a generalisation of the original definition, which has a specific affine notion of direction on the arrangement and a polynomial, rather than analytic, central charge. The definition in [ABM15] assigns bounded t-structures to alcoves, but as bounded t-structures are determined by their hearts, our assignment is equivalent. Notably, the original definition works over a real vector space, which can be thought of as making a choice of origin in $\mathcal{L}$. We lack a way to make this choice in hyperbolic space, motivating the categorical approach in Section 4.2.

Remark 4.2. Observe that if $\mathrm{D}^{\mathrm{b}}(\mathcal{A}) \cong \mathcal{D} \cong \mathrm{D}^{\mathrm{b}}(\mathcal{B})$, that is, the assigned hearts are faithful, then Definition 4.1(2) is a *perverse equivalence* (as in [CR17, Definition 4.1]) with respect to the filtration $\mathcal{D}^{(\bullet)}$. Even if the associated realisation functors are not equivalences, we may still systematically study the relationship between the hearts $\mathcal{A}$ and $\mathcal{B}$ relative to the filtration, using *perverse tilts* from [CR17, §3.7].

§ 4.1.2 | Affine directions

If $\mathcal{H}$ is a collection of affine hyperplanes (for example $\mathcal{H}_\Delta$ with Δ tame), then in [ABM15, §3] a direction is chosen as follows. Let $\mathcal{H}_O$ denote the *linearised arrangement*, obtained by translating each $H \in \mathcal{H}$ to the origin.

Definition 4.3. Let $\mathcal{L}$ be a finite-dimensional affine space containing a discrete collection of hyperplanes $\mathcal{H}$, and choose a connected component $\mathcal{L}_+$ of $\mathcal{L}\setminus\mathcal{H}_O$. Let A and B be two alcoves sharing a hyperplane H. Then A is *above* B, written $A \succ B$, if and only if A lies in the connected component $(\mathcal{L}\setminus H)_+$ of $\mathcal{L}\setminus H$ which contains $\mathcal{L}_+ + H$.

We wish to apply this notion to the Coxeter arrangement within $\mathcal{L} = \mathsf{Level}_\Delta$ for Δ hyperbolic. Unfortunately it is not immediately clear how to generalise, for instance, what it means to translate hyperplanes to the origin of hyperbolic space. In the affine case, $\mathcal{H}_O$ is finite and so there are only finitely many directions we can choose, but this is not the case for hyperbolic arrangements. To get around this issue, we think homologically and convert the notion of direction to that of a 'flow', generalising the idea to work for any (locally finite) arrangement.

§ 4.1.3 | Calibrating reflections and mutations

Setup 4.4. We fix a connected graph Δ with rk vertices of affine or hyperbolic type without loops, that is (2.C) or (2.E) (excluding $\mathbb{L}_n, \mathbb{K}_{n,1}, \mathbb{K}_{n,2}$). The Coxeter arrangement $\mathcal{H}_\Delta$ consists of a hyperplane $H_\alpha \subset \Theta$ dual to each positive real root $\alpha = w\alpha_i$, which we view intersected with the set

$$\mathsf{Level}_\Delta = \left\{ \vartheta \in \Theta \;\middle|\; \textstyle\sum_{i\in\Delta_0} \vartheta_i \geq 0,\ \vartheta^\top (\operatorname{Adj} C_\Delta)\vartheta = 1 \right\}.$$

Each alcove $A \subset \mathsf{Level}_\Delta \backslash \mathcal{H}_\Delta$ is of the form wA_+ for some $w \in W_\Delta$, and each of the rk hyperplanes bordering A are the reflecting hyperplanes $H_{w\alpha_i}$ of the reflections ws_iw^{-1} for $i \in \Delta_0$. Hence a neighbouring alcove B has the form $B = ws_iw^{-1}A = ws_iA_+$.

Motivated by Lemma 3.46, we wish to assign to $A = wA_+$ the heart

$$\mathcal{A} \coloneqq \Phi_{i_\ell}^{\pm_\ell} \cdots \Phi_{i_1}^{\pm_1} \mathcal{A}_+,$$

where $w = s_{i_\ell} \cdots s_{i_1}$ is a reduced expression. This leaves a lot of choice in the powers of $\Phi_{i_\ell}^{\pm_\ell} \cdots \Phi_{i_1}^{\pm_1} \in \operatorname{Br} \mathcal{D}_\Delta$, so it is important to ensure that this assignment is well-defined irrespective of minimal expressions for w.

§ 4.2 | Real charges and real flows

In this section we equip the pair $(\mathcal{H}_\Delta, \mathcal{D}_\Delta)$, constructed in our preliminaries, with a real central charge and an assignment of hearts to alcoves, in line with the data of Definition 4.1.

§ 4.2.1 | Real charges

Let $Z\colon \mathsf{Level}_\Delta \hookrightarrow \Theta$ be the inclusion map. Then, by (3.M), Z is a map to $K(\mathcal{D}_\Delta)^*_{\mathbb{R}}$, as required by Definition 4.1. Since $Z\colon \mathsf{Level}_\Delta \to \Theta$ is injective and $s_i \operatorname{im} Z \subseteq \operatorname{im} Z$, there is an action of W_Δ on Level_Δ making the diagram

$$\begin{array}{ccccc} \mathsf{Level}_\Delta & \xhookrightarrow{Z} & \Theta & \xrightarrow{[M]} & \mathbb{R} \\ {\scriptstyle s_i}\downarrow & & \downarrow{\scriptstyle s_i} & & \| \\ \mathsf{Level}_\Delta & \xhookrightarrow[Z]{} & \Theta & \xrightarrow[[\Phi_i M]]{} & \mathbb{R} \end{array} \tag{4.C}$$

commute for all $M \in \mathcal{D}_\Delta$. By definition of the W_Δ-action on Θ, we have

$$\langle w\vartheta, w[X] \rangle = \langle \vartheta, [X] \rangle \tag{4.D}$$

for all $w \in W_\Delta$, $\vartheta \in \Theta$, $X \in \mathcal{D}_\Delta$.

By parametrising Level_Δ as $(\mathsf{rk}-1)$-dimensional Euclidean or hyperbolic space, we may give an explicit formula for the real central charge Z. This is a real polynomial for Δ affine, in line with the original definition of [ABM15], but becomes a real power series when Δ is hyperbolic, as in Example 2.35. This gives an alternative way of checking the order of vanishing in Definition 4.1(2).

Example 4.5. Consider $\Delta = \mathbb{K}_n$ with $n \geq 3$. As $\mathsf{Level}_\Delta \cong \mathbb{R}$, we may parametrise the real central charge as follows

$$Z_n \colon \mathbb{R} \to \Theta, \qquad a \mapsto \frac{2}{\sqrt{n^2-4}} \begin{pmatrix} \sinh \log m_n^{1-a} \\ \sinh \log m_n^a \end{pmatrix} = \frac{1}{m_n - m_n^{-1}} \begin{pmatrix} m_n^{1-a} - m_n^{a-1} \\ m_n^a - m_n^{-a} \end{pmatrix},$$

recalling the Kronecker constant m_n from Example 2.32. One can show that

$$Z_n(a)_0^2 + nZ_n(a)_0 Z_n(a)_1 + Z_n(a)_1^2 = 1$$

for all $a \in \mathbb{R}$. Viewing n as being continuous, taking the limit as n approaches 2 recovers the classical affine level. Indeed, a simple application of l'Hôpital's rule yields

$$Z_2(a) = \lim_{n \to 2} Z_n(a) = \begin{pmatrix} 1-a \\ a \end{pmatrix},$$

which is Example 2.32(2) as expected.

§ 4.2.2 | Real flows

Recall from Section 2.4 the free category $\operatorname{Free} \mathcal{H}_\Delta$ on the Coxeter arrangement associated with Δ. We may think of each wall-crossing as either a length one reduced positive path or a simple reflection via the identification $A = wA_+, B = ws_iw^{-1}A$ of Setup 4.4. The common abuse of notion s_i will be used for both directions of the wall-crossing.

Definition 4.6. A *real functor* on $\mathcal{H}_\Delta$ is a functor

$$\mathbb{F} \colon \operatorname{Free} \mathcal{H}_\Delta \to \mathcal{A}\mathrm{uteq}\, \mathcal{D}_\Delta, \qquad p \mapsto \mathbb{F}_p,$$

sending every object A to $\mathcal{D}_\Delta$ and every generating morphism $s_i \colon A \to B$ to either Φ_i or Φ_i^{-1}, such that $\mathbb{F}_{B \to A} = (\mathbb{F}_{A \to B})^{-1}$. Here $i \in \Delta_0$ corresponds to the wall between A and B, in the sense that if $\vartheta \in A = wA_+$ for some $w \in W$, then $ws_iw^{-1}\vartheta \in B$. If $\mathbb{F}_{A \to B} = \Phi_i$, then we say that A is *above* B and write $A \succ B$, otherwise A is *below* B, written $A \prec B$. We can summarise this as

$$A \underset{s_i}{\overset{s_i}{\rightleftarrows}} B \qquad \overset{\mathbb{F}}{\longmapsto} \qquad \begin{cases} \mathcal{D}_\Delta \underset{\Phi_i^{-1}}{\overset{\Phi_i}{\rightleftarrows}} \mathcal{D}_\Delta & \text{if } A \succ B, \\ \mathcal{D}_\Delta \underset{\Phi_i}{\overset{\Phi_i^{-1}}{\rightleftarrows}} \mathcal{D}_\Delta & \text{if } A \prec B. \end{cases}$$

If, around every flat (codimension two wall) in $\mathcal{H}_\Delta$, there is a unique source alcove A_s, opposite which is a unique target (or 'sink') alcove A_t, then $\mathbb{F}$ is called a *real flow*.

By Definition 2.16, every flat in our setting is of the form $\mathbb{A}_2$ or $\mathbb{A}_1 \times \mathbb{A}_1$, so a real

flow looks locally like the following.

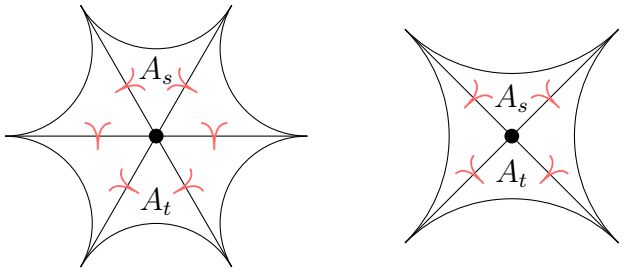

$\mathbb{A}_2$ $\mathbb{A}_1 \times \mathbb{A}_1$ (4.E)

The choice of the 'above' alcove as being the inverse mutation functor (or equivalently, by Lemma 3.47, the right tilt) is in light of Lemma 3.45, since we wish to line up the heart assignment with the shift in (4.B).

Example 4.7. One example of a real flow comes from the (right) Bruhat order $\leq_R$ on W_Δ, discussed in Definition 2.40. To see this, fix a flat of type $\mathbb{A}_2$ (the case $\mathbb{A}_1 \times \mathbb{A}_1$ is easier) and consider the three adjacent hyperplanes H_1, H_2, H_3, viewed in TC. The alcove A_+ is in one of the six regions in TC that form the connected components of the complement of these hyperplanes. Each of the six alcoves neighbouring the flat sits in precisely one of these regions, and therefore the alcove A sitting in the same region as A_+ is the smallest with respect to the length of w, where $wA_+ = A$. This is because any reduced path $A_+ \to A$ does not cross any of H_1, H_2, H_3, but a path to any other alcove B must cross at least one of these, as below.

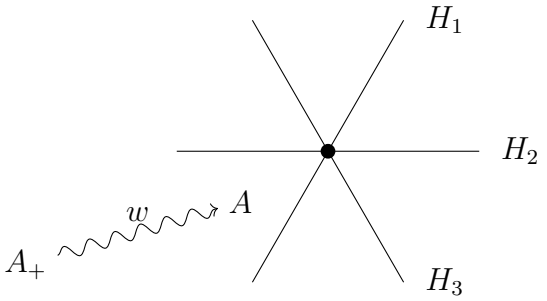

We next claim that A is the unique target alcove in the flat. The claim holds since the path ws_i is reduced (crossing H_1 only once), as is ws_is_j (crossing H_1 and H_2 only once) and $ws_is_js_i$. Thus $w \leq_R ws_i \leq_R ws_is_j \leq_R ws_is_js_i$. The other direction, namely that $w \leq_R ws_j \leq_R ws_js_i \leq_R ws_js_is_j$, is similar.

Example 4.8. We give two examples of real flows on $\mathcal{H}_\Delta$ from Example 2.35.

(1) If $\Delta = \mathbb{A}_2^{\text{aff}}$, then we may recover the notion of direction on affine arrangements used in [ABM15], which involves choosing a connected component of the linearised arrangement. If we consider a flow $\mathbb{F}$ that has the source alcove (and hence the sink alcove) in the same position for every flat, then this has the same effect as fixing the linear component in the same position. In the figure below we

use the 'top left' as the source around every $\mathbb{A}_2$ flat, but the technology of flows allows us to construct many more examples by making local choices at each flat.

(2) If $\Delta = \mathbb{A}^{\text{aff}}_{2,3}$, then W_Δ is the free group on three generators. This means that the associated Coxeter arrangement has no codimension two walls (as no root hyperplanes intersect inside the disc) and hence the condition on flats is vacuously satisfied, so any choice of real functor will automatically be a flow.

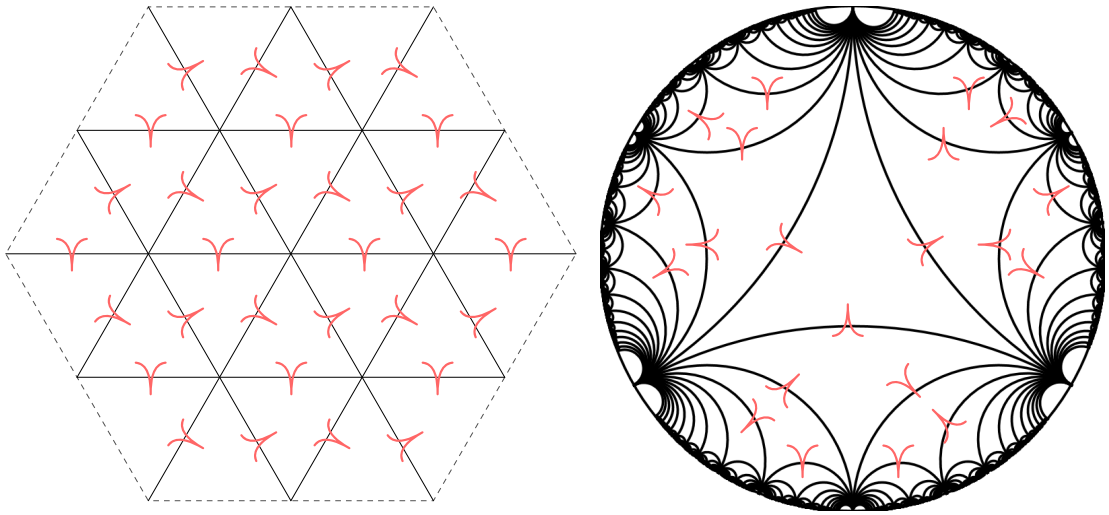

Figure 4.1: Examples of real flows on $\mathcal{H}_\Delta$ for graphs $\mathbb{A}^{\text{aff}}_2$ and $\mathbb{A}^{\text{aff}}_{2,3}$. The former has the most restrictions, whilst the latter has no restrictions.

§ 4.2.3 | Consequences of a real flow

Since the word problem is solved for the braid groups $\text{Br}_{\mathbb{A}_2}$ and $\text{Br}_{\mathbb{A}_1\times\mathbb{A}_1}$, we may easily verify the following cases.

Lemma 4.9. *Let Δ be $\mathbb{A}_1 \times \mathbb{A}_1$ or $\mathbb{A}_2$, and let $i, j \in \Delta_0$ be distinct. The following are the only braid equalities of the form $s_i^{\pm}s_j^{\pm} = s_j^{\pm}s_i^{\pm}$, respectively $s_i^{\pm}s_j^{\pm}s_i^{\pm} = s_j^{\pm}s_i^{\pm}s_j^{\pm}$, that hold in Br_Δ.*

$$\mathbb{A}_1 \times \mathbb{A}_1$$

$$s_is_j = s_js_i$$
$$s_is_j^{-1} = s_j^{-1}s_i$$
$$s_i^{-1}s_j = s_js_i^{-1}$$
$$s_i^{-1}s_j^{-1} = s_j^{-1}s_i^{-1}$$

$$\mathbb{A}_2$$

$$s_is_js_i = s_js_is_j$$
$$s_is_js_i^{-1} = s_j^{-1}s_is_j$$
$$s_i^{-1}s_js_i = s_js_is_j^{-1}$$
$$s_is_j^{-1}s_i^{-1} = s_j^{-1}s_i^{-1}s_j$$
$$s_i^{-1}s_j^{-1}s_i = s_js_i^{-1}s_j^{-1}$$
$$s_i^{-1}s_j^{-1}s_i^{-1} = s_j^{-1}s_i^{-1}s_j^{-1}$$

Each corresponds to a longest diagonal across a 4-gon and a 6-gon, respectively.

Proof. This is readily checked, for example, by the computer algebra package `Magma` [BCP97], iterating over the $2^6 = 64$ choices of positive and negative powers in relations of the form $s_i^{\pm} s_j^{\pm} s_i^{\pm} = s_j^{\pm} s_i^{\pm} s_j^{\pm}$. Each of these expressions determines a source and target alcove. Indeed, fixing a reference alcove A, labelling walls with alternating indices, and thinking of wall-crossing across i to a higher alcove as multiplication by s_i, we obtain the stated expressions by passing from A to its opposite $\overline{A}$ in both ways. The $\mathbb{A}_1 \times \mathbb{A}_1$ case is similar.

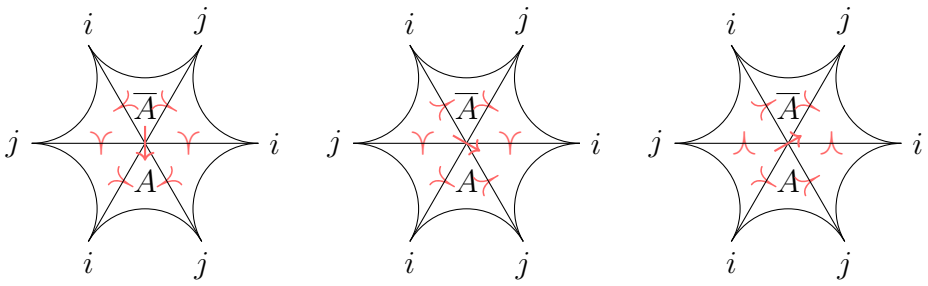

$$(---) = (---) \qquad (--+) = (+--) \qquad (-++) = (++-) \tag{4.F}$$

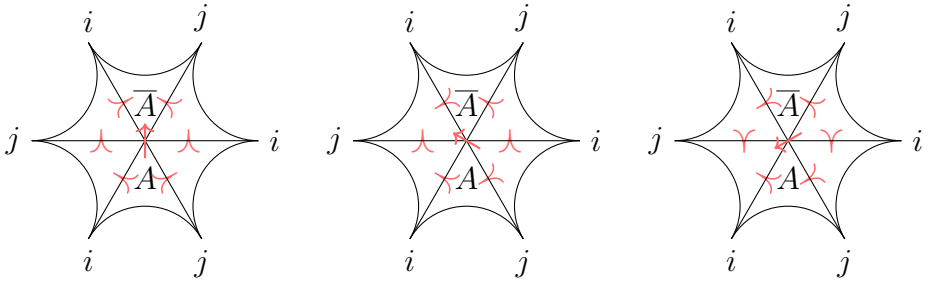

$$(+++) = (+++) \qquad (++-) = (-++) \qquad (++-) = (-++)$$

□

We are now ready to prove the main result of this section, which is that a real flow is precisely the information we need to get a well-defined assignment of hearts to alcoves.

Proposition 4.10. *If $\mathbb{F}$ is a real functor on $\mathcal{H}_\Delta$, then $\mathbb{F}$ is a flow if and only if it descends to a well-defined functor $\mathbb{F}\colon \mathcal{G}_\Delta \to \mathcal{A}\mathrm{uteq}\, \mathcal{D}_\Delta$. In this case, $\mathbb{F}_p = \mathbb{F}_q$ whenever p, q are paths around a codimension two wall from an alcove to its opposite.*

Proof. Consider $\operatorname{Path} \mathcal{H}_\Delta = \operatorname{Free} \mathcal{H}_\Delta / \sim$ defined in Section 2.4. If $\sim_M$ is the smallest equivalence relation in $\operatorname{Free} \mathcal{H}_\Delta$ generated by codimension two (that is, braid) relations, then Matsumoto's Theorem 2.39 implies that $\operatorname{Path} \mathcal{H}_\Delta = \operatorname{Free} \mathcal{H}_\Delta / \sim_M$. This is because any path in the free category can be identified with an element w of the Weyl group, and any two reduced paths give rise to reduced expressions for w and hence differ by a sequence of braid moves. Hence it suffices to check that the paths around codimension two walls give equivalent composition of autoequivalences.

First suppose that $\mathbb{F}$ is a real flow, so (possibly after rotating) each flat locally has the form (4.E). Now by Lemma 4.9 each of the six (or four) relations in $\operatorname{Path} \mathcal{H}_\Delta$

around this flat hold in $\mathrm{Br}_{\mathbb{A}_2}$ (or $\mathrm{Br}_{\mathbb{A}_1\times\mathbb{A}_1}$), so by [SY13, Proposition 2.27] applied to [BIRS09, III.1.8], the relations also hold in $\mathcal{A}\mathrm{uteq}\,\mathcal{D}_\Delta$. Thus, $\mathbb{F}$ descends.

Conversely, suppose that $\mathbb{F}$ descends, and consider a flat of type $\mathbb{A}_2$ as before. Then we have a relation $\mathbb{F}_{s_i}\mathbb{F}_{s_j}\mathbb{F}_{s_i} = \mathbb{F}_{s_j}\mathbb{F}_{s_i}\mathbb{F}_{s_j}$, that is

$$\Phi_i^{\pm}\Phi_j^{\pm}\Phi_i^{\pm} = \Phi_j^{\pm}\Phi_i^{\pm}\Phi_j^{\pm}. \tag{4.G}$$

Now, by [HW18], [BT11], there is a monomorphism $\mathrm{Br}_{\mathbb{A}_2} \hookrightarrow \mathcal{A}\mathrm{uteq}\,\mathcal{D}_\Delta$, $s_i \mapsto \Phi_i$. Therefore (4.G) implies that $s_i^{\pm}s_j^{\pm}s_i^{\pm} = s_j^{\pm}s_i^{\pm}s_j^{\pm}$ holds in $\mathrm{Br}_{\mathbb{A}_2}$. Lemma 4.9 says this can only happen if there is a unique source and sink alcove around the flat. The $\mathbb{A}_1 \times \mathbb{A}_1$ case is similar. □

As a consequence, this explains the 'real' in the terminology, the idea being that we have forced all monodromy to be trivial, as one would expect in a real setting.

Corollary 4.11. *If $\mathbb{F}$ is a real flow then the monodromy monoid homomorphism*

$$\mathrm{End}_{\mathrm{Path}}\,A \to \mathrm{Br}\,\mathcal{D}_\Delta, \qquad p \mapsto \mathbb{F}_p$$

is trivial for all $A \in \mathsf{Alc}_\Delta$.

Proof. We induct on the length of $p\colon A \to A$. If this is two, then $p = (A \xrightarrow{s_i} B \xrightarrow{s_i} A)$ for some $i \in \Delta_0$. By definition of a real functor we have $\mathbb{F}_p = \Phi_i^{\pm}\Phi_i^{\mp} = \mathrm{id}$. If p has length greater than two then it must cross some hyperplane $H = H_{ws_i}$ twice. Thus we have a decomposition $p = \gamma \circ s_i \circ \beta$, where $B \to C$ is the first place p crosses H twice, and β does not cross any hyperplane twice. Then β is reduced.

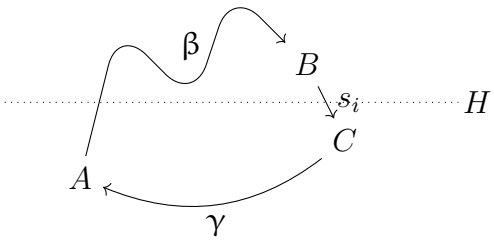

We may choose a reduced path $\beta'\colon A \to C$, which does not cross H because A and C lie on the same side of H, and any path between them crossing H must do so twice and would not be reduced. Then the path $A \to C \to B$ is also reduced because it crosses each hyperplane at most once. Therefore $\beta = s_i \circ \beta'$ in the path category and so

$$\mathbb{F}_p = \mathbb{F}_\gamma\mathbb{F}_{B\to C}\mathbb{F}_\beta = \mathbb{F}_\gamma\mathbb{F}_{B\to C}\mathbb{F}_{C\to B}\mathbb{F}_{\beta'} = \mathbb{F}_\gamma\Phi_i^{\pm}\Phi_i^{\mp}\mathbb{F}_{\beta'} = \mathbb{F}_{\gamma\circ\beta'},$$

which is of smaller length. The claim follows by induction. □

§ 4.3 | Faithfulness of the standard heart

In this section we prove that the standard heart $\operatorname{nilp}\Pi_\Delta \subseteq \mathcal{D}_\Delta$ is faithful in the sense of Definition 3.3, that is,

$$\mathrm{D}^{\mathrm{b}}(\operatorname{nilp}\Pi_\Delta) \cong \mathrm{D}^{\mathrm{b}}_{\operatorname{nilp}}(\Pi_\Delta). \tag{4.H}$$

As a consequence in the next section we are able to greatly simplify the compatibility conditions of Definition 4.1.

§ 4.3.1 | Criteria for faithfulness

Recall from Section 3.1.1 that we need to show that the realisation functor

$$F\colon \mathrm{D}^{\mathrm{b}}(\operatorname{nilp}\Pi_\Delta) \to \mathcal{D}_\Delta, \qquad N^\bullet \mapsto N^\bullet$$

is fully faithful and essentially surjective. The following result shows that, in our case, it is enough for F to be fully faithful.

Proposition 4.12. *Let $\mathcal{A}$ be an abelian category, let $\mathcal{S} \subseteq \mathcal{A}$ be a Serre subcategory, and suppose that the realisation functor*

$$F\colon \mathrm{D}^{\mathrm{b}}(\mathcal{S}) \to \mathrm{D}^{\mathrm{b}}_{\mathcal{S}}(\mathcal{A})$$

is fully faithful. Then F is essentially surjective.

Proof. Since we are working in the bounded setting, we proceed by induction on the number of nonzero cohomology objects of $X \in \mathrm{D}^{\mathrm{b}}_{\mathcal{S}}(\mathcal{A})$. If this is one, then $X \simeq H^k(X)$ for some $k \in \mathbb{Z}$, which is in $\mathcal{S}$ by definition. Hence $X \in \operatorname{im} F$. Now suppose that $H^\bullet(X) = 0$ in degrees less than some $k \in \mathbb{Z}$ but $H^k(X) \neq 0$. Then by (3.B) there exists a triangle

$$\tau^{\leq k}X \longrightarrow X \longrightarrow \tau^{\geq k+1}X \longrightarrow$$

in $\mathrm{D}^{\mathrm{b}}(\Pi)$. As the t-structure restricts (Lemma 3.33), we have $\tau^{\leq k}X, \tau^{\geq k+1}X \in \mathrm{D}^{\mathrm{b}}_{\mathcal{S}}(\mathcal{A})$, which both have nonzero cohomology in fewer degrees than X. Hence by induction,

$$\tau^{\leq k}X, \tau^{\geq k+1}X \in \operatorname{im} F.$$

Moreover, as F is fully faithful, its image is a triangulated subcategory of $\mathrm{D}^{\mathrm{b}}_{\mathcal{S}}(\mathcal{A})$, forcing $X \in \operatorname{im} F$. □

The above result in fact holds for the realisation functor associated to any bounded t-structure (see, for example, [PV18, Theorem 3.11(iv)]). Since $\mathcal{D}_\Delta$ is a full subcategory of $\mathrm{D}^{\mathrm{b}}(\Pi_\Delta)$, we know that F is fully faithful if and only if $\mathrm{D}^{\mathrm{b}}(\operatorname{nilp}\Pi_\Delta) \to \mathrm{D}^{\mathrm{b}}(\Pi_\Delta)$ is fully faithful. The following dévissage result gives a criterion to check this on objects in the Serre subcategory.

Lemma 4.13 ([Kra22, 4.2.13])**.** *Let $\mathcal{A}$ be an abelian category and $\mathcal{B}$ a full exact subcategory. Then the functor $F\colon \mathrm{D}^{\mathrm{b}}(\mathcal{B}) \to \mathrm{D}^{\mathrm{b}}(\mathcal{A})$ is fully faithful if and only if for all*

$L, M \in \mathcal{B}$ and $k \in \mathbb{Z}_{\geq 0}$, there is a bijection

$$F_k \colon \operatorname{Ext}^k_{\mathcal{B}}(L, M) \to \operatorname{Ext}^k_{\mathcal{A}}(L, M).$$

Recall that if $\mathcal{A}$ is an abelian category and $L, M \in \mathcal{A}$, then there is an identification of $\operatorname{Ext}^k_{\mathcal{A}}(L, M)$ with $\operatorname{Hom}_{\mathrm{D}^{\mathrm{b}}(\mathcal{A})}(L, M[k])$, where the latter consists of equivalence classes $[F, q, f]_{\mathcal{A}}$ as discussed at the start of Section 3.1.

§ 4.3.2 | Nilpotent approximations

We now prove the main result of this section directly, leveraging the $\mathbb{N}$-grading of Π_Δ and the resolution (3.21) to approximate extensions $[-,-,-]_\Pi$ over $\operatorname{Mod}\Pi_\Delta$ with extensions $[-,-,-]_{\mathrm{nilp}}$ over $\operatorname{nilp}\Pi_\Delta$.

Theorem 4.14. *The standard t-structure with heart $\operatorname{nilp}\Pi_\Delta$ in $\mathcal{D}_\Delta$ is faithful. That is, there is a fully faithful and essentially surjective functor*

$$F \colon \mathrm{D}^{\mathrm{b}}(\operatorname{nilp}\Pi_\Delta) \xrightarrow{\sim} \mathrm{D}^{\mathrm{b}}_{\mathrm{nilp}}(\Pi_\Delta).$$

Proof. In light of Proposition 4.12 and Lemma 4.13, we need to show that the map

$$F_k \colon \operatorname{Ext}^k_{\mathrm{nilp}}(L, M) \to \operatorname{Ext}^k_{\Pi}(L, M), \qquad [E^\bullet, q, f]_{\mathrm{nilp}} \mapsto [E^\bullet, q, f]_\Pi$$

is a bijection for all $L, M \in \operatorname{nilp}\Pi_\Delta$. By strong induction on module length, we need only verify this for vertex simples S_i, S_j with $i, j \in \Delta_0$. Indeed, for $L, M \in \operatorname{nilp}\Pi_\Delta$, we can apply $\operatorname{Ext}^k_{\mathrm{nilp}}(-, M)$ and $\operatorname{Ext}^k_{\Pi}(-, M)$ to the short exact sequence

$$0 \longrightarrow L' \longrightarrow L \longrightarrow L'' \longrightarrow 0,$$

where L' has smaller length than L and L'' is a vertex simple. This induces the long exact sequence

$$\begin{array}{ccccccccccc}
\cdots \to & \operatorname{Ext}^k_{\mathrm{nilp}}(L'', M) & \to & \operatorname{Ext}^k_{\mathrm{nilp}}(L, M) & \to & \operatorname{Ext}^k_{\mathrm{nilp}}(L', M) & \to & \operatorname{Ext}^{k+1}_{\mathrm{nilp}}(L'', M) & \to \cdots \\
& \downarrow\wr & & \downarrow & & \downarrow\wr & & \downarrow\wr & \\
\cdots \longrightarrow & \operatorname{Ext}^k_{\Pi}(L'', M) & \longrightarrow & \operatorname{Ext}^k_{\Pi}(L, M) & \longrightarrow & \operatorname{Ext}^k_{\Pi}(L', M) & \longrightarrow & \operatorname{Ext}^{k+1}_{\Pi}(L'', M) & \to \cdots
\end{array}$$

and so the five lemma applies. Similarly, we can use a filtration of M and apply $\operatorname{Ext}^k(L, -)$.

(Surjectivity). The Hom case $k = 0$ is immediate, the case $k = 1$ follows since $\operatorname{nilp}\Pi_\Delta \subset \operatorname{Mod}\Pi_\Delta$ is a Serre subcategory, and cases $k > 2$ are trivial since $\mathrm{D}^{\mathrm{b}}(\Pi_\Delta)$ is 2-Calabi–Yau. Hence the only interesting case is $k = 2$. Note that if $i \neq j$ then $\operatorname{Ext}^2_\Pi(S_i, S_j) = 0$ (also by the Calabi–Yau property) and there is nothing to prove, so consider $i = j$. Then $\dim \operatorname{Ext}^2_\Pi(S_i, S_i) = \dim \operatorname{Hom}_\Pi(S_i, S_i) = 1$ implies that any nonzero element of $\operatorname{Ext}^2_\Pi(S_i, S_i) = \operatorname{Hom}_{\mathrm{D}^{\mathrm{b}}(\Pi)}(S_i, S_i[2])$ is equivalent to a roof of the

form

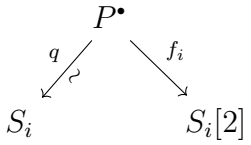

with $P^\bullet$ the projective resolution in Proposition 3.21. To ease notation, we write P for $P^0 = P^{-2} = P_i$, Q for $P^{-1} = Q_i = \bigoplus P_j$, and S for S_i. By noting that the differential $d^\bullet$ in $P^\bullet$ increases path length by one, this resolution can be made $\mathbb{N}$-graded. Indeed, using the grading notation of (3.G),the first three graded pieces are

$$\begin{aligned}
&0 \longrightarrow 0 \longrightarrow 0 \longrightarrow (P)_0 \longrightarrow S \longrightarrow 0,\\
&0 \longrightarrow 0 \longrightarrow (Q)_0 \longrightarrow (P)_1 \longrightarrow 0 \longrightarrow 0,\\
&0 \longrightarrow (P)_0 \longrightarrow (Q)_1 \longrightarrow (P)_2 \longrightarrow 0 \longrightarrow 0.
\end{aligned} \tag{4.I}$$

Since $d^\bullet$ satisfies $d^{-2}(PI) \subseteq QI^2$ and $d^{-1}(QI^2) \subseteq PI^3$ (this can be checked directly as $e_i x \in e_i I = PI$ maps to $ae_i x = e_j ax \in e_j I^2 \subseteq QI^2$, and similarly for the other differential), $P^\bullet$ descends to

$$\begin{array}{ccccccccc}
0 & \longrightarrow & P/PI & \longrightarrow & Q/QI^2 & \longrightarrow & P/PI^3 & \longrightarrow & S/SI^4 & \longrightarrow & 0\\
 & & \| & & \| & & \| & & \| & & \\
0 & \longrightarrow & P/(P)_{\geq 1} & \longrightarrow & Q/(Q)_{\geq 2} & \longrightarrow & P/(P)_{\geq 3} & \longrightarrow & S & \longrightarrow & 0.
\end{array} \tag{4.J}$$

Here, $PI^\ell = (P)_{\geq \ell}$ because $I^\ell = (\Pi_\Delta)_{\geq \ell}$ and P is a direct summand of Π_Δ. Thus, we have defined a 'nilpotent approximation' of $P^\bullet$ by

$$N^\bullet \coloneqq (P/PI \longrightarrow Q/QI^2 \longrightarrow P/PI^3).$$

This is clearly nilpotent in each degree. It is quasi-isomorphic to S concentrated in degree zero because it is equal to the direct sum of the three exact sequences in (4.I). Any map $P^\bullet \to S$ factors through $N^\bullet$ because $SI^2 = 0$. Therefore, f factors through $N^\bullet$ to give a map f' making

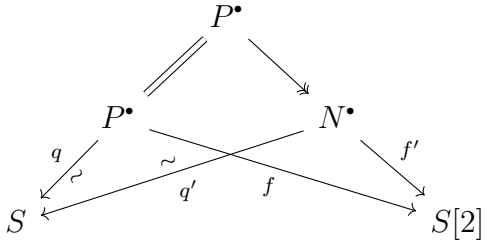

commute in $\mathrm{K}^{\mathrm{b}}(\Pi_\Delta)$. In fact, this diagram is already commutative in $\mathrm{C}^{\mathrm{b}}(\Pi_\Delta)$. Therefore

$$[P^\bullet, q, f]_\Pi = [N^\bullet, q', f']_\Pi = F_k[N^\bullet, q', f']_{\mathrm{nilp}}.$$

(Injectivity). Now let $[E^\bullet, q, f]_{\mathrm{nilp}} \in \mathrm{Ext}^k_{\mathrm{nilp}}(S_i, S_j)$ satisfy $[E^\bullet, q, f]_\Pi = 0$. By definition of the zero morphism in the derived category (see, for example, [Mil, Lemma 2.1.4]), there exists some $Q^\bullet \in \mathrm{D}^{\mathrm{b}}(\Pi_\Delta)$ and a quasi-isomorphism $r\colon Q^\bullet \xrightarrow{\sim} E^\bullet$ such that $f \circ r = 0$. We may then replace $Q^\bullet$ with the projective resolution $P^\bullet$ of S_i using [SPA18, Lemma 0649], which says that there exists a map of complexes $s\colon P^\bullet \to Q^\bullet$, making the diagram

$$\begin{array}{ccc} S_i & \xleftarrow{q\circ r} & Q^\bullet \\ \uparrow & \nearrow_{s} & \\ P^\bullet & & \end{array}$$

commute in $\mathrm{C}^{\mathrm{b}}(\Pi_\Delta)$, provided that $q \circ r$ is surjective in every degree. This is the case for us because S_i is one-dimensional. Then s is also a quasi-isomorphism. Therefore, there is a quasi-isomorphism $r \circ s\colon P^\bullet \to E^\bullet$ with $f \circ (r \circ s) = 0$. Writing $g \coloneqq q \circ r \circ s$, we have

$$[E^\bullet, q, f]_\Pi = [Q^\bullet, q \circ r, 0]_\Pi = [P^\bullet, g, 0]_\Pi.$$

As in the surjectivity argument, we wish to realise the equivalence class $[P^\bullet, g, 0]_\Pi$ as an element of $\mathrm{Ext}^k_{\mathrm{nilp}}(S_i, S_j)$ via a nilpotent approximation. Since $E^\bullet$ is a bounded complex of nilpotent modules, there exists an $\ell \in \mathbb{Z}_{\geq 0}$ such that $E^k I^\ell = 0$ for all $k \in \mathbb{Z}$. Taking m to be the greater of 2 and this ℓ, we define the complex of nilpotent modules

$$N^\bullet \coloneqq (P/PI^m \longrightarrow Q/QI^{m+1} \longrightarrow P/PI^{m+2}),$$

with notation for the terms in $P^\bullet$ as before. Then $r \circ s\colon P^\bullet \to E^\bullet$ factors as $P^\bullet \twoheadrightarrow N^\bullet \to E^\bullet$ in $\mathrm{C}^{\mathrm{b}}(\Pi_\Delta)$. Since the quotient map $\pi\colon P^\bullet \twoheadrightarrow N^\bullet$ and the composition $r \circ s$ are both quasi-isomorphisms, the morphism $q'\colon N^\bullet \xrightarrow{\sim} E^\bullet$ is a quasi-isomorphism. Thus the commutative diagram

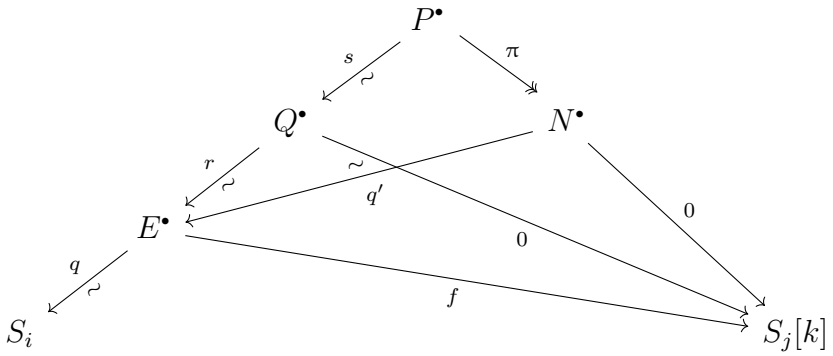

implies that $(f \circ q') \circ \pi = 0$, as $f \circ r \circ s = 0$. Now consider the chain map $f \circ q' \circ \pi\colon P^\bullet \to S_j[k]$, which is null homotopic by the above. This killing homotopy clearly factors

through $N^\bullet$ using the commutative diagram

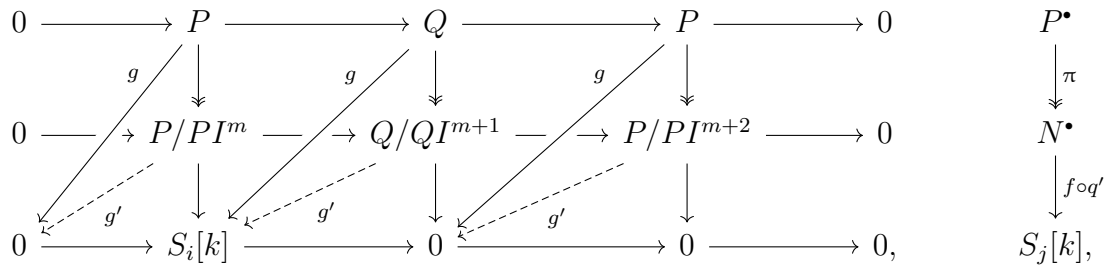

and g' is a killing homotopy by the surjectivity of π. Hence, $f \circ q' = 0$, and then $[E^\bullet, q, f]_{\text{nilp}} = [N^\bullet, q \circ q', 0]_{\text{nilp}} = 0$ by the below

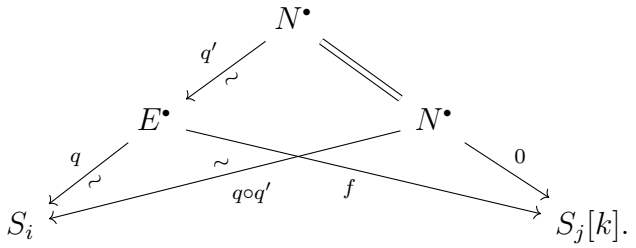

□

Remark 4.15. The above proof is specific to the preprojective algebra, but we expect this proof to hold in greater generality, provided the algebra admits a $\mathbb{N}$-grading and has finite global dimension. An alternative approach to establishing that F_k is an isomorphism is to use one of the equivalent conditions (Ef) or (CoEf) in [PV18, Theorem 3.11(iii)].

§ 4.3.3 | Applications to tilted hearts

As a consequence, all of the hearts we assign to alcoves are faithful.

Corollary 4.16. *If $F \in \operatorname{Auteq} \mathcal{D}_\Delta$, then the heart $F(\operatorname{nilp} \Pi_\Delta) \subseteq \mathcal{D}_\Delta$ is faithful.*

Proof. By [GM94, Theorem 3.7.3], a necessary and sufficient condition for a heart $\mathcal{A} \subseteq \mathcal{D}$ to be faithful is that $\operatorname{Hom}_{\mathcal{D}}(X, Y[k])$ is generated by $\operatorname{Hom}_{\mathcal{D}}(X, Y[1])$ for all $k \in \mathbb{Z}_{\geq 2}$ and all $X, Y \in \mathcal{A}$. Since this condition must hold for $\operatorname{nilp} \Pi_\Delta$ by Theorem 4.14, applying F completes the proof. □

Proposition 4.17. *If $\mathcal{A}$ is an abelian category and $\mathcal{S} \subseteq \mathcal{A}$ is Serre, then $\mathrm{D}^{\mathrm{b}}_{\mathcal{S}}(\mathcal{A}) = \langle \mathcal{S} \rangle$ as thick triangulated subcategories of $\mathrm{D}^{\mathrm{b}}(\mathcal{A})$.*

Proof. One inclusion is immediate, by definition of $\langle \mathcal{S} \rangle$. Now every $E^\bullet \in \mathrm{D}^{\mathrm{b}}_{\mathcal{S}}(\mathcal{A})$ admits a filtration by its cohomology objects (see, for example, [Bay11, Proposition 3.3.1]):

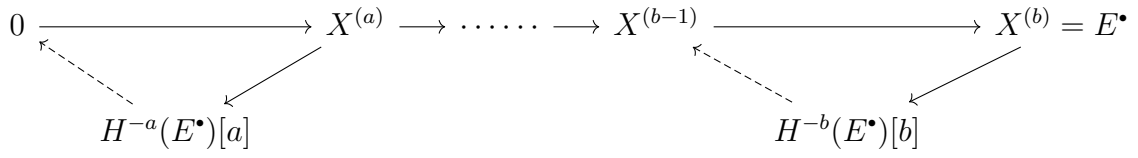

where all triangles are exact and each $H^k(E^\bullet) \in \mathcal{S}$. Hence $E^\bullet$ can be built out of $\mathcal{S}$ in finitely many steps, that is, $E^\bullet \in \langle \mathcal{S} \rangle$. □

§ 4.4 | Constructing real variations

We are now ready to prove the existence of real variations of stability on $\mathcal{D}_\Delta$, which to ease notation we denote by $\mathcal{D}$ for the remainder of the chapter. This generalises the affine examples from [ABM15] into the hyperbolic setting.

§ 4.4.1 | Preparation

First we state important lemmas allowing us to reduce to the case where A is the standard alcove A_+ and B is adjacent across the hyperplane H_i for some $i \in \Delta_0$. Recall that $\mathcal{A}_+$ denotes the standard heart $\operatorname{nilp} \Pi_\Delta$, introduced in Section 3.3.

Lemma 4.18. *In the context of Setup* 4.4*, consider alcoves $A = wA_+$ and $B = ws_iA_+$ separated by the hyperplane $H = H_{w\alpha_i}$. Let $\mathcal{A} = \mathbb{F}_w(\mathcal{A}_+)$ and $\mathcal{B} = \mathbb{F}_w\Phi_i^{\pm}(\mathcal{A}_+)$ be the corresponding hearts, where $\mathbb{F}$ is a real flow on $\mathcal{H}_\Delta$ with the sign depending on whether B is above A $(-)$ or below A $(+)$. Then, with notation from Definition* 4.1*, we have*

(1) $\mathcal{B}_H^{(1)} = \mathbb{F}_w\Phi_i^{\pm}\mathbb{F}_w^{-1}(\mathcal{A}_H^{(1)})$,

(2) $\mathcal{D}_{B,H}^{(1)} \coloneqq \{X \in \mathcal{D} \mid H_{\mathcal{B}}^\bullet(X) \in \mathcal{B}_H^{(1)}\} = \mathbb{F}_w\Phi_i^{\pm}\mathbb{F}_w^{-1}(\mathcal{D}_{A,H}^{(1)})$,

(3) $\mathcal{A}_H^{(1)} = \operatorname{add} \mathbb{F}_w S_i$ *and* $\mathcal{B}_H^{(1)} = \operatorname{add} \mathbb{F}_w S_i[\mp 1]$,

(4) $\mathcal{D}_{A,H}^{(1)} = \langle \mathbb{F}_w S_i \rangle = \langle \mathbb{F}_w S_i[\mp 1] \rangle = \mathcal{D}_{B,H}^{(1)}$,

(5) $\pi_{A,H} \colon \mathcal{D} \twoheadrightarrow \mathcal{D}/\mathcal{D}_{A,H}^{(1)}$ *sends $\mathcal{A}$ and $\mathcal{B}$ to $\mathcal{A}/\mathcal{A}_H^{(1)}$ and $\mathcal{B}/\mathcal{B}_H^{(1)}$, respectively.*

Proof. For (1) and (2) we prove only one inclusion, as the opposite inclusions are analogous.

(1) Suppose that $M \in \mathcal{A}_H^{(1)}$, namely $M \in \mathcal{A}$ and $\langle \vartheta, [M] \rangle = 0$ for all $\vartheta \in H_{w\alpha_i}$. Then $L \coloneqq \mathbb{F}_w\Phi_i^{\pm 1}\mathbb{F}_w^{-1}(M)$ is such that

$$\langle \vartheta, [L] \rangle = \langle \vartheta, ws_iw^{-1}[M] \rangle \overset{(4.D)}{=} \langle s_iw^{-1}\vartheta, w^{-1}[M] \rangle = \langle w^{-1}\vartheta, w^{-1}[M] \rangle = 0,$$

since $s_iw^{-1}\vartheta \in H_i$, and so $L \in \mathcal{B}_H^{(1)}$.

(2) Suppose that $X \in \mathcal{D}_{A,H}^{(1)}$, so $H_{\mathcal{A}}^k(X) \in \mathcal{A}_H^{(1)}$ for all $k \in \mathbb{Z}$. Set $F \coloneqq \mathbb{F}_w\Phi_i^{\pm}\mathbb{F}_w^{-1}$, so that $F(\mathcal{A}) = \mathcal{B}$. If we set $Y \coloneqq FX$, then

$$H_{\mathcal{B}}^k(Y) \overset{3.5}{\cong} FH_{\mathcal{A}}^k(X) \in F(\mathcal{A}_H^{(1)}) = \mathcal{B}_H^{(1)},$$

where the final equality is just an application of (1). Thus $F(\mathcal{D}_{A,H}^{(1)}) \subseteq \mathcal{D}_{B,H}^{(1)}$.

(3) The Serre subcategory $\mathcal{A}_H^{(1)}$ consists of objects $M \in \mathcal{A}$ such that $\langle -, [M] \rangle$ has a zero of order at least one along $H_{w\alpha_i}$. If $\vartheta \in H_{w\alpha_i}$ then $w^{-1}\vartheta \in H_i$. We also have $s_i w^{-1}\vartheta \in H_i$ since $s_i H_i = H_i$. Writing $M = \mathbb{F}_w N$ for some nilpotent module N, we have

$$\langle \vartheta, [M] \rangle = \langle \vartheta, [\mathbb{F}_w N] \rangle = \langle \vartheta, w[N] \rangle = \langle w^{-1}\vartheta, [N] \rangle,$$

which, if zero, forces $[N] \in \mathbb{Z}\boldsymbol{\alpha}_i$. Thus $\mathcal{A}_H^{(1)} = \mathbb{F}_w(\operatorname{add} S_i) = \operatorname{add} \mathbb{F}_w S_i$, and combining Lemma 4.18(1) with Lemma 3.45 gives the result for $\mathcal{B}$.

(4) The thick triangulated subcategory $\mathcal{D}_{A,H}^{(1)}$ consists of objects in $\mathcal{D}$ with cohomology in $\mathcal{A}_H^{(1)} = \operatorname{add} \mathbb{F}_w S_i$. By Proposition 4.17, this is just $\langle \mathbb{F}_w S_i \rangle$, and so

$$\mathcal{D}_{B,H}^{(1)} \overset{(2)}{=} \mathbb{F}_w \Phi_i^{\pm} \mathbb{F}_w^{-1}(\mathcal{D}_{A,H}^{(1)}) = \mathbb{F}_w \Phi_i^{\pm} \langle S_i \rangle \overset{3.45}{=} \mathbb{F}_w \langle S_i[\mp 1] \rangle = \langle \mathbb{F}_w S_i \rangle = \mathcal{D}_{A,H}^{(1)}.$$

(5) For the final claim, consider the following diagram where, for readability, we have suppressed H in the notation.

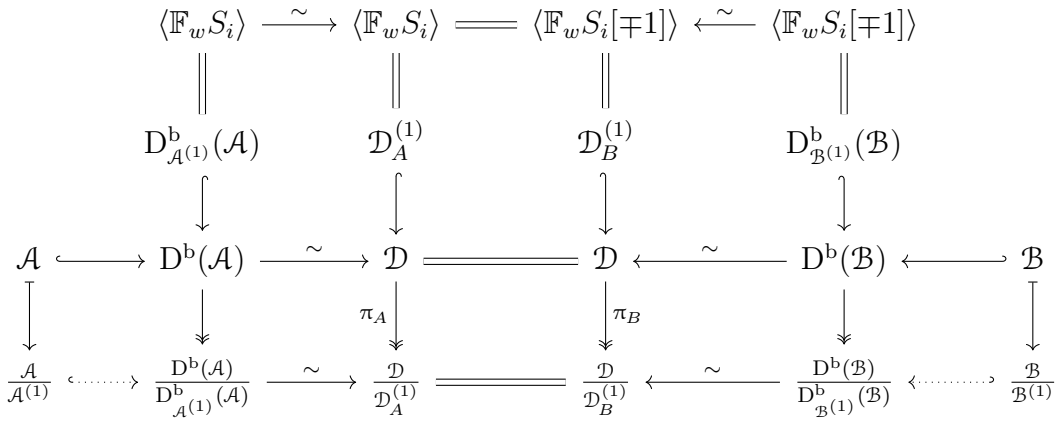

By (4), $\pi_{A,H} = \pi_{B,H}$ since $\mathcal{D}_{A,H}^{(1)} = \mathcal{D}_{B,H}^{(1)}$. The dotted maps in the bottom left and bottom right are fully faithful by Corollary 4.16 and Lemma 3.31 applied to the Serre subcategories $\mathcal{A}_H^{(1)}$ and $\mathcal{B}_H^{(1)}$, respectively. The result follows by commutativity. □

In particular, the above proof shows that $\mathcal{A}/\mathcal{A}_H^{(1)}$ and $\mathcal{B}/\mathcal{B}_H^{(1)}$ are abelian subcategories of $\mathcal{D}/\mathcal{D}_{A,H}^{(1)}$, so it makes sense to compare them in (4.B).

Lemma 4.19. *For all $i \in \Delta_0$ we have*

$$\Phi_i(\operatorname{add} S_i) = \Phi_i(\mathcal{A}_+) \cap \mathrm{D}^{\mathrm{b}}_{\operatorname{add} S_i}(\Pi_\Delta).$$

Proof. Let $M = \Phi_i(N)$ for some $N \in \mathcal{A}_+$. If $N \in \operatorname{add} S_i$, then $M = \Phi_i(S_i^{\oplus m}) = S_i^{\oplus m}[1]$ has cohomology in $\operatorname{add} S_i$, so $M \in \mathrm{D}^{\mathrm{b}}_{\operatorname{add} S_i}(\Pi_\Delta)$. This proves $\subseteq$. Conversely, if $H^k(M) \in \operatorname{add} S_i$ for all $k \in \mathbb{Z}$, then we have

$$[M] = \sum_{k \in \mathbb{Z}} (-1)^k \underline{\dim} H^k(M) \in \mathbb{Z}\boldsymbol{\alpha}_i.$$

Hence $[N] = s_i^2[N] = s_i[M] \in \mathbb{Z}\boldsymbol{\alpha}_i$, which forces $N \in \operatorname{add} S_i$. □

§ 4.4.2 | The main result

Finally, we prove that our construction of real variations of stability is well-defined and satisfies the required compatibility conditions for the t-structures at neighbouring alcoves.

Theorem 4.20. *Let Δ be a connected graph of affine or hyperbolic type and let $\mathbb{F}$ be a real flow on its Coxeter arrangement $\mathcal{H}_\Delta$. Then $(Z, \heartsuit)$ is a real variation of stability on $\mathcal{D}_\Delta$, where Z is the inclusion of Level_Δ into Θ and $\heartsuit$ assigns the heart $\mathbb{F}_w(\operatorname{nilp}\Pi_\Delta)$ to the alcove $A = wA_+ \in \mathsf{Alc}_\Delta$.*

Proof. The fact that $\mathbb{F}$ is a real flow means that the heart $\mathcal{A} \coloneqq \mathbb{F}_w\mathcal{A}_+$ assigned to $A \in \mathsf{Alc}_\Delta$ is well-defined regardless of the reduced expression used for w. Indeed, by Proposition 4.10 one can assign to each $w \in W$ a functor $\mathbb{F}_w = \mathbb{F}_{i_\ell} \cdots \mathbb{F}_{i_1}$. If $w = s_{j_\ell} \cdots s_{j_1}$ is another reduced expression for w, then

$$s_{i_\ell} \cdots s_{i_1} = (s_{i_\ell} \cdots s_{i_1} s_{j_1}^{-1} \cdots s_{j_\ell}^{-1}) s_{j_\ell} \cdots s_{j_1} = \gamma s_{j_\ell} \cdots s_{j_1}$$

for some $\gamma \in \operatorname{End}_{\mathrm{Path}} A$. Then, by Corollary 4.11, $\mathbb{F}_\gamma \in \operatorname{Auteq} \mathcal{D}_\Delta$ is trivial. Therefore $\mathbb{F}_w$ is independent of the reduced expression chosen for w. We now verify the properties of Definition 4.1 in turn.

(1) Let $M \in \mathcal{A}$ be nonzero and let $\vartheta \in A$. Then by construction there exists $\eta \in A_+$ and $N \in \mathcal{A}_+$ such that $\vartheta = w\eta$ and $M = \mathbb{F}_w(N)$. Now repeatedly apply (3.Q) so that

$$Z_\vartheta[M] = \langle \vartheta, [M] \rangle = \langle w\eta, [\mathbb{F}_w(N)] \rangle = \langle \eta, N \rangle.$$

This is clearly positive as the standard alcove A_+ lives in the positive orthant of Θ, and $[N]$ is based by simples with non-negative coefficients. Thus the real central charge $Z \colon \mathsf{Level}_\Delta \to \Theta$ satisfies the positivity property.

(2) Now suppose that B is an alcove adjacent to A across the hyperplane H_α. As in Setup 4.4 we have $\alpha = w\boldsymbol{\alpha}_i$ for some $i \in \Delta_0$, and the heart assigned to B is

$$\mathcal{B} \coloneqq \begin{cases} \mathbb{F}_w\Phi_i(\mathcal{A}_+) & \text{if } A \succ B, \\ \mathbb{F}_w\Phi_i^{-1}(\mathcal{A}_+) & \text{if } A \prec B. \end{cases}$$

We need to prove the compatibility conditions of Definition 4.1 only for $k \in \{0, 1\}$, as the Serre subcategories $\mathcal{A}_H^{(k)}, \mathcal{B}_H^{(k)}$ are zero for $k > 1$. This is because Z is the inclusion map and so the pairing $\langle \vartheta, [M] \rangle$ is linear. Recall that conditions (4.A) and (4.B) are, in order of increasing difficulty,

$$\mathcal{B}_H^{(1)} = \mathcal{A}_H^{(1)}[\pm 1], \qquad \mathcal{B}_H^{(1)} = \mathcal{B}_H \cap \mathcal{D}_{A,H}^{(1)}, \qquad \mathcal{B}/\mathcal{B}_H^{(1)} = \mathcal{A}/\mathcal{A}_H^{(1)}.$$

The first is Lemma 4.18(3), the second follows from Lemma 4.18(4) (or by applying $\mathbb{F}_w$ to Lemma 4.19), and by Lemma 4.18(5) the third reduces to

$$\pi_{A,H}(\mathcal{A}) = \pi_{A,H}(\mathcal{B}). \tag{4.K}$$

To this end, consider the commutative diagram of triangulated categories

$$\begin{array}{ccc} \mathcal{D} & \xrightarrow{\mathbb{F}_w^{-1}} & \mathcal{D} \\ {\scriptstyle \pi_{A,H}}\downarrow & & \downarrow{\scriptstyle \pi_i} \\ \mathcal{D}/\langle \mathbb{F}_w S_i \rangle & \xrightarrow[\overline{\mathbb{F}_w^{-1}}]{} & \mathcal{D}/\langle S_i \rangle, \end{array}$$

where $\pi_i \coloneqq \pi_{A_+,H_i}$. Since the horizontal arrows are equivalences, (4.K) follows from the equality $\pi_i(\mathcal{A}_+) = \pi_i(\Phi_i^{\pm}\mathcal{A}_+)$, because

$$\overline{\mathbb{F}_w^{-1}}(\pi_{A,H}(\mathcal{A})) = \pi_i(\mathbb{F}_w^{-1}(\mathcal{A})) = \pi_i(\mathcal{A}_+),$$

and similarly for $\mathcal{B}$. This allows us to reduce to the case $w = 1$, for which

$$\begin{aligned} A &= A_+, & B &= s_i A_+, \\ \mathcal{A} &= \mathcal{A}_+, & \mathcal{B} &= \Phi_i^{\pm 1}(\mathcal{A}_+), \\ \mathcal{A}_H^{(1)} &= \operatorname{add} S_i, & \mathcal{B}_H^{(1)} &= \operatorname{add} S_i[\pm 1], \end{aligned}$$

by Lemma 4.18(3).

Let $M \in \mathcal{B}$. If we assume that $A \prec B$ with respect to the flow $\mathbb{F}$, then Lemma 3.47 implies $M \in \mathcal{R}_i(\mathcal{A})$ so that $\operatorname{Hom}_{\mathcal{A}}(H^0(M), S_i) = 0$, $H^{-1}(M) \in \operatorname{add} S_i$, and $H^k(M) = 0$ otherwise. Truncating as in (3.B), we obtain the triangle

$$\begin{array}{ccccccc} \tau^{\leq -1}M & \longrightarrow & M & \longrightarrow & \tau^{\geq 0}M & \longrightarrow \\ \wr\| & & \| & & \wr\| & \\ S_i^{\oplus m}[1] & \longrightarrow & M & \longrightarrow & N & \longrightarrow \end{array}$$

for some $N \in \mathcal{T}_i \subseteq \mathcal{A}_+$. Applying π_i kills the first term as we quotient by $\mathcal{D}_{A,H}^{(1)} = \langle S_i \rangle$. Therefore $\pi_i(M)$ is isomorphic to $\pi_i(N)$, giving $\pi_i(\mathcal{B}) \subseteq \pi_i(\mathcal{A})$. For the reverse inclusion, take $N \in \mathcal{A}$ and use left tilts with the triangle

$$\tau^{\leq 0}N \longrightarrow N \longrightarrow \tau^{\geq 1}N \longrightarrow$$

This entire argument is analogous if instead $A \succ B$. □

Chapter 5

Intersection arrangements

In this chapter we generalise the Coxeter arrangements defined in Chapter 2 to intersection arrangements in the sense of [IW], providing a dimension two classification in the hyperbolic setting.

§ 5.1 | Setup

We recall the key concepts of Iyama and Wemyss [IW, §1], before explaining differences between the hyperbolic and affine case. As usual, let Δ be a finite connected graph of rank rk without loops.

Through our Coxeter preliminaries we have defined an associated generalised Cartan matrix C_Δ (2.1), a Weyl group W_Δ (2.16), and a Coxeter arrangement $\mathcal{H}_\Delta$ (2.28). This arrangement lives inside a region known as the real level Level_Δ (2.31), which itself is a codimension one slice of the Tits cone TC_Δ (2.29), and the hyperplanes correspond to real roots $\alpha \in \mathsf{R}^{\mathsf{re}}_\Delta$ (2.22).

§ 5.1.1 | What is an intersection arrangement?

Let $\mathcal{J}$ be a subset of the vertices of Δ. Abusing notation slightly we write $\mathcal{J} \subseteq \Delta$, viewing it as a full subgraph of Δ throughout.

Example 5.1. Viewing $\mathcal{J}$ as shaded vertices, consider the following examples of the data $(\Delta, \mathcal{J})$.

(1) $(\mathbb{A}_3^{\mathrm{hyp}}, \{0,2\}) =$  .

(2) $(\mathbb{D}_6^{\mathrm{hyp}}, \{\infty,0,1,5,6\}) =$ 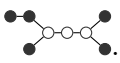 .

(3) $(\mathbb{E}_8^{\mathrm{hyp}}, \{\infty,1,2,3,5,7,8\}) =$ 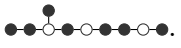 .

The indexing of $\mathcal{J}$ used above is that of diagrams (2.B)–(2.D) and is required for computations, but is otherwise unimportant. Going forward, it suffices to use the shaded diagram to convey $\mathcal{J} \subseteq \Delta$.

Notation 5.2. For $\mathcal{J} \subseteq \Delta$, we write:

(1) $\mathcal{J}^c := \Delta \backslash \mathcal{J}$.

(2) $\mathcal{J} + i \coloneqq \mathcal{J} \cup \{i\}$ for $i \in \mathcal{J}^c$.

(3) $\mathcal{J} - j \coloneqq \mathcal{J} \backslash \{j\}$ for $j \in \mathcal{J}$.

Again, these are all viewed as full subgraphs of Δ.

Definition 5.3. The *corank* of $\mathcal{J} \subseteq \Delta$ is $\mathsf{crk} \coloneqq |\mathcal{J}^c| = \mathsf{rk} - |\mathcal{J}|$.

Of interest in this thesis is the case $\mathsf{crk} = 3$, as in Example 5.1, in order to obtain a three dimensional arrangement. This becomes two dimensional after taking a suitable level in the affine or hyperbolic case.

Definition 5.4. Let $\mathcal{H}_\Delta$ be the Coxeter arrangement associated with a graph Δ. Then

$$\mathcal{H}_\mathcal{J} \coloneqq \mathcal{H}_\Delta \cap \{\vartheta \in \Theta \mid \vartheta_j = 0 \text{ for all } j \in \mathcal{J}\} = \mathcal{H}_\Delta \cap \bigcap_{j \in \mathcal{J}} H_j$$

is the *intersection arrangement* associated with $\mathcal{J} \subseteq \Delta$.

Note that if Δ is affine or hyperbolic then $\mathcal{H}_\mathcal{J}$ is $(\mathsf{crk} - 1)$-dimensional, viewing $\mathcal{H}_\Delta$ inside Level_Δ as in Section 2.3. However, in general $\mathcal{H}_\mathcal{J}$ is a real hyperplane arrangement in dimension crk. In their memoir [IW], Iyama and Wemyss go on to classify all affine tilings arising as intersection arrangements, seen in Theorem 1.3. Interestingly, they obtain all of these arrangements from type $\mathbb{E}^{\text{aff}}$, but as we will see in the hyperbolic setting, $\mathbb{A}^{\text{hyp}}$, $\mathbb{D}^{\text{hyp}}$, and $\mathbb{E}^{\text{hyp}}$ all contribute unique arrangements.

The main result of this chapter is an analogous classification for Δ hyperbolic, which must also be a finite list as by Theorem 2.26 there are only finitely many hyperbolic graphs with $\mathsf{rk} \geq 3$. To avoid the computational costs of determining a high dimensional Coxeter arrangement only to then reduce to dimension two or three, the next subsections outline a direct approach using $\mathcal{J}$-roots and the $\mathcal{J}$-level. First however, Definition 5.4 is made more precise, by defining analogous combinatorial objects to those in Chapter 2, but now depending on $\mathcal{J} \subseteq \Delta$.

§ 5.1.2 | $\mathcal{J}$-roots and $\mathcal{J}$-chambers

We recall the wall and chamber structure of intersection arrangements $\mathcal{H}_\mathcal{J}$, which provides a richer combinatorial structure than that of $\mathcal{H}_\Delta$. Just as the hyperplanes in the Coxeter arrangement correspond to positive real roots in the root system of Δ (now termed 'full roots'), hyperplanes in $\mathcal{H}_\mathcal{J}$ correspond to the following.

Definition 5.5. The set of *restricted roots* (or $\mathcal{J}$-roots) associated with $(\Delta, \mathcal{J})$ is

$$\mathsf{R}^{\mathsf{re}}_\mathcal{J} \coloneqq \{\alpha \in \mathsf{R}^{\mathsf{re}}_\Delta \mid \alpha|_{\mathcal{J}^c} \neq 0\}.$$

The condition $\alpha|_{\mathcal{J}^c} \neq 0$ ensures that $H_\alpha \cap \bigcap_{j \in \mathcal{J}} H_j$ is not the whole space $\mathbb{R}^{\mathsf{crk}}$. Then $\mathcal{H}_\mathcal{J}$ can be expressed as the union of restricted root hyperplanes, analogously to Definition 2.28, living in the $\mathcal{J}$-*cone*

$$\mathsf{TC}_\mathcal{J} \coloneqq \{\vartheta \in \mathsf{TC}_\Delta \mid \vartheta_j = 0 \text{ for all } j \in \mathcal{J}\}.$$

Definition 5.6. A $\mathcal{J}$-*chamber* in the intersection arrangement of $(\Delta, \mathcal{J})$ is a connected component of $\mathsf{TC}_{\mathcal{J}} \backslash \bigcup_{\alpha \in \mathsf{R}^{\mathrm{re}}_{\mathcal{J}}} H_\alpha$.

Despite the combinatorics of the intersection arrangement being more complicated, it is still possible to label the set of $\mathcal{J}$-chambers $\mathsf{Cham}_{\mathcal{J}}$. Let $W_{\mathcal{J}} \coloneqq \langle s_j \mid j \in \mathcal{J} \rangle \leq W_\Delta$ be the *parabolic (Weyl) subgroup*. If $\mathcal{J}$ is disconnected, then $W_{\mathcal{J}}$ is the product of the Weyl groups corresponding to each connected component.

Theorem 5.7 ([IW, Theorem 1.12])**.** *Let $\mathcal{J} \subseteq \Delta$. There is a bijection between chambers in the intersection arrangement $\mathcal{H}_{\mathcal{J}}$ and pairs (x, J), where $x \in W_\Delta$ and $J \subseteq \Delta$ satisfy*

(1) $\ell(x) = \min\{\ell(y) \mid y \in xW_J\}$,

(2) $W_{\mathcal{J}} x = xW_J$.

Clearly the pair $(1, \mathcal{J})$ satisfies the above conditions, and so plays the role of a fundamental chamber for $\mathcal{H}_{\mathcal{J}}$.

Example 5.8. The extreme situation is $\mathcal{J} = \varnothing$, which we call 'full corank'. In this case, Theorem 5.7 gives the chambers as

$$\mathsf{Cham}_\varnothing = \{(x, \varnothing) \mid x \in W_\Delta\} \cong W_\Delta,$$

and so recovers the correspondence between chambers and Weyl group elements seen in Section 2.3.

§ 5.1.3 | Simple wall-crossing

With the walls and chambers understood, we now discuss how to move between neighbouring chambers, generalising the Weyl group action.

Definition 5.9. Let Δ be a graph, let $\mathcal{J} \subseteq \Delta$, and let $i \in \mathcal{J}^c$. If the parabolic subgroup $W_{\mathcal{J}+i} \leq W_\Delta$ is finite then $\mathcal{J}$ is said to be *i-Dynkin*, and if this holds for all $i \in \mathcal{J}^c$ then $\mathcal{J}$ is called *strongly Dynkin*.

In other words, $\mathcal{J} + i$ is a *finitary subset* of Δ_0, and as a full subgraph it must be a disjoint union of ADE diagrams. In this case, recalling (2.J) we see that $W_{\mathcal{J}+i}$ has a longest element $w_{\mathcal{J}+i}$ and the graph $\mathcal{J} + i$ admits a Dynkin involution $\iota_{\mathcal{J}+i}$.

Definition 5.10. Let $A = (x, J)$ be a $\mathcal{J}$-chamber and suppose that J is i-Dynkin for some $i \in J^c$. The *simple wall-crossing* of A with respect to i is the chamber

$$\omega_i A \coloneqq (x w_J w_{J+i},\ J + i - \iota_{J+i}(i)).$$

We call the effect of this operation in the second slot *mutation*, which does not depend on the ambient $\mathcal{J}$.

Therefore if $J \subseteq \Delta$ is strongly Dynkin then the simple wall-crossing ω_i is well-defined for all $i \in J^c$. Starting from the 'standard chamber' $(1, \mathcal{J})$ we may repeatedly mutate to navigate the intersection arrangement. In this way, simple wall-crossings gives rise to the 1-skeleton of the intersection arrangement.

Example 5.11. We compute a simple wall-crossing for Example 5.1(1), that is

$$(\Delta, \mathcal{J}) = (\mathbb{A}_3^{\text{hyp}}, \{0, 2\}) =$$

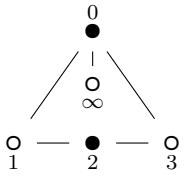

with the standard $\mathcal{J}$-chamber ($x = 1, J = \mathcal{J}$). Then $J + \infty$ is $\mathbb{A}_1 \times \mathbb{A}_2$ which has finite Weyl group, so we may mutate with respect to $i = \infty$ (indeed, J is strongly Dynkin). The longest elements are $w_J = s_0 s_2$ and $w_{J+\infty} = s_\infty s_0 s_\infty s_2$, and the Dynkin involution $\iota_{J+\infty}$ interchanges 0 and ∞. Hence the new chamber is

$$(y, K) \coloneqq \omega_\infty \left(1, \right) = \left(1 \cdot s_0 s_2 \cdot s_\infty s_0 s_\infty s_2, \right) = \left(s_\infty s_0, \right).$$

The simplification of the Weyl element is because s_2 commutes with s_0 and s_∞ in W_Δ, which then braid in W_Δ. This mutation process may then be continued by computing $\omega_j(y, K)$ for some $j \in K^c$, such as 0.

Theorem 5.12 ([IW, Theorem 1.20])**.** *Let $\mathcal{H}_\mathcal{J}$ be the intersection arrangement associated with $\mathcal{J} \subseteq \Delta$. Then the following statements hold:*

(1) *If $A = (x, J)$ is a $\mathcal{J}$-chamber, $i \in \mathcal{J}^c$, and J is i-Dynkin, then $B \coloneqq \omega_i A \in \mathsf{Cham}_\mathcal{J}$ and the wall between A and B is the restricted root hyperplane corresponding to $x\alpha_i$.*

(2) *If $\mathcal{J}$ is strongly Dynkin, then any two $\mathcal{J}$-chambers are connected by a finite sequence of simple wall-crossings, and this sequence has length one precisely when the $\mathcal{J}$-chambers are adjacent.*

(3) *Simple wall-crossing is involutive, that is, $\omega_{\iota_{J+i}(i)} \omega_i (x, J) = (x, J)$.*

Lemma 5.13. *If Δ is hyperbolic and $\mathcal{J} \subseteq \Delta$ has $\mathsf{crk} \geq 3$, then $\mathcal{J}$ is strongly Dynkin.*

Proof. Let $i \in \mathcal{J}^c$ be arbitrary and suppose that $|W_{\mathcal{J}+i}| = \infty$. Then $\mathcal{J} + i \subset \Delta$ is a tame or wild subgraph of rank at most $\mathsf{rk} - 3 + 1 = \mathsf{rk} - 2$. The wild option is impossible as Δ is hyperbolic, and the tame option is impossible since tame subgraphs must have rank $\mathsf{rk} - 1$ by Lemma 2.13. Hence $W_{\mathcal{J}+i}$ must be finite. □

Therefore we do not need to worry about satisfying the strongly Dynkin condition in the classification of hyperbolic intersection arrangements with corank three, allowing us to wall-cross with impunity.

Remark 5.14. In [IW, Proposition 3.2], it is observed that type $\mathbb{A}$ (sub)graphs only ever give type $\mathbb{A}$ relations, in the sense that if $\mathcal{J} \subseteq \Delta$ is strongly Dynkin and $\mathcal{J} + i + k = \mathbb{A}_n$ then $\omega_{i'}\omega_k\omega_i = \omega_{k'}\omega_i\omega_k$. It is also easy to see that if i and k belong to disjoint components in $\mathcal{J} + i + k$, then $\omega_i\omega_k = \omega_k\omega_i$. More complicated braid relations arise when $\mathcal{J} + i + k$ is type $\mathbb{D}$ or $\mathbb{E}$, giving behaviour not usually associated with a simply laced graph.

As might be expected from the study of hyperbolic Coxeter arrangements, free relations (and hence ∞-gons in the dual graph) between simple wall-crossings ω_i and ω_k can arise for Δ hyperbolic, as by crossing codimension two walls it is possible to leave the Tits cone. This happens precisely when $\mathcal{J} + i + k$ is affine, such as $\mathcal{J} + 1 + 3$ in Example 5.11. This cannot happen for Δ affine and $\mathcal{J}$ corank three, as seen in Theorem 1.3.

§ 5.2 | Hyperbolic computations

In this section we discuss the process of drawing the arrangements defined in Section 5.1 in the hyperbolic setting. Our main result is that if Δ is hyperbolic then restricting C_Δ to a corank three submatrix still gives rise to a hyperbolic quadratic form. This is then implemented using the computer algebra in Appendix A.

§ 5.2.1 | The $\mathcal{J}$-Level

As in the case of the Coxeter arrangements, we wish to take a real level, reducing the dimension by one to aid visualisation without losing any combinatorial structure. The natural choice is to use the principal submatrix of C_Δ^{-1}, with rows and columns corresponding to the vertices in $\mathcal{J}^c$, and consider the associated quadratic form. However, it is not clear a priori (indeed, we show that $\mathsf{crk} \geq 3$ is important) that this submatrix retains the hyperbolic signature of C_Δ^{-1} from Lemma 2.10, which we need in order to view a hyperbolic intersection arrangement on the Poincaré disc. To this end, we invoke two classical results from the theory of matrices.

Theorem 5.15 (Jacobi complementary minor, cf. [Lal96, (1)])**.** *Let C be a square matrix and let J, K be subsets of its indices with $|J| = |K|$. Then*

$$\det C^{-1}[K^c, J^c] = (-1)^{\Sigma J^c + \Sigma K^c} \frac{\det C[J, K]}{\det C},$$

where $C[J, K]$ is the $|J| \times |K|$ submatrix of C with rows in J and columns in K, and $\Sigma J^c, \Sigma K^c$ are the sum of the indices in J, K, respectively.

Theorem 5.16 (Poincaré separation, cf. [Bel97, §7.10])**.** *Let C be an $r \times r$ real symmetric matrix with eigenvalues $\lambda_1 \geq \ldots \geq \lambda_r$, and let D be an $r \times s$ semi-orthogonal matrix such that $D^\top D$ is the identity matrix. Then the eigenvalues μ_i of the $s \times s$ matrix $D^\top CD$ satisfy $\lambda_i \geq \mu_i \geq \lambda_{r-s+i}$ for all $i \in \{1, \ldots, s\}$.*

Now consider the *restricted GCM* (or $\mathcal{J}$-Cartan) $C_\mathcal{J} \coloneqq C_\Delta^{-1}[\mathcal{J}^c, \mathcal{J}^c] = D_\mathcal{J}^\top C_\Delta^{-1} D_\mathcal{J}$. Here $D_\mathcal{J}$ is the $\mathsf{rk} \times \mathsf{crk}$ semi-orthogonal matrix with columns $\{\alpha_i \mid i \in \mathcal{J}^c\}$, which clearly satisfies $D_\mathcal{J}^\top D_\mathcal{J} = I_{\mathsf{crk}}$.

Lemma 5.17 (Cf. 2.10)**.** *If Δ is hyperbolic and $\mathcal{J} \subseteq \Delta$ has corank at least three, then $C_\mathcal{J}$ has hyperbolic signature.*

Proof. If Δ is hyperbolic then $\det C_\Delta$ is negative by Lemma 2.10. Since $\mathcal{J}$ has $\mathsf{crk} \geq 3$, by Lemma 2.13 the principal submatrix $C_\Delta[\mathcal{J}, \mathcal{J}]$ must be a GCM of finite type as Δ is hyperbolic. Hence $\det C_\Delta[\mathcal{J}, \mathcal{J}]$ is positive, and so

$$\det C_\mathcal{J} = \det C_\Delta^{-1}[\mathcal{J}^c, \mathcal{J}^c] \overset{5.15}{=} (-1)^{2\Sigma\mathcal{J}^c} \frac{\det C_\Delta[\mathcal{J}, \mathcal{J}]}{\det C_\Delta} < 0.$$

Therefore, zero is not an eigenvalue of the restricted GCM, and $C_\mathcal{J}$ has at least one negative eigenvalue. Now suppose that $\mu_i \geq \mu_j$ are two negative eigenvalues of $C_\mathcal{J} = D_\mathcal{J}^\top C_\Delta^{-1} D_\mathcal{J}$. Then Theorem 5.16 implies that the eigenvalues λ_i of C_Δ^{-1} satisfy

$$0 > \mu_i \geq \lambda_{\mathsf{rk}-\mathsf{crk}+i}, \qquad 0 > \mu_j \geq \lambda_{\mathsf{rk}-\mathsf{crk}+j},$$

contradicting Lemma 2.10. Thus $C_\mathcal{J}$ must have at most one negative eigenvalue. □

In light of Lemma 5.17, we may visualise corank three hyperbolic intersection arrangements as in Section 2.3, but now on the $\mathcal{J}$-*Level*

$$\mathsf{Level}_\mathcal{J} \coloneqq \left\{ \vartheta \in \mathsf{TC}_\mathcal{J} \;\middle|\; \vartheta^\top C_\mathcal{J} \vartheta = -1 \right\} \cong \mathsf{Level}_\Delta \cap \bigcap_{j \in \mathcal{J}} H_j, \tag{5.A}$$

where the last bijection accounts for the fact that Level_Δ was defined using $\operatorname{Adj} C_\Delta$ and so we must scale by the determinant. Furthermore, as this result holds for higher corank, the same computation may be used for hyperbolic intersection arrangements in higher dimension. We discuss this possibility further in Section 6.2.

Finally we mimic the end of Section 2.3 and redefine the intersection arrangement associated with $(\Delta, \mathcal{J})$ (where Δ is hyperbolic and $\mathcal{J}$ has corank at least three) to be

$$\mathcal{H}_\mathcal{J} = \bigcup_{\alpha \in \mathsf{R}^{\mathsf{re}}_\mathcal{J}} (H_\alpha \cap \mathsf{Level}_\mathcal{J}).$$

Just as we passed from chambers to alcoves in the global Coxeter setting, we now consider $\mathcal{J}$-alcoves, the connected components of $\mathsf{Level}_\mathcal{J} \setminus \mathcal{H}_\mathcal{J}$. By [Hum90, §6.5], $\mathcal{J}$-alcoves are in bijection with $\mathcal{J}$-chambers, and so they are also labelled using Theorem 5.7.

Definition 5.18 (Cf. 2.34)**.** The connected component $(1, \mathcal{J}) = \Theta_+ \cap \mathsf{Level}_\Delta$ (respectively $\Theta_+ \cap \mathsf{TC}_\Delta$) is called the *standard $\mathcal{J}$-alcove* (respectively, chamber) in the intersection arrangement associated with $(\Delta, \mathcal{J})$.

§ 5.2.2 | Diagonalisation and intersection

Next, for completeness, we make precise the identification of $\mathsf{Level}_{\mathcal{J}}$ with the disc model for hyperbolic space. For simplicity we work in corank three as this is the case to be classified, but a generalisation to higher dimensions is clear.

Let $\mathcal{J} \subseteq \Delta$ be corank three hyperbolic, so that by Lemma 5.17 the restricted GCM $C_{\mathcal{J}}$ has two positive eigenvalues μ_1, μ_2, and one negative eigenvalue μ_3. Define the $\mathsf{crk} \times \mathsf{crk}$ matrix product

$$Q_{\mathcal{J}} \coloneqq \begin{pmatrix} | & | & | \\ u_1 & u_2 & u_3 \\ | & | & | \end{pmatrix} \cdot \begin{pmatrix} \sqrt{|\mu_1|} & 0 & 0 \\ 0 & \sqrt{|\mu_2|} & 0 \\ 0 & 0 & \sqrt{|\mu_3|} \end{pmatrix},$$

where u_1, u_2, u_3 are the orthonormalised eigenvectors of $C_{\mathcal{J}}$. By Sylvester's law of inertia [Syl52], the $\mathcal{J}$-Cartan decomposes as

$$C_{\mathcal{J}} = Q_{\mathcal{J}} \begin{pmatrix} 1 & 0 & 0 \\ 0 & 1 & 0 \\ 0 & 0 & -1 \end{pmatrix} Q_{\mathcal{J}}^{\top}. \tag{5.B}$$

Using the change of variables $\eta \coloneqq Q_{\mathcal{J}}\vartheta$, the intersection $\mathsf{Level}_{\mathcal{J}} \cap H_\alpha$ for some $\alpha \in \mathsf{R}^{\mathsf{re}}_{\mathcal{J}}$ satisfies the system of equations

$$\eta_1^2 + \eta_2^2 - \eta_3^2 = -1, \qquad \beta_1\eta_1 + \beta_2\eta_2 + \beta_3\eta_3 = 0,$$

where $\beta \coloneqq Q_{\mathcal{J}}^{-1}\alpha$. This is now easily solved in terms of η_3 to give a curve (η_1, η_2, η_3) in $\mathbb{R}^3$ with parametrisation

$$\begin{aligned} \eta_1 &= \frac{-\beta_1\beta_3\eta_3 - \beta_2\sqrt{(\beta_1^2+\beta_2^2-\beta_3^2)(\eta_3^2-1)-\beta_3^2}}{\beta_1^2+\beta_2^2}, \\ \eta_2 &= \frac{-\beta_2\beta_3\eta_3 - \beta_1\sqrt{(\beta_1^2+\beta_2^2-\beta_3^2)(\eta_3^2-1)-\beta_3^2}}{\beta_1^2+\beta_2^2}. \end{aligned} \tag{5.C}$$

We then stereographically project this curve to the unit disc via the point $(0, 0, -1)$, which is the map $(\eta_1, \eta_2, \eta_3) \longmapsto (\frac{\eta_1}{1+\eta_3}, \frac{\eta_2}{1+\eta_3})$. The image of (5.C) under this projection tends to the following as $\eta_3 \to \infty$:

$$\begin{aligned} I_1 &= \left(\frac{-\beta_1\beta_3 - \beta_2\sqrt{\beta_1^2+\beta_2^2-\beta_3^2}}{\beta_1^2+\beta_2^2}, \ \frac{-\beta_2\beta_3 + \beta_1\sqrt{\beta_1^2+\beta_2^2-\beta_3^2}}{\beta_1^2+\beta_2^2} \right), \\ I_2 &= \left(\frac{-\beta_1\beta_3 + \beta_2\sqrt{\beta_1^2+\beta_2^2-\beta_3^2}}{\beta_1^2+\beta_2^2}, \ \frac{-\beta_2\beta_3 - \beta_1\sqrt{\beta_1^2+\beta_2^2-\beta_3^2}}{\beta_1^2+\beta_2^2} \right). \end{aligned} \tag{5.D}$$

These *ideal points* lie on the boundary of the unit disc and have entries depending solely on root data. Hence we see that the restricted root α leads to a wall in the intersection arrangement if and only if β satisfies $\beta_1^2 + \beta_2^2 \geq \beta_3^2$, which is easy to

check with computer algebra. If β, β' are the image of two restricted roots α, α' under change of coordinates and $\gamma = \beta \times \beta'$ is their vector product, then the intersection of the corresponding geodesics in the disc is the point

$$\left(\frac{\gamma_1}{\gamma_3 + \operatorname{sign}(\gamma_3)\sqrt{\gamma_3^2 - \gamma_1^2 - \gamma_2^2}}, \frac{\gamma_2}{\gamma_3 + \operatorname{sign}(\gamma_3)\sqrt{\gamma_3^2 - \gamma_1^2 - \gamma_2^2}} \right), \tag{5.E}$$

provided that $\gamma_3^2 \geq \gamma_1^2 + \gamma_2^2$.

Finally we can draw the geodesic between these points in $\mathbb{H}^2$. Recall from hyperbolic geometry (see [CFKP97, §7]) that this geodesic is the minor arc of a circle that is perpendicular to the disc and passes through the points (5.D). By considering the points I_1, I_2 as complex numbers with phases φ_1, φ_2, we can express the radius and centre of this geodesic as

$$R = \tan \tfrac{|\varphi_1 - \varphi_2|}{2}, \qquad C = \operatorname{sign}(R)\sqrt{1 + R^2}(\cos \tfrac{\varphi_1 + \varphi_2}{2}, \sin \tfrac{\varphi_1 + \varphi_2}{2}). \tag{5.F}$$

If I_1 and I_2 are on opposite sides of the disc then $|\varphi_1 - \varphi_2| = \pi$, and (5.F) becomes a circle of infinite radius through the points I_1 and I_2, that is, a straight line.

§ 5.2.3 | Drawing intersection arrangements

We conclude this computational section by briefly outlining the process in which the arrangements in Section 5.4 are drawn.

We start with the standard $\mathcal{J}$-alcove $A_+ := (1, \mathcal{J})$, which is bounded by the simple (restricted) root hyperplanes $\{H_i \mid i \in \mathcal{J}^c\}$. For each such i, compute $\omega_i A_+$, which is of the form (x, J) for some $w \in W_\Delta$ and $J \subseteq \Delta$. Now mutate again for this new alcove, where we do not need to mutate with respect to $i' := \iota_{\mathcal{J}+i}(i)$ as this would be moving 'backwards'. At each step record the roots $x\alpha_i$ which correspond to the walls of the $\mathcal{J}$-alcoves. Proceed until d wall-crossing steps have been carried out, where $d \in \mathbb{Z}_{\geq 0}$.

For each unique $\alpha \in \mathsf{R}^{\mathsf{re}}_{\mathcal{J}}$ found this way, restrict to $\mathcal{J}^c$ and intersect with $\mathsf{Level}_{\mathcal{J}}$ as outlined in the previous subsection, after applying the coordinate change (5.B) using the eigenspace of $C_{\mathcal{J}}$. The intersections are then drawn as geodesics in the Poincaré disk following (5.D) and (5.F).

Example 5.19. We give the restricted GCM, the change of basis matrix, and the

intersection arrangement associated with the data in Example 5.1.

5.1	(1)	(2)	(3)
Δ	$\mathbb{A}_3^{\text{hyp}}$	$\mathbb{D}_6^{\text{hyp}}$	$\mathbb{E}_8^{\text{hyp}}$
$\mathcal{J}$		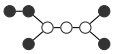	
$C_{\mathcal{J}}$	$-\frac{1}{4}\begin{pmatrix} 0 & 4 & 4 \\ 4 & 5 & 7 \\ 4 & 7 & 5 \end{pmatrix}$	$-\begin{pmatrix} 6 & 6 & 6 \\ 6 & 5 & 5 \\ 6 & 5 & 4 \end{pmatrix}$	$-2\begin{pmatrix} 1 & 6 & 4 \\ 4 & 21 & 15 \\ 4 & 15 & 10 \end{pmatrix}$
$Q_{\mathcal{J}}$	$\begin{pmatrix} 0.697 & 0.000 & 0.697 \\ -0.196 & 0.500 & 1.240 \\ -0.196 & -0.500 & 1.240 \end{pmatrix}$	$\begin{pmatrix} 0.702 & 0.223 & 2.557 \\ -0.061 & -0.478 & 2.287 \\ -0.768 & 0.242 & 2.156 \end{pmatrix}$	$\begin{pmatrix} 0.986 & 0.456 & 1.783 \\ -0.549 & 0.336 & 6.513 \\ 0.400 & -0.662 & 4.539 \end{pmatrix}$
$\mathcal{H}_{\mathcal{J}}$	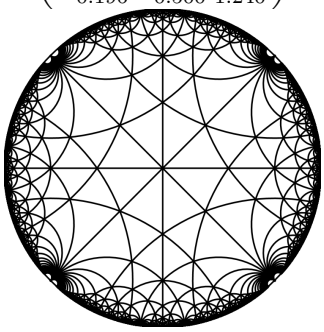	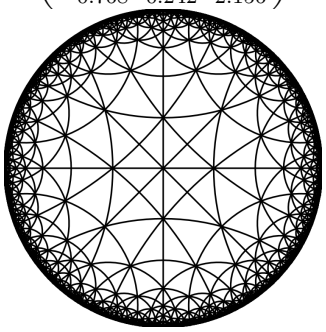	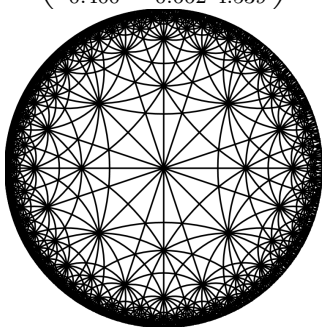

One can verify in these examples that $Q_{\mathcal{J}}^{-1} C_{\mathcal{J}} Q_{\mathcal{J}}^{-\top}$ gives the hyperbolic-signature diagonal matrix.

§ 5.3 | Symmetric mutation classes

Having defined intersection arrangements and outlined how to compute them directly, this section begins the process of classifying the hyperbolic intersection arrangements in dimension two, that is, the number of 'different' arrangements $\mathcal{H}_{\mathcal{J}}$ that arise from the data $(\Delta, \mathcal{J})$, where:

(1) Δ is hyperbolic,

(2) $\mathcal{J} \subseteq \Delta$ has corank three.

§ 5.3.1 | Number of subsets

We start with a simple combinatorial calculation to give an upper bound for the number of arrangements. Taking from (2.E) the hyperbolic graphs that admit corank three subsets, that is the 23 graphs in rank three and above, the total number of such subsets is

$$5\binom{3}{3} + 3\binom{4}{3} + 2\binom{5}{3} + 3\binom{6}{3} + 2\binom{7}{3} + 3\binom{8}{3} + 3\binom{9}{3} + 2\binom{10}{3} = 827. \tag{5.G}$$

Thankfully, many of these subsets will lead to the same arrangement. This is because starting at two different $\mathcal{J}$-alcoves (x, J) and (y, K), applying wall-crossing would eventually yield the same as if we had started at $(1, \mathcal{J})$. It follows that $\mathcal{H}_J = \mathcal{H}_K$, and this motivates the main definition of the section.

Definition 5.20. Two subsets J and K of a graph Δ are *symmetric mutation equivalent*, denoted $J \sim K$, if either

(1) there exist a sequence of mutations (in the sense of Definition 5.10) connecting J and K,

(2) J and K are isomorphic as bicoloured graphs.

The *symmetric mutation class* of $\mathcal{J} \subseteq \Delta$ is the set $[\mathcal{J}] := \{J \subseteq \Delta \mid J \sim \mathcal{J}\}$.

Case (2) in Definition 5.20 identifies subsets that are technically different at the level of sets (and can't be mutated to each other), but are essentially the same and will clearly give identical intersection arrangements. Consider, for example, the subsets

of the graph $\mathbb{D}_4^{\text{hyp}}$. These cannot reach each other via simple wall-crossing but are the same as bicoloured graphs.

Example 5.21. Recalling the data $(\Delta, \mathcal{J})$ from Example 5.1, we compute the symmetric mutation class of each. By colouring the three vertices in $\mathcal{J}^c$, we may easily keep track of the mutation process.

(1) 

In J_1 we can mutate with respect to any coloured vertex. However, only the vertex $\bullet$ moves under mutation, as both $\bullet$ and $\bullet$ lie in the middle of an $\mathbb{A}_3$ graph so are fixed under the associated Dynkin involution. Applying the mutation $\omega_{\bullet}$ gives J_2, from which mutating with respect to the vertex $\bullet$ would return us to J_1 by Theorem 5.12(3). However, now $\bullet$ lives in an $\mathbb{A}_2$ graph so will move under mutation, giving J_3. From here we notice that $\bullet$ and $\bullet$ are 'stuck', but we may apply a symmetry of $\mathbb{A}_3^{\text{hyp}}$ to obtain J_4. This is the final element of $[J]$, as $\bullet$ and $\bullet$ are fixed under mutation, and applying $\omega_{\bullet}$ gives back J_2.

(2) 

Applying $\omega_{\bullet}$ to K_1 yields K_2, noting that $\bullet$ and $\bullet$ live in the middle of graphs $\mathbb{A}_1$ and $\mathbb{A}_3$, respectively. In K_2 however, $\bullet$ is in the graph $\mathbb{A}_4$ and is free to move under mutation (this results in K_3) whilst $\bullet$ is still stuck. The mutation $\omega_{\bullet}$ then gives K_4, trapping $\bullet$ and closes the symmetric mutation class $[K]$, as this is also fixed under symmetries of the graph $\mathbb{D}_6^{\text{hyp}}$.

(3) 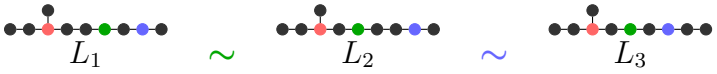

With $\bullet$ and $\bullet$ in the middle of graphs $\mathbb{E}_6$ and $\mathbb{A}_3$ respectively, the only nontrivial choice of mutation from L_1 is with respect to $\bullet$. Obtaining L_2, we see that $\bullet$ is now in an $\mathbb{A}_4$ graph (with $\bullet$ still at a branch vertex, unaffected by Dynkin involutions) and so using $\omega_{\bullet}$ results in L_3. Here $\bullet$ and $\bullet$ will not move under mutation, and the graph $\mathbb{E}_8^{\text{hyp}}$ does not admit automorphisms, so $[L]$ is closed.

In each case we see that no other sets of shaded vertices can be obtained by symmetric mutation.

The colouring for $\mathcal{J}^c$ introduced in Example 5.21 is used going forward to compute symmetric mutation classes, which we may describe using the following useful invariant.

Definition 5.22. The *cotype* of $\mathcal{J} \subseteq \Delta$ is the unordered list $\Delta_1 \cdots \Delta_\ell$ of disjoint graphs in the full subgraph corresponding to $\mathcal{J}$.

The cotype is constant across a symmetric mutation equivalence class, which follows from the fact that Dynkin involutions keep the type of shaded graph unchanged. Any corank three subset $\mathcal{J}$ in the hyperbolic setting is a disjoint union of ADE graphs, so the indices in the cotype should always add to $\mathsf{rk} - 3$.

Example 5.23. We continue with Example 5.1.

(1)  has cotype $\mathbb{A}_1^2$.

(2) 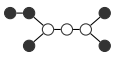 has cotype $\mathbb{A}_1^3\mathbb{A}_2$.

(3)  has cotype $\mathbb{A}_1^3\mathbb{A}_2^2$.

Comparing with Example 5.21 we see that the cotype is indeed constant throughout the classes $[J]$, $[K]$, and $[L]$.

§ 5.3.2 | Summary of hyperbolic symmetric mutation classes

The following is the main result of this section, and is proven via a series of direct computations. The mutation computations were first carried out by hand and then independently verified using the function `SMC` in Appendix A.2. All angle data were computed using standard `Magma` Coxeter group commands.

Theorem 5.24. *The* 827 *corank three subsets of a hyperbolic graph* Δ *partition into the* 200 *symmetric mutation classes summarised below.*

rk	$\binom{\mathsf{rk}}{3}$	Δ	classes	sizes (multiplicity)	Prop.
3	1	$\mathbb{A}_1^{\text{hyp}}$	1	1	5.25
		$\mathbb{A}_{1,1}^{\text{hyp}}$	1	1	
		$\mathbb{A}_{2,1}^{\text{aff}}$	1	1	
		$\mathbb{A}_{2,2}^{\text{aff}}$	1	1	
		$\mathbb{A}_{2,3}^{\text{aff}}$	1	1	
4	4	$\mathbb{A}_2^{\text{hyp}}$	1	4	5.26
		$\mathbb{A}_{2,1}^{\text{hyp}}$	1	4	
		$\mathbb{A}_{2,2}^{\text{hyp}}$	1	4	

5	10	$\mathbb{A}_3^{\mathrm{hyp}}$	3	$1, 4, 5$	5.27
		$\mathbb{A}_{3,1}^{\mathrm{hyp}}$	3	$1, 3, 6$	5.28
6	20	$\mathbb{A}_4^{\mathrm{hyp}}$	3	$3, 7, 10$	5.29
		$\mathbb{D}_4^{\mathrm{hyp}}$	5	$1, 3, 4, 6(2)$	5.30
		$\mathbb{S}_5$	2	$10(2)$	5.31
7	35	$\mathbb{A}_5^{\mathrm{hyp}}$	8	$1(3), 3, 4, 7, 8, 10$	5.32
		$\mathbb{D}_5^{\mathrm{hyp}}$	10	$1(3), 2(2), 3(2), 6, 7, 9$	5.33
8	56	$\mathbb{A}_6^{\mathrm{hyp}}$	8	$2(2), 3, 5, 8, 9, 13, 14$	5.34
		$\mathbb{D}_6^{\mathrm{hyp}}$	18	$1(3), 2(6), 3(4), 4, 5, 6(2), 8$	5.35
		$\mathbb{E}_6^{\mathrm{hyp}}$	10	$1(2), 3(2), 4, 5, 6, 10, 11, 12$	5.36
9	84	$\mathbb{A}_7^{\mathrm{hyp}}$	17	$1(5), 2(2), 3(2), 4(2), 6, 8, 10, 11, 12, 14$	5.37
		$\mathbb{D}_7^{\mathrm{hyp}}$	25	$1(7), 2(3), 3(3), 4(5), 5(4), 7(2), 8$	5.38
		$\mathbb{E}_7^{\mathrm{hyp}}$	20	$1(5), 2(3), 3(3), 4(3), 5(2), 8, 9(2), 16$	5.39
10	120	$\mathbb{D}_8^{\mathrm{hyp}}$	40	$1(10), 2(10), 3(8), 4(5), 5(4), 6, 9, 11$	5.40
		$\mathbb{E}_8^{\mathrm{hyp}}$	20	$1(2), 2(3), 3(2), 4(4), 5, 6, 7, 8, 9(2), 13, 14, 19$	5.41

Here 'size' is the number of corank three subsets in each class, and the multiplicity $m(n)$ means that there are n symmetric mutation classes of size m.

Proof. We first observe that the number of classes sum to 200 and the class sizes (after taking multiplicity) sum to 827 as expected from (5.G). The computation of the symmetric mutation classes is split over Propositions 5.25 to 5.41 in the following subsections. We proceed by rank, giving a list of class representatives for each graph in the form $[\mathcal{J}]^{(m;\Delta_1\cdots\Delta_\ell)}$ where the parenthetical data is the size of the class and its cotype, respectively. For Δ of fixed rank $3 \leq \mathsf{rk} \leq 10$, the classes are directly computed as follows:

(1) Start with any subset $\mathcal{J} \subseteq \Delta$, of which there are $\binom{\mathsf{rk}}{3}$.

(2) Compute $\boldsymbol{\omega}_i(1, \mathcal{J})$ for each $i \in \mathcal{J}^c$.

(3) If a new subset J is obtained then we know that $J \in [\mathcal{J}]$.

(4) Repeat this process until simple wall-crossings no longer give different subsets.

(5) Take the closure of the current collection of subsets with respect to bicoloured graph automorphisms, viewing $\mathcal{J}^c$ as a single colour (unshaded).

Now choose $\mathcal{J} \neq \mathcal{J}' \subseteq \Delta$ and repeat, until all subsets of Δ have been accounted for. Writing $\mathcal{J}^c = \{\bullet, \bullet, \bullet\}$ as in Example 5.21, we illustrate the steps above using a (symmetric) mutation table:

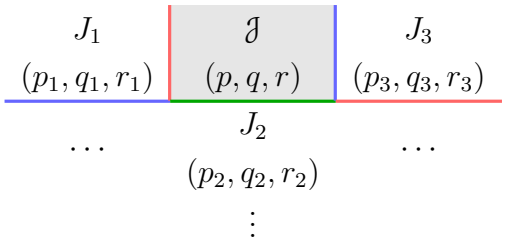

The shaded cell denotes the class representative $\mathcal{J}$. Each cell represents a unique subset of Δ, and a wall (coloured by vertices in $\mathcal{J}^c = \{i, j, k\}$) is drawn between two cells if and only if the corresponding subsets are related by mutation in the sense of Definition 5.20(1). Below each subset we include its *angle data*, a triple of exponents (p, q, r) corresponding to the pairs $\{i, j\}$, $\{i, k\}$, and $\{j, k\}$, such that

$$(\omega_{\color{red}\bullet}\omega_{\color{green}\bullet})^p(x, J) = (\omega_{\color{red}\bullet}\omega_{\color{blue}\bullet})^q(x, J) = (\omega_{\color{green}\bullet}\omega_{\color{blue}\bullet})^r(x, J) = (x, J). \tag{5.H}$$

This provides a local version of the Coxeter data m_{ij} from Definition 2.16. Whilst not required until Section 5.4, the angle data is convenient to compute while doing wall-crossing calculations, and by [IW, Remark 3.4] it suffices to keep track of the length of Weyl elements when determining the braid length of a pair of mutations.

If a wall of a certain colour is missing beside a cell, by convention this is because mutating with respect to that colour gives a cell already present in the table, up to some permutation of the coloured vertices. Similarly we use a dashed wall to represent mutation with respect to that colour leaving the subset unchanged. Every subset is adjacent to at least one wall, so it is always be possible to get between any two members of the symmetric mutation class via a finite sequence of wall-crossings, as in Theorem 5.12(2). □

§ 5.3.3 | Rank three classes

This is the trivial case $\mathcal{J} = \varnothing$, and as such all symmetric mutation classes are singletons and the resulting intersection arrangements are Coxeter. Hence we recover Example 2.35.

Proposition 5.25. *There are five corank three symmetric mutation classes for hyperbolic graphs of rank three, shown below.*

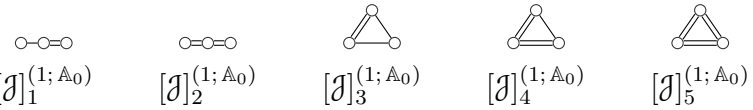

Proof. For each graph above there is only one way to choose a corank three subset, that is the empty set, and so the symmetric mutation class must be a singleton. □

§ 5.3.4 | Rank four classes

This is only slightly less trivial, with again a single class for each Δ but this time with local structure, as the angle data varies across the class.

Proposition 5.26. *Let Δ be a hyperbolic graph of rank four. Then any corank three subset of Δ belongs in one of the following symmetric mutation classes.*

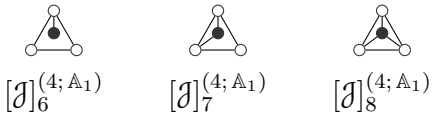

$[\mathcal{J}]_6^{(4;\,\mathbb{A}_1)}$ $[\mathcal{J}]_7^{(4;\,\mathbb{A}_1)}$ $[\mathcal{J}]_8^{(4;\,\mathbb{A}_1)}$

Proof. We start with $[\mathcal{J}]_6$, taking the proposed representative and mutating repeatedly to obtain the symmetric mutation table below.

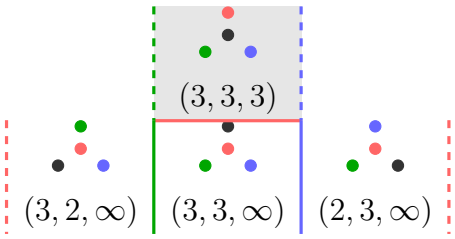

From the representative in cell $(2,1)$, notice that only $\bullet$ will mutate in a nontrivial way, as $\bullet$ and $\bullet$ are stuck in an $\mathbb{A}_1$ graph. This is indicated by a solid red wall but dashed green and blue walls. Applying $\omega_{\bullet}$ we move into cell $(2,2)$, wherein now $\bullet$ and $\bullet$ sit in an $\mathbb{A}_2$ graph, and will mutate. In doing the mutations $\omega_{\bullet}$ and $\omega_{\bullet}$, we obtain the subsets in cells $(1,2)$ and $(3,2)$ respectively. At this point we can stop, since every possible corank three subset has been observed. In general, it is harder to check if a symmetric mutation class is closed.

For the angle data of $[\mathcal{J}]_6$, this may be directly computed or one can invoke Remark 5.14. Consider, for example, the subset in cell $(1,2)$. Shading both $\bullet$ and $\bullet$ gives a $\mathbb{A}_3$, so the corresponding simple wall-crossings have a braid relation of length three. The vertices $\bullet$ and $\bullet$ belong to different components, so $\omega_{\bullet}$ and $\omega_{\bullet}$ commute. Finally, shading $\bullet$ and $\bullet$ yields $\mathbb{A}_2^{\text{aff}}$, implying that there is no relation between their simple wall-crossings. Hence the angle data for this subset is $(3,2,\infty)$, which we note is locally the Coxeter arrangement for $\mathbb{A}_1^{\text{hyp}}$.

Moving to the classes $[\mathcal{J}]_7$ and $[\mathcal{J}]_8$, the procedure is largely the same, with the only difference being the angle data obtained and the mutations used.

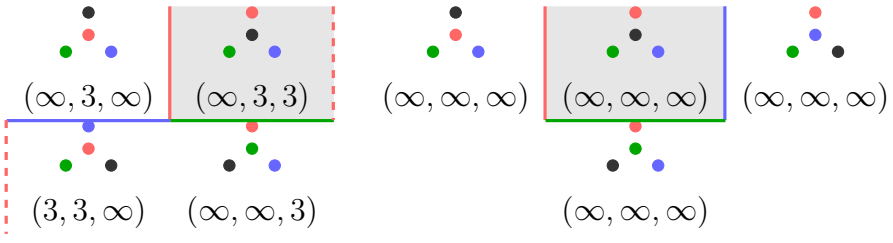

It follows that each hyperbolic graph of rank four gives rise to a single mutation class. □

§ 5.3.5 | Rank five classes

Proposition 5.27. *The* $\binom{5}{3} = 10$ *corank three subsets of* $\mathbb{A}_3^{\text{hyp}}$ *partition into the following three symmetric mutation classes.*

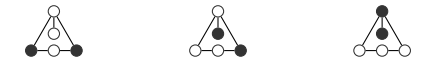

Proof. Consider the subset representing $[\mathcal{J}]_9$. The overextended vertex is disconnected from $\mathcal{J}$, and the other vertices lie in the centre of the graph $\mathbb{A}_3$. Furthermore, $\mathcal{J}$ is symmetric with respect to the only automorphism of $\mathbb{A}_3^{\text{hyp}}$, so the class $[\mathcal{J}]_9$ is a singleton. We have already computed $[\mathcal{J}]_{10}$ in Example 5.21(1), confirming its mutation table and that of $[\mathcal{J}]_{11}$ below.

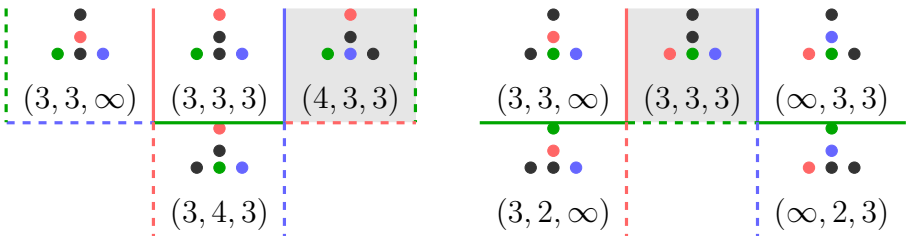

Both tables are closed under graph automorphisms, and the left table has three walls for every cell so is clearly closed under mutation. In the right table, applying $\omega_\bullet$ to the subset in cell $(1,1)$ gives cell $(3,1)$ after forgetting colours, and the bottom two subsets are related similarly. As we have accounted for all ten subsets of $\mathbb{A}_{3,1}^{\text{hyp}}$, this completes the partition into symmetric mutation classes. □

From now on only the largest stated class is explicitly described. The other classes have been determined similarly and then double-checked alongside the angle data using the `Magma` code in Appendix A.2 and Appendix A.3.

Proposition 5.28. *The* $\binom{5}{3} = 10$ *corank three subsets of* $\mathbb{A}_{3,1}^{\text{hyp}}$ *partition into the following three symmetric mutation classes.*

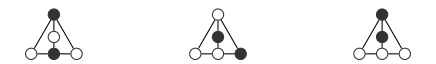

Proof. For the largest class, $[\mathcal{J}]_{14}$, we have the mutation table

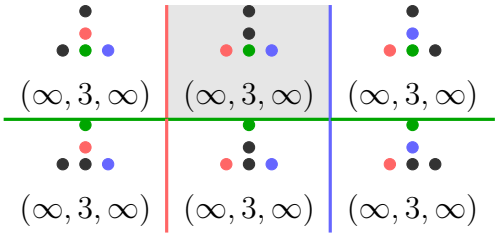

which is closed under mutation and the only automorphism of $\mathbb{A}_{3,1}^{\text{hyp}}$. Indeed, the subsets in the left column are symmetric to the subsets in the right column, and the middle column has already been mutated fully. □

§ 5.3.6 | Rank six classes

Proposition 5.29. *The* $\binom{6}{3} = 56$ *corank three subsets of* $\mathbb{A}_4^{\text{hyp}}$ *partition into the following three symmetric mutation classes.*

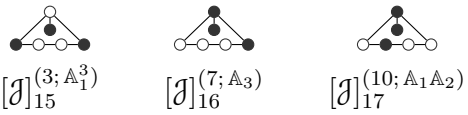

Proof. The mutation table for $[\mathcal{J}]_{17}$ is

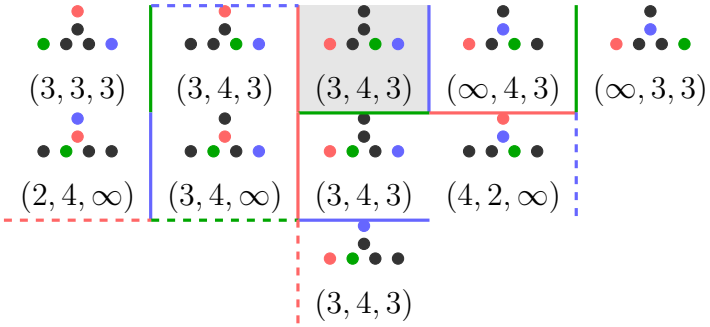

Note that again this is closed under mutation, which can be surmised by checking each cell with a missing wall. For example, mutating the subset in cell $(1, 1)$ with respect to • gives the same diagram (after forgetting colours) as in the cell $(5, 1)$. Further the above table is closed under the only graph automorphism of $\mathbb{A}_4^{\text{hyp}}$. □

Proposition 5.30. *The* $\binom{6}{3} = 20$ *corank three subsets of* $\mathbb{D}_4^{\text{hyp}}$ *partition into the following five symmetric mutation classes.*

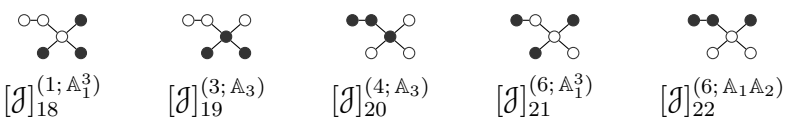

Proof. The symmetric mutation table for $[\mathcal{J}]_{22}$ is

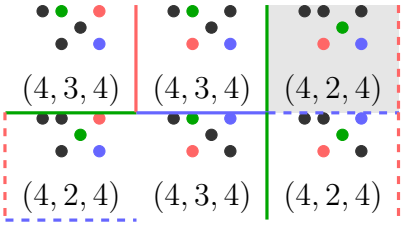

and, in a similar way to Proposition 5.29, is readily seen to be closed under mutation and symmetries. □

Proposition 5.31. *The* $\binom{6}{3} = 20$ *corank three subsets of* $\mathbb{S}_5$ *partition into the following two symmetric mutation classes.*

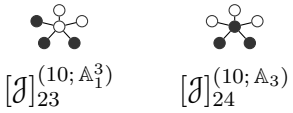

Proof. Each corank three subset of $\mathbb{S}_5$ is fixed under any simple wall-crossing. Indeed, for both representatives above we have $\mathcal{J} + i = \mathbb{D}_4$ for all $i \in \mathcal{J}^c$, which has a trivial Dynkin involution as per (2.J). Hence every mutation class is a singleton. However, under symmetries this clearly reduces to two classes, one where subsets contain the central vertex and one where subsets do not. Each class has ten members, as can be easily checked. The angle data for each $J \in [\mathcal{J}]_{23}$ is $(2, \infty, \infty)$, and similarly for $[\mathcal{J}]_{24}$ we have (∞, ∞, ∞). □

§ 5.3.7 | Rank seven classes

Proposition 5.32. *The* $\binom{7}{3} = 35$ *corank three subsets of* $\mathbb{A}_5^{\text{hyp}}$ *partition into the following eight symmetric mutation classes.*

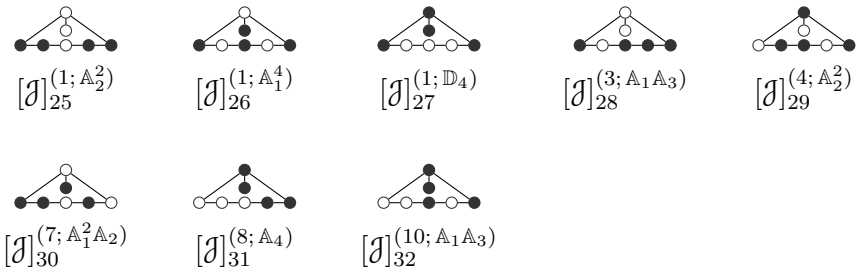

Proof. The symmetric mutation table for $[\mathcal{J}]_{32}$ is

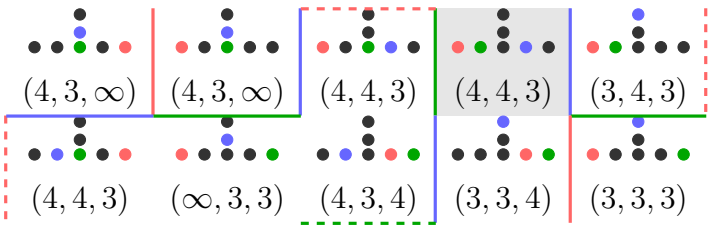

and this is readily seen to be closed under mutation and symmetries. The other classes are similar. □

Proposition 5.33. *The* $\binom{7}{3} = 35$ *corank three subsets of* $\mathbb{D}_5^{\text{hyp}}$ *partition into the following ten symmetric mutation classes.*

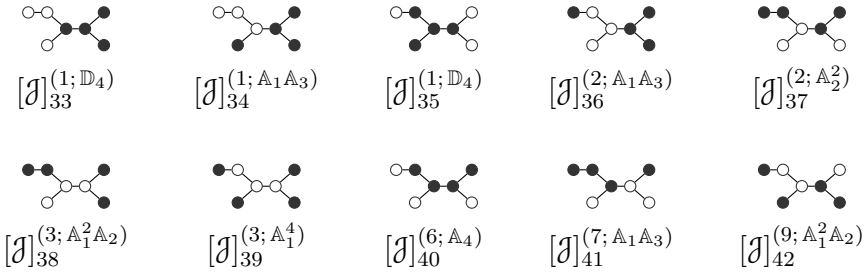

Proof. We present only the full class for $[\mathcal{J}]_{42}$, whose mutation table is

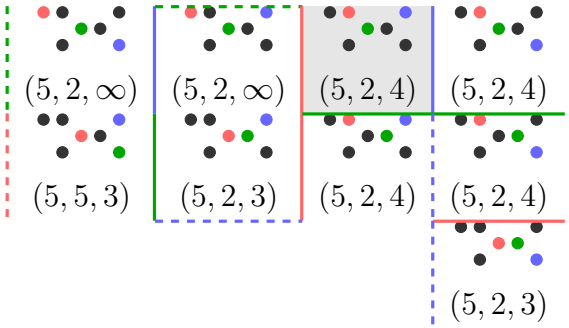

□

§ 5.3.8 | Rank eight classes

Proposition 5.34. *The* $\binom{8}{3} = 56$ *corank three subsets of* $\mathbb{A}_6^{\text{hyp}}$ *partition into the following eight symmetric mutation classes.*

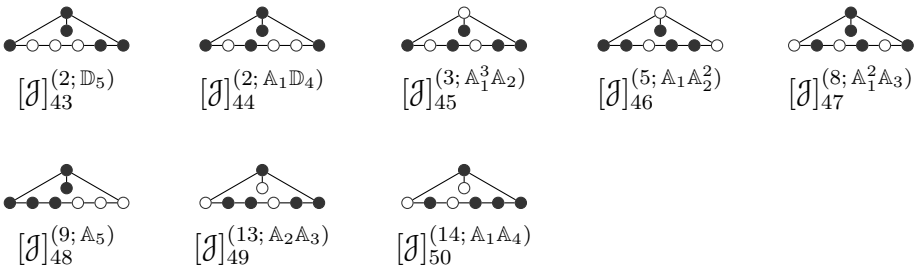

Proof. Again we show only the largest class, here $[\mathcal{J}]_{50}$, which has mutation table

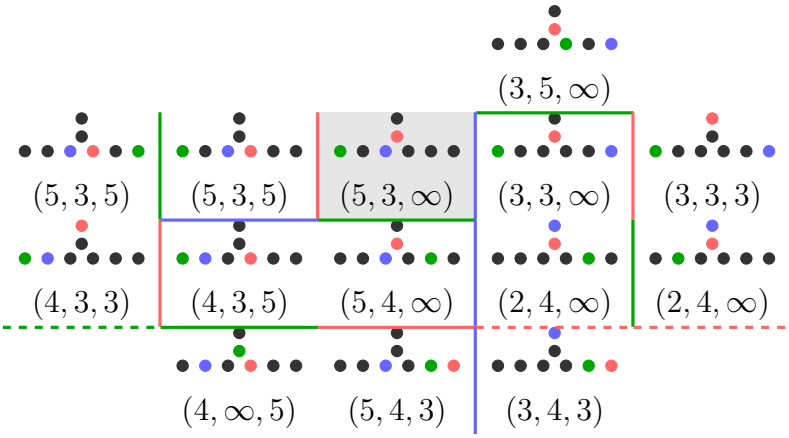

□

Proposition 5.35. *The* $\binom{8}{3} = 56$ *corank three subsets of* $\mathbb{D}_6^{\text{hyp}}$ *partition into the following eighteen symmetric mutation classes.*

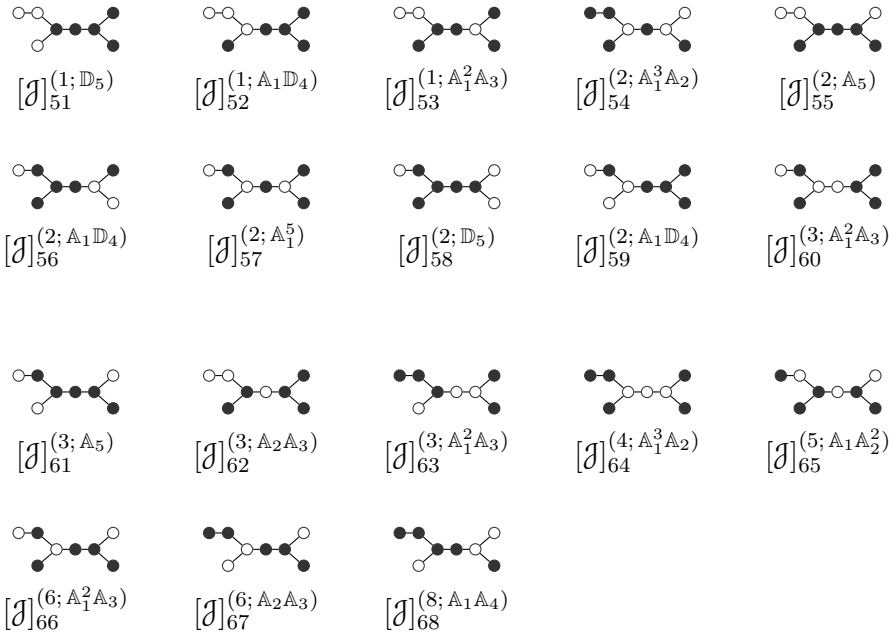

Proof. Notice that $[\mathcal{J}]_{64}$ is Example 5.21(2). Verifying only the largest case, the mutation table for $[\mathcal{J}]_{68}$ is

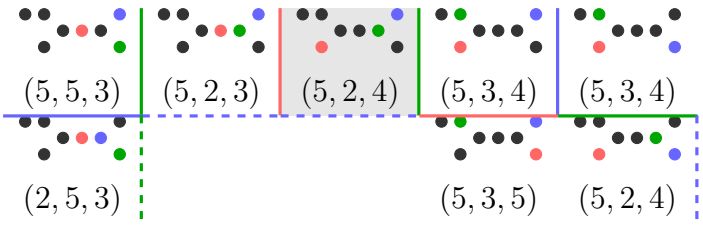

□

Proposition 5.36. *The* $\binom{8}{3} = 56$ *corank three subsets of* $\mathbb{E}_6^{\text{hyp}}$ *partition into the following ten symmetric mutation classes.*

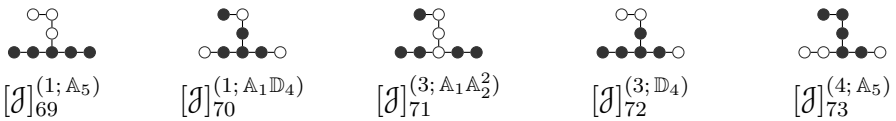

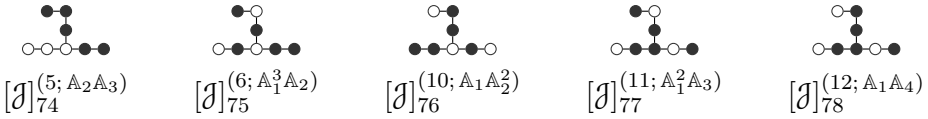

Proof. The mutation table for $[\mathcal{J}]_{78}$, the largest class for $\mathbb{E}_6^{\text{hyp}}$, is

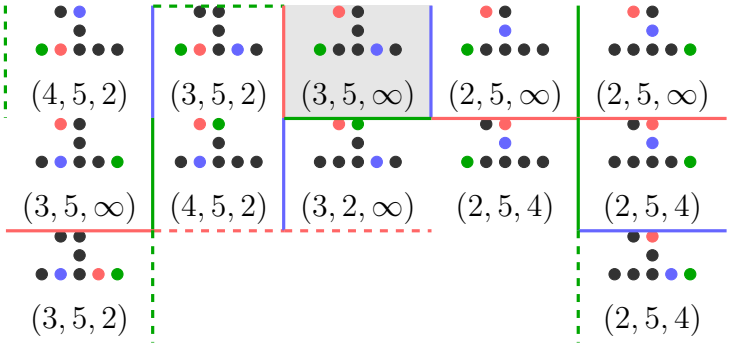

□

§ 5.3.9 | Rank nine classes

Proposition 5.37. *The* $\binom{9}{3} = 84$ *corank three subsets of* $\mathbb{A}_7^{\text{hyp}}$ *partition into the following seventeen symmetric mutation classes.*

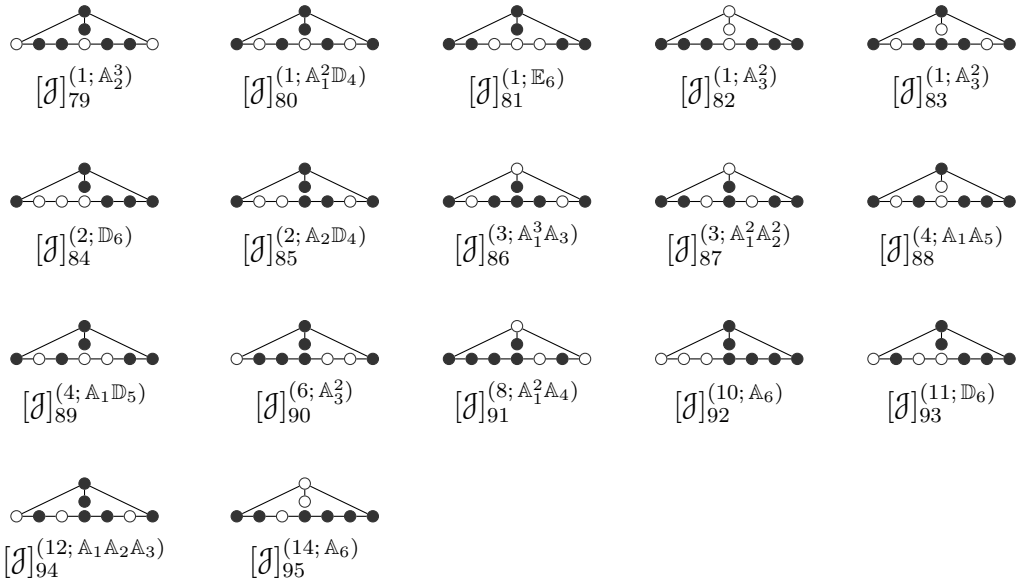

Proof. Verifying the largest class only, the mutation table for $[\mathcal{J}]_{95}$ is

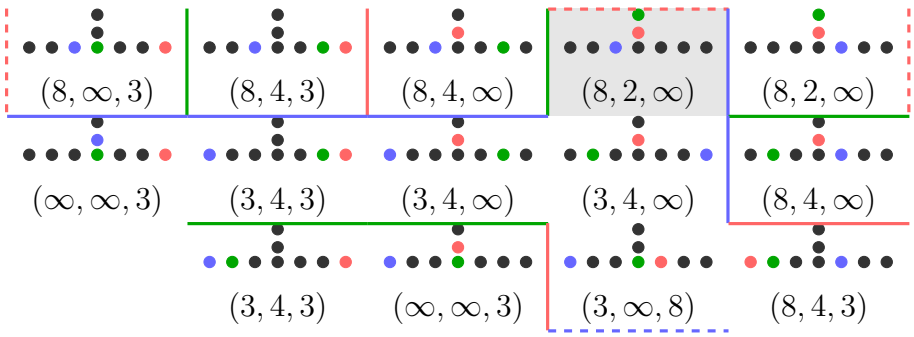

Proposition 5.38. *The* $\binom{9}{3} = 84$ *corank three subsets of* $\mathbb{D}_7^{\text{hyp}}$ *partition into the following twenty-five symmetric mutation classes.*

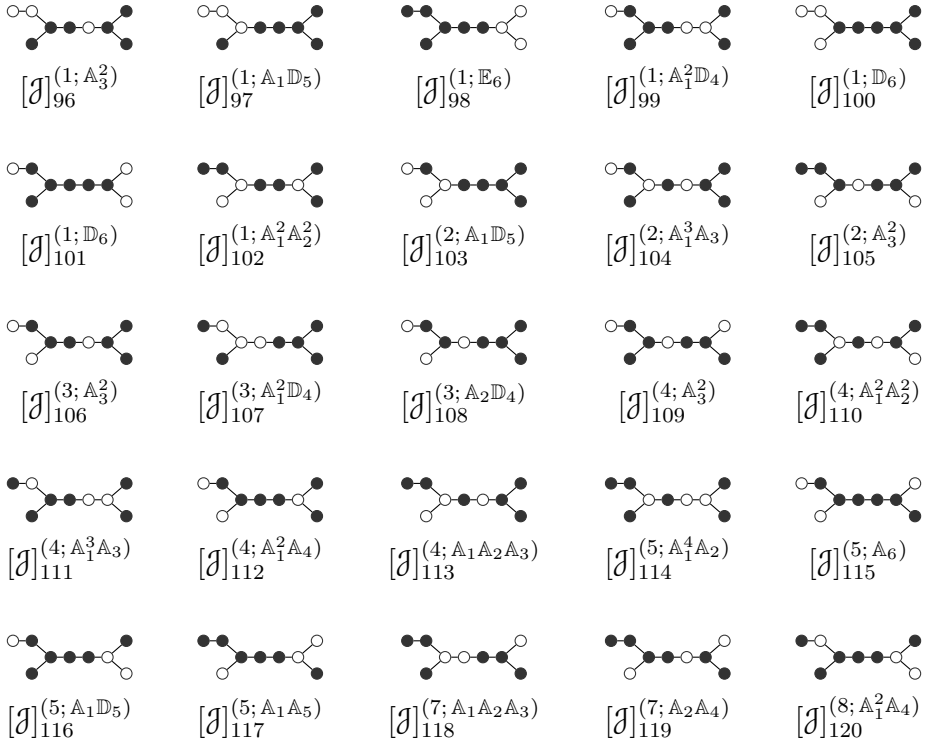

Proof. The largest case in this setting is $[\mathcal{J}]_{120}$, with mutation table

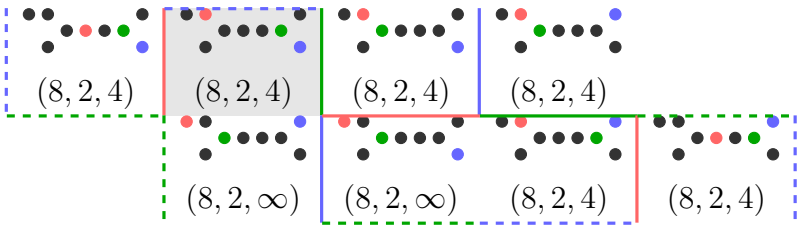

□

Proposition 5.39. *The* $\binom{9}{3} = 84$ *corank three subsets of* $\mathbb{E}_7^{\text{hyp}}$ *partition into the following twenty symmetric mutation classes.*

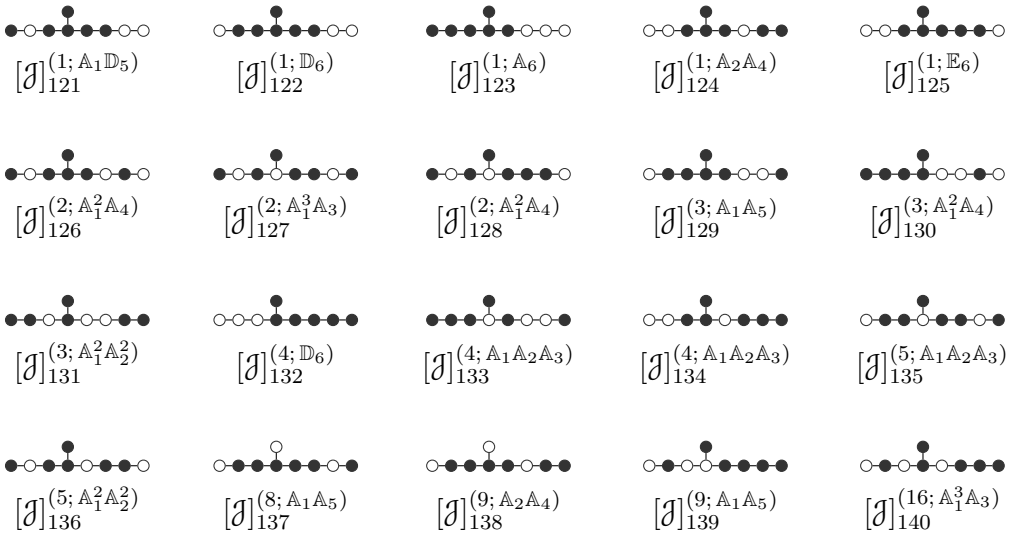

Proof. Here, the largest case is $[\mathcal{J}]_{140}$, which is summarised in the following

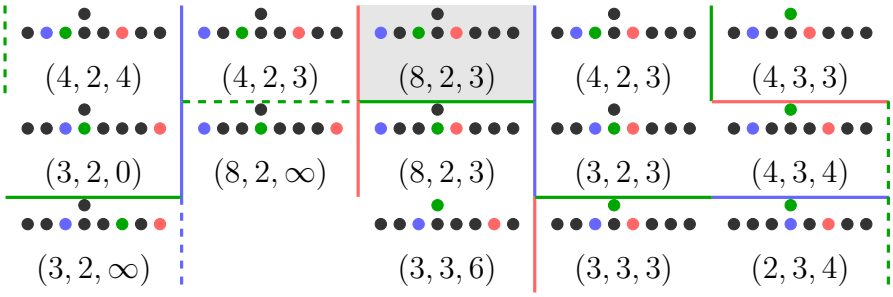

□

§ 5.3.10 | Rank ten classes

Proposition 5.40. *The* $\binom{8}{3} = 120$ *corank three subsets of* $\mathbb{D}_8^{\text{hyp}}$ *partition into the following forty symmetric mutation classes.*

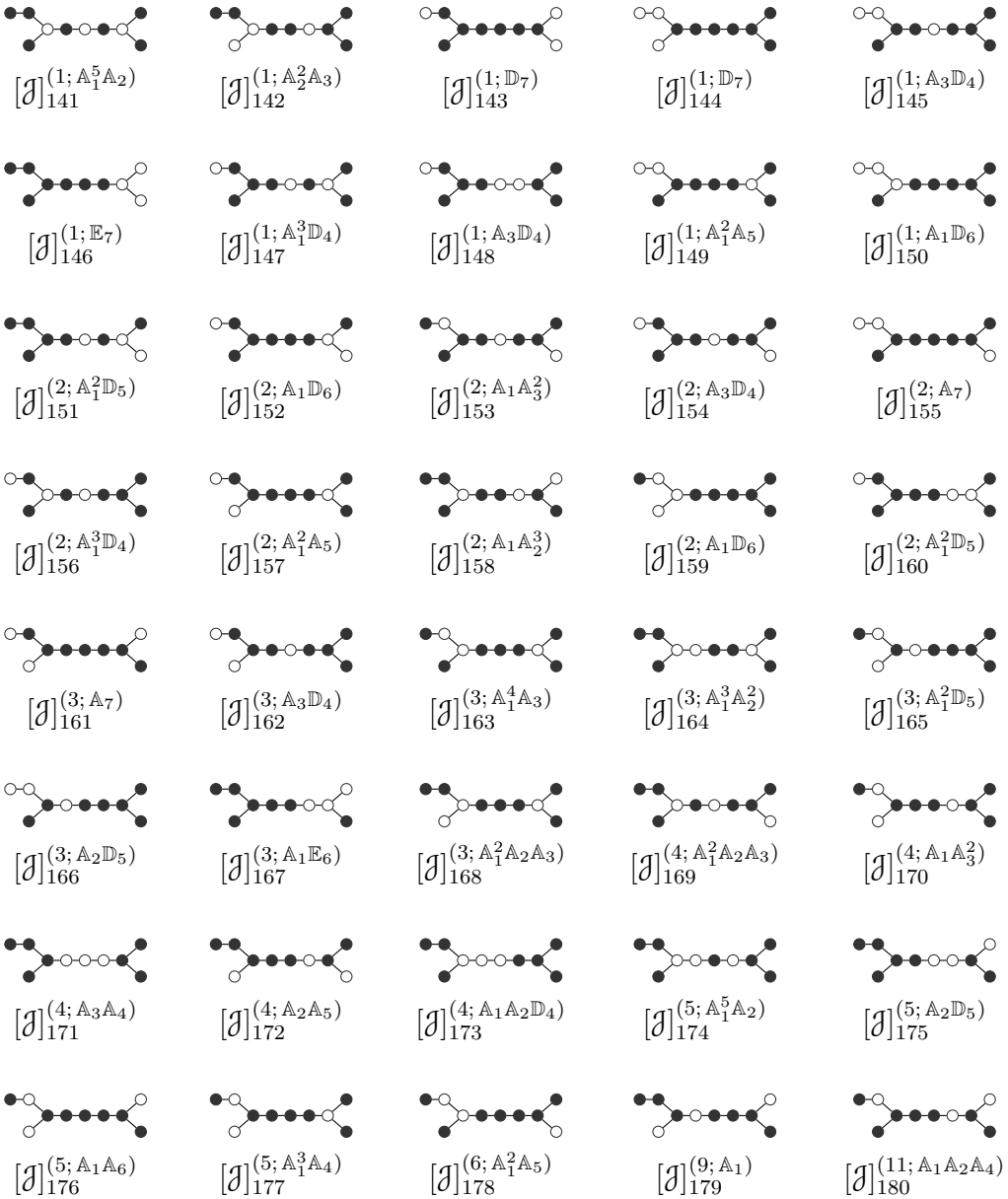

Proof. The mutation table for the largest case, $[\mathcal{J}]_{180}$, is

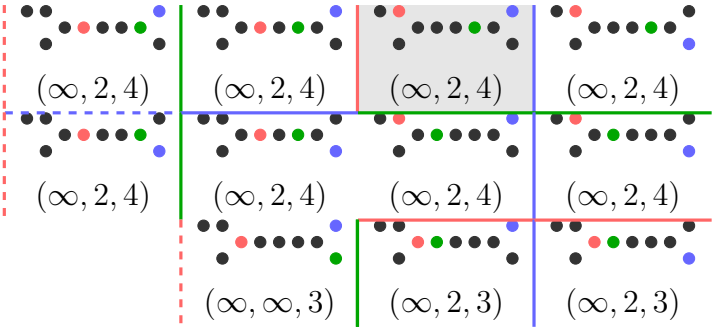

□

Proposition 5.41. *The* $\binom{8}{3} = 120$ *corank three subsets of* $\mathbb{E}_8^{\text{hyp}}$ *partition into the following twenty symmetric mutation classes.*

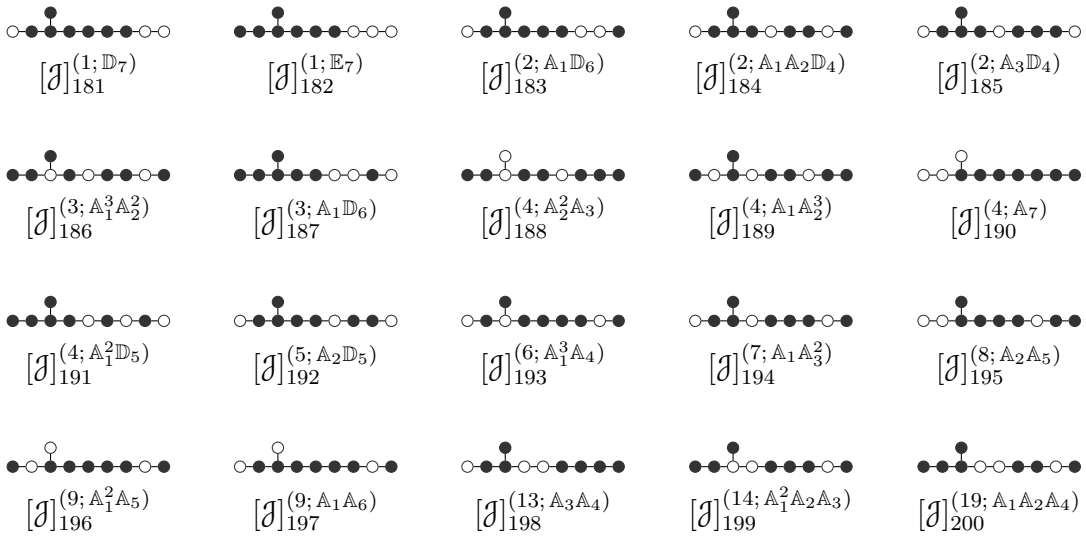

Proof. Notice that $[\mathcal{J}]_{186}$ is Example 5.21(3). Again verifying only the largest class, the mutation table for $[\mathcal{J}]_{200}$ is

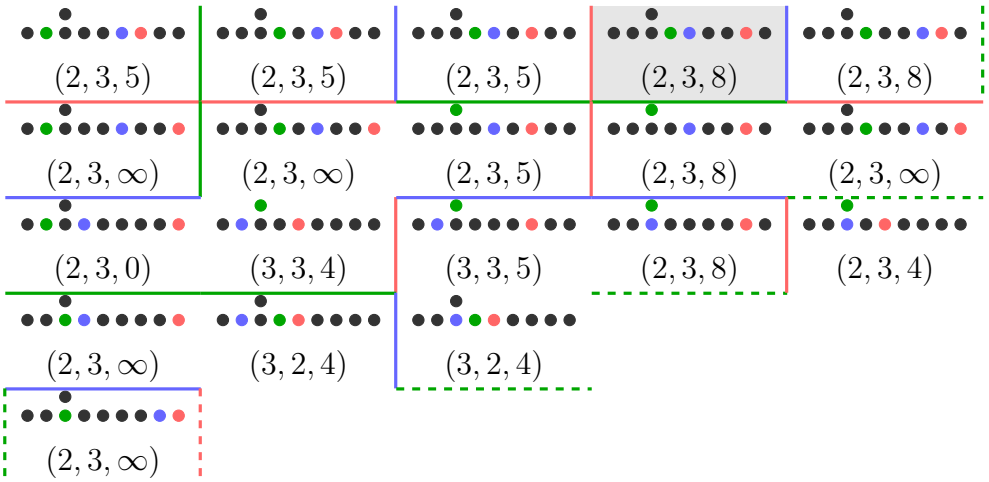

□

§ 5.3.11 | Higher corank

Analogously to (5.G), there are 4929 subsets of hyperbolic graphs with nonzero corank. Motivating future work, the following generalisation gives an upper bound on the number of hyperbolic intersection arrangements in higher dimension.

Theorem 5.42. *Let Δ be a hyperbolic graph with $\mathsf{rk} \geq 3$, and let $\mathcal{J} \subseteq \Delta$ have $\mathsf{crk} \geq 3$. Then $\mathcal{J}$ is in one of 485 symmetric mutation classes enumerated below.*

	crk							
Δ	3	4	5	6	7	8	9	10
$\mathbb{A}_1^{\mathrm{hyp}}$	1							
$\mathbb{A}_{1,1}^{\mathrm{hyp}}$	1							
$\mathbb{A}_{2,1}^{\mathrm{aff}}$	1							
$\mathbb{A}_{2,2}^{\mathrm{aff}}$	1							
$\mathbb{A}_{2,3}^{\mathrm{aff}}$	1							
$\mathbb{A}_2^{\mathrm{hyp}}$	1	1						
$\mathbb{A}_{2,1}^{\mathrm{hyp}}$	1	1						
$\mathbb{A}_{2,2}^{\mathrm{hyp}}$	1	1						
$\mathbb{A}_3^{\mathrm{hyp}}$	3	1	1					
$\mathbb{A}_{3,1}^{\mathrm{hyp}}$	3	1	1					
$\mathbb{A}_4^{\mathrm{hyp}}$	3	2	1	1				
$\mathbb{D}_4^{\mathrm{hyp}}$	5	3	1	1				
$\mathbb{S}_5$	2	2	1	1				
$\mathbb{A}_5^{\mathrm{hyp}}$	8	4	2	1	1			
$\mathbb{D}_5^{\mathrm{hyp}}$	10	5	3	1	1			
$\mathbb{A}_6^{\mathrm{hyp}}$	8	6	3	2	1	1		
$\mathbb{D}_6^{\mathrm{hyp}}$	18	12	6	3	1	1		
$\mathbb{E}_6^{\mathrm{hyp}}$	10	7	3	2	1	1		
$\mathbb{A}_7^{\mathrm{hyp}}$	17	10	7	3	2	1	1	
$\mathbb{D}_7^{\mathrm{hyp}}$	25	16	10	5	3	1	1	
$\mathbb{E}_7^{\mathrm{hyp}}$	20	13	8	4	2	1	1	
$\mathbb{D}_8^{\mathrm{hyp}}$	40	32	18	11	5	3	1	1
$\mathbb{E}_8^{\mathrm{hyp}}$	20	15	9	6	3	2	1	1
	200	132	74	41	20	11	5	2

Proof. This is completely analogous to Theorem 5.24. □

§ 5.4 | Hyperbolic classification

We classify rank three hyperbolic intersection arrangements, by reducing further from symmetric mutation classes to distinct arrangements of hyperplanes.

§ 5.4.1 | Distinguishing arrangements

First we make precise what we mean when regarding two intersection arrangements to be the same. As motivation, in the classical setting of hyperbolic triangle groups the data (p, q, r) globally determines the corresponding hyperplane arrangement. We now extend this to intersection arrangements by considering the angle data at each alcove. Indeed, just as the Coxeter exponents m_{ij} determine the angles in each alcove of a

Coxeter arrangement, we have a more general version of this where locally each alcove has the structure of a potentially different triangle group.

Each alcove in a Coxeter arrangement is a triangle with a fixed set of angles, but for an intersection arrangement there may be more than one type of triangle. By recording this set of angle triples which correspond to braiding of simple wall-crossings we get a patch of triangles that determines the arrangement.

If two symmetric mutation classes have a different set of triangles then we can immediately conclude they give different intersection arrangements. Two classes can be identified with the same arrangement if their angle set is the same and further the configuration in which these triangles are attached is the same, all of which can be extracted from the mutation process from Section 5.3. To illustrate this, consider the following example.

Example 5.43. Consider from Proposition 5.33 and Proposition 5.35 the symmetric mutation classes $[\mathcal{J}]_{36}$ and $[\mathcal{J}]_{57}$ of $\mathbb{D}_5^{\text{hyp}}$ and $\mathbb{D}_6^{\text{hyp}}$ respectively. Both classes contain two subsets; the former has angle data $(2,4,4)$ and $(2,4,\infty)$, and the latter has $(4,2,\infty)$ and $(4,2,4)$. In this way both arrangements consist of these two triangles, attached by a single wall-crossing. Below we overlay the triangles on their respective arrangements.

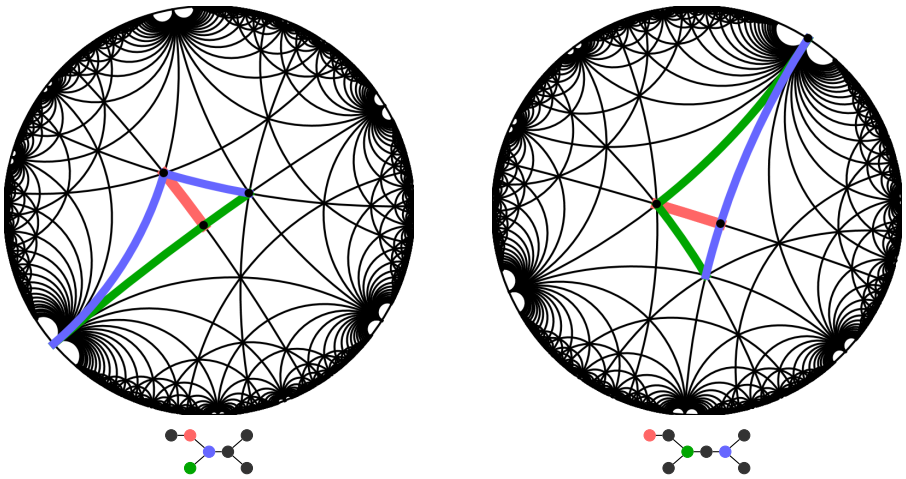

Hence we can identify the two intersection arrangements associated with these symmetric mutation classes. This repeating region of triangles suggests the existence of a fundamental region for the arrangement, which may similarly be classified and is discussed further in Section 6.2.

Definition 5.44. Two intersection arrangements $\mathcal{H}_J$ and $\mathcal{H}_K$ are *combinatorially equivalent* if their finite set of triangles, together with gluing data coming from mutation, determine the same tiling.

The gluing and angle data captures how polygons are attached in the dual graph, and is often the easiest way to distinguish two arrangements that have the same set of triangles.

§ 5.4.2 | The main result

We now present the hyperbolic intersection arrangements in dimension two which are combinatorially different in the sense of Definition 5.44. This uses the angle data generated by computer algebra in the proof of Theorem 5.24, with the mutation structure checked by hand when two symmetric mutation classes have the same set of triangles. In this case we also draw the two arrangements that potentially coincide, to give a partial double verification by inspection.

Recall from (2.16) that every flat in $\mathcal{H}_\mathcal{J}$ gives rise to a polygon in the dual graph. The superscripts in the following list denote the polygons present in the dual graph of the arrangement, with only the first of each combination decorated as such. Below each arrangement is a representative of the earliest symmetric mutation class in Theorem 5.24 that gives rise to the arrangement.

Theorem 5.45. *Let Δ be hyperbolic and let $\mathcal{J} \subseteq \Delta$ be of corank three. Then, up to isomorphism of 1-skeleta, the associated intersection arrangement $\mathcal{H}_\mathcal{J}$ is one of the following 102 tilings of $\mathbb{H}^2$, where the dashed boxes represent Coxeter arrangements.*

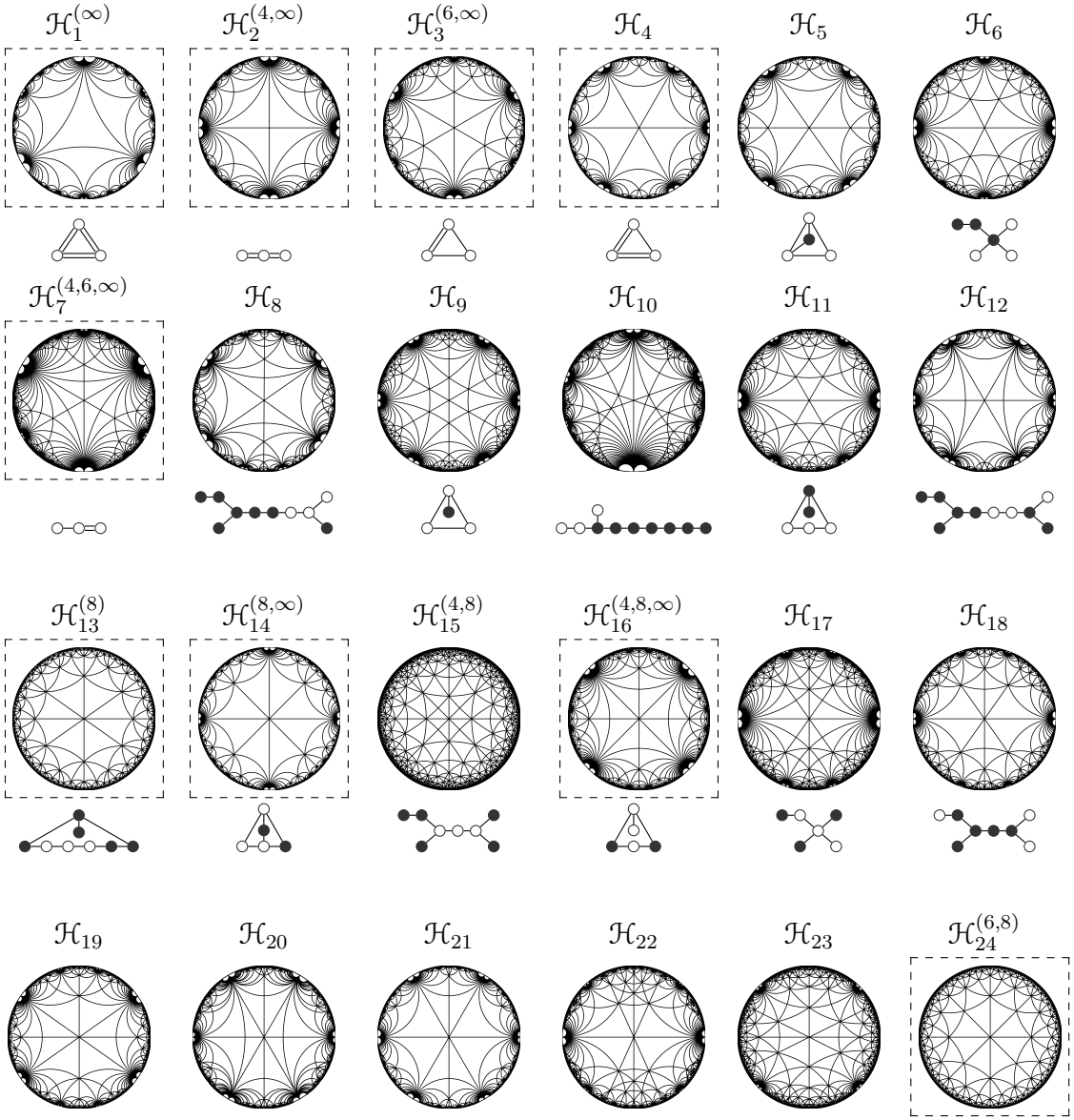

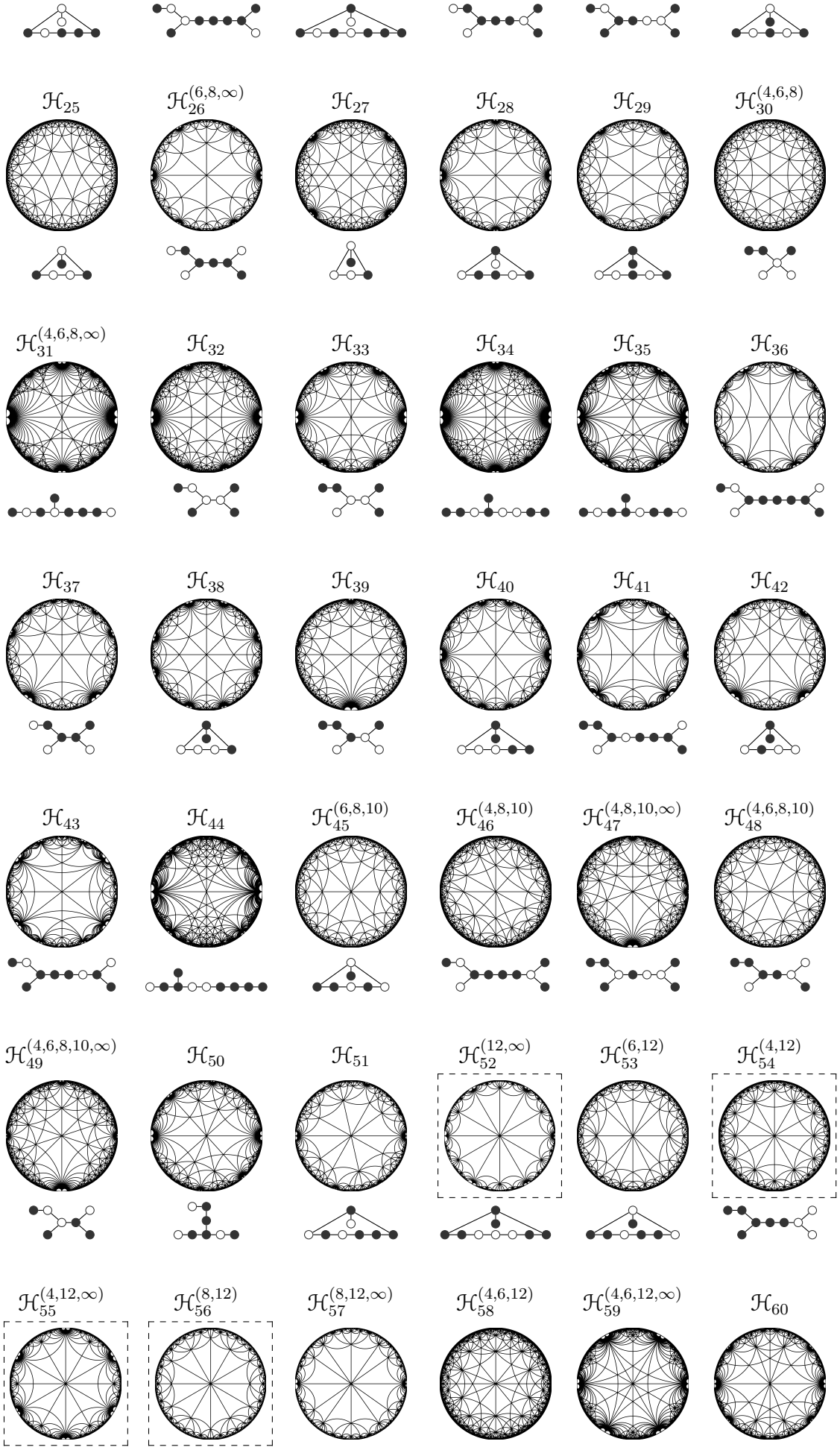
$\mathcal{H}_{25}$
$\mathcal{H}_{26}^{(6,8,\infty)}$
$\mathcal{H}_{27}$
$\mathcal{H}_{28}$
$\mathcal{H}_{29}$
$\mathcal{H}_{30}^{(4,6,8)}$
$\mathcal{H}_{31}^{(4,6,8,\infty)}$
$\mathcal{H}_{32}$
$\mathcal{H}_{33}$
$\mathcal{H}_{34}$
$\mathcal{H}_{35}$
$\mathcal{H}_{36}$
$\mathcal{H}_{37}$
$\mathcal{H}_{38}$
$\mathcal{H}_{39}$
$\mathcal{H}_{40}$
$\mathcal{H}_{41}$
$\mathcal{H}_{42}$
$\mathcal{H}_{43}$
$\mathcal{H}_{44}$
$\mathcal{H}_{45}^{(6,8,10)}$
$\mathcal{H}_{46}^{(4,8,10)}$
$\mathcal{H}_{47}^{(4,8,10,\infty)}$
$\mathcal{H}_{48}^{(4,6,8,10)}$
$\mathcal{H}_{49}^{(4,6,8,10,\infty)}$
$\mathcal{H}_{50}$
$\mathcal{H}_{51}$
$\mathcal{H}_{52}^{(12,\infty)}$
$\mathcal{H}_{53}^{(6,12)}$
$\mathcal{H}_{54}^{(4,12)}$
$\mathcal{H}_{55}^{(4,12,\infty)}$
$\mathcal{H}_{56}^{(8,12)}$
$\mathcal{H}_{57}^{(8,12,\infty)}$
$\mathcal{H}_{58}^{(4,6,12)}$
$\mathcal{H}_{59}^{(4,6,12,\infty)}$
$\mathcal{H}_{60}$

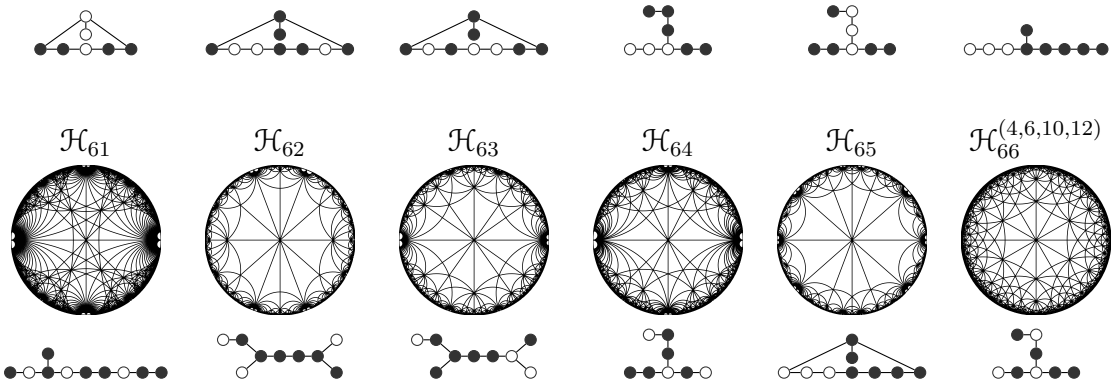

$\mathcal{H}_{61}$
$\mathcal{H}_{62}$
$\mathcal{H}_{63}$
$\mathcal{H}_{64}$
$\mathcal{H}_{65}$
$\mathcal{H}_{66}^{(4,6,10,12)}$

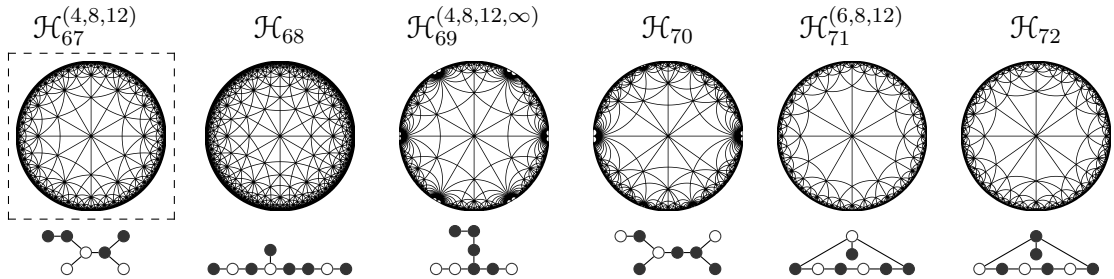
$\mathcal{H}_{67}^{(4,8,12)}$
$\mathcal{H}_{68}$
$\mathcal{H}_{69}^{(4,8,12,\infty)}$
$\mathcal{H}_{70}$
$\mathcal{H}_{71}^{(6,8,12)}$
$\mathcal{H}_{72}$

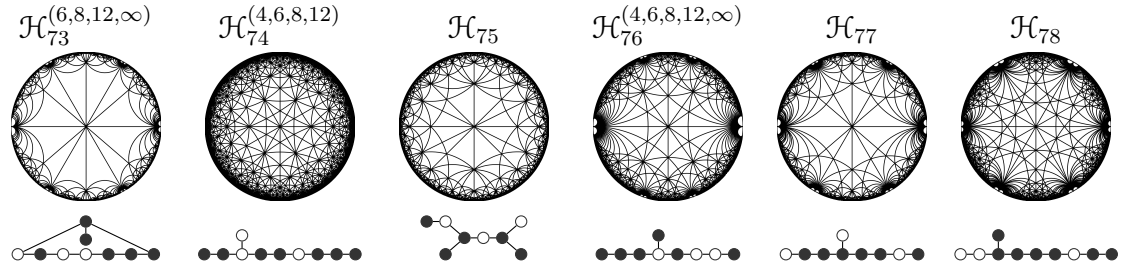
$\mathcal{H}_{73}^{(6,8,12,\infty)}$
$\mathcal{H}_{74}^{(4,6,8,12)}$
$\mathcal{H}_{75}$
$\mathcal{H}_{76}^{(4,6,8,12,\infty)}$
$\mathcal{H}_{77}$
$\mathcal{H}_{78}$

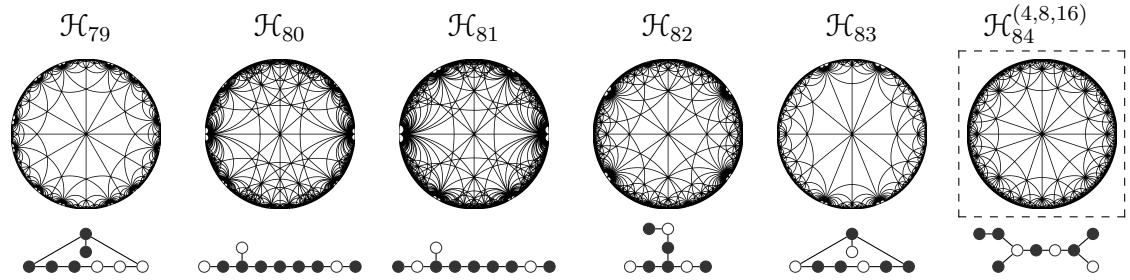
$\mathcal{H}_{79}$
$\mathcal{H}_{80}$
$\mathcal{H}_{81}$
$\mathcal{H}_{82}$
$\mathcal{H}_{83}$
$\mathcal{H}_{84}^{(4,8,16)}$

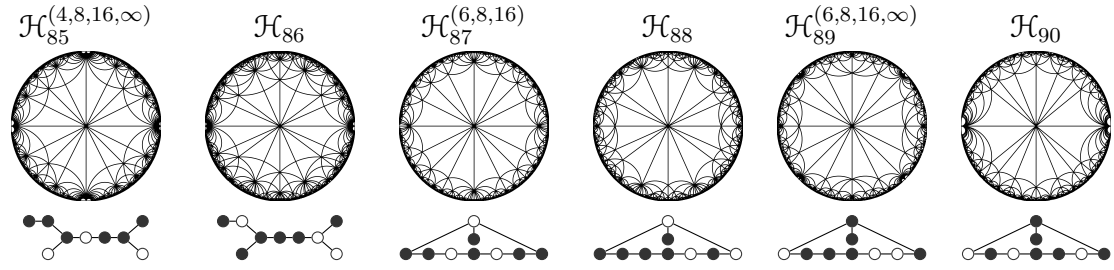
$\mathcal{H}_{85}^{(4,8,16,\infty)}$
$\mathcal{H}_{86}$
$\mathcal{H}_{87}^{(6,8,16)}$
$\mathcal{H}_{88}$
$\mathcal{H}_{89}^{(6,8,16,\infty)}$
$\mathcal{H}_{90}$

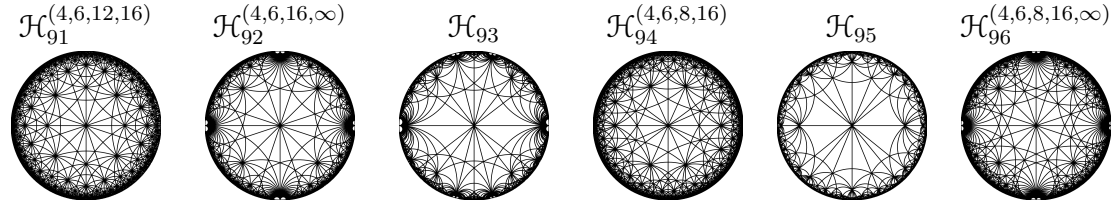
$\mathcal{H}_{91}^{(4,6,12,16)}$
$\mathcal{H}_{92}^{(4,6,16,\infty)}$
$\mathcal{H}_{93}$
$\mathcal{H}_{94}^{(4,6,8,16)}$
$\mathcal{H}_{95}$
$\mathcal{H}_{96}^{(4,6,8,16,\infty)}$

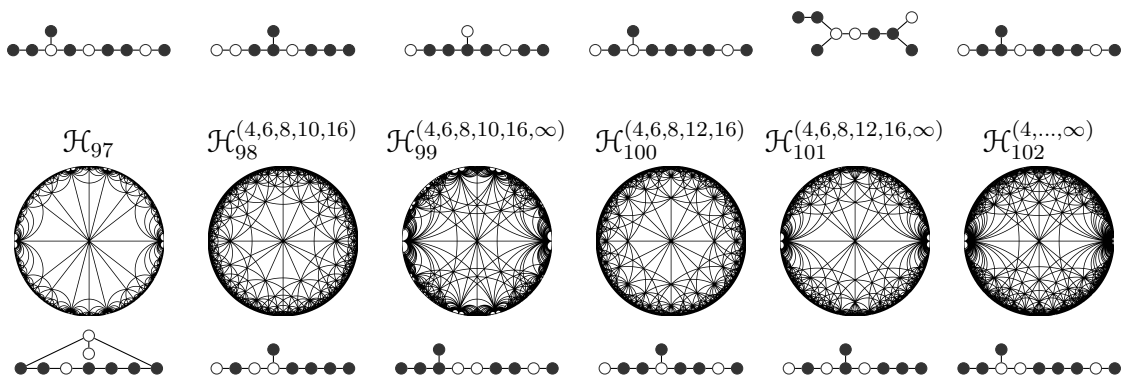

Proof. Similarly to Theorem 5.24, this is largely a direct computation. The list of arrangements is ordered by the largest finite polygon that arises in the dual graph, and the centre of this polygon is always at the centre of the arrangement.

The table at the end of the proof contains the classes that correspond to each arrangement, along with the list of triangles present, in the form of angle data. The arrangements which are Coxeter (boxed) correspond to the singleton classes appearing in Section 5.3, and so contain a single triangle. In particular, we see from the table that all 200 symmetric mutation classes are present, with multiplicities arising in the same way as Example 5.43.

First we distinguish the 102 arrangements listed. Clearly if the set of triangles is different then the arrangements are different, but if the set of triangles coincide we check the order and gluing data in the sense of Definition 5.44. Within each of the 45 polygon combinations of the dual graphs (separated by a horizontal line) we list the arrangements in increasing order of 'complexity', with the number of polygons, angle combinations, and mutation class member increasing going down the table. This reduces the classification problem to checking that all arrangements with a given polygon combination are different. In most cases, such as $\mathcal{H}_{16}$ through $\mathcal{H}_{23}$, just the list of unique triangles is enough to distinguish two arrangements with the same polygons. This leaves the small number of cases for which the set of triangles is the same but are attached with different orders or orientation. Observe in the table that there are four cases when a pair of arrangements contain the exact same set of triangles. We go through these cases in turn and verify that the arrangements are indeed different, overlaying their angle data and using $\bullet$ to mark the corners of the standard $\mathcal{J}$-alcove.

(1) $\mathcal{H}_9$ and $\mathcal{H}_{11}$: the difference is that the former has one ideal triangle neighbouring

every equilateral triangle but the latter has two.

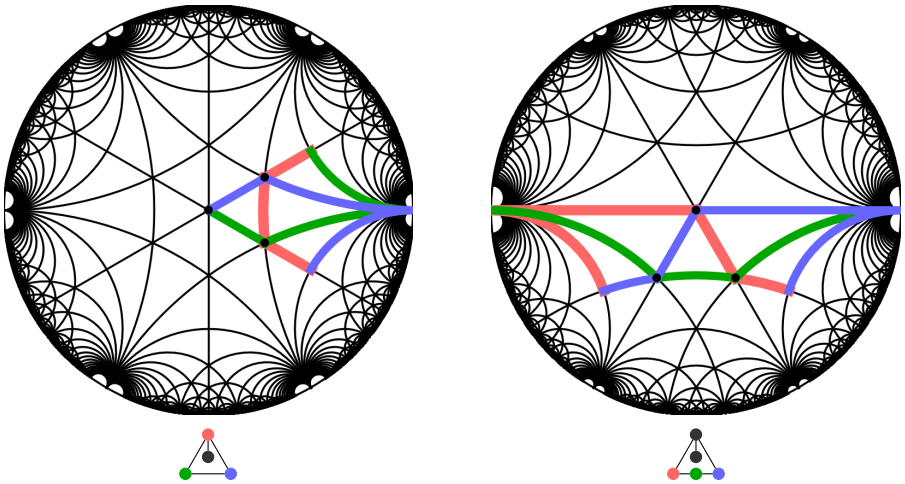

(2) $\mathcal{H}_{26}$ and $\mathcal{H}_{28}$: the former has 8-gons neighbouring other 8-gons, whilst the latter does not. In other words, the angles of $\frac{\pi}{4}$ in $\mathcal{H}_{28}$ are reflected across adjacent alcoves.

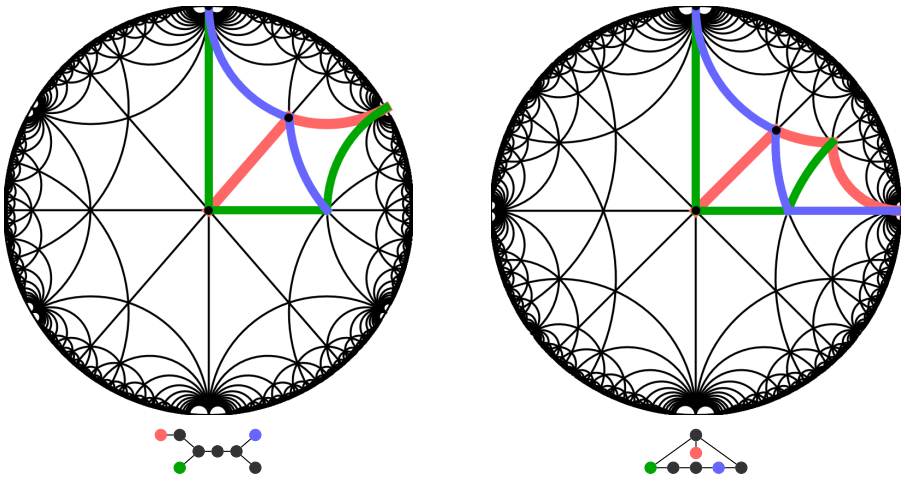

(3) $\mathcal{H}_{59}$ and $\mathcal{H}_{61}$: the former never has ∞-gons neighbouring 12-gons, whilst this occurs in the latter.

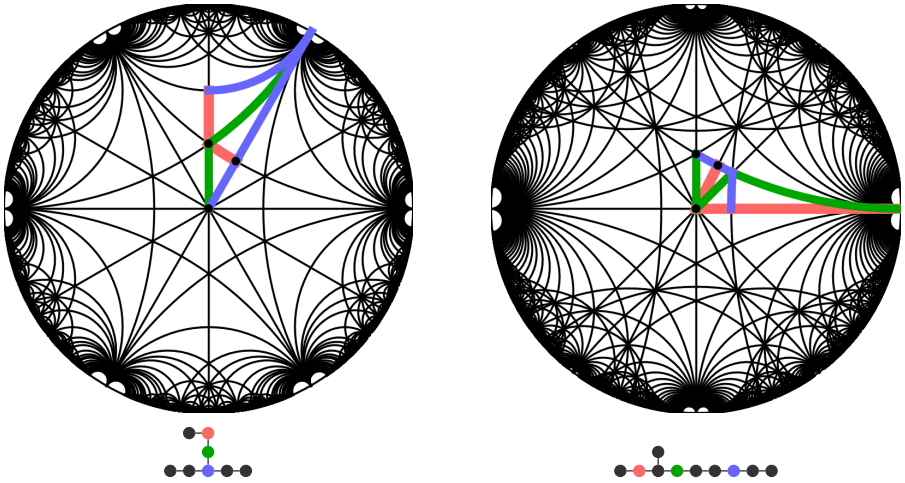

(4) $\mathcal{H}_{85}$ and $\mathcal{H}_{86}$: the former has four ∞-gons surrounding every 16-gon, but the latter only has two.

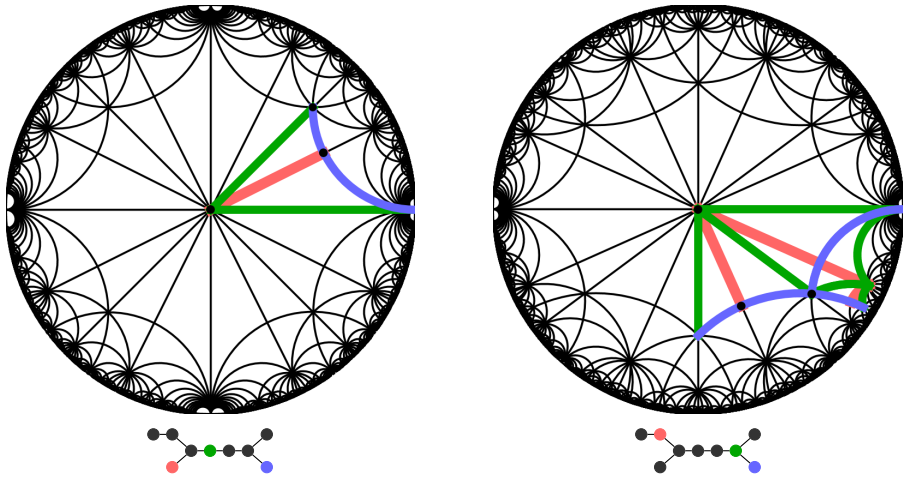

This gives 102 as a lower bound, so it remains to check that all symmetric mutation classes in a row indeed give the same intersection arrangement. Since most of the duplicates are for Coxeter arrangements, this case is clear, as there is only one tiling that is determined by a single triangle. For cases with a larger set of triangles, we check by hand that the mutation structure is the same using the angle data with multiplicity. This can be cross-referenced with the dual graph of the arrangements.

$\mathcal{H}_\bullet$	$[\mathcal{J}]_\bullet$	triangles
[1]	5, 8, 12, 24, 143	(∞,∞,∞)
[2]	2, 23, 82, 146, 152, 154, 155	$(2,\infty,\infty)$
[3]	3, 35, 79	$(3,3,\infty)$
[4]	4, 14, 161	$(3,\infty,\infty)$
5	7	$(3,3,\infty)$; $(3,\infty,\infty)$
6	20	$(3,3,3)$; $(3,3,\infty)$
[7]	1, 18, 34, 52, 69, 97, 99, 123, 148, 150, 182	$(2,3,\infty)$
8	167	$(2,3,\infty)$; $(3,\infty,\infty)$
9	6	$(2,3,\infty)$; $(3,3,3)$; $(3,3,\infty)$
10	190	$(2,3,3)$; $(2,3,\infty)$
11	11	$(2,3,\infty)$; $(3,3,3)$; $(3,3,\infty)$
12	175	$(2,3,\infty)$; $(2,\infty,\infty)$; $(3,\infty,\infty)$
[13]	43, 44	$(4,4,4)$
[14]	13, 80, 83, 84, 101	$(4,4,\infty)$
15	64, 113, 173	$(2,4,4)$; $(4,4,4)$
[16]	9, 19, 33, 51, 53, 56, 96, 100, 121, 125,	$(2,4,\infty)$

$\mathcal{H}$.	$[\mathcal{J}]$.	triangles
	144, 145, 147, 151, 153,	
	158, 169, 172, 181	
17	21, 36, 57, 59, 103, 104,	$(2,4,4);(2,4,\infty)$
	126, 156, 159, 160, 183	
18	58, 157	$(2,4,4);(4,4,\infty)$
19	28, 72	$(2,4,\infty);(4,4,\infty)$
20	178	$(2,4,\infty);(2,\infty,\infty)$
21	88	$(2,4,\infty);(4,\infty,\infty)$
22	112, 171	$(2,4,4);(2,4,\infty);(4,4,\infty)$
23	111, 170	$(2,4,4);(2,4,\infty);(4,4,4)$
24	26, 27, 70	$(3,4,4)$
25	15	$(3,3,4);(3,4,4)$
26	61, 86	$(3,3,4);(3,4,\infty)$
27	10	$(3,3,3);(3,3,4);(3,3,\infty)$
28	29	$(3,3,4);(3,4,\infty)$
29	32	$(3,3,3);(3,3,4);(3,3,\infty);(3,4,4);(3,4,\infty)$
30	22	$(2,4,4);(3,4,4)$
31	128, 185	$(2,3,4);(2,4,\infty)$
32	39, 60, 107, 165	$(2,3,4);(2,3,\infty);(3,4,4)$
33	38, 62, 63, 106, 108,	$(2,3,4);(2,3,\infty);(3,4,\infty)$
	162, 166	
34	131	$(2,3,4);(2,3,\infty);(3,3,4)$
35	136, 192	$(2,3,4);(2,3,\infty);(2,4,4);(2,4,\infty)$
36	176	$(2,4,\infty);(3,4,\infty);(3,\infty,\infty)$
37	40	$(2,4,4);(2,4,\infty);(3,4,4);(3,4,\infty)$
38	16	$(2,3,\infty);(3,3,4);(3,3,\infty)$
39	41	$(2,4,4);(2,4,\infty);(3,4,4)$
40	31	$(2,3,\infty);(3,3,4);(3,3,\infty);(3,4,\infty)$
41	179	$(2,3,\infty);(2,4,\infty);(2,\infty,\infty);(3,\infty,\infty)$
42	17	$(2,4,\infty);(3,3,3);(3,3,4);(3,3,\infty);(3,4,\infty)$
43	180	$(2,3,\infty);(2,4,\infty);(3,\infty,\infty)$
44	198	$(2,3,3);(2,3,4);(2,3,\infty);(2,4,4);(2,4,\infty);$
		$(3,3,4);(3,4,4)$
45	30	$(3,3,4);(3,3,5);(3,4,5)$
46	177	$(2,4,5);(4,4,5)$
47	114, 174	$(2,4,5);(2,5,\infty)$
48	68	$(2,3,5);(2,4,5);(3,4,5);(3,5,5)$
49	42	$(2,3,5);(2,4,5);(2,5,\infty);(3,5,5)$
50	78	$(2,3,5);(2,3,\infty);(2,4,5);(2,5,\infty);(3,5,\infty)$

$\mathcal{H}$.	$[\mathcal{J}]$.	triangles
51	50	$(2,4,\infty)$; $(3,3,3)$; $(3,3,4)$; $(3,3,\infty)$; $(3,4,5)$; $(3,5,5)$; $(3,5,\infty)$; $(4,5,\infty)$
[52]	81	$(6,6,\infty)$
53	46	$(3,3,6)$; $(3,6,6)$
[54]	98	$(2,6,6)$
[55]	25, 55, 122, 149	$(2,6,\infty)$
[56]	85	$(4,4,6)$
57	89	$(4,6,6)$; $(4,6,\infty)$
58	74	$(2,3,6)$; $(3,6,6)$
59	71, 130, 187	$(2,3,6)$; $(2,3,\infty)$
60	132	$(2,3,6)$; $(2,3,\infty)$; $(3,6,\infty)$
61	189	$(2,3,6)$; $(2,3,\infty)$
62	115	$(2,6,\infty)$; $(3,6,6)$; $(3,6,\infty)$
63	116	$(2,3,6)$; $(2,3,\infty)$; $(3,6,6)$
64	76	$(2,3,3)$; $(2,3,6)$; $(2,3,\infty)$; $(2,6,\infty)$; $(3,3,6)$
65	92	$(2,3,\infty)$; $(3,3,6)$; $(3,3,\infty)$; $(3,6,\infty)$; $(6,\infty,\infty)$
66	75	$(2,3,5)$; $(2,5,6)$; $(3,3,3)$; $(3,3,5)$
[67]	37, 54, 102, 124, 141, 142, 164	$(2,4,6)$
68	127, 184	$(2,4,4)$; $(2,4,6)$
69	73	$(2,4,6)$; $(2,4,\infty)$
70	66, 67, 129, 163, 168	$(2,4,6)$; $(2,6,\infty)$
71	45	$(3,4,4)$; $(3,4,6)$
72	47	$(3,3,4)$; $(3,3,6)$; $(3,4,6)$
73	93	$(3,3,3)$; $(3,3,4)$; $(3,3,\infty)$; $(3,4,\infty)$; $(3,6,\infty)$; $(6,6,\infty)$
74	188	$(2,3,6)$; $(2,4,6)$
75	65, 117	$(2,3,6)$; $(2,4,6)$; $(3,6,6)$
76	133, 191	$(2,3,6)$; $(2,3,\infty)$; $(2,4,6)$
77	137	$(2,3,3)$; $(2,3,4)$; $(2,3,6)$; $(2,3,\infty)$; $(2,6,\infty)$; $(3,3,\infty)$; $(3,4,6)$
78	195	$(2,3,3)$; $(2,3,4)$; $(2,3,\infty)$; $(2,4,6)$; $(3,3,4)$; $(3,4,4)$
79	48	$(2,3,\infty)$; $(3,3,6)$; $(3,3,\infty)$; $(3,4,\infty)$; $(4,4,\infty)$
80	197	$(2,3,3)$; $(2,3,4)$; $(2,3,6)$; $(2,3,\infty)$; $(2,4,6)$; $(3,3,\infty)$; $(3,4,6)$
81	196	$(2,3,3)$; $(2,3,4)$; $(2,3,6)$; $(2,3,\infty)$; $(2,4,\infty)$; $(3,3,3)$; $(3,3,6)$
82	77	$(2,3,3)$; $(2,3,4)$; $(2,3,6)$; $(2,3,\infty)$; $(2,6,6)$; $(3,3,\infty)$; $(3,4,6)$
83	49	$(2,6,\infty)$; $(3,3,4)$; $(3,4,4)$; $(3,4,6)$; $(3,4,\infty)$;

$\mathcal{H}$.	$[\mathcal{J}]$.	triangles
		$(3,6,\infty)$; $(4,4,\infty)$
$\boxed{84}$	110	$(2,4,8)$
85	105, 109	$(2,4,8)$; $(2,8,\infty)$
86	120	$(2,4,8)$; $(2,8,\infty)$
87	87	$(3,4,8)$; $(3,8,8)$
88	91	$(3,3,4)$; $(3,3,8)$; $(3,4,8)$; $(3,8,8)$
89	90	$(3,4,4)$; $(3,4,8)$; $(3,8,\infty)$
90	94	$(3,3,8)$; $(3,3,\infty)$; $(3,4,8)$; $(3,4,\infty)$; $(3,8,\infty)$
91	186	$(2,3,6)$; $(2,3,8)$
92	134	$(2,3,3)$; $(2,3,8)$; $(2,3,\infty)$; $(3,3,8)$
93	138	$(2,3,3)$; $(2,3,8)$; $(2,3,\infty)$; $(2,8,\infty)$; $(3,3,8)$; $(3,3,\infty)$
94	193	$(2,3,4)$; $(2,3,8)$; $(2,4,4)$; $(2,4,8)$
95	118, 119	$(2,3,8)$; $(2,4,8)$; $(3,8,8)$
96	194	$(2,3,4)$; $(2,3,8)$; $(2,3,\infty)$; $(2,4,4)$; $(2,4,8)$; $(3,3,4)$
97	95	$(2,8,\infty)$; $(3,3,4)$; $(3,4,8)$; $(3,4,\infty)$; $(3,8,\infty)$; $(3,\infty,\infty)$; $(4,8,\infty)$
98	139	$(2,3,4)$; $(2,3,5)$; $(2,3,8)$; $(2,4,5)$; $(2,5,8)$; $(3,4,5)$
99	200	$(2,3,4)$; $(2,3,5)$; $(2,3,8)$; $(2,3,\infty)$; $(3,3,4)$; $(3,3,5)$
100	135	$(2,3,4)$; $(2,3,6)$; $(2,4,8)$; $(2,6,8)$
101	140	$(2,3,3)$; $(2,3,4)$; $(2,3,6)$; $(2,3,8)$; $(2,3,\infty)$; $(2,4,4)$; $(2,4,8)$; $(2,8,\infty)$; $(3,3,3)$; $(3,3,4)$; $(3,3,6)$; $(3,4,4)$
102	199	$(2,3,5)$; $(2,3,6)$; $(2,3,8)$; $(2,3,\infty)$; $(2,4,5)$; $(2,4,6)$

□

Chapter 6

Future work

Motivated by the results on real variations of stability in Chapter 4 and the novel combinatorial structures discovered in Chapter 5, we conclude the thesis by exploring further research directions and open problems.

§ 6.1 | Towards full stability conditions

In this section we discuss future work building on from Section 4.4.

§ 6.1.1 | Covering maps

The first priority is to use the examples of real variations of stability on $\mathcal{D}_\Delta$ we have constructed in Chapter 4 to realise $\operatorname{Stab}\mathcal{D}_\Delta$ as a covering space, a question of much interest. This would give a novel approach to studying the $K(\pi,1)$ conjecture both within and outside the Coxeter setting, and investigating topological properties of the stability manifold.

Problem 6.1. Prove that the real variations of stability conditions constructed on the category $\mathcal{D}_\Delta$ in Theorem 4.20 induce a regular covering map from $\operatorname{Stab}\mathcal{D}_\Delta$.

§ 6.1.2 | Almost regular points

We now wish to give an analogue of the main theorem of [ABM15], which constructs a connected submanifold $\widetilde{U}$ of the space of stability conditions. This submanifold is controlled by the t-structures appearing in real variations of stability, and related to the following region.

Definition 6.2 ([ABM15, §2.3])**.** Let Δ be a connected graph of affine of hyperbolic type. The *almost regular* part of Level_Δ is the set $\mathsf{Level}_\Delta^{\mathrm{ar}}$ consisting of ϑ whose stabiliser in W_Δ has at most two elements. In other words, $\vartheta \in \mathsf{Level}_\Delta^{\mathrm{ar}}$ is either strictly inside an alcove or on a single hyperplane.

Recall the complexification $\mathsf{Level}_\Delta^{\mathbb{C}}\backslash\mathcal{H}_\Delta^{\mathbb{C}}$ from Definition 2.45, wherein lies the region

$$U \coloneqq \{(\vartheta,\vartheta') \in \mathsf{Level}_\Delta^{\mathrm{ar}} \times \mathsf{Level}_\Delta \mid \vartheta \in \mathsf{Level}_\Delta\backslash\mathcal{H}_\Delta \text{ or } (\vartheta,\vartheta') \in \overline{A}\times A \text{ for some } A \in \mathsf{Alc}_\Delta\},$$

which is related to an open neighbourhood of the almost regular points in $\mathsf{Level}_\Delta^{\mathbb{C}}$.

Example 6.3. Consider the graph $\Delta = \mathbb{K}_2$, so $\mathsf{Level}_\Delta \cong \mathbb{R}$ and $\mathcal{H}_\Delta \cong \mathbb{Z}$, that is alcoves are open intervals $(a, a+1)$. In this case we also have $\mathsf{Level}_\Delta^{\mathrm{ar}} = \mathsf{Level}_\Delta$, as there are no codimension two walls. Clearly any element of the form $((a, a+1), \mu)$ is in U, and if $\lambda = a \in \mathbb{Z}$ then this forces $\mu \in (a-1, a) \cup (a, a+1)$. Hence

$$U \cong \{z \in \mathbb{C} \mid \Re(z) \notin \mathbb{Z} \text{ or } \Re(z) - 1 < \Im(z) < \Re(z) + 1, \Im(z) \neq \Re(z)\}$$

in this case. For higher Kronecker graphs we obtain a similar picture but with non-uniform alcove length.

§ 6.1.3 | Connected submanifolds

Fix a universal cover of $\mathsf{Level}_\Delta^{\mathbb{C}} \backslash \mathcal{H}_\Delta^{\mathbb{C}}$, and let $\widetilde{U}$ be the preimage of U in this cover.

Since the region

$$U_+ \coloneqq \{(\eta, \eta') \in \mathsf{Level}_\Delta^{\mathbb{C}} \mid \eta \in A_+ \text{ or } (\eta, \eta') \in \overline{A_+} \times A_+\}$$

is a fundamental domain for the action of W_Δ on U, a point in $\widetilde{U}$ can be expressed as a pair (p, z). Here $z = (\eta, \eta') \in U_+$ and p is the homotopy class of a path between A_+ and some $A \in \mathsf{Alc}_\Delta$, which we can identify with an element in the braid group. Thus there is a projection

$$\pi \colon \widetilde{U} \to U, \qquad (p, z) \mapsto \overline{p}(z),$$

where $\overline{p} \in W_\Delta$ is the Weyl element corresponding to p. If $\mathbb{F}$ is a real flow on $\mathcal{H}_\Delta$ then there is also an inclusion

$$\iota \colon \widetilde{U} \hookrightarrow \operatorname{Stab} \mathcal{D}_\Delta, \qquad (p, z) \mapsto (\sqrt{-1}\overline{p}(z), \mathbb{F}_{\overline{p}(\mathcal{A}_+)}).$$

The following theorem, which we wish to replicate using the technology of flows, was first given in [ABM15] in the context of a simple Lie algebra $\mathfrak{g}$ over $\mathbb{C}$, with $\mathcal{D}$ being the derived category of coherent sheaves on a resolution of a Slodowy slice singularity.

Conjecture 6.4 (Cf. [ABM15, Theorem 1])**.** *Let $(Z, \heartsuit)$ be a real variation of stability on $\mathcal{D}_\Delta$. Then there exists a unique continuous Br_Δ-equivariant map $\iota \colon \widetilde{U} \to \operatorname{Stab} \mathcal{D}_\Delta$ such that*

$$\begin{array}{ccc} \widetilde{U} & \xrightarrow{\iota} & \operatorname{Stab} \mathcal{D}_\Delta \\ {\scriptstyle\pi}\downarrow & & \downarrow{\scriptstyle Z} \\ U & \xrightarrow[\sqrt{-1}E]{} & K(\mathcal{D}_\Delta)^*_{\mathbb{C}} \cong \Theta_{\mathbb{C}} \end{array} \tag{6.A}$$

commutes and for all $A \in \mathsf{Alc}_\Delta$, $z \in \widetilde{A}$, the heart of $\iota(z)$ is $\heartsuit(A)$.

Whilst such a $\widetilde{U}$ would be connected, as observed by [ABM15] it is far from being universal, hence the following problem.

Problem 6.5. Construct an explicit subset of $\operatorname{Stab} \mathcal{D}_\Delta$ which is a universal covering of a some domain whose fundamental group is isomorphic to Br_Δ, similarly to [Ike14].

§ 6.2 | Understanding intersection arrangements

We next discuss generalisations of the results in Section 5.4.

§ 6.2.1 | Higher dimensional intersections

Building on the work in Chapter 5, the first natural question to ask is can we extend this classification to higher corank. An ambitious classification is that of *all* hyperbolic intersection arrangements, which is possible due to there only being finitely many diagrams of this type.

Problem 6.6. Give a full list of hyperbolic intersection arrangements in dimensions two to nine. That is, classify the unique arrangements $\mathcal{H}_\mathcal{J}$ arising from the data of a hyperbolic graph Δ and a subset $\mathcal{J} \subseteq \Delta$ of corank $3 \leq \mathsf{crk} \leq 10$.

Whilst visualising the arrangements in higher dimensions would be more tricky, the combinatorial invariants used in the previous chapter still apply. For example, alcoves in a corank four intersection arrangement would be (hyperbolic, in our case) tetrahedrons with faces corresponding to the simple wall-crossings and dihedral angles between faces given by braiding as before. This may be of independent interest to geometric group theorists as a family of hyperbolic non-Coxeter arrangements. We are interested in how many intersection arrangements are 'old' Coxeter, 'new' Coxeter, and non-Coxeter.

Example 6.7. Consider the following corank four subset of $\mathbb{S}_5$,

$\mathcal{J} =$ 

coloured as in Example 5.21 but with an additional colour. Similarly to Proposition 5.31, this subset is fixed under mutation, so its intersection arrangement is a Coxeter arrangement in $\mathbb{H}^3$, which is possible to visualise using the Poincaré ball model. Each alcove is a hyperbolic tetrahedron, with each of the four faces corresponding to a simple wall-crossing with respect to the coloured vertices. The six dihedral angles correspond to a braid between two repeated wall-crossings, and so by listing these angles we can visualise the intersection arrangement. Each alcove in the first intersection arrangement is a hyperbolic tetrahedron and it can be directly computed that its dihedral angles are $\frac{\pi}{2}$ (wall-crossing pairs ●●, ●●, ●●) and $\frac{\pi}{4}$ (wall-crossing pairs ●●, ●●, ●●).

Our intuition is that as the corank increases so does the proportion of symmetric mutation classes that give different intersection arrangements. This is because each alcove has $\binom{\mathsf{crk}}{2}$ angles and so there is more choices of unique tetrahedra and ways that the arrangements could differ in their gluing.

§ 6.2.2 | Hyperbolic Dynkin diagrams

In the context of intersection arrangements we restricted to a graph (symmetric GCM) and a subset of its vertices, but the general theory laid out in [IW] holds for any Coxeter group provided strongly Dynkin subsets exist. For example, Lemma 5.17 immediately generalises to any hyperbolic GCM, regardless of symmetry.

This means that a larger classification, of both affine and hyperbolic intersection arrangements, is possible by considering symmetrisable GCMs. By giving a convenient criterion for symmetrisability, [CCC+10] enumerate the 142 symmetrisable GCMs of hyperbolic type. This opens up the possibility of studying intersection arrangements of types $\mathbb{B}$, $\mathbb{C}$, $\mathbb{F}$, and $\mathbb{G}$, which admit overextended vertices.

Problem 6.8. Classify the tilings of $\mathbb{H}^2$ occurring as intersection arrangements of symmetrisable hyperbolic Dynkin diagrams. Determine if the only polygons appearing in the dual graph of such tilings are those in Theorem 5.45.

In this level of generality we may obtain even richer combinatorial structure, in the form of new polygons and angle combinations, reflecting non-simply laced behaviour.

§ 6.2.3 | The mutation groupoid

In order to capture the full complexity and structure of the arrangements proposed above, we formally introduce a powerful invariant.

Definition 6.9. The *mutation groupoid* $\mathcal{G}_\mathcal{J}$ associated with $(\Delta, \mathcal{J})$ has objects the mutation class members, where $J \in [\mathcal{J}]$ is now an ordered set, and morphisms corresponding to mutation. The relations in $\mathcal{G}_\mathcal{J}$ are given by braidings (5.H) of simple-wall crossings.

In other words, $\mathcal{G}_\mathcal{J}$ is the same data as in the symmetric mutation table of Theorem 5.24, but now we also keep track of the specific colours of vertices in J^c. As an example, $\mathbb{A}_2^{\text{hyp}}$ has four elements in its (only) mutation class but eight in the mutation groupoid, encoding the fact that the coloured vertices can become rearranged if one continues the first mutation table in Proposition 5.26. Using the language of angle data, this notion of rearranging the coloured vertices captures alcoves admitting different orientations, leading to a more intricate arrangement.

A problem related to classifying intersection arrangements is to determine a fundamental region for each unique tiling and the group that acts on that region to produce the tiling. This should come from a minimal spanning tree within the fundamental groupoid, giving some global structure to our tessellations and further illuminating the hyperbolic geometry in the background.

Problem 6.10. Use the mutation groupoid of $(\Delta, \mathcal{J})$ to construct a fundamental region for $\mathcal{H}_\mathcal{J}$ and a Coxeter group that acts upon it to tile $\mathsf{Level}_\mathcal{J}$. Use this information to precisely classify intersection arrangements in higher dimensional and more general settings.

§ 6.3 | Local systems of categories

This section acts as a way to combine the novel technology of intersection arrangements and tilted hearts from the previous two chapters, further generalising notions of stability and connecting them with rich combinatorial structure. In Chapter 4 we used a groupoid structure where at every alcove the object was a copy of the category $\mathcal{D}_\Delta$. With a more local hyperplane structure established in Chapter 5 we may now assign a triangulated category $\mathcal{D}_J$ that varies as we move through alcoves. This takes advantage of the full generality of real variations: instead of a fixed category at each alcove and varying the hearts, we now have a varying ambient category within which sits a bounded heart.

§ 6.3.1 | Local systems of categories

We now wish for an algebraic structure akin to the local rules for intersection arrangements, lifting Chapter 4 out of the Coxeter setting. In the construction of Theorem 4.20, the hearts assigned to each alcove live inside the same triangulated category. However this restriction is not used anywhere, suggesting that a more local construction is possible. Indeed, Anno, Bezrukavnikov, and Mirković anticipate this with the following concept.

Definition 6.11 ([ABM15, Definition 3])**.** Let $\mathcal{H} \subseteq \mathcal{L}$ be a locally finite hyperplane arrangement and let Alc be its set of alcoves. A *local system of categories with a stability condition* is a choice of triangulated category $\mathcal{D}_A$ and bounded heart $\heartsuit(A)$ for each alcove, such that for every homotopy class of a path p connecting $A, B \in \mathsf{Alc}$ there exists a triangulated equivalence $\Phi_p \colon \mathcal{D}_A \to \mathcal{D}_B$ satisfying $\Phi_{pq} \cong \Phi_p \Phi_q$ and $\Phi_{A \to A} \cong \mathrm{id}_{\mathcal{D}_A}$. Finally fix a central charge map $Z \colon \mathcal{L} \to K(\mathcal{D}_A)^*_{\mathbb{R}}$ for some (equivalently, any) alcove A, such that the following hold:

(1) $\langle Z_\vartheta, [M] \rangle > 0$ for all $\vartheta \in A$ and all nonzero M in $\heartsuit(A)$.

(2) If A and B share a hyperplane H and p is the path between them around H in the positive direction, then the hearts $\heartsuit(A)$ and $\heartsuit(B)$ are related as in Definition 4.1(2).

We aim to construct a large class of examples of local systems of categories, which would specialise to Theorem 4.20 in the case $\mathcal{J} = \varnothing$. This would then explore, for the first time, stability conditions on *contracted* preprojective algebras and *singular* K3 categories, not considered in previous work such as [Ike14], [HW23].

Problem 6.12. Generalise Theorem 4.20 to intersection arrangements by showing that the data of $\mathcal{H}_\mathcal{J}$ and $\mathcal{D}_\mathcal{J}$, the latter defined in the next subsection, give rise to a local system of categories with a stability condition.

§ 6.3.2 | Contracted preprojective algebras

Definition 6.13 ([IW, §5.1])**.** The *contracted preprojective algebra* of $(\Delta, \mathcal{J})$ is defined as the corner algebra

$$\Pi_{\mathcal{J}} \coloneqq e_{\mathcal{J}} \Pi e_{\mathcal{J}},$$

where $e_{\mathcal{J}} \coloneqq 1 - \sum_{j \in \mathcal{J}} e_j$ is the idempotent corresponding to $\mathcal{J}$.

For $\mathcal{J} \subseteq \Delta$ we may then associate the triangulated category

$$\mathcal{D}_{\mathcal{J}} \coloneqq \mathrm{D}^{\mathrm{b}}_{\mathrm{nilp}}(\Pi_{\mathcal{J}}),$$

which is *singular* 2-Calabi–Yau (see [IW, Proposition 5.10]).

As seen in Section 3.4, the 'global' preprojective algebra Π_Δ admits classical tilting objects that correspond to reduced expressions of Weyl group elements, which are in bijection with chambers in the Coxeter arrangement. The main result of [IW, Part 2] is that this idea generalises to the intersection arrangements $\mathcal{H}_{\mathcal{J}}$ using $\Pi_{\mathcal{J}}$, partitioning the contracted preprojective algebra into derived equivalence classes.

Theorem 6.14 ([IW, Theorem 5.2])**.** *If Δ is extended ADE and $\mathcal{J} \subseteq \Delta$ is strongly Dynkin, then the map*

$$(x, J) \mapsto e_{\mathcal{J}} T_x e_J$$

is a bijection between alcoves in the intersection arrangement and tilting modules in $\Pi_{\mathcal{J}}$. Furthermore, wall-crossing is compatible with mutation functors.

For an arbitrary graph Δ, it is unknown whether this map is bijective. However, we can still use the assignment to connect wall-crossing in local arrangements with mutation functors on the contracted preprojective algebra. Indeed, the tilting module $e_J T_x e_K$ induces a derived equivalence $\mathbb{R}\mathrm{Hom}_{\Pi_{\mathcal{J}}}(e_J T_x e_K, -)$ between categories $\mathcal{D}_J$ and $\mathcal{D}_K$, corresponding to alcoves (x, J) and (y, K), respectively. Hence there is candidate data for a local system of categories in the sense of Definition 6.11.

§ 6.3.3 | Atomic Matsumoto

It is important to check that everything we assumed regarding wall-crossing still holds in this setting, such as Matsumoto's Theorem 2.39 relating reduced expressions. A key ingredient in this direction is a result by Ko relating reduced expressions of paths between $\mathcal{J}$-alcoves, using the following language from Coxeter theory.

Definition 6.15 (Cf. [Ko24, Definition 1.1])**.** Let (W, S) be a Coxeter system. A parabolic double coset $W_J w W_K$ is a *core coset* if we have

$$W_J w = W_J w W_K = w W_K.$$

By [Ko24, Proposition 9.2], there is a bijection between core cosets and $\mathcal{J}$-alcoves.

Theorem 6.16 ([Ko24, Theorem 5.1])**.** *Two atomic reduced expressions of the same core coset (which correspond to $\mathcal{J}$-alcoves) are related by atomic braid relations.*

§ 6.4 | Beyond hyperbolic type

A general motivation of this thesis has been to be able to say as much as possible about the preprojective algebra in the wild setting. Indeed, we worked in this direction when showing that the category of nilpotent modules over Π_Δ forms a faithful heart inside its derived category (Theorem 4.14). With Theorem 3.18 showing noetherianity failing for Π_Δ when Δ is wild, we continue in this spirit and ask whether a natural weaker property holds.

Definition 6.17. A ring Λ is *(right) coherent* if every finitely generated (right) ideal is finitely presented.

Clearly if Δ is finite type or tame then its noetherian preprojective algebra is coherent, but in general this is still an open problem. Showing that Π_Δ is coherent would simplify many of the approaches used in this thesis, such as being able to use the (now abelian) category $\operatorname{fp}\Pi_\Delta$ of finitely presented modules. Moreover, many theorems about finitely generated modules over noetherian rings could then be applied.

Problem 6.18. Let Δ be a graph of wild type and let Π be the preprojective algebra of any quiver with underlying graph Δ. Determine if Π_Δ is coherent as a ring; if not, is there a hyperbolic counterexample?

This problem has seen some progress in the work of Minamoto, as it is a consequence of [Min12, Proposition 5.1] that if Δ is acyclic then Π_Δ is *graded coherent*. In other words, the category $\operatorname{gr}\operatorname{fp}\Pi_\Delta$ of graded finitely presented modules is abelian whenever Δ is acyclic. In [Min18, Proposition 3.2], Minamoto also provides a criterion for the preprojective algebra to be graded coherent, based on the Auslander-Reiten translations of the underlying path algebra. However, it is known that graded coherence does not imply coherence in general.

Definition 6.19. A noetherian $\mathbb{C}$-algebra Λ is *Iwanaga–Gorenstein* if it has finite injective dimension as both an Λ-module and a Λ^{op}-module. In this case a finitely generated Λ-module M is said to be *Cohen–Macaulay* if $\operatorname{Ext}^\bullet_\Lambda(M,\Lambda)=0$.

This motivates an alternative approach.

Theorem 6.20 ([AIR15, Theorem 2.2])**.** *Let Λ be a $\mathbb{C}$-algebra with idempotent $e\neq 1$, and suppose that Λ is bimodule CY_d, noetherian, and $\Lambda/\langle e\rangle$ is finite-dimensional over $\mathbb{C}$. Then $e\Lambda e$ is Iwanaga–Gorenstein, Λe is a $(d-1)$ cluster tilting Cohen–Macaulay $e\Lambda e$-module, and there is a natural isomorphism $\operatorname{End}_{e\Lambda e}(\Lambda e)\cong\Lambda$.*

We expect it is possible to remove the noetherian assumption from this result and a well-chosen idempotent e to reduce the question of coherence to the simpler algebraic objects of $e\Pi_\Delta e$ and $\Pi_\Delta e$.

Appendix A

Arrangement code

In the interest of reproducibility, this appendix contains computer algebra code, written in `Magma` (Appendix A.1–A.3) and `Mathematica` (Appendix A.4). This verifies the classification of symmetric mutation classes in Section 5.3 and draws the hyperbolic intersection arrangements in Section 5.4. We give the minimal code required for this, but much more functionality has been implemented, such as a way to 'explore' arrangements, a colouring of the tilings, and the overlay of angle data.

Throughout the code excerpts in this appendix, the symbol ↪ represents a line break, which should disappear when copied from most document readers.

§ A.1 | Initialisation

This section includes preliminary code that will be used in the rest of the scripts.

§ A.1.1 | Hyperbolic graphs

We first encode the hyperbolic graphs in rank three to ten via their generalised Cartan matrices, following Theorem 2.26 with indexing $\{\infty, 0, 1, 2, \dots\}$. In `Magma` these are simply sequence objects indexed $\{1, \dots, \mathsf{rk}\}$, which are converted into matrix objects by the functions to follow.

```
// rank three
A1hyp := [[2,-1,0],[-1,2,-2],[0,-2,2]];
A1hyp1 := [[2,-2,0],[-2,2,-2],[0,-2,2]];
A2aff1 := [[2,-2, -1],[-2,2,-1],[-1,-1,2]];
A2aff2 := [[2,-2,-2],[-2,2,-1],[-2,-1,2]];
A2aff3 := [[2,-2,-2],[-2,2,-2],[-2,-2,2]];
// rank four
A2hyp := [[2,-1,0,0],[-1,2,-1,-1],[0,-1,2,-1],[0,-1,-1,2]];
A2hyp1 := [[2,-1,-1,0],[-1,2,-1,-1],[-1,-1,2,-1],[0,-1,-1,2]];
A2hyp2 := [[2,-1,-1,-1],[-1,2,-1,-1],[-1,-1,2,-1],[-1,-1,-1, 2]];
// rank five
A3hyp := [[2,-1,0,0,0],[-1,2,-1,0,-1],[0,-1,2,-1,0],
         [0,0,-1,2,-1],[0,-1,0,-1,2]];
A3hyp1 := [[2,-1,0,-1,0],[-1,2,-1,0,-1],[0,-1,2,-1,0],
```

```
          [-1, 0,-1,2, -1],[0,-1,0,-1,2]];
// rank six
A4hyp := [[2,-1,0,0,0,0],[-1,2,-1,0,0,-1],[0,-1,2,-1,0,0],
          [0,0,-1,2,-1,0],[0,0,0,-1,2,-1],[0,-1,0,0,-1,2]];
D4hyp := [[2,-1,0,0,0,0],[-1,2,0,-1,0,0],[0,0,2,-1,0,0],
          [0,-1,-1,2,-1,-1],[0,0,0,-1,2,0],[0,0,0,-1,0,2]];
S5 := [[2,-1,-1,-1,-1,-1],[-1,2,0,0,0,0],[-1,0,2,0,0,0],
       [-1,0,0,2,0,0],[-1,0,0,0,2,0],[-1,0,0,0,0,2]];
// rank seven
A5hyp := [[2,-1,0,0,0,0,0],[-1,2,-1,0,0,0,-1],[0,-1,2,-1,0,0,0],
          [0,0,-1,2,-1,0,0],[0,0,0,-1,2,-1,0],[0,0,0,0,-1,2,-1],
          [0,-1,0,0,0,-1,2]];
D5hyp := [[2,-1,0,0,0,0,0],[-1,2,0,-1,0,0,0],[0,0,2,-1,0,0,0],
          [0,-1,-1,2,-1,0,0],[0,0,0,-1,2,-1,-1],[0,0,0,0,-1,2,0],
          [0,0,0,0,-1,0,2]];
// rank eight
A6hyp := [[2,-1,0,0,0,0,0,0],[-1,2,-1,0,0,0,0,-1],[0,-1,2,-1,0,0,0,0],
          [0,0,-1,2,-1,0,0,0],[0,0,0,-1,2,-1,0,0],[0,0,0,0,-1,2,-1,0],
          [0,0,0,0,0,-1,2,-1],[0,-1,0,0,0,0,-1,2]];
D6hyp := [[2,-1,0,0,0,0,0,0],[-1,2,0,-1,0,0,0,0],[0,0,2,-1,0,0,0,0],
          [0,-1,-1,2,-1,0,0,0],[0,0,0,-1,2,-1,0,0],[0,0,0,0,-1,2,-1,-1],
          [0,0,0,0,0,-1,2,0],[0,0,0,0,0,-1,0,2]];
E6hyp := [[2,-1,0,0,0,0,0,0],[-1,2,0,0,-1,0,0,0],[0,0,2,-1,0,0,0,0],
          [0,0,-1,2,0,-1,0,0],[0,-1,0,0,2,-1,0,0],[0,0,0,-1,-1,2,-1,0],
          [0,0,0,0,0,-1,2,-1],[0,0,0,0,0,0,-1,2]];
// rank nine
A7hyp := [[2,-1,0,0,0,0,0,0,0],[-1,2,-1,0,0,0,0,0,-1],
          [0,-1,2,-1,0,0,0,0,0],[0,0,-1,2,-1,0,0,0,0],
          [0,0,0,-1,2,-1,0,0,0],[0,0,0,0,-1,2,-1,0,0],
          [0,0,0,0,0,-1,2,-1,0],[0,0,0,0,0,0,-1,2,-1],
          [0,-1,0,0,0,0,0,-1,2]];
D7hyp := [[2,-1,0,0,0,0,0,0,0],[-1,2,0,-1,0,0,0,0,0],
          [0,0,2,-1,0,0,0,0,0],[0,-1,-1,2,-1,0,0,0,0],
          [0,0,0,-1,2,-1,0,0,0],[0,0,0,0,-1,2,-1,0,0],
          [0,0,0,0,0,-1,2,-1,-1],[0,0,0,0,0,0,-1,2,0],
          [0,0,0,0,0,0,-1,0,2]];
E7hyp := [[2,-1,0,0,0,0,0,0,0],[-1,2,-1,0,0,0,0,0,0],
          [0,-1,2,-1,0,0,0,0,0],[0,0,-1,2,0,-1,0,0,0],
          [0,0,0,0,2,-1,0,0,0],[0,0,0,-1,-1,2,-1,0,0],
          [0,0,0,0,0,-1,2,-1,0],[0,0,0,0,0,0,-1,2,-1],
```

```
         [0,0,0,0,0,0,0,-1,2]];
// rank ten
D8hyp := [[2,-1,0,0,0,0,0,0,0,0],[-1,2,0,-1,0,0,0,0,0,0],
         [0,0,2,-1,0,0,0,0,0,0],[0,-1,-1,2,-1,0,0,0,0,0],
         [0,0,0,-1,2,-1,0,0,0,0],[0,0,0,0,-1,2,-1,0,0,0],
         [0,0,0,0,0,-1,2,-1,0,0],[0,0,0,0,0,0,-1,2,-1,-1],
         [0,0,0,0,0,0,0,-1,2,0],[0,0,0,0,0,0,0,-1,0,2]];
E8hyp := [[2,-1,0,0,0,0,0,0,0,0],[-1,2,0,0,0,0,0,0,0,-1],
         [0,0,2,-1,0,0,0,0,0,0],[0,0,-1,2,0,-1,0,0,0,0],
         [0,0,0,0,2,-1,0,0,0,0],[0,0,0,-1,-1,2,-1,0,0,0],
         [0,0,0,0,0,-1,2,-1,0,0],[0,0,0,0,0,0,-1,2,-1,0],
         [0,0,0,0,0,0,0,-1,2,-1],[0,-1,0,0,0,0,0,0,-1,2]];
```

§ A.1.2 | Helper functions

The following procedures are used routinely in our computations, and are modifications to existing procedures in `Magma`. The function `Phase(x,y)` takes a point (x, y), such as the ideal points (5.D) viewed as a complex number, and returns its argument. and returns the argument. The function `CrossProduct(v, w)` computes $\boldsymbol{v} \times \boldsymbol{w}$ in order to find intersections of geodesics via (5.E).

```
// compute the phase in [0, 2pi] of a point on the unit circle
Phase := function(x, y)
  pi := Pi(RealField(1000));
  if y gt 0 then
    quo := x/y;
    // trick to make Sign(0) = 0
    return(Arccot(quo) + (1-Sign(quo)^Sign(quo))*pi/2);
  elif y lt 0 then
    quo := x/y;
    return(Arccot(quo) + (3-Sign(quo))*pi/2);
  elif x lt 0 then
    return(pi);
  else
    return(0);
  end if;
end function;
// compute the cross product of two vectors in R3
CrossProduct := function(v, w)
  return([v[2]*w[3]-v[3]*w[2], v[3]*w[1]-v[1]*w[3], v[1]*w[2]-v[2]*w
     ↪ [1]]);
end function;
```

§ A.2 | Symmetric mutation classes

This section implements checks of the classification of hyperbolic symmetric mutation classes in Section 5.3.

§ A.2.1 | Simple wall-crossing

The function `SimpleWallCrossing(Delta, J, i, (x))` implements $\omega_i(x, J)$ from Definition 5.10, and is crucial in the rest of the code. The function takes the following arguments:

(1) `Delta` — Δ as in §A.1.1,

(2) `J` — J encoded as a sequence of indices,

(3) `i` — $i \in J^c$ encoded as a positive integer at most `rk`,

(4) `x` — $x \in W_\Delta$, an optional argument (by default the identity), encoded as a sequence of simple reflection indices.

For example, `J = [1,3,4,5], x = [1,2]` represents the $\mathcal{J}$-alcove $(s_1s_2, \{1,3,4,5\})$. Checks are first made to ensure that $i \in J^c$ and J is i-Dynkin in the sense of Definition 5.9. The new Weyl element y and subset K are returned encoded in the same way, along with the image of i under the involution $\iota_{J+i}(i)$, so that this process may be repeated.

```
// mutate alcove (x, J) to (y, K)
SimpleWallCrossing := function(Delta, J, i: x := [])
  // checks
  error if i in J,
  "Can only mutate with respect to i not in J";
  // setup
  r := #Delta; // rank
  C := Matrix(Rationals(), Delta); // Cartan matrix
  W<[s]> := CoxeterGroup(C); // Weyl group
  Graph := Graph<r | ScalarMatrix(r, 2) - C>;
  V := VertexSet(Graph);
  if #J gt 0 then
    GraphJ := sub<Graph | {V!j : j in J}>;
  else
    GraphJ := NullGraph();
  end if;
  GraphJi := sub<Graph | {V!j : j in Include(J, i)}>;
  v := VertexSet(GraphJi)!V.i;
  WJ := CoxeterGroup(GrpFPCox, GraphJ); // parabolic subgroups
  WJi := CoxeterGroup(GrpFPCox, GraphJi);
```

```
  error if not IsFinite(WJi),
  "Subset must be strongly Dynkin";
  JiC := Component(v);
  Aut, VJi := AutomorphismGroup(JiC);
  // compute Weyl element y
  lJ := Length(LongestElement(WJ));
  lJi := Length(LongestElement(WJi));
  wJ := W![Index(V!VertexSet(GraphJ)!ElementToSequence(LongestElement(
     ↪ WJ))[s]) : s in [1..lJ]];
  wJi := W![Index(V!VertexSet(GraphJi)!ElementToSequence(LongestElement
     ↪ (WJi))[s]) : s in [1..lJi]];
  y := (W!x)*wJ*wJi;
  // compute subset K
  if #Aut eq 1 then
    iotav := V!v; // trivial involution
  elif CartanName(JiC)[1] eq "D" and IsEven(StringToInteger(CartanName(
     ↪ JiC)[2])) then
    iotav := V!v; // D4, D6, D8: trivial involution
  elif CartanName(JiC)[1] eq "E" and CartanName(JiC)[2] ne "6" then
    iotav := V!v; // E7, E8: trivial involution
  else
    iotav := V!Image(Aut.1, VJi, v); // nontrivial involution
  end if;
  K := [j : j in Include(J, i) | V.j ne iotav];
  // output
  return<ElementToSequence(y), K, Index(iotav)>; // record image of i
end function;
```

§ A.2.2 | List of classes

Next we define the function `SMC(Delta)`, which as input takes Δ as above and computes its symmetric mutation classes from corank 3 to corank `rk`, returning the full class decomposition, the cotype of each class, and the number of total classes. The corank three output of this function coincides with Theorem 5.24.

```
// compute all symmetric mutation classes in corank at least three
SMC := function(Delta)
  // setup
  rk := #Delta; // rank
  C := Matrix(Rationals(), Delta); // Cartan matrix
  Graph := Graph<rk | ScalarMatrix(rk, 2) - C>;
  V := VectorSpace(Rationals(), rk); // root lattice
```

```
e := Basis(V); // simple roots
MC := [];
// mutation classes
for crk in [3..rk] do
  print "Corank:", crk;
  mc := [];
  for Jc in Subsets({1..rk}, crk) do
    J := {1..rk} diff Jc;
    Jmc := {Jc};
    if Jc in &join(mc) then // check if we've seen subset before
      continue Jc;
    end if;
    GraphJ := Graph;
    AssignVertexLabels(~GraphJ, [(&+[e[j] : j in Jc])[i] : i in [1..rk
      ↪ ]]);
    for Kc in &join(mc) do
      GraphK := Graph;
      AssignVertexLabels(~GraphK, [(&+[e[k] : k in Kc])[i] : i in [1..
        ↪ rk]]);
      if IsIsomorphic(GraphJ, GraphK) then // symmetry
        Kpos := Position([Kc in Kmc : Kmc in mc], true);
        Include(~mc[Kpos], Jc);
        continue Jc;
      end if;
    end for;
    ncls := 0;
    while #Jmc gt ncls do
      ncls := #Jmc;
      for Kc in Jmc do
        K := {1..rk} diff Kc;
        for i in Kc do
          GraphKi := sub<Graph | {VertexSet(Graph)!k : k in Include(K,
            ↪  i)}>;
          WKi := CoxeterGroup(GrpFPCox, GraphKi);
          if IsFinite(WKi) then // mutation
            Include(~Jmc, Include(Exclude(Kc, i), SimpleWallCrossing(
              ↪ Delta, K, i)[3]));
          end if;
        end for;
      end for;
```

```
      end while;
      Include(~mc, Jmc);
    end for;
    Append(~MC, mc);
    mc;
  end for;
  print "Symmetric mutation classes:", &+[#mc : mc in MC];
  // output
  print "Cotypes:", Append([[CartanName(sub<Graph | {VertexSet(Graph)!j
      ↪  : j in ({1..rk} diff Random(cls))}>) : cls in mc] : mc in
      ↪ Prune(MC)], ["Empty"]);
  return MC;
end function;
```

§ A.3 | Arrangement data

This section implements Section 5.2, namely the restricted root system, change of variables, and restricted hyperplane intersections (5.D). This data can then be passed to `Mathematica` in order to draw the hyperplanes in an intersection arrangement $\mathcal{H}_{\mathcal{J}}$, following (5.F).

§ A.3.1 | Diagonalisation to unit hyperboloid

First we perform the coordinate transformation, in particular computing the matrices $E_{\mathcal{J}}$ and $Q_{\mathcal{J}}$ from Section 5.2.2, which are used to view the intersection arrangement as living in the hyperbolic plane. The function `DiagonaliseLevel(Delta, Jc, (p))` receives as input:

(1) `Delta` — Δ, as in §A.1.1,

(2) `Jc` — $\mathcal{J}^c$, encoded as a sequence of indices,

(3) `p` — an optional positive integer (by default 15), controlling the precision of arithmetic over $\mathbb{R}$.

The eigenspace of the restricted GCM $C_{\mathcal{J}}$ is computed over the splitting field of its characteristic polynomial, and we verify that (5.B) is satisfied. The eigenspace computations have only been implemented for the case $\mathsf{crk} = 3$, but the generalisation is straightforward.

```
// change of variables to unit hyperboloid
DiagonaliseLevel := function(Delta, Jc: p := 15)
  // setup
  r := #Delta; // rank
  R := RealField(p); // reals to precision p
```

```
C := Matrix(Rationals(), Delta); // Cartan matrix
CJ := Submatrix(C^-1, Jc, Jc); // restricted Cartan
F := SplittingField(CharacteristicPolynomial(CJ)); // splitting field
V := VectorSpace(R, 3); // root space
if Type(F) ne FldRat then
  z := R!Zeroes(F, p)[1]; // primitive root
else
  z := 0; // F = Q
end if;
CJ := MatrixRing(F, 3)!CJ; // work over field
// eigenvalues
evalF := &cat[[e[1] : j in [1..e[2]]] : e in Setseq(Eigenvalues(CJ))
   ↪ ];
if Type(F) ne FldRat then
  evalR := [&+[Eltseq(e)[i]*z^(i-1) : i in [1..#Eltseq(e)]] : e in
     ↪ evalF];
else
  evalR := [R!e : e in evalF];
end if;
evalsort := Reverse(Sort(evalR)); // negative eigenvalue last
ord := [];
for i in [1..3] do
  pos := Position(evalR, evalsort[i]);
  evalR[pos] := 0;
  Append(~ord, pos);
end for;
evalR := evalsort;
print "Eigenvalues:", evalR;
EJ := DiagonalMatrix([Sqrt(AbsoluteValue(evalR[i])) : i in [1..3]]);
// eigenvectors
mult := [#[i : i in [1..3] | evalR[i] eq evalR[j] and i le j] : j in
   ↪ [1..3]]; // geometric multiplicity
evecF := [Basis(Eigenspace(CJ, evalF[ord[i]]))[mult[i]] : i in
   ↪ [1..3]];
if not Type(F) eq FldRat then
  evecR := [V![&+[Eltseq(v[k])[j]*z^(j-1) : j in [1..#Eltseq(v[k])]]
     ↪ : k in [1..3]] : v in evecF];
else
  evecR := [V!v : v in evecF];
end if;
```

```
  print "Eigenvectors:", evecR;
  P := Matrix(evecR);
  for i in [1..3] do // orthonormalise eigenvectors
    if mult[i] eq 1 then
      P[i] := P[i]/Sqrt(Norm(P[i]));
    elif mult[i] eq 2 then
      P[i] := P[i] - (DotProduct(P[i], P[i-1])/Norm(P[i-1]))*P[i-1];
      P[i] := P[i]/Sqrt(Norm(P[i]));
    end if;
  end for;
  P := Transpose(P);
  // diagonalisation
  CJ := MatrixRing(R, 3)!CJ; // work over R to precision p
  QJ := P*EJ; // change of basis matrix
  diag := [[Round((Inverse(QJ)*CJ*Inverse(Transpose(QJ)))[i][j]) : i in
     ↪  [1..3]] : j in [1..3]]; // check diag(1, 1, -1) output
  print "Verification:", diag;
  // output
  return(QJ);
end function;
```

§ A.3.2 | Restricted root data

We may now compute all of the root system and geodesic data required to understand the intersection arrangement associated with $(\Delta, \mathcal{J})$. The following function `IntersectionArrangement(Delta, Jc, d, (p), (name))` is the main implementation, using all of the previous functions and takes the arguments:

(1) `Delta` — Δ, as in §A.1.1,

(2) `Jc` — $\mathcal{J}^c$, as in §A.2.1,

(3) `d` — a positive integer d representing the number of wall-crossing steps to take from the $\mathcal{J}$-alcove $(1, \mathcal{J})$,

(4) `p` — the precision parameter, as in §A.3.1

(5) `name` — an optional string for exporting data (by default nothing is saved) for future use.

We summarise the main steps of the command.

Step 1 uses `DiagonaliseLevel` to give a change of variables that makes intersecting $\mathsf{Level}_{\mathcal{J}}$ with restricted root hyperplanes $\mathcal{H}_\Delta$ simpler, as in (5.C).

Step 2, the longest step, the $\mathcal{J}$-alcoves (x, J) are computed by repeated wall-crossing up to d steps. The higher the value of d the more detailed the resulting arrangement, as more restricted roots (and hence geodesics) are computed..

Step 3 calculates the geodesics in the disc that correspond to the root hyperplanes above, after first applying the change of variables from the first step, so that they will intersect with the unit hyperboloid. The output at this stage are the phases of the endpoints of each geodesics, which are then passed to `Mathematica` for drawing.

Step 4 consists of optional data to better understand the arrangement, by computing the vertices of each alcove, the angles at each vertex, and summarises the polygons present in the dual graph. In particular, this step double-checks the angle data computed in the proof of Theorem 5.24 and used for the classification Theorem 5.45.

Step 5 is an optional final export to the file `/dat/<name>/<name>J<Jc>.csv`, depending on whether the `name` optional parameter is given. This output file is directly read as input to `Mathematica`.

```
IntersectionArrangement := function(Delta, Jc, d: p := 15, name := "")
  // setup
  rk := #Delta; // rank
  R := RealField(p); // Reals
  V := VectorSpace(Rationals(), rk); // root space
  e := Basis(V); // simple roots
  VJ := VectorSpace(R, #Jc); // restricted root space
  C := Matrix(Rationals(), Delta); // Cartan matrix
  W<[s]> := CoxeterGroup(C); // Weyl group
  Graph := Graph<rk | ScalarMatrix(rk, 2) - C>;
  J := [j : j in [1..rk] | not j in Jc]; // shaded vertices
  print "Shaded vertices:", J;
  Graph0 := VertexSet(Graph); // vertices
  GraphJc := Graph; // mutation labels
  AssignLabels(~GraphJc, [Graph0.i : i in Jc], ["r", "g", "b"]);
  // diagonalisation
  print "\n"; print "Step 1: Diagonalisation";
  QJ := DiagonaliseLevel(Delta, Jc); // diagonalisation matrix
  print "Coordinate change:", QJ;
  Qinv := Inverse(QJ);
  // mutation
  print "\n"; print "Step 2: Mutation";
  Alc := [[[], Jc]]; elts := [[]]; subs := [Jc]; // J-alcoves
  queue := Alc; muts := [""]; class := ["Y"]; // mutations
  tri := [Jc]; // triangles
  walls := [[ElementToSequence(e[j])[Jc] : j in Jc]];
```

```
Gcls := [GraphJc]; // labelled graphs
vert := [0]; // keep track of mutated vertices
for step in [1..d] do // wall crossing
  print "Wall crossing step:", step;
  for alc in queue do;
    y := alc[1]; Kc := alc[2];
    pos := Position(Alc, alc);
    for i in Exclude(Kc, vert[pos]) do // avoid mutating 'backwards'
      newmc := "N";
      swc := SimpleWallCrossing(Delta, [k : k in [1..rk] | not k in Kc
          ↪ ], i : x := y);
      ynew := swc[1]; // Weyl element
      inew := swc[3]; // image of mutated vertex
      Knew := Exclude(Insert(Kc, Position(Kc, i), inew), i); // subset
      if not [ynew, Knew] in Alc then
        Append(~elts, ynew); Append(~subs, Knew);
        G := Gcls[pos]; G0 := VertexSet(G);
        Append(~muts, Label(G0.i) cat muts[pos]);
        AssignLabel(~G, G0.inew, Label(G0.i));
        if inew ne i then // only delete label if it moves
          DeleteLabel(~G, G0.i);
        end if;
        Append(~Gcls, G);
        if #ynew gt 0 then // restricted roots for walls
          res := [ElementToSequence(e[j]*&*[MatrixRing(Rationals(), rk
              ↪ )!ReflectionGroup(W).x : x in Reverse(ynew)])[Jc] : j
              ↪ in Knew];
          H := [[Abs(vi) : vi in v] : v in res];
        else
          H := [ElementToSequence(e[j])[Jc] : j in Knew];
        end if;
        if not (Seqset(Knew) in {Seqset(alc[2]) : alc in Alc}) and
            ↪ class[pos] eq "Y" then // Kc in mutation class
          newmc := "Y";
          Append(~tri, Knew);
        end if;
        Append(~Alc, [ynew, Knew]);
        Append(~queue, [ynew, Knew]);
        Append(~walls, H);
        Append(~vert, inew);
```

```
        Append(~class, newmc);
      end if;
    end for;
    Exclude(~queue, alc); // remove alcove from queue
  end for;
  print "Alcoves computed:", #Alc;
end for;
// geodesics
print "\n"; print "Step 3: Geodesics";
I1 := []; I2 := []; // ideal points
roots := []; // restricted roots
ngeo := 1; // geodesic count
for v in &cat[H : H in walls] do
  if Position(&cat[H : H in walls], v) eq ngeo then
    A := Qinv[1][1]*v[1] + Qinv[1][2]*v[2] + Qinv[1][3]*v[3]; // Q^-1v
    B := Qinv[2][1]*v[1] + Qinv[2][2]*v[2] + Qinv[2][3]*v[3];
    C := Qinv[3][1]*v[1] + Qinv[3][2]*v[2] + Qinv[3][3]*v[3];
    if A^2 + B^2 ge C^2 and A^2 + B^2 ne 0 then
      Append(~I1, [(-A*C-B*Sqrt(A^2+B^2-C^2))/(A^2+B^2), (-B*C+A*Sqrt(
        ↪ A^2+B^2-C^2))/(A^2+B^2)]);
      Append(~I2, [(-A*C+B*Sqrt(A^2+B^2-C^2))/(A^2+B^2), (-B*C-A*Sqrt(
        ↪ A^2+B^2-C^2))/(A^2+B^2)]);
    end if;
    Append(~roots, IntegerToString(Integers()!v[1]) cat ":" cat
      ↪ IntegerToString(Integers()!v[2]) cat ":" cat
      ↪ IntegerToString(Integers()!v[3]));
      end if;
  ngeo +:= 1;
end for;
arg1 := [Phase(i[1], i[2]) : i in I1];
arg2 := [Phase(i[1], i[2]) : i in I2];
ngeo := #arg1;
print "Geodesics computed:", ngeo;
// triangles
print "\n"; print "Step 4: Triangles";
angs := ["" : k in [1..#tri]]; gons := {};
for k in [1..#tri] do
  Kc := tri[k]; K := [i : i in [1..rk] | not i in Kc];
  for i, j in [1..3] do
    if j gt i then
```

```
      GraphKij := sub<Graph | {Graph0!v : v in K cat [Kc[i], Kc[j]]}>;
      Wij := CoxeterGroup(GrpFPCox, GraphKij);
      if not IsFinite(Wij) then // no relation
        angs[k] := angs[k] cat IntegerToString(Integers()!(0/2));
        Include(~gons, "Infinity");
        continue j;
      end if;
      ynew := []; Knew := K; iodd := Kc[i]; ieve := Kc[j];
      for mut in [1..25] do // repeated wall-crossing
        if mut mod 2 eq 1 then
          swc := SimpleWallCrossing(Delta, Knew, iodd: x := ynew);
          ynew := swc[1]; Knew := swc[2]; iodd := swc[3];
        else
          swc := SimpleWallCrossing(Delta, Knew, ieve: x := ynew);
          ynew := swc[1]; Knew := swc[2]; ieve := swc[3];
        end if;
        if ynew eq [] then // relation
          angs[k] := angs[k] cat IntegerToString(Integers()!(mut/2));
          Include(~gons, IntegerToString(mut));
          break mut;
        end if;
      end for;
    end if;
  end for;
end for;
print "Polygons in arrangement:", gons;
// optional export
print "\n"; print "Step 5: Export";
SetAutoColumns(false); // manual line breaks
SetColumns(0);
if name ne "" then
  sub := &cat[IntegerToString(i) : i in Jc];
  out := "dat/" cat name cat "/" cat name cat "J" cat sub cat ".csv";
  PrintFile(out, "ngeo,arg1,arg2": Overwrite := true);
  for k in [1..ngeo] do
    fprintf out, "%o, %o, %o \n",
    (k eq 1) select ngeo else "", arg1[k], arg2[k];
  end for;
  print "File saved:", out;
else
```

```
    print "No file saved.";
  end if;
  // output
  print "\n"; print "Arrangement data generated."; print "\n";
  return <arg1, arg2, roots, elts, subs, muts, angs>;
end function;
```

§ A.4 | Drawing intersection arrangements

We now pass to `Mathematica` in order to draw the intersection arrangements, using the data generated by `IntersectionArrangement`.

§ A.4.1 | Drawing hyperbolic geodesics

The following `Mathematica` module `PhaseGeo` takes the phase of two complex numbers of unit magnitude and uses (5.F) to draw the unique geodesic between them in the Poincaré disc model of $\mathbb{H}^2$. The parametrisation is slightly involved, requiring a number of cases to ensure that the geodesic is drawn inside the unit disc.

```
PhaseGeo[{ph1_, ph2_}] := Module[{phi, R, C, I1, I2, t1, t2},
  (*setup*)
  phi = Abs[ph1 - ph2]/2;
  R = If[Abs[phi - Pi/2] < 10^-8 || Abs[phi - (3Pi)/2] < 10^-8,
        0, Tan[phi]]; (*check for opposite points*)
  C = Sign[R/2]Sqrt[1+R^2]{Cos[ph1 + ph2], Sin[ph1 + ph2]};
  I1 = {Cos[ph1], Sin[ph1]}; (*ideal points*)
  I2 = {Cos[ph2], Sin[ph2]};
  t1 = If[Abs[R] > 0, Min[
    If[Abs[I1[[1]] - C[[1]] + Abs[R]] > 10^-8,
      2ArcTan[(I1[[2]] - C[[2]])/(I1[[1]] - C[[1]] + Abs[R])], Pi],
    If[Abs[I2[[1]] - C[[1]] + Abs[R]] > 10^-8,
      2ArcTan[(I2[[2]] - C[[2]])/(I2[[1]] - C[[1]] + Abs[R])], Pi]]];
  t2 = If[Abs[R] > 0, Max[
    If[Abs[I1[[1]] - C[[1]] + Abs[R]] > 10^-8,
      2ArcTan[(I1[[2]] - C[[2]])/(I1[[1]] - C[[1]] + Abs[R])], Pi],
    If[Abs[I2[[1]] - C[[1]] + Abs[R]] > 10^-8,
      2ArcTan[(I2[[2]] - C[[2]])/(I2[[1]] - C[[1]] + Abs[R])], Pi]]];
  (*output*)
  If[Abs[R] > 0, Circle[C, Abs[R],
    If[Pi + Min[t1, t2] < Max[t1, t2], {Min[t1, t2] + 2Pi,
    Max[t1, t2]}, {Min[t1, t2], Max[t1, t2]}]],
  Line[{I1, I2}]]
]
```

§ A.4.2 | Creating arrangements

All that remains is importing the phase data calculated in Appendix A.3 and then applying `PhaseGeo` to draw the hyperplanes between each pair of points. To this end we make a choice of Δ and $\mathcal{J}^c$, the former encoded as the same string used for the `name` argument in `IntersectionArrangement`, and import the data saved by this function. This will work provided that `Magma` and `Mathematica` are pointing to the same root directory. An example is given below, and all hyperbolic arrangements in this thesis are created using this process.

```
(*setup*)
graph = "A7hyp";
Jc = {4, 6, 7};
(*import*)
subset = StringJoin[
  ToString[Jc[[1]]], ToString[Jc[[2]]], ToString[Jc[[3]]]];
file = StringJoin[graph, "J", subset, ".csv"];
dat = Import[StringJoin["dat\\", graph, "\\", file],
  "Dataset", HeaderLines -> 1];
ngeo = dat[1, "ngeo"];
(*arrangement*)
arr = Graphics[{{Thickness[0.001], Table[PhaseGeo[{
  Mod[dat[i, "arg1"], 2Pi], Mod[dat[i, "arg2"], 2Pi]}], {i,1,ngeo}]},
  {Thickness[0.001], Circle[]}},
  PlotRange -> {{-1, 1}, {-1, 1}},
  ImageSize -> Full]
```

Bibliography

[ABM15] Rina Anno, Roman Bezrukavnikov, and Ivan Mirković. Stability conditions for Slodowy slices and real variations of stability. *Moscow Mathematical Journal*, 15(2):187–203, 403, 2015.

[Ach21] Pramod N Achar. *Perverse Sheaves and Applications to Representation Theory*, volume 258. American Mathematical Soc., 2021.

[AIR15] Claire Amiot, Osamu Iyama, and Idun Reiten. Stable categories of Cohen–Macaulay modules and cluster categories. *American Journal of Mathematics*, 137(3):813–857, 2015.

[ARS95] Maurice Auslander, Idun Reiten, and Sverre O. Smalø. *Representation Theory of Artin Algebras*. Cambridge Studies in Advanced Mathematics. Cambridge University Press, Cambridge, 1995.

[AW22] Jenny August and Michael Wemyss. Stability conditions for contraction algebras. *Forum of Mathematics. Sigma*, 10:Paper No. e73, 20, 2022.

[Bay11] Arend Bayer. A tour to stability conditions on derived categories. Lecture notes, University of Edinburgh, 2011.

[BB05] Anders Björner and Francesco Brenti. *Combinatorics of Coxeter Groups*, volume 231 of *Graduate Texts in Mathematics*. Springer, New York, 2005.

[BBD82] A. A. Beilinson, J. Bernstein, and P. Deligne. Faisceaux pervers. In *Analysis and Topology on Singular Spaces, I (Luminy, 1981)*, volume 100 of *Astérisque*, pages 5–171. Soc. Math. France, Paris, 1982.

[BBK02] Sheila Brenner, Michael C. R. Butler, and Alastair D. King. Periodic algebras which are almost Koszul. *Algebras and Representation Theory*, 5(4):331–367, 2002.

[BCP97] Wieb Bosma, John Cannon, and Catherine Playoust. The Magma algebra system. I. The user language. *Journal of Symbolic Computation*, 24(3-4):235–265, 1997.

[BCS23] Gwyn Bellamy, Alastair Craw, and Travis Schedler. Birational geometry of quiver varieties and other GIT quotients, 2023. arXiv:2212.09623.

[Bei87] A. A. Beilinson. On the derived category of perverse sheaves. In Yuri I. Manin, editor, *K-Theory, Arithmetic and Geometry: Seminar, Moscow University, 1984–1986*, pages 27–41. Springer, Berlin, Heidelberg, 1987.

[Bel97] Richard Bellman. *Introduction to Matrix Analysis: Second Edition*. SIAM, 1997.

[BGL87] Dagmar Baer, Werner Geigle, and Helmut Lenzing. The preprojective algebra of a tame hereditary Artin algebra. *Communications in Algebra*, 15(1-2):425–457, 1987.

[BIRS09] Aslak B. Buan, Osamu Iyama, Idun Reiten, and Jeanne Scott. Cluster structures for 2-Calabi–Yau categories and unipotent groups. *Compositio Mathematica*, 145(4):1035–1079, 2009.

[BK89] Alexey I. Bondal and Mikhail M. Kapranov. Representable functors, Serre functors, and reconstructions. *Izvestiya Akademii Nauk SSSR. Seriya Matematicheskaya*, 53(6):1183–1205, 1337, 1989.

[BKOP14] Georgia Benkart, Seok-Jin Kang, Se-jin Oh, and Euiyong Park. Construction of Irreducible Representations over Khovanov–Lauda–Rouquier Algebras of Finite Classical Type. *International Mathematics Research Notices*, 2014(5):1312–1366, 2014.

[Bri07] Tom Bridgeland. Stability conditions on triangulated categories. *Annals of Mathematics. Second Series*, 166(2):317–345, 2007.

[Bri09] Tom Bridgeland. Stability conditions and Kleinian singularities. *International Mathematics Research Notices. IMRN*, 2009(21):4142–4157, 2009.

[BT11] Christopher Brav and Hugh Thomas. Braid groups and Kleinian singularities. *Mathematische Annalen*, 351(4):1005–1017, 2011.

[CCC+10] Lisa Carbone, Sjuvon Chung, Leigh Cobbs, Robert McRae, Debajyoti Nandi, Yusra Naqvi, and Diego Penta. Classification of hyperbolic Dynkin diagrams, root lengths and Weyl group orbits. *Journal of Physics. A. Mathematical and Theoretical*, 43(15):155209, 30, 2010.

[CFKP97] James W. Cannon, William J. Floyd, Richard Kenyon, and Walter R. Parry. Hyperbolic geometry. In *Flavors of Geometry*, volume 31 of *Math. Sci. Res. Inst. Publ.*, pages 59–115. Cambridge Univ. Press, Cambridge, 1997.

[CH98] William Crawley-Boevey and Martin P. Holland. Noncommutative deformations of Kleinian singularities. *Duke Mathematical Journal*, 92(3):605–635, 1998.

[Cox34] H. S. M. Coxeter. Discrete Groups Generated by Reflections. *Annals of Mathematics*, 35(3):588–621, 1934.

[CR17] Joseph Chuang and Raphaël Rouquier. Perverse equivalences. Preprint, 2017.

[Del72] Pierre Deligne. Les immeubles des groupes de tresses généralisés. *Inventiones mathematicae*, 17:273–302, 1972.

[Del10] Emanuele Delucchi. Combinatorics of covers of complexified hyperplane arrangements. In *Arrangements, Local Systems and Singularities*, volume 283 of *Progr. Math.*, pages 1–38. Birkhäuser Verlag, Basel, 2010.

[DW22] Will Donovan and Michael Wemyss. Stringy Kähler moduli, mutation and monodromy, 2022. To appear J. Diff. Geom. arXiv:1907.10891.

[EL21] Alexey Elagin and Valery A. Lunts. Thick subcategories on curves. *Advances in Mathematics*, 378:107525, 2021.

[Gab72] Peter Gabriel. Unzerlegbare Darstellungen. I. *Manuscripta Mathematica*, 6:71–103; 309, 1972.

[GM94] S. I. Gelfand and Yu. I. Manin. Homological algebra. In *Algebra, V*, volume 38 of *Encyclopaedia Math. Sci.*, pages 1–222. Springer, Berlin, 1994.

[GP79] Israel M. Gel'fand and Vladimir A. Ponomarev. Model algebras and representations of graphs. *Functional Analysis and Its Applications*, 13(3):1–12, 1979.

[Hal13] Brian C Hall. *Lie Groups, Lie Algebras, and Representations*. Springer, 2013.

[HRS96] Dieter Happel, Idun Reiten, and Sverre O. Smalø. Tilting in abelian categories and quasitilted algebras. *Memoirs of the American Mathematical Society*, 120(575):viii+ 88, 1996.

[Hum90] James E. Humphreys. *Reflection Groups and Coxeter Groups*. Cambridge Studies in Advanced Mathematics. Cambridge University Press, Cambridge, 1990.

[HW18] Yuki Hirano and Michael Wemyss. Faithful actions from hyperplane arrangements. *Geometry & Topology*, 22(6):3395–3433, 2018.

[HW23] Yuki Hirano and Michael Wemyss. Stability conditions for 3-fold flops. *Duke Mathematical Journal*, 172(16):3105–3173, 2023.

[Ike14] Akishi Ikeda. Stability conditions for preprojective algebras and root systems of Kac-Moody Lie algebras, 2014. arXiv:1402.1392.

[Inc] Wolfram Research Inc. Mathematica, Version 14.0. Champaign, IL, 2024.

[IR08] Osamu Iyama and Idun Reiten. Fomin–Zelevinsky mutation and tilting modules over Calabi–Yau algebras. *American Journal of Mathematics*, 130(4):1087–1149, 2008.

[IW] Osamu Iyama and Michael Wemyss. Tits cones intersections and applications. Draft.

[Kac80] Victor G. Kac. Some remarks on representations of quivers and infinite root systems. In *Representation Theory, II (Proc. Second Internat. Conf., Carleton Univ., Ottawa, Ont., 1979)*, volume 832 of *Lecture Notes in Math.*, pages 311–327. Springer, Berlin, 1980.

[Kac83] Victor G. Kac. *Infinite-Dimensional Lie Algebras*, volume 44 of *Progress in Mathematics*. Birkhäuser Boston, Inc., Boston, MA, 1983.

[Kac90] Victor G. Kac. *Infinite-Dimensional Lie Algebras*. Cambridge University Press, Cambridge, third edition, 1990.

[Kel08] Bernhard Keller. Calabi-Yau triangulated categories. In *Trends in Representation Theory of Algebras and Related Topics*, EMS Ser. Congr. Rep., pages 467–489. Eur. Math. Soc., Zürich, 2008.

[Kil88] Wilhelm Killing. Die Zusammensetzung der stetigen endlichen Transformationsgruppen. *Mathematische Annalen*, 33(1):1–48, 1888.

[Ko24] Hankyung Ko. An atomic Coxeter presentation, 2024. arXiv:2312.16666.

[Kra22] Henning Krause. *Homological Theory of Representations*, volume 195 of *Cambridge Studies in Advanced Mathematics*. Cambridge University Press, Cambridge, 2022.

[KS06] Masaki Kashiwara and Pierre Schapira. *Categories and Sheaves*, volume 332 of *Grundlehren Der Mathematischen Wissenschaften*. Springer, Berlin, Heidelberg, 2006.

[Lal96] Pierre Lalonde. A non-commutative version of Jacobi's equality on the cofactors of a matrix. *Discrete Mathematics*, 158(1-3):161–172, 1996.

[Lew24] Samuel Lewis. Real variations of stability on K3 categories, 2024. arXiv:2407.07621.

[Li88] Wang Lai Li. Classification of generalized Cartan matrices of hyperbolic type. *Chinese Annals of Mathematics. Series B. Shuxue Niankan. B Ji*, 9(1):68–77, 1988.

[Mag74] Wilhelm Magnus. *Noneuclidean Tesselations and Their Groups*. Academic Press, 1974.

[Mat64] Hideya Matsumoto. Générateurs et relations des groupes de Weyl généralisés. *Comptes Rendus Hebdomadaires des Séances de l'Académie des Sciences*, 258:3419–3422, 1964.

[McK80] John McKay. Graphs, singularities, and finite groups. In *The Santa Cruz Conference on Finite Groups (Univ. California, Santa Cruz, Calif., 1979)*, volume 37 of *Proc. Sympos. Pure Math.*, pages 183–186. Amer. Math. Soc., Providence, R.I., 1980.

[Mil] Dragan Miličić. Lectures on derived categories. Lecture notes, University of Utah.

[Min12] Hiroyuki Minamoto. Ampleness of two-sided tilting complexes. *International Mathematics Research Notices*, 2012(1):67–101, 2012.

[Min18] Hiroyuki Minamoto. A criterion for graded coherence of tensor algebras and applications to higher dimensional AR-theory. *European Journal of Mathematics*, 4(2):612–621, 2018.

[Miy91] Junichi Miyachi. Localization of triangulated categories and derived categories. *Journal of Algebra*, 141(2):463–483, 1991.

[Moo79] Robert V. Moody. Root systems of hyperbolic type. *Advances in Mathematics*, 33(2):144–160, 1979.

[MS17] Emanuele Macrì and Benjamin Schmidt. Lectures on Bridgeland Stability. In *Moduli of Curves: CIMAT Guanajuato, Mexico 2016*, pages 139–211. Springer International Publishing, Cham, 2017.

[Mum65] David Mumford. *Geometric Invariant Theory*. Ergebnisse Der Mathematik Und Ihrer Grenzgebiete, Neue Folge, Band 34. Springer-Verlag, Berlin-New York, 1965.

[Par00] Luis Paris. On the fundamental group of the complement of a complex hyperplane arrangement. In *Arrangements–Tokyo 1998*, volume 27, pages 257–273. Mathematical Society of Japan, 2000.

[PV18] Chrysostomos Psaroudakis and Jorge Vitória. Realisation functors in tilting theory. *Mathematische Zeitschrift*, 288(3):965–1028, 2018.

[Ric89] Jeremy Rickard. Morita theory for derived categories. *Journal of the London Mathematical Society. Second Series*, 39(3):436–456, 1989.

[Rin12] Claus Michael Ringel. Introduction to the representation theory of quivers. Lecture notes, Universität Bielefeld, 2012.

[Saç89] Cihan Saçlıoğlu. Dynkin diagrams for hyperbolic Kac–Moody algebras. *Journal of Physics. A. Mathematical and General*, 22(18):3753–3769, 1989.

[Sal87] M. Salvetti. Topology of the complement of real hyperplanes in $\mathbb{C}^N$. *Inventiones Mathematicae*, 88(3):603–618, 1987.

[Ser53] Jean-Pierre Serre. Groupes d'homotopie et classes de groupes abéliens. *Annals of Mathematics. Second Series*, 58:258–294, 1953.

[SPA18] The Stacks Project Authors. *Stacks Project*, 2018. Link.

[SY13] Yuhi Sekiya and Kota Yamaura. Tilting theoretical approach to moduli spaces over preprojective algebras. *Algebras and Representation Theory*, 16(6):1733–1786, 2013.

[Syl52] J.J. Sylvester. XIX. A demonstration of the theorem that every homogeneous quadratic polynomial is reducible by real orthogonal substitutions to the form of a sum of positive and negative squares. *The London, Edinburgh, and Dublin Philosophical Magazine and Journal of Science*, 4(23):138–142, 1852.

[Ver96] Jean-Louis Verdier. Des catégories dérivées des catégories abéliennes. *Astérisque*, 1996(239):xii+253, 1996.

[Vis08] Sankaran Viswanath. Embeddings of Hyperbolic Kac–Moody Algebras into E 10. *Letters in Mathematical Physics*, 83(2):139–148, 2008.

[VS93] E. B. Vinberg and O. V. Shvartsman. Discrete Groups of Motions of Spaces of Constant Curvature. In E. B. Vinberg, editor, *Geometry II: Spaces of Constant Curvature*, pages 139–248. Springer, Berlin, Heidelberg, 1993.

[Wem18] Michael Wemyss. Flops and clusters in the homological minimal model programme. *Inventiones Mathematicae*, 211(2):435–521, 2018.

[Woo10] Jonathan Woolf. Stability conditions, torsion theories and tilting. *Journal of the London Mathematical Society. Second Series*, 82(3):663–682, 2010.